

**POWER SYSTEM RELIABILITY ANALYSIS
WITH SPECIAL EMPHASIS ON
RENEWABLE DISTRIBUTED GENERATION
AND ELECTRIC VEHICLE**



BIPUL KUMAR TALUKDAR

DEPARTMENT OF ELECTRICAL ENGINEERING

ASSAM ENGINEERING COLLEGE

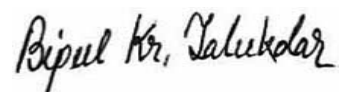
**THIS THESIS IS SUBMITTED TO
GAUHATI UNIVERSITY FOR THE AWARD OF DEGREE OF
DOCTOR OF PHILOSOPHY**

**FACULTY OF ENGINEERING
GAUHATI UNIVERSITY
2022**

Declaration

I hereby declare that this thesis is the result of my own research work which has been carried out under the guidance of Dr. Bimal Chandra Deka, Professor, Department of Electrical Engineering, Assam Engineering College (Supervisor) and Dr. Arup Kumar Goswami, Associate Professor, Department of Electrical Engineering, National Institute of Technology Silchar (Co-supervisor). I further declare that this thesis as a whole or any part thereof has not been submitted to any university (or institute) for the award of any degree or diploma.

This thesis contains less than 90,000 (ninety thousand) words excluding bibliography and captions.




.....
(Bipul Kumar Talukdar)

March 2022

Certificate

This is to certify that the thesis titled "Power System Reliability Analysis with Special Emphasis on Renewable Distributed Generation and Electric Vehicle" is the result of research work of Bipul Kumar Talukdar, carried under our supervision, submitted to Gauhati University for the award of the degree of Doctor of Philosophy in Electrical Engineering.

This thesis conforms to the standard of PhD Thesis under Gauhati University including the standard related to plagiarism and has a similarity index not more than 10% (Ten percent), excluding the bibliography.

.....

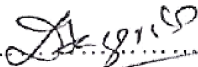
Prof. (Dr.) Bimal Chandra Deka
(Supervisor)

.....


Dr. Arup Kumar Goswami,
(Co-supervisor)

Members of the Research Advisory Committee:

(a) Dr. Durlav Hazarika

.....

(b) Dr. Damodar Agarwal

.....

(c) Dr. Sarmila Patra

.....

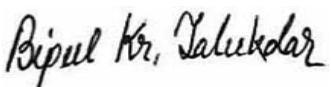
Acknowledgements

First of all, I would like to show immense gratitude to my supervisor, Dr. Bimal Chandra Deka, Professor, Department of Electrical Engineering, Assam Engineering College. I sincerely thank him for his exemplary guidance and encouragement, without whose supervision and persistent help, this research would not have been materialized.

I would like to thank my co-supervisor, Dr. Arup Kumar Goswami, Associate Professor, Department of Electrical Engineering, National Institute of Technology Silchar, for his valuable support, encouragement, and guidance during the course of the research.

It is my heartiest thank to the Department of Electrical Engineering, Assam Engineering College. I would like to acknowledge Prof. (Dr.) Damodar Agarwal, Head of the Department, and all other teachers of the department for their enthusiastic support and encouragement I received throughout this endeavor.

Finally, I thank my parents, family, and friends. I am indebted to them for being constant sources of motivation, care and support.



.....

(Bipul Kumar Talukdar)

March 2022

Abstract

Power system reliability (PSR) refers to the probability of a power system performing its intended function, i.e., to provide electrical power to all of its customers at a reasonable cost with an assurance of continuity and quality. However, it is neither technically nor economically feasible to plan, construct and operate a power system with zero likelihood of failure. System failures are stochastic in nature. The probability of customers being interrupted can be reduced up to a certain extent by increased investment and proper planning during the designing phase or the operating phase, or both. For this, it is extremely important to assess the reliability of the entire system considering all aspects like load growth, available operating reserve, capacity expansion, transmission constraints, etc. A thorough analysis of PSR helps system planners, designers, and operators to monitor the system's overall risk level. It also provides information on the weak zone in the system and helps to prepare preventive and corrective maintenance schedules for its components.

Over the years, PSR has been an operational issue for the power system operators (PSOs). However, deregulation of power industry makes PSR more customer-centric and price-specific. In a deregulated power system (DPS), customers have more freedom to select not only the energy utilities but also to purchase power at their preferred reliability levels. Therefore, maintaining PSR as per customers' specifications becomes challenging for the PSOs in DPSs. Centralized operations that aid in easier decision-making at all levels are no more relevant in the deregulated environment. Cost-based mechanisms of vertically integrated utilities have transitioned to price-based mechanisms in horizontally operated power systems. A judicious reliability-centered operating reserve management (ORM) strategy is vital in such environments. This research covers this aspect. Reliability assessment of a power system under deregulated scenario is one of the objectives of this research.

For a highly reliable power supply, the adequacy of operating reserve is an important factor. With the integration of renewable distributed generation (DG), smart management

of the operating reserve becomes possible, enabling high efficiency and reliability of power supply at reasonably lower costs. However, integration of large volumes of renewable energy sources (RESs) brings some technical challenges and complexities in power system operation. Therefore, modern power system requires enhanced techniques to evaluate its reliability and minimize the frequency and duration of outages. In this research work, a method has been proposed to develop a reliability model of a system having multiple RESs. The thesis analyzes the reliability worth in terms of energy and costs due to the integration of solar, wind, and tidal energy sources with the help of two new performance metrics.

In addition to RESs, the emergence of electric vehicles (EVs) brings many new aspects to PSR studies. EVs can be treated as variable loads (in grid-to-vehicle mode) and also as portable DG (in vehicle-to-grid mode). The increased volume of plug-in EVs in grid-to-vehicle mode reduces the grid's reserve capacity and thus reduces the reliability of power supply to its customer load-points. Moreover, uncontrolled scheduling of EV charging distorts the load curve, causing peaks on the peaks; and pushes the system operator for load curtailment, and thus reduces the system reliability. The present research considers this aspect also. It analyzes how the reliability of a distribution network is impacted due to the charging of plug-in EVs.

The operational effectiveness of a plug-in EV is primarily dependent on the availability of a reliable charging station at the desired location. Thus, the grid's reliability directly impacts the operation of an EV. Furthermore, EVs are built with a large number of electrical components, which makes EVs more failure-prone as compared to conventional vehicles. This thesis presents an approach to conducting comprehensive reliability, availability, and maintainability studies of a plug-in EV covering all the above-mentioned aspects. In addition to this, the thesis also investigates the reliability and availability of a solar-powered vehicle. The study quantitatively justifies that a solar EV with a standby plug-in facility can be the most effective EV option from reliability perspective.

The present studies implement the Markov modeling concepts and well-being framework to develop different reliability models. In addition to the conventional reliability indices, some newly designed reliability metrics have been proposed in this thesis. Developed models are exemplified in some standard test systems. Input data sets are collected from the state of the art literature. Calculations are carried out through programming/simulations in MATLAB/Simulink ■

Table of Contents

| | |
|--|--------------|
| List of Figures | xix |
| List of Tables | xxiii |
| List of Abbreviations | xxv |
| 1 Introduction | 1 |
| 1.1 Background | 1 |
| 1.1.1 Power System Reliability | 2 |
| 1.1.2 Hierarchical Levels for Reliability Studies | 3 |
| 1.1.3 Changing Scenarios | 5 |
| 1.2 Research Problems | 9 |
| 1.3 Aim | 12 |
| 1.4 Research Objectives | 12 |
| 1.5 Outline of the Thesis | 12 |
| 2 Review of Literature | 17 |
| 2.1 Introduction | 17 |
| 2.2 Requirements for Power System Reliability Assessment | 18 |
| 2.2.1 Generation System (HL-I) Studies | 18 |
| 2.2.2 Composite System (HL-II) Studies | 19 |
| 2.2.3 Distribution System Studies | 20 |

| | | |
|----------|--|-----------|
| 2.3 | Reliability Cost/Worth | 21 |
| 2.4 | Power System Reliability Evaluation Techniques | 23 |
| 2.4.1 | Deterministic Approach | 26 |
| 2.4.2 | Probabilistic Approach | 26 |
| 2.4.3 | Well-being Approach | 27 |
| 2.4.4 | Markov Model Approach | 27 |
| 2.5 | Some Emerging Areas for Reliability Study | 28 |
| 2.5.1 | Reserve Management under Deregulated Scenario | 28 |
| 2.5.2 | Impacts of Distributed Generation | 30 |
| 2.5.3 | Reliability of Renewable Energy Incorporated Network | 31 |
| 2.5.4 | Grid Integration with Electric Vehicles | 34 |
| 2.5.5 | RAM Studies for Electric Vehicles | 35 |
| 2.5.6 | Solar EV: A Step toward Green Transportation | 37 |
| 2.6 | Conclusion | 41 |
| 3 | Methods and Materials | 43 |
| 3.1 | Introduction | 43 |
| 3.2 | Basic Concepts, Terms and Definitions | 44 |
| 3.2.1 | Reliability Function | 45 |
| 3.2.2 | Maintainability Function | 46 |
| 3.2.3 | Availability Function | 47 |
| 3.3 | System Reliability Evaluation | 48 |
| 3.3.1 | Series System | 48 |
| 3.3.2 | Parallel System | 49 |
| 3.3.3 | Standby System | 50 |
| 3.4 | Markov Model | 51 |
| 3.4.1 | Differential Equations Method | 53 |
| 3.4.2 | Matrix Multiplication Method | 56 |
| 3.4.3 | Availability Calculation Steps | 58 |
| 3.5 | Well-being Model | 58 |
| 3.5.1 | Well-being Indices Evaluation Methods | 60 |

| | | |
|----------|--|-----------|
| 3.5.2 | Flowchart for Well-being indices | 61 |
| 3.6 | Distribution System Reliability Assessment (DSRA) | 62 |
| 3.6.1 | Distribution System Reliability Indices | 63 |
| 3.6.2 | Distribution System Reliability Indices Calculation | 67 |
| 3.7 | Reliability Test Systems | 70 |
| 3.7.1 | Roy Billinton Test System (RBTS) | 70 |
| 3.7.2 | RBTS Bus-2 Distribution System | 72 |
| 3.8 | Conclusion | 73 |
| 4 | Reliability-Centered Reserve Management in Deregulated Power System | 75 |
| 4.1 | Introduction | 75 |
| 4.1.1 | Principle of Operating Reserve | 76 |
| 4.1.2 | Operating Reserve in Conventional Power System | 77 |
| 4.1.3 | Operating Reserve in Deregulated Power System | 78 |
| 4.2 | Methodology | 79 |
| 4.3 | Description of the Test System | 83 |
| 4.4 | Case Studies | 84 |
| 4.4.1 | Considering RBTS as a Vertically Integrated System | 84 |
| 4.4.2 | Considering RBTS as a Deregulated System | 87 |
| 4.5 | Conclusion | 91 |
| 5 | Reliability Modeling and Worth Analysis of a Renewable Energy Incorporated Distribution Network | 93 |
| 5.1 | Introduction | 93 |
| 5.2 | Reliability of Active Distribution Network | 95 |
| 5.3 | Power Generation Model under consideration | 96 |
| 5.3.1 | Modeling of Solar Power Generation | 96 |
| 5.3.2 | Modeling of Wind Power Generation | 100 |
| 5.3.3 | Modeling of Tidal Power Generation | 102 |
| 5.3.4 | Reliability Modeling of the Hybrid Generation System (HGS) | 104 |
| 5.4 | Reliability Modeling of the Radial Network | 109 |

| | | |
|----------|---|------------|
| 5.5 | Flowchart of the Study | 111 |
| 5.6 | Description of the Test System | 112 |
| 5.7 | Results and Discussion | 113 |
| 5.7.1 | Reliability investigation with a perfect distribution network | 113 |
| 5.7.2 | Reliability investigation with an imperfect distribution network | 114 |
| 5.7.3 | Reliability worth/cost assessment using the proposed metrics | 119 |
| 5.8 | Conclusion | 120 |
| 6 | Reliability Analysis of Distribution Network Integrated with Electric Vehicle | 123 |
| 6.1 | Introduction | 123 |
| 6.2 | Methodology | 124 |
| 6.2.1 | Battery Charging Model | 124 |
| 6.2.2 | Vehicle Charging Demand Model | 126 |
| 6.2.3 | Time Distribution Modeling of schedulable PEV | 128 |
| 6.2.4 | PEV Load Modeling | 129 |
| 6.2.5 | Reliability of the Network | 131 |
| 6.3 | Description of the Test System | 131 |
| 6.4 | Results and Discussion | 132 |
| 6.5 | Conclusion | 135 |
| 7 | Reliability, Availability and Maintainability Analysis of Plug-in Electric Vehicle | 137 |
| 7.1 | Introduction | 137 |
| 7.2 | PEV Configuration | 139 |
| 7.3 | Reliability Modeling of PEV System | 141 |
| 7.3.1 | Modeling of Energy Source Subsystem | 142 |
| 7.3.2 | Modeling of the Electric Propulsion Subsystem | 145 |
| 7.3.3 | Modeling of the PEV System | 147 |
| 7.4 | Charging Station's Role on PEV's Availability | 149 |
| 7.5 | Results and Discussion | 152 |
| 7.5.1 | RAM Assessment of the PEV System | 152 |
| 7.5.2 | Impact of <i>ASAI</i> on the PEV | 154 |

| | | |
|----------|---|------------|
| 7.6 | Conclusion | 156 |
| 8 | Reliability Modeling and Availability Analysis of Solar Electric Vehicle | 157 |
| 8.1 | Introduction | 157 |
| 8.2 | Description of the SEV System | 160 |
| 8.3 | Reliability Modeling of SEV | 161 |
| 8.3.1 | Fault-Tree model of the SEV under study | 162 |
| 8.3.2 | Modeling of Power Supply System (PSS) | 163 |
| 8.3.3 | Modeling of Energy Storage System (ESS) | 169 |
| 8.3.4 | Modeling of Motor-Drive System (MDS) | 173 |
| 8.3.5 | Modeling of Energy Management and Control System(EMCS) . . . | 175 |
| 8.3.6 | Modeling of Electrical Propulsion System (EPS) | 176 |
| 8.3.7 | Composite Reliability Modeling of the SEV System | 178 |
| 8.4 | Results and Discussion | 179 |
| 8.4.1 | Reliability Assessment of SEV | 180 |
| 8.4.2 | Availability Assessment of SEV | 183 |
| 8.4.3 | Impact of <i>mPAI</i> on SEV's Availability | 185 |
| 8.5 | Conclusion | 186 |
| 9 | Conclusions and Future Scope | 189 |
| 9.1 | Conclusions | 189 |
| 9.1.1 | General Conclusions | 190 |
| 9.1.2 | Specific Conclusions | 192 |
| 9.2 | Future Scope | 195 |
| | References | 197 |
| | Appendix A Input Data Set | 211 |
| | Appendix B List of Publications | 217 |

List of Figures

| | | |
|-----|--|----|
| 1.1 | Basic power system functional zones | 4 |
| 1.2 | Problem Identification Flowchart | 11 |
| 2.1 | Conceptual tasks for HL-I evaluation | 19 |
| 2.2 | Consumer, utility, and total cost a function of system reliability | 22 |
| 2.3 | Prototype SEV models: (a) Sunmobile (b) Sion (c) Lightyear One | 39 |
| 3.1 | Reliability block diagram of a 2-component series system | 49 |
| 3.2 | Reliability block diagram of a 2-component parallel system | 49 |
| 3.3 | Reliability block diagram of a standby system | 50 |
| 3.4 | State-space diagram of a system having single repairable component | 52 |
| 3.5 | System well-being model | 59 |
| 3.6 | Flowchart to determine the basic well-being indices | 61 |
| 3.7 | Simple 3-load point RDS | 67 |
| 3.8 | Single-line diagram of RBTS | 71 |
| 3.9 | Distribution System at Bus-2 of RBTS | 72 |
| 4.1 | System Well-being Model | 80 |
| 4.2 | Flowchart for determination of operating reserve | 82 |
| 4.3 | Single-line diagram of RBTS | 83 |
| 4.4 | Well-being model for Vertically integrated RBTS | 85 |

| | | |
|------|--|-----|
| 4.5 | Power transactions in deregulated market | 87 |
| 4.6 | CRAI at different capacities of GENCO 1 | 88 |
| 4.7 | CRAI at different Capacity of GENCO 2 | 89 |
| 5.1 | Subdivision of ADN reliability | 95 |
| 5.2 | Abstract model of the system under consideration | 96 |
| 5.3 | PV power output vs. Solar irradiation characteristics | 100 |
| 5.4 | Wind power output vs. wind speed characteristics curve | 102 |
| 5.5 | Layout of Tidal Power Plant | 103 |
| 5.6 | State -space diagram of a two-state system | 104 |
| 5.7 | State -space diagram of a n-state system | 104 |
| 5.8 | State-space diagram of the HGS | 105 |
| 5.9 | Well-being indices of the HGS | 108 |
| 5.10 | Flowchart of the proposed study | 111 |
| 5.11 | Modified DS of BUS-2 (RBTS) with SPP, WPP and TPP integration | 112 |
| 5.12 | Reliability of the hybrid generation system | 114 |
| 5.13 | Improvements in (a) SAIFI, (b)SAIDI, (c) CAIDI, (d) AENS , (e) EENS and (f) IEAR under different modes of HGS operation | 118 |
| 5.14 | Improvements in (a) ECOST and (b) Savings in ECOST under different modes of HGS operation | 119 |
| 6.1 | Equivalent circuit of charger | 125 |
| 6.2 | Distribution Network at BUS-2 of IEEE-RBTS | 132 |
| 6.3 | Impact of different sizes of EV loads on system load curve | 133 |
| 7.1 | Schematic diagram of a typical plug-in electric vehicle (PEV) system. | 140 |
| 7.2 | Fault-tree diagram of the PEV system. | 141 |
| 7.3 | State-space diagram of the Energy Source Subsystem. | 142 |
| 7.4 | State-space diagram of the Electric Propulsion Subsystem. | 146 |
| 7.5 | State-space diagram of the PEV system. | 147 |
| 7.6 | State-space diagram of the CS-Battery Model. | 150 |

| | | |
|------|---|-----|
| 7.7 | Reliability, Availability, and Maintainability curves for the PEV. | 153 |
| 7.8 | Vehicle's availability at different restoration rates (RR). | 154 |
| 7.9 | Availability of PEV at different ASAI. | 155 |
| 8.1 | Schematic diagram of the SEV under study | 161 |
| 8.2 | Fault-tree of the SEV under study | 162 |
| 8.3 | Power supply scheme for the SEV under study | 164 |
| 8.4 | n-state model of PVG. | 165 |
| 8.5 | Three-state model of a battery. | 169 |
| 8.6 | State-space diagram of the ESS model | 172 |
| 8.7 | State-space diagram of the Motor-Drive system | 174 |
| 8.8 | State-space diagram of the EMCS | 175 |
| 8.9 | State-space diagram of the EPS | 177 |
| 8.10 | Reliability block diagram of the SEV. | 178 |
| 8.11 | Comparison of reliability of SEV with and without plug-in facility | 181 |
| 8.12 | Reliability of a SEV with different energy source options | 182 |
| 8.13 | Effectiveness of the SEV with different maintenance strategies. | 183 |
| 8.14 | Comparison of availability of the SEV with different component failure rates(FR) | 185 |
| 8.15 | Availability of the SEV at different <i>mPAI</i> | 186 |

List of Tables

| | | |
|-----|---|-----|
| 3.1 | Component data for the system of Fig. 3.7 | 68 |
| 3.2 | Load-point reliability indices for the system of Fig. 3.7 | 68 |
| 3.3 | Details of the distribution system | 68 |
| 3.4 | Interruption effects in a given calendar year | 69 |
| 4.1 | System well-being indices for unit commitment using single criterion . . . | 85 |
| 4.2 | System well-being indices for unit commitment using multiple criterion . . | 86 |
| 4.3 | Well-being indices for DISCO B with different reserves allocation | 88 |
| 4.4 | Well-being indices with different capacity reserves allocation at GENCO 2 . | 89 |
| 4.5 | Well-being indices after the reserve agreement between DISCO B and GENCO 2 | 90 |
| 4.6 | Well-being indices after the CR agreement between DISCO A,C-E and GENCO 1 | 90 |
| 5.1 | Well-being indices of the HGS | 109 |
| 5.2 | Results of the case studies | 117 |
| 5.3 | Incremental energy and cost benefits from the HGS under different modes of operation | 120 |
| 6.1 | Logarithmic normal distribution parameters | 129 |
| 6.2 | Reliability parameters of elements of the DN | 132 |

| | | |
|------|---|-----|
| 6.3 | Impact of PEV charging on DS reliability | 134 |
| 6.4 | Parameters of the different PEVs | 134 |
| 6.5 | DS Reliability under different PEV charging modes | 134 |
| 8.1 | Reliability of key subsystems of the SEV | 180 |
| A.1 | Generating Unit Rating and Reliability Data of RBTS [1] | 211 |
| A.2 | Priority order of generating units of RBTS [1] | 212 |
| A.3 | Specifications of SPP, WPP and TPP [2, 3] | 212 |
| A.4 | Weather effect coefficient (τ) for SPP [4] | 212 |
| A.5 | Customer Data at BUS-2 of RBTS [5] | 213 |
| A.6 | Component Reliability Data for BUS-2 of RBTS [6] | 213 |
| A.7 | Interruption Cost (\$/kW) of different consumer types [7] | 213 |
| A.8 | Component Reliability Data for PEV [MIL-HDBK-217E,F] | 213 |
| A.9 | Charging Station Data for PEV [8] | 214 |
| A.10 | Reliability data of a typical SEV [MIL-HDBK-217E,F] | 214 |
| A.11 | PV Generation Data [9] | 214 |
| A.12 | Charging Station Data for SEV [9] | 215 |
| A.13 | Radial System Reliability Parameter: RBTS (Bus-2) [6] | 215 |

List of Abbreviations

| | |
|-------|--|
| ADN | Active Distribution Network |
| AENS | Average Energy Not Supplied |
| AS | Auxiliary System |
| ASAI | Average Service Availability Index |
| BB | Battery Bank |
| BLP | Bulk Load Point |
| BSP | Bulk Supply Point |
| CAIDI | Customer Average Interruption Duration Index |
| CC | Charge Controller |
| CS | Charging Station |
| DG | Distributed Generation |
| DN | Distribution Network |
| DS | Distribution System |
| DSR | Distribution System Reliability |
| DSRA | Distribution System Reliability Assessment |
| ECOST | Expected Interruption Cost |
| EENS | Expected Energy Not Supplied |
| EFR | Effective Failure Rate |
| EMCS | Energy Management and Control System |
| EMU | Energy Management Unit |
| EPS | Electric Propulsion Subsystem |

| | |
|-------|------------------------------------|
| ERR | Effective Restoration Rate |
| ESS | Energy Source Subsystem |
| EV | Electric Vehicle |
| FOR | Forced Outage Rate |
| FR | Failure Rate |
| G2V | Grid-to-Vehicle |
| GS | Generating System |
| HGS | Hybrid Generating System |
| ICB | Incremental Cost Benefits |
| ICE | Internal Combustion Engine |
| IEAR | Interrupted Energy Assessment Rate |
| IEB | Incremental Energy Benefits |
| LP | Load Point |
| MDS | Motor-Drive System |
| MDT | Mean Down Time |
| MOT | Mean Operating Time |
| mPAI | Minimum Power Availability Index |
| MRT | Mean Restoration Time |
| MTBF | Mean Time Between Failure |
| MTS | Mechanical Transmission System |
| MTTFF | Mean Time To First Failure |
| MUP | Minimum Useful Power |
| NOC | Normal Operating Condition |
| PC | Power Controller |
| PEV | Plug-in Electric Vehicle |
| PSR | Power System Reliability |

| | |
|-------|--|
| PSS | Power Supply System |
| PVG | Photovoltaic Generation |
| PVS | Photovoltaic System |
| RAM | Reliability, Availability, and Maintainability |
| RBD | Reliability Block Diagram |
| RBTS | Roy Billinton Test System |
| RDG | Renewable Distributed Generation |
| RE | Renewable Energy |
| RES | Renewable Energy Source |
| RR | Repair Rate |
| SAIDI | System Average Interruption Duration Index |
| SAIFI | System Average Interruption Frequency Index |
| SEV | Solar Electric Vehicle |
| SOC | State of Charge |
| SOH | State of Health |
| SPP | Solar Power Plant |
| STPM | Stochastic Transitional Probability Matrix |
| TGS | Traditional Generating System |
| TPP | Tidal Power Plant |
| V2G | Vehicle-to-Grid |
| VC | Vehicle Controller |
| VIPS | Vertically Integrated Power System |
| WPP | Wind Power Plant |
| WTG | Wind Turbine-Generator |

1

Introduction

1.1 Background

The primary function of a power system is to provide electrical energy to its customers as economically as possible and with an acceptable degree of continuity and quality [10]. Modern society has come to expect that the supply of electrical energy will be uninterruptedly available on demand. However, this is not possible due to the stochastic failures of equipment and the system, which are generally outside the control of power system personnel. Electricity supply generally involves a very complex and highly integrated system. Failures in any part of it can cause interruptions, ranging from inconveniencing a small number of local residents to major and widespread catastrophic disruptions of supply. The economic impact of these

interruptions is not restricted to loss of revenue by the utility or loss of energy utilization by the customer but includes indirect costs imposed on society and the environment due to the outage. System failure probability can be reduced to a certain extent with increased investment and proper planning during the designing phase or the operating phase, or both [11]. However, overinvestment can lead to excessive operating costs, which will be reflected in the tariff structure. This has always been a critical system issue, and power system planners and operators have always strived to ensure that customers receive adequate and secure supplies within reasonable economic constraints [7].

1.1.1 Power System Reliability

The term, “Power System Reliability (PSR)” refers to the ability of the system to perform its intended function, i.e., to supply electricity to consumers at a reasonable cost with an assurance of the least possible interruption [7]. The concept of PSR covers numerous aspects of power system performance. One of those aspects is “System Adequacy”. It is important to appreciate that most of the probabilistic techniques for reliability analysis are in the domain of system adequacy, i.e., the existence of sufficient facilities within the system to satisfy consumer load demand or system operational constraints. This includes the facilities necessary to generate sufficient energy and the associated transmission and distribution facilities required to transport the energy to the actual consumer load points [12].

The adequacy of power supply mostly depends on how much operating reserve is available in the system to meet the system load during contingencies. Therefore, a fundamental problem in system planning is the correct estimation of reserve capacity [7]. Too low a value means excessive interruption; while too high a value results in excessive costs. The cost of an interruption from the customer’s point of view is related to the nature of the degree to which the activities interrupted are dependent on power supply. In turn, this dependency is a function of both customer and interruption characteristics. Customer characteristics include the type

of customer, nature of the customer's activities, size of operation, and other demographic data, demand, and energy requirements, energy dependency as a function of time of day, etc. Interruption characteristics include duration, frequency, and time of occurrence of interruptions; whether an interruption is complete or partial; if advance warning or duration information is supplied by the utility; and whether the area affected by the interruption is localized or wide-spread. The impact of an outage is partially dependent on the attitude and preparedness of customers, which in turn is related to existing reliability levels [11].

For proper planning, designing, and operation of a power system, it is crucial to conduct a comprehensive reliability assessment considering all aspects such as equipment failure characteristics, load growth, available operating reserve, future capacity expansion, transmission constraints, etc.[13]. Analysis of power system reliability helps engineers in identifying the weak links in the system; encourages replacing the failure-prone elements with more reliable options and provides the necessary information to the system operators in making decisions on load management, unit commitment, and component maintenance, etc. It also helps to establish existing indices which serve as a guide for acceptable values in future reliability assessments; enables previous predictions to be compared with actual operating experience; and gives performance measures to monitor the response to system design changes [14].

1.1.2 Hierarchical Levels for Reliability Studies

Since modern electric power systems are very large and complex, it is almost impossible to analyze the whole power system as a single entity using a completely realistic and exhaustive procedure. Power system reliability studies, therefore, have traditionally been performed in parts, i.e., the reliability performances of the major parts of the system have been evaluated separately. The functional zones of a power system, viz. generation, transmission, and distribution, are combined to form a series of hierarchical levels for reliability assessment, as shown in Fig. 1.1.

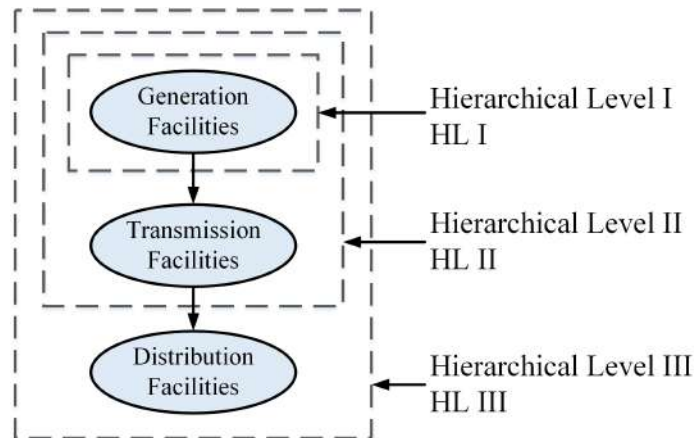


Fig. 1.1 Basic power system functional zones

Hierarchical Level I (HL-I) is concerned only with the availability of generation facilities to fulfill the total system load requirement. The transmission system and its limitations in transferring generated energy to the load points are ignored in HL-I. Hierarchical Level II (HL-II) includes both generation and transmission facilities, while HL-III consists of all three functional zones in assessing customer load point adequacy. HL-III studies are not usually conducted directly due to the enormity of the problem in a practical system. The analysis is generally performed in the distribution system functional zone in which the input points may or may not be considered as completely reliable [15].

Functional zone studies are often performed which do not cover hierarchical levels above them. These studies are usually conducted on a subset of the system to examine a particular configuration or topological change. These analyses are frequently undertaken in the sub-transmission and distribution systems as these areas are less influenced by the actual location of the generating facilities. Again, in composite system adequacy studies of relatively large-scale transmission systems, it is reasonable to limit a study area and, in doing so, provide more realistic results than by evaluating the whole system.

1.1.3 Changing Scenarios

(a) Restructuring and Deregulation

Over the years, power system has been undergone significant restructuring throughout the world [16]. Earlier, virtually all power systems either have been state-controlled and hence regulated by governments directly or indirectly through agencies, or have been in the control of private companies, which were highly regulated and, therefore, again controlled by government policies and regulations. This has created systems that have been centrally planned and operated, with energy transported from large-scale sources of generation through transmission and distribution systems to individual consumers [17].

The deregulation of the power industry has initiated the transition of centralized, monopolistic systems towards a competitive market structure [18]. The intention is to unbundle or disaggregate the various sectors and allow access to the system by an increased number of parties, not only consumers and generators but also traders of energy. The trend has, therefore, been toward the “market forces” concepts, with trading taking place at various interfacing levels throughout the system. This has led to the concept of “customers” rather than “consumers” since some customers need not consume but resell the energy as a commodity [19]. A consequence of these developments is that there is an increasing amount of energy generated at local distribution levels by independent nonutility generators and a rising number of renewable energy sources (RESs) [20].

Although this changing scenario has a very large impact on the way the system may be developed and operated and on the future reliability levels and standards, it does not obviate the need to assess the effect of system developments on customers and the fundamental bases of reliability studies. The need to assess the present performance and predict the future behavior of systems remains and probably even more important given the increasing number of players in the bilateral energy market [20].

In a conventional, vertically integrated power system (VIPS), the operating reserve allocation is centrally managed to meet the system performance standards under any outage condition [21]. In contrast, in a deregulated power system (DPS), customers can select not only the energy and transmission providers but also their reliability levels. This implies that the reliability levels at different bulk load points are different. The reliability measures are expressed in terms of operating reserve [1]. The deregulated environment enables customers to purchase the operating reserve directly from generation providers in a reserve market. The individual consumer is concerned more with its own load point reliability rather than system reliability [22]. The different reliability requirements by customers can be achieved by purchasing different capacities of reserve. Similarly, the capacity of spinning reserve in the agreements can be determined based on the reliability level required by customers [23].

(b) Renewable Energy Integration

In recent years, power industries have been directed at utilizing more and more renewable energy sources (RESs) for electricity generation in order to mitigate energy security and environmental concerns. The increasing penetration of renewable distributed generations (RDGs) has brought substantial changes in the technological development of the power distribution system, such as a shift from passive distribution network to active one and the upgrade of the automation of distribution system to self-healing control [24–26]. Distributed Generation (DG) can be used in an isolated way, supplying the consumer's local demand, or in an integrated way, supplying energy to the grid. DGs provide benefits to both consumers and utilities, especially in sites where the central generation is impracticable or where there are deficiencies in the transmission system [27]. The integration of RDGs in a distribution system increases the system's adequacy at considerably lower costs and thus enables utilities to provide a higher reliability to customers through smart utilization of reserve capacity.

However, due to the intermittent generation and uncertainties associated with RESs, integration of RDGs brings many technical and economic challenges in grid operation. The increase in the size and complexity of distribution systems integrated with RDGs, together with the need of supplying the demand economically and reliably, necessitates the assessment of the stochastic nature of network failures and generation outages, given that such events can lead to interruptions in the power supply. The main direct contribution of DG to reliability is on the customer side rather than on the utility or system side. The utility always provides the base level of reliability, and the DG's role is to boost the level of reliability by supplying the local load during interruptions [28]. The duration of interruptions at the load bus is expected to be fewer when a standby DG is connected. Integration of multiple RDGs also significantly lowers the monetary losses involved in customer interruptions in the network.

(c) Emergence of Electric Vehicle

The reliability concerns of power systems have further increased with the emergence of electric vehicles (EVs). The large-scale EV integration with a distribution network challenges the operation and control of a power grid. Electric vehicle load characteristics are different from those of conventional loads [29]. The increased volume of plug-in EVs in grid-to-vehicle (G2V) mode reduces the grid's reserve capacity and thus reduces the adequacy of power supplied to the load points. Again, uncontrolled scheduling of plug-in EV (PEV) charging distorts the load curve, causing peaks on the peaks; and pushes the system operator for load curtailment, and thus reduces the system reliability [30]. However, the integration of EV has some positive impacts on the grid also. EVs can be utilized as portable DGs. Injection of EV generation into a distribution network (vehicle-to-grid, V2G) improves the system's stability and reliability [31].

(d) RAM issues of electric vehicle

Although EVs find growing global importance because of their pollution-free and low-cost operation, the Reliability, Availability, and Maintainability (RAM) related issues still have limited large-scale commercial utilization of these vehicles. People are mainly concerned about the vehicle's reliability, safety, cost, and maintainability while purchasing a vehicle [8]. EVs are designed with a large number of electrical components and systems which are highly failure-prone. Therefore, such vehicles offer less reliability than mechanically driven internal combustion engine-based vehicle systems. To achieve higher reliability, the vehicle system must be designed with more reliable components. Among all the parts, the battery's reliability is the most sensitive to the reliability of a plug-in EV. The operation of a plug-in EV is also affected by the reliability of a charging station. For a reliable charging station, the reliability of the power supply must be high. Because of frequent load shedding, charging stations offer fewer charging hours to a discharged EV. As a result, the operational effectiveness or availability of a plug-in EV decreases considerably. Thus, PSR plays a crucial role in the operation of a plug-in EV [8].

(e) Emergence of Solar Electric Vehicle

Limited driving range and the absence of a charging station at the desired location limit the adaptability of a plug-in EV [32]. Moreover, EV takes much longer refueling (i.e., recharging) time as compared to conventional vehicles. People may not have enough time to recharge the vehicle at a public charging station. As mentioned earlier, frequent load shedding is a major issue in many countries [8]. A solar electric vehicle (SEV), which is powered entirely or considerably by direct solar energy utilizing photovoltaic (PV) technology, seems to be one of the best last-mile solutions to these problems [33]. SEVs are regarded as the future of transportation. The ability to get recharged during the running as well as the parking period is one of the most outstanding advantages of a SEV. It can be operated without grid support

and so its operation does not impacted by the reliability of the grid. SEV in V2G mode is similar to a portable renewable DG. A large volume of SEV integration to a distribution network can significantly enhance the network's reliability, particularly during the peak load period.

This thesis addresses some of the emerging areas of power system reliability studies. The research problems identified from these areas are stated in the following section.

1.2 Research Problems

After carrying out an extensive literature review (presented in Chapter-2) on the themes illustrated in Section 1.1.3, some important research problems have been identified. The aim and objectives of the present research are defined based on those problems. The identified research problems/gaps are stated as follows:

(a) Operating Reserve Allocation: The determination of the required size of operating reserve to ensure a highly reliable power supply to customers is an important aspect of power system planning and operation. In a vertically integrated power system (VIPS), a fixed amount of operating reserve is allocated to all load points, and hence, the reliability level is uniform for all customers. However, in a deregulated power system (DPS), operating reserve allocation is based on the customer's reliability demand. Customers can set their own reliability levels by purchasing operating reserves as per their requirements. Thus, operating reserve management(ORM) in a deregulated environment is a much more complex problem than VIPS. Most of the current research works were directed to address the ORM issue for VIPS only. Preparing a customer-defined reserve schedule considering reliability as a constraint is therefore taken as a subject of interest in this research.

(b) Lack of Suitable Methodology for Multiple RESs-integrated Systems: Reliability analysis of renewable energy sources (RESs) had received little attention in the past. It was due to their less contribution in power generation as compared to the conventional power

plants. Moreover, the traditional reliability evaluation techniques have many limitations in incorporating the intermittent output characteristics of RESs. Most of the available literature have used either deterministic or probabilistic approach. A few research works have applied the well-being approach, which bridges the gap between the deterministic and probabilistic approaches.[34] Although the well-being approach has many advantages, it fails to analyze the reliability of systems having derated states. Thus this method cannot correctly estimate the reliability of power systems integrated with multiple RESs. Markov framework [35] can solve this problem; however, this method is purely probabilistic and cannot handle the deterministic criteria of system operation. To develop an approach that can solve all the issues described above can be an important research problem. This thesis is directed at solving this problem.

(c) Limited Studies on Reliability Worth: Reliability worth assessment is an important task for power system planning and operation. Reliability worth is usually quantified in the form of customer interruption costs which provides an indirect measure of the monetary losses connected with power interruptions and serves as input for cost implications and operational decisions. Very few research works have reported the reliability cost-benefit aspects of RESs-integrated systems. To determine how much energy and monetary benefits can be attained from using RESs, is taken as a research problem in this thesis.

(d) Very few Researches on Electric Vehicles' Reliability: The impact of electric vehicle (EV) charging on power distribution networks is a fascinated research topic these days. However, reliability-centric studies are still minimal. Again, how the reliability of a power distribution network impacts the operation of a plug-in EV is still an unexplored subject of research. Reliability, availability, and maintainability studies on an EV system carry great significance for customers and manufacturers. However, no proper mathematical modelings and formulation are available in the state of the art literature in this regard so far. This thesis attempts to accomplish these research gaps.

(e) Reliability Modeling of Solar Electric Vehicle: Solar electric vehicle (SEV) is an emerging transport utility which primarily uses solar energy for its propulsion. It is regarded as an ideal solution for clean and sustainable transportation. SEV's effectiveness mainly depends on the reliability of its onboard photovoltaic system (PVS). The power generated by PVS is intermittent in nature and affected by various factors like solar irradiation, vehicle's geographic location, ambient temperature, weather condition, dust deposition, wind speed, etc. Designing a PVS on the roof of the vehicle to produce reliable electrical power for charging the battery at a standard rate is a major challenge for SEV manufacturers. There are few research works that focus on the reliability issues of SEV, and no proper methodology is available to investigate the effectiveness of a SEV at a particular geographic location. As such, this thesis efforts to carry out a comprehensive study on it.

A detailed review of literature on various topics relevant to the theme is covered in the next chapter. The following flowchart gives an idea about the area of problems that have been identified for the present study.

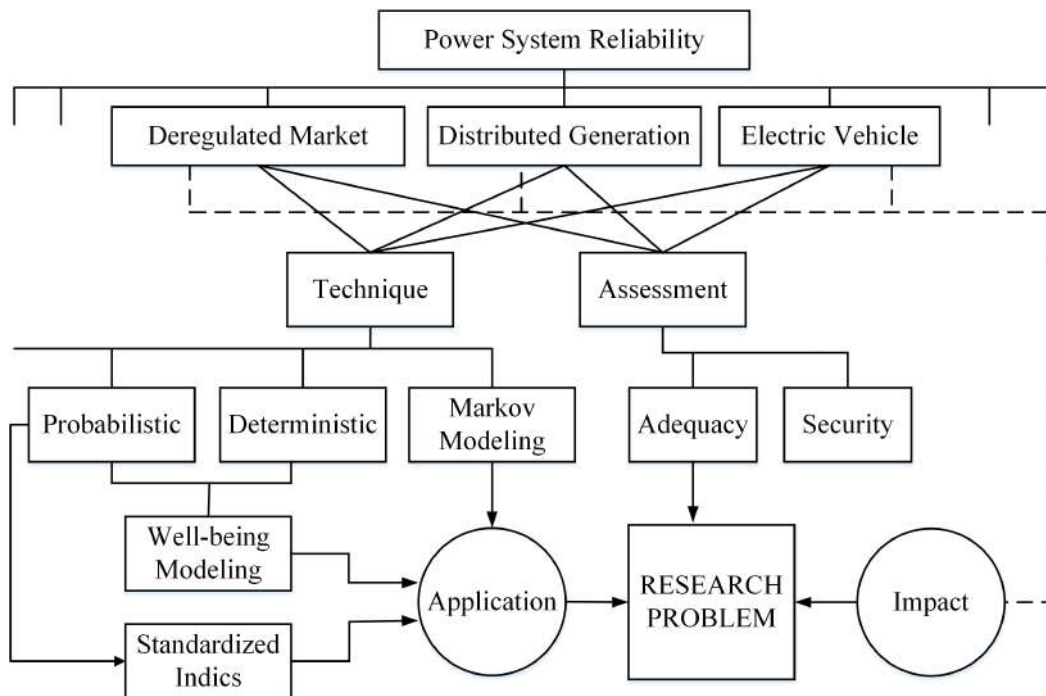


Fig. 1.2 Problem Identification Flowchart

1.3 Aim

The aim of the present research is to conduct a comprehensive reliability analysis of modern power systems with special emphasis on renewable distributed generation and electric vehicle.

1.4 Research Objectives

The main objectives of the present research are as follows:

1. To conduct a reliability-centered operating reserve assessment in a deregulated power system.
2. To develop an approach to carry out a comprehensive reliability worth assessment of a power distribution network integrated with multiple renewable energy sources.
3. To investigate the impact of electric vehicle integration on the reliability of a distribution network.
4. To carry out a reliability, availability and maintainability (RAM) analysis of a plug-in electric vehicle.
5. To construct a reliability model of a solar electric vehicle for carrying out a comprehensive reliability and availability analysis of the vehicle.

1.5 Outline of the Thesis

Based on the research objectives, the research works reported in this thesis can be categorized into five parts: (a) Reliability-centered operating reserve management in deregulated power system (b) Reliability analysis of a renewable energy incorporated distribution network, (c) Reliability analysis of electric vehicle integrated distribution network, (d) RAM assessment of plug-in EV and (d) Reliability modeling and availability analysis of solar EV. The thesis is comprised of total nine chapters, which are organized as follows:

- Chapter 1 presents an overview of the research work. Section 1.1 introduces the major areas of research. The research gaps are reported in Section 1.2. From the research gaps, the aims and objectives of the research have been deduced and presented in Sections 1.3 and 1.4, respectively. After that, the outline of the thesis is presented in Section 1.5.
- Chapter 2 presents an extensive review of literature relevant to the present study. The fundamentals of power system reliability (PSR) are discussed at the beginning of the chapter. The details of available methods for PSR studies are also included. After that, the chapter presents some emerging areas of power systems and identifies the research scopes in those areas, carrying out an extensive literature survey. The main objective of this chapter is to present the theoretical parts and identify the research problems for the study.
- Chapter 3 presents the methods and materials used in the present research work. Basic terms, definitions, and mathematical expressions of various parameters are explained in Sections 3.2 and 3.3. The concepts of Markov modeling and well-being framework have been extensively used in this research. These two methods are discussed in depth in sections 3.4 and 3.5, respectively. Section 3.6 discusses the reliability indices and techniques used in distribution systems. This chapter also describes the various test systems used in the present research.
- Chapter 4 presents an approach to carry out a reliability assessment of a deregulated power system. An effort has been made to illustrate how capacity reserve management in a deregulated environment is done based on customer's reliability satisfaction. The well-being framework has been applied to develop the reliability model of a bilateral power market. A new index, CRAI, has been introduced to measure the percentage

reserve margin and risk in the system. The proposed concepts have been exemplified in Roy Billinton Test System (RBTS).

- Chapter 5 presents a comprehensive reliability assessment of a power distribution network integrated with renewable energy sources (RESs). Solar, wind, and tidal energy sources are considered for the study. For each RES, the mathematical model has been formulated incorporating all critical input variables. A multi-state reliability model has been developed to determine the reliability of the hybrid generation system. Two popular reliability frameworks, namely the Markov and well-being frameworks, have been merged together to evaluate the reliability of the integrated system. This is a new concept presented in this chapter. The load point reliability and worth-oriented indices are assessed to analyze the impacts of the three RESs on the distribution system's reliability. In addition to that, two new performance metrics have been proposed to estimate the benefits of adding RESs from the reliability worth and cost perspectives. The analyses have been carried out on RBTS. The results show that the maximum reliability worth and cost benefits can be extracted from a combined operation of multiple RESs. Therefore, a combination of solar-wind-tidal energy sources can be an effective solution for countries with long coastlines to fulfill sustainable energy goals and improve the grid's reliability and reduce the monetary losses incurred due to customer interruptions.
- Chapter 6 presents a reliability assessment of a distribution system integrated with electric vehicles (EVs). It examines how the reliability of a distribution network is affected due to the increased EV charging from the grid. The vehicle's charging and load models are developed for this purpose. The distribution network associated with the Bus-2 of the IEEE- RBTS is considered as the test system. Distribution system reliability indices, namely SAIFI, SAIDI, CAIDI, ASAI, and ENS, are evaluated to

- investigate the impact on system reliability due to the controlled and uncontrolled charging of plug-in EVs.
- Chapter 7 presents an approach to carry out a quantitative RAM analysis of a plug-in electric vehicle. A mathematical model is developed in the Markov Framework incorporating the reliability characteristics of all significant electrical components of the vehicle system, namely battery, motor, drive, controllers, charging unit, and energy management unit. The chapter also investigates the role of a charging station on the availability of the vehicle. It illustrates how the grid power supply's reliability influences the operational effectiveness of a plug-in electric vehicle.
 - Chapter 8 presents an approach to investigate the reliability and availability of a solar electric vehicle (SEV) facilitated with a standby plug-in option. It introduces a composite reliability model, which is developed in Markov framework incorporating the stochastic failure and repair characteristics of all critical electrical systems of the vehicle. A new probabilistic index, *mPAI* is proposed to determine the availability of power generated by the photovoltaic modules mounted on the SEV. The reliability improvement due to the standby plug-in facility is also examined. Reliability-centric sensitivity analyses have been carried out to investigate the impacts of key parameters on the performance of a SEV. The study presented in the chapter quantitatively justifies that a SEV with a plug-in facility is much more reliable and effective than a regular plug-in EV or SEV.
 - Chapter 9 presents the summary and conclusion of the overall study. Some important future works of the present research have also been put forwarded in this chapter.
 - In addition to the above chapters, there are two appendices provided. Appendix A presents the input data which are used in case studies throughout the thesis. A list of publications on the present research has been included in Appendix B.

2

Review of Literature

2.1 Introduction

Reliability is an inherent characteristic and a specific measure that defines the capacity of any system to perform its assigned function [10]. For a power system, the “assigned function” refers to supplying electrical power to its end customers at a reasonable cost with a high degree of reliability and quality [15]. In the days of global, fully integrated, and nationalized electricity supply industries, the only significant measure was the reliability seen by actual end-users. Also, the system was restructured in a relatively simplistic way such that generation, transmission, and distribution could be evaluated as a series of sequential hierarchical levels [7]. Failures at any level could cause an outage in power supply to the end-user. All planning and operational standards (both deterministic and probabilistic) were designed to minimize such outages within economic constraints. Later, the system has been or is being restructured quite remarkably, and now many private utilities are involved,

often competitively, including generators (both large-scale remote generators and small-scale, renewable distributed generators), network owners and operators, energy distributors, regulators, as well as the consumers. Each of these parties needs to know the quality and performance of the system sector or subsector for which they are responsible [36]. This necessitates a wide range of reliability measures. This chapter reviews existing approaches and how these may be used or adapted to suit the needs and the required indices of the new competitive industry and the different emerging aspects associated with it.

2.2 Requirements for Power System Reliability Assessment

In order to review the functionality of a power system and the way it reacts with reliability, the concept of hierarchical levels has been introduced (Section 1.1.2). The first level (HL-I) relates to generation facilities, the second level (HL-II) refers to the integration of generation and transmission, and the third level (HL-III) refers to the complete system, including distribution [15]. However, distribution system reliability (DSR) is often analyzed separately due to the complexities of entire system studies. This traditional categorization needs to be reassessed due to two effects. First, distribution systems are now directly connected to distributed generating systems, and hence the impact of transmission utilities gets omitted. Second, power can be purchased directly from the wholesale power market through bilateral transactions. This eliminates the effects of generation system failures in DSR studies. However, basic principles in PSR studies are still valuable in these changing scenarios.

2.2.1 Generation System (HL-I) Studies

In a generation system study, the total system generation is examined to determine its adequacy to meet the total system load requirement. This activity is usually termed “generating

capacity reliability evaluation". The basic modeling approach for the HL-I study is shown in Fig. 2.1.

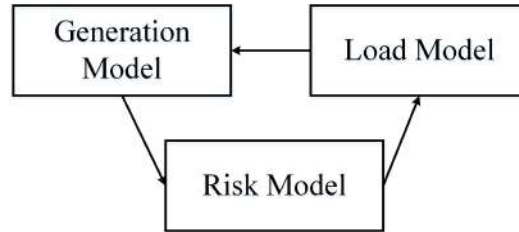


Fig. 2.1 Conceptual tasks for HL-I evaluation

The transmission system and its ability to move the generated energy to customer load points are ignored in generating system adequacy assessment. The basic concern is to estimate the generating capacity required to satisfy the system demand and to have sufficient capacity to perform corrective and preventive maintenance on the generating facilities. The basic indices in generating system adequacy assessment are: Loss of Load Expectation (LOLE), Loss of Energy Expectation (LOEE), Loss of Load Frequency (LOLF), and Loss of Load Duration (LOLD).[37]

2.2.2 Composite System (HL-II) Studies

Composite system studies intend to assess the adequacy of an existing or proposed system, including the impact of various reinforcement options at both the generation and transmission levels. These effects are examined by evaluating two sets of indices: load point indices and overall system indices. The system indices give an estimation of overall adequacy. The load point indices show the effect at individual busbars and provide input values to subsequent distribution system adequacy evaluation. Both system and load point indices can be classified as annualized and annual indices. Annualized indices are evaluated using a single load level (usually the system peak load level) and expressed yearly. Annual indices are determined considering complete load fluctuations throughout one year. Usually, annualized indices give a satisfactory indication when examining the adequacies of various

reinforcement alternatives. Annual indices give a more practical and complete understanding of system adequacy. Probability of Load Curtailment (PLC), Expected Frequency of Load Curtailment (EFLC), Expected Duration of Load Curtailment (EDLC), Average Duration of Load Curtailment (ADLC), Expected Load Curtailment (ELC), Expected Demand Not Supplied (EDNS), Expected Energy Not Supplied (EENS), Bulk Power Interruption Index (BPPI), Bulk Power/Energy Curtailment Index (BPECI), etc. are some of the most frequently used metrics in composite system adequacy studies.

2.2.3 Distribution System Studies

Distribution system studies involve the assessment of suitable adequacy indices at the actual consumer load points. There are two basic types of distribution systems: meshed and radial arrangements. Assessment techniques for meshed distribution networks are conceptually the same as those used for composite systems. The techniques for a radial configuration are based on failure-mode analysis, including considerations of all practical failure and restoration processes. These techniques can also be applied for assessing substation adequacy since a substation has similar configurations and failure modes.

There are three primary load point indices for distribution system reliability assessment (DSRA). These are: load point failure rate λ , load point outage duration r , and load point unavailability U . With the help of three primary indices, a number of performance metrics for the overall distribution system are defined. Amongst them, the most commonly used metrics are: System Average Interruption Frequency Index (SAIFI), System Average frequency Duration Index (SAIDI), Customer Average Interruption Frequency Index (CAIFI), Customer Average Interruption Duration Index (CAIDI), Average Service Availability Index (ASAI), Average Service Unavailability Index (ASUI), Energy Not Supplied (ENS), Average Energy Not Supplied (AENS), and Average Customer Curtailment Index (ACCI). A detailed description of these indices is presented in Section 3.6.1 of Chapter-3.

2.3 Reliability Cost/Worth

The economics of alternate facilities play a significant role in the decision-making process. In order to provide meaningful input to electric power utility decision-making, customer interruption costs (CIC) must be linked to quantitative indices which respond to system capital and operating investment [38]. The increase in reliability due to the various alternatives should be assessed together with the investment cost associated with each scheme. Dividing this cost by the increase in reliability gives the incremental cost of reliability, i.e., how much it will cost for a per-unit increase in reliability. This approach is practical when comparing alternatives, given that the reliability of a section of the power system is inadequate. In this case, the lowest incremental cost of reliability is the most cost-effective. This is still a significant step forward from comparing alternatives and making major capital investment decisions using deterministic techniques [38].

Establishing the worth of service reliability is a difficult and subjective task, as direct evaluation appears to be infeasible at this time. A practical alternative, which is being widely utilized, is to evaluate the impacts and the monetary losses incurred by customers due to electric power supply failures. CICs provide a valuable surrogate for the actual worth of electric power supply reliability.

Figure 2.2 shows that utility costs will generally increase as consumers are provided with higher reliability. On the other hand, consumer costs associated with supply interruptions will decrease as the reliability increases. The total costs to society are the sum of these two individual costs. This total cost exhibits a minimum point at which an “optimum” or target level of reliability is achieved.

Several studies have been reported on the subject of interruption and outage costs. Billinton gave a brief outline in [37] to evaluate customer worth assessments. The procedure of calculating CIC and Value of Lost Load (VoLL) is also presented in the literature. The interrupted Energy Assessment Rate (IEAR) is one of the factors that can be used to evaluate

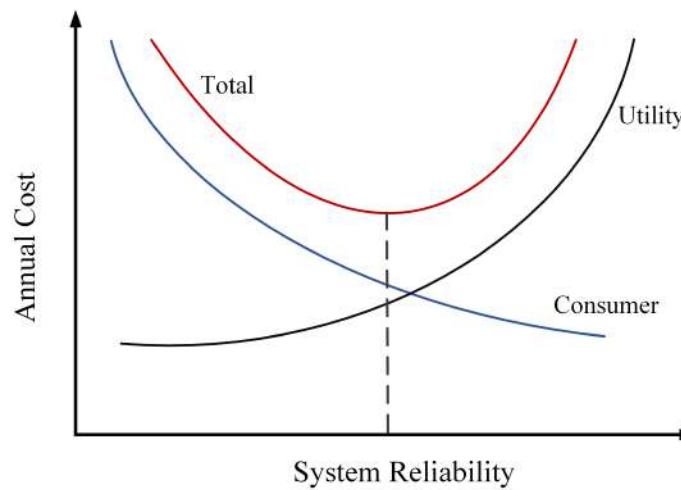


Fig. 2.2 Consumer, utility, and total cost a function of system reliability

the worth of system reliability. Oteng-Adjei [39] described how the basic concepts associated with IEAR estimation could be used for the worth analysis of composite systems.

Ghajar and Billinton [40] proposed a method for calculating the marginal interruption costs (MIC) at bulk customer load points in a composite generation and transmission system. The exact method of calculating the MIC in HL-II is very time-consuming and may not be suitable for applications in the operating environment. It is observed that the removal of a large generating unit for maintenance has a noticeable effect on the MIC, while the effect of removing transmission lines for maintenance in large systems is very small.

Monte-Carlo simulation method is used by Sankarakrishnan and Billinton [41] for reliability worth assessment in the composite power system network. They proposed a methodology for evaluating the CIC with time-varying loads at the load buses.

Several other authors [42–48] have broadly covered various aspects of reliability cost/worth assessment of composite power systems.

2.4 Power System Reliability Evaluation Techniques

PSR indices can be evaluated using a variety of methods. The two main approaches are analytical and simulation. Most methods have been analytically based. Simulation methods have taken a minor role in specific applications. It is because simulation techniques generally necessitate a large amount of computational time. Moreover, analytical models and procedures have been adequate to provide planners and designers with the results needed to make objective decisions. This is now changing, and increasing interest is being shown in modeling the system behavior more comprehensively and evaluating a more informative set of system reliability indices [7].

Analytical approaches represent the system by a mathematical model and assess the reliability indices applying straightforward mathematical solutions. They usually provide expectation indices in a relatively short computational period. Unfortunately, assumptions are frequently required to interpret the problem and create mathematical modeling of the system. This is especially the case if complicated procedures and complex systems have to be modeled. The resulting assessment can therefore lose some or much of its significance. Simulation techniques are to be used for reliability assessment in such situations [15].

The simulation techniques estimate the reliability indices by simulating the actual process and stochastic behavior of the system. These techniques, therefore, treat the problem as a series of real experiments. These techniques theoretically consider virtually all aspects and contingencies inherent in power system planning, design, and operation. These include stochastic events such as interruptions and restoration of elements that can be expressed by general probability distributions, dependent events, and system behavior, queuing of failed components, load variations, variation of energy input such as that occurring in hydrogeneration, and all different types of operating policies [7].

Billinton and Bhavaraju [49] conducted pioneering work on the reliability evaluation of a composite power system. Billinton illustrates the application of a conditional probability

approach to determine a reliability index at any point in a composite system [50]. A general design criterion is postulated in terms of quality of service rather than continuity. Billinton and Bhavaraju proposed a composite system reliability evaluation approach, which includes a complete system representation of the form used in AC and DC load flow analysis. This technique also utilizes the quality of service criterion rather than continuity. An important aspect of this method is the calculation of reliability levels at each load busbar. Line and transformer overloads due to simultaneous independent outage conditions are included in the analysis by removing the overloaded component from the network. A computer algorithm was developed for the analysis.

Billinton and Medichera [51] developed a method at the University of Saskatchewan, Canada, for evaluating the reliability of composite generation and transmission systems. A set of busbar and system indices is defined based upon the load curtailment required to alleviate transmission line overloads. A brief description of the common-cause outage models is also included. The effectiveness of the techniques for assessing the busbar and system reliability indices of a practical system configuration is also illustrated. A digital computer program based on the technique is described, which calculates the reliability indices by examining all possible first and second-order overlapping independent outage conditions and common cause outages. An extension of the above technique to include common-cause and common-mode outages is presented by Billinton, *et al.* in [52]. The effect of station-originated interruptions in HL-II is illustrated by the same author in [53] and Allan and Ocha in [54].

A practical power system tends to be quite large. Therefore, a thorough examination of all credible outages involving system components is not practical due to the considerable computation time required to solve the network under these outage situations. Attempts have been made to calculate the adequacy indices of large power systems using approximate techniques that either simplify assumptions or utilize approximate solution techniques.

Kumar and Billinton [55, 56] proposed a method for the adequacy assessment of a small area in a large power network. This method is simple and can be used with the existing computer program to determine the adequacy performance of a power network. However, the efficiency of the method depends upon the number of the small area as compared to the size of the entire power network. In the mentioned paper, the authors have made a qualitative treatment to compare with other methods. Billington and Zhang [57] also proposed similar techniques. Another way is suggested by Oliveira et al. [58] to reduce the computational effort in Monte- Carlo-based composite reliability evaluation. The technique uses analytical information from “simpler” models as “regression variables” to minimize the variance of the estimate of reliability indices, such as LOLP, EPNS, in the “complete” model.

A hybrid approach is proposed by Billinton and Wenyuan in [59] that considers Monte-Carlo simulation and enumeration technique for reliability evaluation of large composite power systems. Ubeda and Allan, Sankarakrishnan and Billinton [60] and Jonnavithula [61] use a sequential simulation approach for HL-II reliability evaluation. The technique shows how the nature of sequential simulation can significantly reduce the computational effort that the simulation of composite systems initially involves.

All of the available techniques for quantitative reliability evaluation of power systems are in adequacy domain. Many utilities have difficulties interpreting the expected load-curtailement indices since the existing indices are based on adequacy assessment and, in many cases, do not consider realistic operating conditions in the system under study. Most of the reliability evaluation techniques proposed by various authors are primarily concerned with solution techniques’ computation speed and efficiency.

Quantitative reliability assessment methods are developed based on some specific approaches. The most popular approaches are explained in the following subsections.

2.4.1 Deterministic Approach

In the past, assessments of PSR were mainly done using deterministic approaches. Here, the system performance is assessed for various scenarios, interpreting both severe and plausible operating conditions. Available reserve margin, peak load, failures in largest generating units, faults in a single line, faults in multiple lines, etc., are some standard criteria based on which deterministic approaches are usually designed. The system planner or operator selects the most suitable and economical option among these deterministic criteria to define the system's reliability [15].

The deterministic approaches have several attractive features. These techniques are straightforward to implement and easier to understand. The engineering judgment about critical and credible operating conditions is usually consistent. However, the inability to incorporate the stochastic nature of system failure in risk assessment is the main limitation of deterministic approaches [10].

2.4.2 Probabilistic Approach

Most of the reliability indices are based on probabilistic criteria. It is because system failures are mostly stochastic in nature. Probabilistic techniques in various applications have reached very different stages of maturity, with the composite power system evaluation methods somewhat lagging behind. However, there are some major difficulties in applying the probabilistic approach [15]. These are:

- Unavailability of statistical data on system failures
- Complexity in system modeling for probabilistic assessment
- Heavy computational burden

Despite these difficulties, probabilistic approaches become an integral part of the decision-making process in power system planning and operation. With the recent trend toward dereg-

ulation and renewable energy integration, probabilistic approaches get further widespread acceptance for reliability studies.

2.4.3 Well-being Approach

As mentioned earlier, system designers and planners are sometimes reluctant to apply probabilistic techniques for power system reliability evaluation because of the difficulties in interpreting and accepting a single numerical risk index. Moreover, there is a lack of system operating information and appropriate data on generating units or transmission lines performance in addition to the actual load demand. The dilemma between the probabilistic and deterministic approaches can be alleviated by embedding deterministic considerations into the probabilistic framework using a model known as the “well-being model”, which bridges the gap between these two approaches.

In well-being approach, the composite system is classified into three system well-being indices, namely, health, marginal, and at risk, which is closely associated with the system operating states. Considering this well-being framework, Goel and Feng evaluated the reliability of composite generation and transmission systems [12]. The approach was used for generating system’s reliability assessment by Abdulwhab and Billinton in [62]. The same approach was implemented to assess the reliability of spinning reserve by Goel *et al.* in [1].

Because of its ability to accept both deterministic and probabilistic criteria, the well-being approach has been used to determine the reliability of deregulated power system in chapter 4 and renewable energy incorporated distribution system in Chapter 5. Detailed discussion on the well-being approach is presented in Chapter 3.

2.4.4 Markov Model Approach

Markov modeling is a popular approach for reliability assessment. It can incorporate the derated states of a system. Moreover, this approach can incorporate the stochastic behaviors

of both failure and repair processes. Other analytical techniques do not have this property. Therefore, many researchers have regarded this framework as a useful tool for the reliability modeling of engineering systems. The theory of the Markov approach has been well-explained by R. Billinton, and R. Allan in [63]. Z. Esau *et al.*, M. Al-Muhaini *et al.* and T. Adefarati *et al.* implemented this framework for reliability assessment of renewable energy incorporated electrical systems in [64–66].

This thesis extensively uses the Markov modeling concepts. The detailed procedure of this method has been illustrated in Section 3.4 of the next chapter.

2.5 Some Emerging Areas for Reliability Study

As mentioned earlier, electrical power system is in a significant phase of shifting toward a restructured, deregulated, and inverter-dominated grid system. The growing thrust over renewable distributed generation and the arrival of electric vehicles have also brought many notable changes in power system operation and design. Following are some of the emerging areas having great potential for power system reliability research.

2.5.1 Reserve Management under Deregulated Scenario

The latest liberalization trend in electric power systems all over the world has raised a wide range of planning and operational issues into perspective, significant being the reliability aspects [67]. The hierarchical control and management structure of vertically integrated power systems (VIPS) have given way to a decentralized environment, resulting in the structural changes that necessarily warrant the remodeling of existing reliability analysis formulations [19]. Though the reliability evaluation techniques suitable for traditional power systems are well entrenched, recent developments in this area have seen improvisations with far-reaching implications in the horizontally operated power systems as well [23].

Quantification of the stochasticity inherent in power systems from a reliability point of view (adequacy assessment), primarily by way of a wide variety of indices, has been the main research focus in VIPS over the past few decades. In the deregulated environment, there is an economic division of entities into individual generation, transmission, and distribution companies, operated under different types of market design – pool market structure, bilateral market structure, or a hybrid market structure [17]. Each structure involves a unique reliability modeling framework. More prone to uncertainties than ever before, the complexities arising from decentralized electricity markets dictate a comprehensive, probabilistic power systems analysis. The concept of reliability network equivalents has been proposed by Roy Billinton, which were later used in tandem with power flow tracing procedures to propose a compact framework for deregulated power system (DPS) reliability frameworks.

In VIPS, “system reliability” is a major concern of the system operators. The operators must provide the necessary ancillary critical services to customers. Operating reserve (OR) is one of the critical ancillary services to maintain system reliability in case of contingency [16]. It refers to the surplus generation capacity available to the system operators for meeting the demand in case a generator goes down or there is any disruption in the power supply. Most power systems maintain the reserve above the capacity of the largest generators plus a fraction of peak load [68].

In VIPS, the allocation and size of the reserve are centrally managed and used following a contingency to meet the disturbance condition requirements. However, in DPS, customers can purchase the operating reserve directly from the generation providers in a wholesale power market [22]. Customers can select not only the power and transmission providers but also their reliability levels [18]. The reliability levels are different at different bulk load points (BLP). The different reliability level requirements by customers can be achieved by purchasing different amounts of the reserve. Similarly, the cost of the reserve can be determined based on the reliability level specified by customers.

In 1997, Billinton R. presented the concept of a new electric power utility industry with consideration of system reliability [67]. Singh C. demonstrated the role of reliability, risk, and probabilistic analysis in the competitive environment in 1999 [69]. Shahidehpour M *et al.* illustrated the operation, trading, and volatility issues in a restructured power system [70]. Rahmi A.F. *et al.* discussed effective market monitoring in the deregulated electricity market [19]. Again, Zhu J. *et al.* proposed a new spinning reserve market structure to utilize the available resources best to meet load with the transmission constraints [71]. Allen EH *et al.* explain how reserve markets are managed for maintaining power system reliability [72]. Mehmet T described the deployment of reserve requirements into the power systems considering the cost, loss, and reliability parameters based on sustainable energy [73]. They also investigated the impact of Demand Side Management (DSM) on operating reserve requirements [74]. Helseth A *et al.* examined the benefits of capacity reserve exchanges within the hydro-dominated nordic market [75]. Reddy SS *et al.* proposed an optimal dynamic reserve activation strategy using spinning, hydro, and demand-side reserves [76]. Many other researchers have carried out similar researches; however, reliability-constrained operating reserve management (ORM) under a deregulated environment has received the least focus in those studies.

Chapter 4 of this thesis aims at conducting a reliability-centered ORM study in a DPS. A new performance index has been introduced to measure the percentage of operating reserve required to maintain the system's health above the desired reliability level. The well-being framework [77] has been implemented to develop a reliability model of DPS. The concepts are exemplified in the Roy Billinton Test System (RBTS) [78].

2.5.2 Impacts of Distributed Generation

The importance of distributed generation (DG) is increasing day by day with increased liberalization of the economy and deregulation of energy sectors. There have been considerable

research works on DG for the last several decades with a lot of reforms. The increased penetration of DG has many impacts on distribution systems. It supports the system voltage and improves the power quality. It helps to reduce the power losses, decrease the burden of transmission and distribution. It supports the installation of new transmission and distribution lines and improves the reliability of the system. But it is not easy to obtain these benefits. Moreover, there are certain issues like voltage flicker, harmonics, increased impact of short circuit level, etc., to be addressed so that DG does not lead to degrading the system.

Generally, the distribution networks are passive in nature. However, the connection of DG converts the distribution network into an active one. The power flow and voltage of the DG-connected distribution network are regulated by the generation and loads. The distribution system with DG develops different power quality issues like flicker, transient voltage variations, harmonics, etc.

2.5.3 Reliability of Renewable Energy Incorporated Network

Modern distribution networks (DN) are mostly active networks that not only transmit power but also generate power at strategic locations using small, scattered, and preferably renewable power generating units [79]. Micro and nano grids are primarily designed for supplying smartly and locally controllable power to a DN [80]. They have additional objectives of utilizing clean and sustainable energy resources to alleviate socio-economic, environmental, and energy security issues associated with conventional power plants [81]. The biggest advantage of integrating renewable DG in a DN is that it increases the adequacy of the system at considerably lower costs and thus enables utilities to provide a higher reliability to customers through smart utilization of reserve capacity.

Among all, solar and wind have been the most prioritized renewable energy sources (RESs) worldwide over the last few years. Presently, wind energy contributes the highest share to the growth of renewable electricity generation (160TWh), followed closely by

solar (140TWh) [82]. In 2018, India placed the concept of "One Sun, One World, One Grid" (OSOWOG) in the assembly of the International Solar Alliance (ISA), [83] which outlines that the modern grid system is going to be a trans-national electricity grid, driven by RESs, and solar will be the prime contributor. However, to achieve a 100% renewable grid, integration of extremely high volumes of variable RESs will be required, and for that, other renewable resources also must be judiciously utilized. The intermittent characteristics and uncertainties associated with renewable DGs bring technical and economic challenges in grid operation [84, 85]. A hybrid renewable power generation strategy can neutralize these challenges in many ways. For countries with large coastal regions, tidal energy is a potential resource for power generation. Therefore, a coordinated operation of solar, wind, and tidal power plants can be an effective way to meet their sustainable energy goals. It will not only enhance the grid's reliability but also significantly lower the monetary losses involved in customer interruptions in the network.

Significant numbers of research works have been published in recent times addressing the issues and benefits of renewable microgrids [86–89]. Eluri *et al.* presented a comprehensive analysis of active distribution network (ADN) incorporating RESs highlighting the fundamental concepts of microgrid, challenges during grid integration, and different techniques for its optimized operation [90]. Escalera *et al.* presented a critical review on the reliability techniques for DS considering the effects of increased dispersed generation and control, protection, and communication schemes [91]. Man-Im *et al.* proposed an optimal and cost-effective dispatch strategy for the operation of hybrid RESs with storage facilities. Solar, wind, and storage system were the basic elements of interest constituting the hybrid system [92]. Esau *et al.* examined the reliability of an ADN incorporating the stochastic effects of solar generation. They stated that the reliability of an ADN might be affected by the high solar penetration at stressed operating conditions [79]. Wang *et al.* analyzed how the reliability of an on-grid solar plant is affected under cloudy, overcast, and rainy weather

conditions in the four seasons of a year [4]. Kalkhambkar *et al.* proposed methodologies for optimal allocation of RESs for economic benefits [84, 93]. Chuong *et al.* demonstrated a multi-stage reliability model for a DN integrating wind energy sources [94]. Lin *et al.* carried out an extensive review for reliability-centric planning and operation of DS with wind energy integration [95]. Similar types of research works have been conducted by several other researchers discussing the reliability of DS integrated with RES(s). However, observation on the existing literature reveals that most of the reliability studies have considered solar and/or wind and the least focus has been given on examining the benefits from grid integration of other RESs like tidal energy, biomass, etc. Murali *et al.* reported the feasibility and potential of tidal power plants in India in their research work [96]. Nazir also reported that a hybrid solar-hydro coastal power plant is technically feasible as well as commercially viable in supplying electricity in coastal areas [97]. Again, Chowdhury *et al.* discussed the ongoing trends, ecological impacts, and technological prospects of tidal energy penetration [98]. However, the reliability aspects were missing in the aforesaid studies.

As mentioned earlier, reliability worth assessment is an important task for planning and operation of a system. Reliability worth is usually quantified in the form of customer interruption costs (CIC) [6]. CIC provides an indirect measure of the monetary losses connected with power interruptions and serves as input for cost implications and making operational decisions [99]. Very few research works have reported the reliability cost-benefit aspects of RESs-integrated distribution network. Chapter 5 of this thesis includes the reliability-worth aspects of a RESs-incorporated distribution system. How much energy and monetary benefits can be attained from integrating solar, wind, and tidal energy sources are assessed with the help of two new metrics.

Probabilistic and deterministic approaches have traditionally been exercised for distribution system reliability assessment (DSRA) [100, 101]. However, the probabilistic approach needs large computations and has challenges in interpretation and acceptance of a single

quantitative risk index [102]. In contrast, deterministic approaches are straightforward to implement but cannot account for stochastic characteristics of system behavior and are not responsive to many of the parameters such as load and risk nature [10]. These limitations can be alleviated by using the well-being approach, which bridges the gap between the probabilistic and deterministic approaches. The well-being approach has found many applications in reliability studies [34, 103–105]. However, this approach cannot alone incorporate the intermittent or derated states of RESs. Derated states can be modeled in ‘Markov framework’ only. Another outstanding advantage of the Markov approach is that it can incorporate both the failure and repair processes of a system [35]. Other reliability assessment methods ignore the repair process and consider only the system’s stochastic failure characteristics. Markov approach has gained considerable weightage in many research works [79, 106, 2]. In Chapter 5, the Markov framework has been merged with the well-being framework. It is a novel concept proposed in Chapter 5. The availability models of RESs are developed in Markov framework, and the system’s deterministic operational criteria are linked with the probabilistic indices using the well-being framework. The proposed approach is expected to be helpful in reliability modeling and analysis of a generating system comprising of multiple RESs.

2.5.4 Grid Integration with Electric Vehicles

Electric vehicle has been a centre of discussion in automobile sector in recent times. EVs have been rapidly developed nowadays due to mainly their zero carbon emission property, environmental protection, and low operating cost [107, 108]. However, if a large number of EVs are integrated with the grid in uncontrolled mode, the operation and planning of the power system will be affected by the non-negligible [109]. These effects mainly include the increase of load, the difficulty of optimization of power grid operation control, increased distortion affecting power quality and reliability, putting forward new requirements for

distribution network planning [110]. Therefore, it has practical importance to analyze the impact of large-scale EV grid integration on distribution network reliability. Zhou Jiaqi studied the influence of EVs connected to the grid on the grid's reliability under time-sharing electricity price, indicating that the grid's reliability under controlled charging mode is higher than that of the uncontrolled method. A coordinated charging strategy can reduce distribution system losses and improve voltage profiles [111]. Charging algorithms can be developed by coordinating EVs considering feeder losses, load factor, and load variance [112]. The real-time charging coordination strategy of PEVs has been proposed in [113] to minimize power losses and improve voltage profile by considering priority-based charging schemes. The impacts of V2G strategies are discussed in [31, 114–117]. The achievable power capacity (APC) in the V2G mode of operation of PEVs is addressed in [114]. The optimal charging control strategies for V2G frequency control services are presented in [115]. V2G mode of operation can generate revenue for the vehicle owners and fleet operators. The different concept of EV's V2G mode of operation is discussed in [116].

The impact on the reliability of a distribution network due to EV charging can be studied for various purposes and in many ways. In this thesis, the system's reliability has been investigated by evaluating some standard reliability indices, such as SAIFI, SAIDI, EENS, ASAI, etc.

2.5.5 RAM Studies for Electric Vehicles

Reliability, availability, and maintainability (RAM) are the main issues that people are mostly concerned about while purchasing a vehicle. As mentioned earlier, PEVs are designed with a large number of electrical components and systems (e.g., battery, motor-drive, controllers, energy management systems, etc.). These systems are highly failure-prone. Therefore, such vehicles offer less reliability than mechanically driven ICE-based vehicle systems. To achieve a higher reliability, the vehicle system must be designed with reliable components. Among all

the parts, the battery's reliability is the most sensitive to the reliability of a PEV. The vehicle's protective schemes must also fulfill the minimum reliability criteria to ensure safety to the personnel. Although a highly reliable vehicle system demands a higher price, it reduces the frequency of maintenance and lowers the servicing cost.

The operation of a PEV is also affected by the reliability of a charging station. For a reliable charging station, the reliability of the power supply is a dominant factor. In many countries, load shedding is a major issue. Because of frequent load shedding, charging stations offer fewer charging hours to a discharged PEV. As a result, the operational effectiveness or availability of a PEV decreases considerably.

A thorough investigation of the RAM of the vehicle system can help manufacturers to identify the failure-prone zones in the design and to estimate their contributions to the overall system failure. It encourages searching for more reliable alternatives. RAM analysis ascertains the critical performance metrics, such as Survivability, Mean Time to Failure, Mean Down Time, and Frequency of Failure. Apart from these, RAM analysis is also essential from the customer's point of view. A large investment is associated while purchasing a PEV, and such investments deserve dedicated research in order to ensure that the most critical reliability criteria are satisfied. The components' reliability information can help to follow proper maintenance strategies and improve the vehicle's health [8].

In the existing literature, reliability-oriented researches for a PEV system are found to be very limited. However, some notable research works deal with evaluating the reliability of some vital components of a PEV system. For example, Shu *et al.* evaluated the electric motors' reliability using the fault-tree method [118]. They proposed an integrated motor-drive reliability model. Xia *et al.* developed a reliability model for Li-ion batteries used in EVs [119, 120]. This model integrated the degradation model and multiphysics model. They cited various relevant research works. Sakhdari *et al.* proposed an energy management strategy for EVs [121]. The dynamic programming method was applied in order to optimize

the distribution of energy and improve the health of the battery. Bolvashenkov *et al.* proposed a model for predictive reliability assessment of electric drive trains [122]. They illustrated various factors that can affect the reliability of a drive train. Ammaiyappan *et al.* illustrated a simulation model focusing on the reliability of lead-acid battery, controller, and brushless dc motor required for EV operation [123]. Khalilzadeh *et al.* developed a reliability model of a DC-DC converter system used in the Plug-in hybrid EV in [124]. They applied the Markov concepts to determine the useful lifetime of the bidirectional converter. The latest research works were centered on discussing the reliability issues that are faced by power distribution networks due to electric vehicle charging. However, no significant research work has been noticed addressing the RAM of the overall PEV system.

Observing the literature gap as illustrated above, this thesis aims to model a mathematical framework to analyze the RAM of an EV. Chapter 7 of the thesis has been mainly designed for this purpose. It explores how the RAM of a plug-in EV is impacted by various factors and suggests how it can be improved.

2.5.6 Solar EV: A Step toward Green Transportation

The transport sector accounts for roughly one-fourth of worldwide CO_2 emissions in the atmosphere [125, 126]. The growing concerns of air quality deterioration, global warming, and the rapid diminution of petroleum resources have pushed the governments and policy-makers of many countries to promote clean and sustainable automotive options for road transportation [127, 128]. At first sight, electric vehicles (EV) can be a potential solution to the emission problem. However, the electricity required for an EV still needs to be produced, in part by fossil fuels in many countries. Thus, attaining a truly carbon-free solution on the horizon is not fulfilled. There are some other concerns also which make people hesitate to buy an EV. Unlike a conventional car, an EV needs a much longer refueling time. Many drivers do not want to switch to EVs because of the lack of a charging facility at home

or at work, or they do not have enough time to charge the car at a public charging station. The reliability of the power supply at the charging station is another critical factor for the operation of an EV. A solar electric vehicle (SEV) seems to be one of the best last-mile solutions providing extra energy to reach home or the nearest charging station. The ability to recharge during the running as well as the parking period is one of the main advantages when designing cars with solar panels. Solar energy is expected to be the future of mobility, and solar energized EVs are regarded as the next big step in tackling carbon neutrality and energy security issues [129].

The concept of SEV is not a new one. The world's first SEV model, named 'Sunmobile', was developed by W. G. Cobb [130]. It was presented at the General Motors Powerama Convention held in Chicago on August 31, 1955. Since then, efforts have been made by many designers and manufacturers to bring commercially viable SEVs to the market. For example, in October 2013, the Solar Team Eindhoven (STE) presented a solar-powered family car called 'Stella' with four people intake capacity and a driving range of 600 kilometers [131]. Grandstudio, an automotive design consultancy based in Turin, Italy, is coming up with an all-electric advanced solar car named 'Lightyear One' by 2021 [132]. 'Sion' is another announced solar-powered, fully electric car, currently being developed by the German start-up Sono Motors [133]. A California-based start-up called 'Humble Motors' is looking to join the fray, and it has unveiled the One electric Sport Utility Vehicle called 'Humble One' [134]. It uses over 80 sq. feet of solar modules and generates nearly 96 km of range per day. Apart from these, Tesla, Lucid, Faraday Future, and Fisker have proven that the zero-emission vehicle technology will get better than it already is in the coming years.

The operation of a SEV mainly depends on the reliability of its onboard photovoltaic system (PVS). The power generated by PVS is intermittent in nature and affected by various factors like solar irradiation, vehicle's geographic location, ambient temperature, weather condition, dust deposition, wind speed, etc.[135–138]. Designing a PVS on the roof of

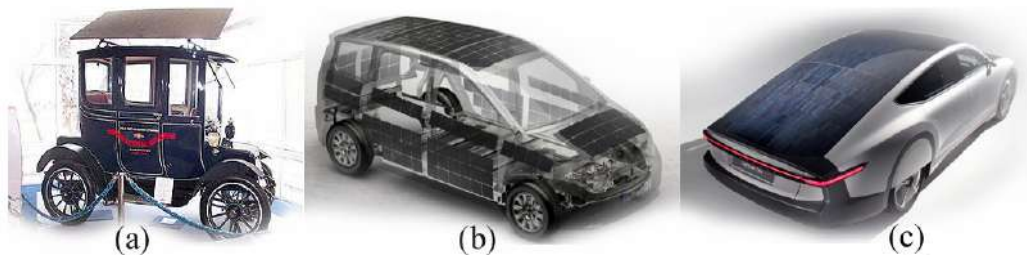


Fig. 2.3 Prototype SEV models: (a) Sunmobile (b) Sion (c) Lightyear One

the vehicle to produce reliable electrical power for charging the battery at a standard rate is a major challenge for the SEV manufacturers. Most manufacturers try to mitigate this challenge by providing a standby power source such as plug-in option, fuel cell, swappable spare battery, etc. The standby power supply option significantly improves the reliability of the SEV. Apart from the power source, the reliability of other electrical components of the SEV such as battery, energy management system, propulsion system, controllers, etc., have also considerable impacts on the overall operational effectiveness of the vehicle. For better survivability, the vehicle system must be manufactured with a reliable design using reliable components [139]. Moreover, the vehicle's protective schemes must fulfill the minimum reliability criteria to ensure safety to the personnel. Although a system with high reliability incurs higher manufacturing costs, it reduces the frequency of maintenance and, therefore, lowers the service costs [63].

To fulfill the desired reliability criteria, a comprehensive reliability assessment of the entire vehicle system is very important during the period of design and manufacturing of a SEV. It helps manufacturers to identify the failure-prone zone in the vehicle system and estimate their contribution to the overall system failures and thus encourages searching for better alternatives. On the other hand, the usefulness or the operational effectiveness of the vehicle system can be estimated by calculating its steady-state availability [139]. A thorough reliability and availability assessment not only helps to investigate the risk, survivability, and effectiveness of the vehicle system but also guides to prepare better corrective and preventive maintenance strategies for the vehicle [140]. For a SEV, these studies carry more significance

due to its solar irradiance-dependent operation. The customers also get benefited from such analysis in deciding on purchasing an effective and reliable SEV.

The reliability assessment of a solar-energized EV is still an unexplored research area. Most of the studies carried out so far were confined to the design and performance analysis of a few selected components of a SEV system. Subudhi PS *et al.* proposed a battery charging system for PV system and grid interfaced plug-in EVs [64]. Gobhinath S *et al.* demonstrated a practical approach to design and fabricate a four-wheeled SEV [65]. Rachid T *et al.* proposed an IRAMY Inverter Control strategy for a SEV [141]. Khan S *et al.* carried out a review assessment of solar-energized charging systems used to recharge the battery of an EV [66]. Again, Sankar AB *et al.* developed a simulation model of a SEV considering the performance of the PVS, charge controller, battery, motor, and inverters, etc. [142] Ismail M *et al.* designed a charge controller (CC) for a solar-energized storage system [143]. Rodriguez AS *et al.* investigated the feasibility of solar-powered car considering CO_2 emissions and economic aspects [125]. However, in the aforesaid studies, the reliability issues of a SEV system were not addressed at all.

The reliability-centric researches noticed in the literature were mainly directed at some critical components of plug-in EVs. Xia Q *et al.* proposed a reliability model of Li-ion batteries used in an EV [144, 145]. Their study was mainly aimed at constructing a multiphysics-based model incorporating the Stochastic Capacity Degradation and Dynamic-Response Impedance characteristics of a battery pack. Shu X *et al.* concentrated on evaluating the reliability of a traction motor using the fault tree method [146]. Sakhdari B *et al.* proposed a strategy for energy management in EVs [147]. Dynamic Programming technique was used for optimizing the energy distribution and enhance the reliability of the battery. Ammaiyappan BS *et al.* investigated the reliability of lead-acid batteries, controllers, and brushless dc-motors used in EVs [148]. Khalilzadeh M *et al.* proposed a reliability model for DC-DC converter system applying Markov concepts [124]. Bolvashenkov I *et al.* demonstrated a

reliability model for an electric drive-train highlighting modern maintenance strategies [149]. All these studies help to examine the reliability of the selected components but cannot comment on the reliability of the entire EV system.

The impact of intermittency of solar generation must be taken into account while carrying out a reliability study for a SEV. Alferidi A *et al.* proposed a probabilistic model for PV system topologies for adequacy assessment [150]. Borges CLT discussed how PV generation (PVG) is dependent on the solar irradiation level at a particular location [151]. Wang H *et al.* considered the temperature and weather effect while studying the reliability of PVG [136]. Many other researchers have carried out similar studies; however, most of those studies are intended for grid-connected PV systems, not for SEVs.

The reliability of a CS will be an important factor if the SEV is facilitated with a backup charging option. An unreliable CS offers fewer charging hours and increases the downtime of an EV. The contribution of the plug-in option toward the SEV's operational effectiveness cannot be ignored. The research gap in this area is also quite visible.

From the above discussion, it is evident that there are ample scopes of research on SEVs in different aspects. This thesis considers the reliability aspect of a SEV. Chapter 8 presents mathematical modeling of a SEV and carries out a reliability and availability assessment of it. The study shows that SEV with a standby plug-in facility is the best EV option from a reliability perspective.

2.6 Conclusion

This chapter describes the fundamental concepts of power system reliability, various methods for power system reliability assessment, and a brief review of literature on some emerging areas for power systems reliability study. The main focused areas for the current reliability studies are: deregulated power system, distribution system integrated with renewable energy sources, electric vehicle integration with a distribution network, plug-in electric vehicle, and

solar electric vehicle. Presenting the theoretical concepts and the research gaps in the existing literature related to the aforesaid subjects were the prime objectives of this chapter. In the very next chapter, detailed analyses of the methods and materials used in the current research work are presented.

3

Methods and Materials

3.1 Introduction

In the preceding chapter, a literature review on different methodologies and approaches used in power system reliability analysis has been reported. This chapter presents a detailed description of various terms, definitions, methods, and materials used in the present research work. As explained in Section 2.4.3, the well-being approach has many advantages over other deterministic and probabilistic approaches. Therefore, this approach has been applied in Chapter 4 to analyze the reliability of a deregulated power system. The detailed methodology of this approach is explained in Section 3.5. In Chapter 5, a new method has been proposed

based on the well-being framework and Markov concept. As mentioned in Section 3.4, the Markov framework is suitable for developing a multi-state reliability model. One of the outstanding advantages of this method is that it can incorporate both failure and repair characteristics of a component or system. In this research, the Markov framework is used in Chapters 5, 7, and 8. Section 3.4 of the present chapter illustrates this approach in detail. Again, for distribution system reliability assessment (DSRA), the well-established DSRA indices are used. The descriptions of these indices and the procedure to evaluate these indices are explained in Section 3.6.

The Roy Billinton Test System (RBTS) has been used as the test system in the present research work. The detailed descriptions of RBTS and its associated distribution system are illustrated in Section 3.7.

3.2 Basic Concepts, Terms and Definitions

The life cycle of a component encounters three types of failure rates or hazard rates in three stages of life. It experiences a decreasing failure rate during early life, constant failure rate during a useful life, and increasing failure rate during the wear out period. The probability that a failure may not occur in a specified time interval is called “reliability” [35]. Poor design and incorrect manufacturing techniques are the main reasons for low reliability. Poor maintenance policies and human errors due to a lack of understanding of the system and process, carelessness, forgetfulness, poor judgmental skills, etc. also contribute to a system’s unreliability. Despite the designer’s best effort, a system cannot be 100% reliable. The system is likely to fail during its operation. It might be costly in terms of money and time, or sometimes dangerous in terms of safety. Therefore, maintenance becomes an essential consideration in the long-term performance of a system. The system demands preventive maintenance to keep away from any possible failures. The term “maintainability” refers to the probability that a failed system is restored to the operable condition in a specified time

[14]. It characterizes the system's adaptability to the detection and the elimination of failures and their prevention. "Availability" is another measure of the effectiveness of a maintained system. It integrates both reliability and maintainability parameters, and it depends on the number of failures that occur and how quickly any faults are rectified. The long-term or steady-state availability is the proportion of time during which the system is available for use.

3.2.1 Reliability Function

The term 'reliability' means the probability of success. Let us consider a system having N components. After operation of t hours, only $N_s(t)$ have survived due to the failure of $N_f(t)$ components. The probability of success ,i.e., reliability, $R(t)$ is given by,

$$R(t) = \frac{N_s(t)}{N} = 1 - \frac{N_f(t)}{N} \quad (3.1)$$

The hazard rate which is a measure of instantaneous speed of failures is defined as,

$$z(t) = \lim_{\Delta t \rightarrow 0} \frac{N_s(t) - N_s(t + \Delta t)}{N_s(t) \Delta t} = \frac{1}{N_s(t)} \left(-\frac{dN_s(t)}{dt} \right) \quad (3.2)$$

Differentiating $R(t)$ w.r.t t ,

$$\frac{dR(t)}{dt} = \frac{1}{N} \frac{dN_s(t)}{dt} \quad (3.3)$$

Substituting in terms of the hazard rate,

$$\frac{dR(t)}{dt} = -\frac{N_s(t)z(t)}{N} = -R(t)z(t) \quad (3.4)$$

$$z(t) = -\frac{1}{R(t)} \frac{dR(t)}{dt} \quad (3.5)$$

Integrating both the sides, and simplifying Eq. (3.4), the expression of reliability can be derived as:

$$R(t) = \exp \left[- \int_0^t z(\tau) d\tau \right] \quad (3.6)$$

The Mean Operating Time (MOT) or Mean Time To Failure (MTTF) is:

$$MTTF = \int_0^{\infty} R(t) dt \quad (3.7)$$

For constant-hazard model, $z(t) = \lambda$ where, λ is the constant failure rate of a component and is independent of time. Therefore, a system with constant failure rate will have the reliability and MTTF as:

$$R(t) = e^{-\lambda t} \quad (3.8)$$

$$MTTF = \frac{1}{\lambda} \quad (3.9)$$

3.2.2 Maintainability Function

Maintainability is an index associated with a system under repair. It is the probability that the failed system will be repaired within time t [14]. If T is a random variable representing the repair time, then maintainability is defined as:

$$M(t) = \text{Prob}(T \leq t) \quad (3.10)$$

If the repair time is exponentially distributed with parameter μ , then the repair-density function is:

$$g(t) = \mu e^{-\mu t} \quad (3.11)$$

and therefore,

$$M(t) = \text{Prob}(T \leq t) = \int_0^t \mu e^{-\mu \tau} d\tau = 1 - e^{-\mu t} \quad (3.12)$$

The expected value of repair time is called mean time to repair (MTTR) or mean down time (MDT) and is given by:

$$MTTR = \int_0^{\infty} t g(t) dt = \frac{1}{\mu} \quad (3.13)$$

3.2.3 Availability Function

With the introduction of repair capability that restores a system to an operative state, an alternative measure of system performance is availability. Availability, $A(t)$ may be interpreted as the probability that a system is operational at a given point in time t or as the percentage of time, over some interval in which the system is operational [152]. Accordingly, the definition of availability will change as follows:

1. **Inherent Availability:** It is based solely on the failure distribution and repair-time distribution. It can therefore be viewed as an equipment design parameter, and reliability-maintainability trade-offs can be based on this interpretation.

$$A_{inh} = \lim_{T \rightarrow \infty} A(T) = \frac{MTBF}{MTTR + MTBF} \quad (3.14)$$

where, MTBF stands for Mean Time Between Failures and MTTR refers to Mean Time To failure.

2. **Achieved Availability:** Achieved availability, A_a is defined as

$$A_a = \frac{MTBM}{MTBM + \overline{M}} \quad (3.15)$$

where the mean time between maintenance (MTBM) includes both unscheduled and preventive maintenance and is computed from Eq. (3.16),

$$MTBM = \frac{t_d}{m(t_d) + t_d/T_{pm}} \quad (3.16)$$

and \bar{M} is the mean system downtime, T_{pm} is the preventive maintenance interval, t_d is the design life and $m(t_d)$ is the cumulative average number of failures over the design life. For constant failure rates, $m(t_d) = \lambda t_d$ and t_d can be factored out of Equation (3.16)

3. **Steady-state Availability:** The exponential form of availability of a repairable system having a constant failure rate of λ and repair rate of μ is given by

$$A(t) = \frac{\mu}{\lambda + \mu} + \frac{\lambda}{\lambda + \mu} e^{-(\lambda + \mu)t} \quad (3.17)$$

Steady-state availability is defined as,

$$A_{ss} = \lim_{t \rightarrow \infty} A(t) = \frac{\mu}{\lambda + \mu} \quad (3.18)$$

This research basically deals with steady-state availability in Chapters 7 and 8.

3.3 System Reliability Evaluation

A relatively standard procedure to estimate the reliability of any system is to decompose it into its constituent components, evaluate the reliability of each of these components, and combine the component reliabilities using one or more numerical techniques. The level to which the decomposition is taken must be such that the reliabilities of the resulting components are known within reasonable and acceptable precision. The constituent components may be connected in series, parallel, or standby mode as illustrated below.

3.3.1 Series System

A system is said to be reliability-wise in series, if failure of even a single constituent component results in the failure of the whole system [14]. The reliability of a 2-component

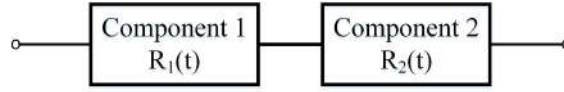


Fig. 3.1 Reliability block diagram of a 2-component series system

series system (Fig. 3.1) at time t is determined using

$$R_s(t) = R_1(t) \times R_2(t) \quad (3.19)$$

From Equation (3.6),

$$R_s(t) = \exp \left[- \int_0^t z_1(\tau) d\tau \right] \times \exp \left[- \int_0^t z_2(\tau) d\tau \right] \quad (3.20)$$

For an n -component series system with failure rates $\lambda_1(t), \lambda_2(t), \lambda_3(t), \dots, \lambda_n(t)$,

$$R_s(t) = \prod_{i=1}^n \exp \left[- \int_0^t \lambda_i(t) dt \right] \quad (3.21)$$

3.3.2 Parallel System

A system is said to be reliability-wise parallel if it fails to operate only if all of its constituent components fail simultaneously. For an n -component parallel system, reliability is given by

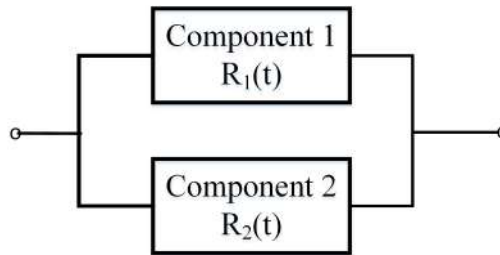


Fig. 3.2 Reliability block diagram of a 2-component parallel system

$$R_p(t) = 1 - \prod_{i=1}^n Q_i(t) \quad (3.22)$$

where $Q_i(t)$ is the unreliability of the i^{th} component at time t . If λ_i is the hazard rate of the i_{th} component, then

$$R_p(t) = 1 - \prod_{i=1}^n \left(1 - \exp \left[- \int_0^t \lambda_i(t) dt \right] \right) \quad (3.23)$$

3.3.3 Standby System

In a standby system, one or more components are in a standby mode, ready to take over system operation when the main or normally operating component(s) fail. Such a system may be used when it is impractical to simultaneously operate the main component(s) and the standby component(s)[14]. This type of system may also be particularly advantageous when the redundant standby component(s) has a lower failure rate in standby or idle mode than in operating mode [35]. Based on the reliability of the switching device, two cases arise

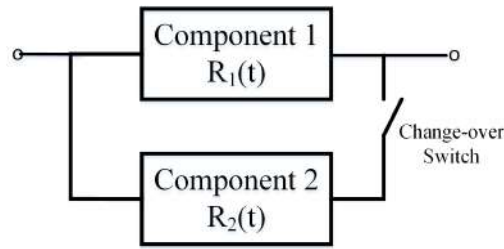


Fig. 3.3 Reliability block diagram of a standby system

as follows:

1. **Perfect Switching:** In this case, the sensing and changeover switch is 100% reliable. For a two identical component system having a single main component as one standby component with constant failure rate of λ , the reliability of the system is:

$$R(t) = (1 + \lambda t) e^{-\lambda t} \quad (3.24)$$

For n identical standby components,

$$R(t) = \sum_{x=0}^n \frac{(\lambda t)^x e^{-\lambda t}}{x!} \quad (3.25)$$

If the primary and standby components are not identical, system reliability can be evaluated using Equation (3.26).

$$R(t) = e^{-\lambda_1 t} + \frac{\lambda_1}{\lambda_2 - \lambda_1} \left[e^{-\lambda_1 t} - e^{-\lambda_2 t} \right] \quad (3.26)$$

where λ_1 is the failure rate of the primary component and λ_2 is the failure rate of the standby component.

2. **Imperfect Switching:** In this case the sensing and changeover switch is not 100% reliable. The reliability of the normally operating component is unaffected by the unreliability of the sensing and switching device. If r_{sw} be the reliability of the sensing and switching device, then the reliability of the overall system is given by Equation (3.27).

$$R(t) = e^{-\lambda_1 t} + \frac{r_{sw} \lambda_1}{\lambda_2 - \lambda_1} \left[e^{-\lambda_1 t} - e^{-\lambda_2 t} \right] \quad (3.27)$$

3.4 Markov Model

As discussed in Section 3.3, a fundamental computation in reliability engineering is the determination of system reliability from the knowledge of component reliabilities and their system configuration. However, when component failures are dependent, more powerful methods, such as the Markov framework, are needed. Using the Markov approach, the random behavior of systems that vary discretely or continuously with time and space can be modeled [35]. Markov framework can incorporate both the stochastic failure and repair processes, which is one of the major limitations of other analytical techniques.

Markov analysis looks at a system as being in one of several states. One possible state, for example, is that in which all the components forming the system are operating. Another possible state is that in which one component has failed, but the other components continue to work. The fundamental assumption in a Markov process is that the probability that a system undergoes a transition from one state to another depends only on the system's current state and not on any previous states of the system that may have experienced. In other words, the transition probability is not dependent on the past state history of the system. This is equivalent to the memorylessness of the exponential distribution [152]. The system should be stationary, i.e., transitions between states are constant and time-invariant. From these two aspects of lack of memory and being stationary, it is evident that the Markov approach is suitable to those systems only whose behavior can be described by a probability distribution that is characterized by a constant hazard rate.

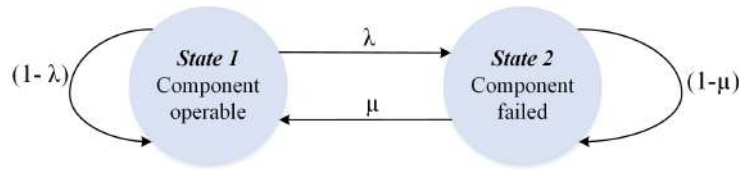


Fig. 3.4 State-space diagram of a system having single repairable component

The basic concepts of Markov modeling is explained by a single component repairable system. As demonstrated in Fig. 3.4, the system has two states: UP (Operable) and DOWN (Failed). The parameter λ and μ are the state transition rates. They denote the rates at which the component transits from one state to another. In other words, the transition rate is the ratio of the number of times that a transition occurs from a given state to the time spent in that state [35]. Based on this definition, the failure rate (λ) and repair rate (μ) can be defined as:

$$\lambda = \frac{\text{Number of failures in a given period}}{\text{Total period of time the system was operating}} \quad (3.28)$$

$$\mu = \frac{\text{Number of repairs in a given time period}}{\text{Total period of time taken in the repair process}} \quad (3.29)$$

The reciprocals of failure rate and repair rate are called Mean Operating Time (MOT) and Mean Down Time (MDT), respectively. Transition probabilities can be represented by a matrix. This matrix is known as “Stochastic Transitional Probability Matrix” (STPM) [14]. In STPM, the summation of the elements in a row is always equal to unity.

$$STPM = \begin{bmatrix} P_{11} & P_{12} \\ P_{21} & P_{22} \end{bmatrix} \quad (3.30)$$

where P_{ij} is the probability of transition from state i to state j . For the system that is shown in Fig. 3.4, the STPM will be:

$$STPM = \begin{bmatrix} 1 - \lambda & \lambda \\ \mu & 1 - \mu \end{bmatrix} \quad (3.31)$$

Under steady-state condition ($t \rightarrow \infty$), the probability P_{ij} is called steady-state or limiting state probability. There are several techniques for the evaluation of the limiting state probabilities. Out of those, the Differential Equations Method and the Matrix Multiplication Method are the most widely used methods. Concepts from both these methods have been used in the present research work. The detailed descriptions of the methods are discussed in Sections 3.4.1 and 3.4.2.

3.4.1 Differential Equations Method

Suppose, an incremental interval of time dt which is made sufficiently small so that probability of two or more events occurring during this increment of time is negligible. The probability of being in the operating state after the interval of dt , i.e., the probability of being in state 1 of Fig. 3.4 at time $t + dt$ is equal to

[Probability of being operative at time t AND of not failing in time dt] + [Probability of being failed at time t AND of being repaired in time dt].

Mathematically,

$$P_0(t + dt) = P_0(t)(1 - \lambda dt) + P_1(t)(\mu dt) \quad (3.32)$$

Similarly,

$$P_1(t + dt) = P_1(t)(1 - \mu dt) + P_0(t)(\lambda dt) \quad (3.33)$$

Form Equation (3.32),

$$\frac{P_0(t + dt) - P_0(t)}{dt} = -\lambda P_0(t) + \mu P_1(t) \quad (3.34)$$

As $dt \rightarrow 0$,

$$\frac{P_0(t + dt) - P_0(t)}{dt} \Big|_{dt \rightarrow 0} = \frac{P_0(t)}{dt} = P_0'(t) \quad (3.35)$$

Thus,

$$P_0'(t) = -\lambda P_0(t) + \mu P_1(t) \quad (3.36)$$

Similarly, from Equation (3.33),

$$P_1'(t) = \lambda P_0(t) - \mu P_1(t) \quad (3.37)$$

Equations (3.36) and (3.37) are linear differential equations with constant coefficients. Taking Laplace transform of Equation (3.36),

$$sP_0(s) - P_0(0) = -\lambda P_0(s) + \mu P_1(s) \quad (3.38)$$

where $P_1(s)$ is the Laplace transform of $P_1(t)$ and $P_0(0)$ is the initial value of $P_0(t)$. Rearranging Equation (3.38) gives,

$$P_0(s) = \frac{\mu}{s + \lambda} P_1(s) + \frac{1}{s + \lambda} P_0(0) \quad (3.39)$$

Similarly Equation (3.37) can be transformed into

$$P_1(s) = \frac{\lambda}{s+\mu}P_0(s) + \frac{1}{s+\mu}P_1(0) \quad (3.40)$$

where $P_1(0)$ is the initial value of $P_1(t)$. Solving Equations (3.39) and (3.40) for $P_0(s)$ and $P_1(s)$,

$$P_0(s) = \frac{\mu}{\lambda+\mu} \left[\frac{P_0(0) + P_1(0)}{s} \right] + \frac{1}{\lambda+\mu} \cdot \frac{1}{s+\lambda+\mu} [\lambda P_0(0) - \mu P_1(0)] \quad (3.41)$$

$$P_1(s) = \frac{\lambda}{\lambda+\mu} \left[\frac{P_0(0) + P_1(0)}{s} \right] + \frac{1}{\lambda+\mu} \cdot \frac{1}{s+\lambda+\mu} [\mu P_1(0) - \lambda P_0(0)] \quad (3.42)$$

Taking inverse Laplace transform of Equations (3.41) and (3.42),

$$P_0(t) = \frac{\mu}{\lambda+\mu} [P_0(0) + P_1(0)] + \frac{e^{-(\lambda+\mu)t}}{\lambda+\mu} [\lambda P_0(0) - \mu P_1(0)] \quad (3.43)$$

and

$$P_1(t) = \frac{\lambda}{\lambda+\mu} [P_0(0) + P_1(0)] + \frac{e^{-(\lambda+\mu)t}}{\lambda+\mu} [\mu P_1(0) - \lambda P_0(0)] \quad (3.44)$$

The term $P_0(0) + P_1(0) = 1$ for the initial conditions. Therefore, Equations (3.43) and (3.44) becomes:

$$P_0(t) = \frac{\mu}{\lambda+\mu} + \frac{e^{-(\lambda+\mu)t}}{\lambda+\mu} [\lambda P_0(0) - \mu P_1(0)] \quad (3.45)$$

and

$$P_1(t) = \frac{\lambda}{\lambda+\mu} + \frac{e^{-(\lambda+\mu)t}}{\lambda+\mu} [\mu P_1(0) - \lambda P_0(0)] \quad (3.46)$$

In practice, the most likely state in which the system starts is State-1 (i.e., Operating State).

In this case, $P_0(0) = 1$ and $P_1(0) = 0$, and Equations (3.45) and (3.46) reduce to:

$$P_0(t) = \frac{\mu}{\lambda+\mu} + \frac{1}{\lambda+\mu} e^{-(\lambda+\mu)t} \quad (3.47)$$

and

$$P_1(t) = \frac{\lambda}{\lambda + \mu} + \frac{1}{\lambda + \mu} e^{-(\lambda + \mu)t} \quad (3.48)$$

The probabilities $P_0(t)$ and $P_1(t)$ are the probabilities of being found in the operating state and failed state respectively as a function of time given that the system started at time $t = 0$ in the operating state.

The limiting state probabilities will be:

$$P_0 = P_0(\infty) = \frac{\mu}{\lambda + \mu} \quad (3.49)$$

$$P_1 = P_1(\infty) = \frac{\lambda}{\lambda + \mu} \quad (3.50)$$

The values of P_0 and P_1 are generally referred to as steady -state availability (A) and un-availability (U) respectively. The time dependent availability, $A(t)$ of the system is given by Equation (3.51).

$$A(t) = P_0(t) = \frac{\mu}{\lambda + \mu} + \frac{1}{\lambda + \mu} e^{-(\lambda + \mu)t} \quad (3.51)$$

3.4.2 Matrix Multiplication Method

In this method, the stochastic transitional probability matrix (STPM) is developed for a small interval of time, dt . The actual value of dt should be chosen such that the probability of two or more transitions occurring in this interval of time is negligible. The principle of this method is that, once the limiting state probabilities have been reached by the matrix multiplication method, any further multiplication by the STPM does not change the values of the limiting state probabilities [35], i.e., if α represents the limiting state probability vector and P is the STPM, then,

$$\alpha P = \alpha \quad (3.52)$$

This principle can be applied to the simple two state system shown in Fig. 3.4. If P_1 and P_2 are the limiting state probabilities of being in the operating state (State 1) and failed state (State 2) respectively, then

$$\alpha = [P_1 \ P_2] \quad (3.53)$$

Now, Equation (3.31), (3.52) and (3.53) give,

$$[P_1 \ P_2] \begin{bmatrix} 1 - \lambda & \lambda \\ \mu & 1 - \mu \end{bmatrix} = [P_1 \ P_2] \quad (3.54)$$

Again, as per total probability theorem,

$$P_1 + P_2 = 1 \quad (3.55)$$

Solving Equation (3.54) and (3.55), the value of P_1 and P_2 are found to be:

$$P_1 = \frac{\mu}{\lambda + \mu} \quad (3.56)$$

$$P_2 = \frac{\lambda}{\lambda + \mu} \quad (3.57)$$

P_1 is called the steady-state availability (A) and P_2 is known as the steady-state unavailability (U) of the system.

In complex systems, there will be several states, and most of these states will be absorbing states. Based on the number of states and the series-parallel configuration of constituent components or subsystems, the system availability is determined. The necessary steps to evaluate the limiting state probabilities and availability of such complex systems are as follows:

3.4.3 Availability Calculation Steps

- **Step 1:** Identify all states in which the system can reside.
- **Step 2:** Identify all possible transitions between these states and specify the quantitative values of these transitions.
- **Step 3:** Construct the appropriate set of differential equations or the stochastic transitional probability matrix.
- **Step 4:** Using the methods explained in Sections 3.4.1 and 3.4.2 and , determine the time dependent state probabilities, if required.
- **Step 5:** Using the principle of $\alpha P = \alpha$ given in Equation (3.52), evaluate the limiting state probabilities.
- **Step 6:** Identify the system up states, down states and derated states (if any).
- **Step 7:** Combine the appropriate state probabilities to find the probability of system being in up, down or in derated state(s).
- **Step 8:** Using the principle of absorbing states, solve the modified differential equations to evaluate the system availability.

3.5 Well-being Model

System well-being modeling gives a new perspective to power system adequacy studies and helps when conventional probabilistic techniques are generally not applicable. It bridges the gap between probabilistic and deterministic approaches and estimates the system reliability based on some prespecified deterministic risk criteria [34].

In the well-being framework, based on reliability level, the system is considered to reside in a set of mutually exclusive states. The probabilities of occurring those states form the well-being indices [12]. The basic well-being model for a system is shown in Fig. 3.5. Here, the system has three states, namely, healthy, marginal, and risk. The well-being indices for this system are, namely, probability of health $p(H)$, probability of margin $p(M)$, and probability of risk $p(R)$.

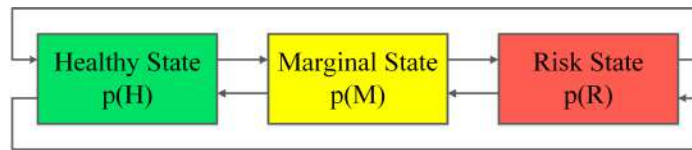


Fig. 3.5 System well-being model

In the healthy state, all components are operational within their constraints, and the generation is adequate to meet the system load. There is sufficient reserve margin such that the loss of any significant system components such as generating units and transmission lines specified by an acceptable deterministic criterion will not result in an operating limit being violated or load curtailed. The particular criterion will depend on the planning and operating philosophy of the utility in question.

In the marginal state (alert state), the system operates within its limits, but it no longer has sufficient reserve to satisfy the acceptable deterministic criterion. The failure of some major components will result in constraint violation or load curtailment. If the individual load is either equal to (emergency) or greater than (extreme emergency) the available capacity of the component, the system will enter the state of risk.

The probability of risk, $p(R)$ measures the likelihood of the system being in the risk state. System enters at the risk state from the healthy or marginal state due to either the loss of certain operating capacity or a sizable increase in the system load. In this state, equipment or system constraints are violated, and some loads may have to be curtailed due to insufficient reserve in the system.

3.5.1 Well-being Indices Evaluation Methods

Well-being indices are evaluated using either simulation or analytical techniques. Monte Carlo Simulation (MCS) is the most popular simulation technique [12]. However, the requirement of a large computation time is a major drawback of MCS technique. The analytical approaches are of two types: Contingency Enumeration (CE) approach and the Conditional Probability Capacity Outage Probability Table (CPCOPT) approach [62].

In the CE approach, a power generation model is developed considering all the possible combinations of the existing generating unit states along with corresponding probabilities. For adequacy assessment, the available reserve in each system state is compared with the capacity of the largest available unit (CLU) in that state (deterministic criterion). If the available capacity reserve is greater than or equal to the CLU, this state is designated as a healthy state. When the demand is less than the CLU but greater than zero, the state is treated as a marginal state. When the reserve is negative, the state is marked as a risk state. The health probability, $p(H)$ is the summation of the probabilities of the healthy states. The margin probability, $p(M)$ is the summation of the marginal state probabilities. Again, the risk probability, $p(R)$ is the summation of all risk state probabilities in the system [62].

On the other hand, in the CPCOPT approach, well-being indices are derived in three steps. In the first step, $p(R)$ is determined using the basic loss of load probability (LOLP) method. Next, $p(H)$ is evaluated, creating a series of COPT convolved with the load model. The $p(H)$ is weighted with the corresponding generating unit probabilities in each case. In the final step, $p(M)$ is determined by subtracting the sum of $p(H)$ and $p(R)$ from 1, since $p(H) + p(M) + p(R) = 1$

Due to simplicity, the CE approach has been preferred in the present research work. The flowchart to determine the well-being indices based on the CE approach is given in Section 3.5.2.

3.5.2 Flowchart for Well-being indices

The flowchart to determine the basic well-being indices of a system based on the CE approach is presented in Fig. 3.6.

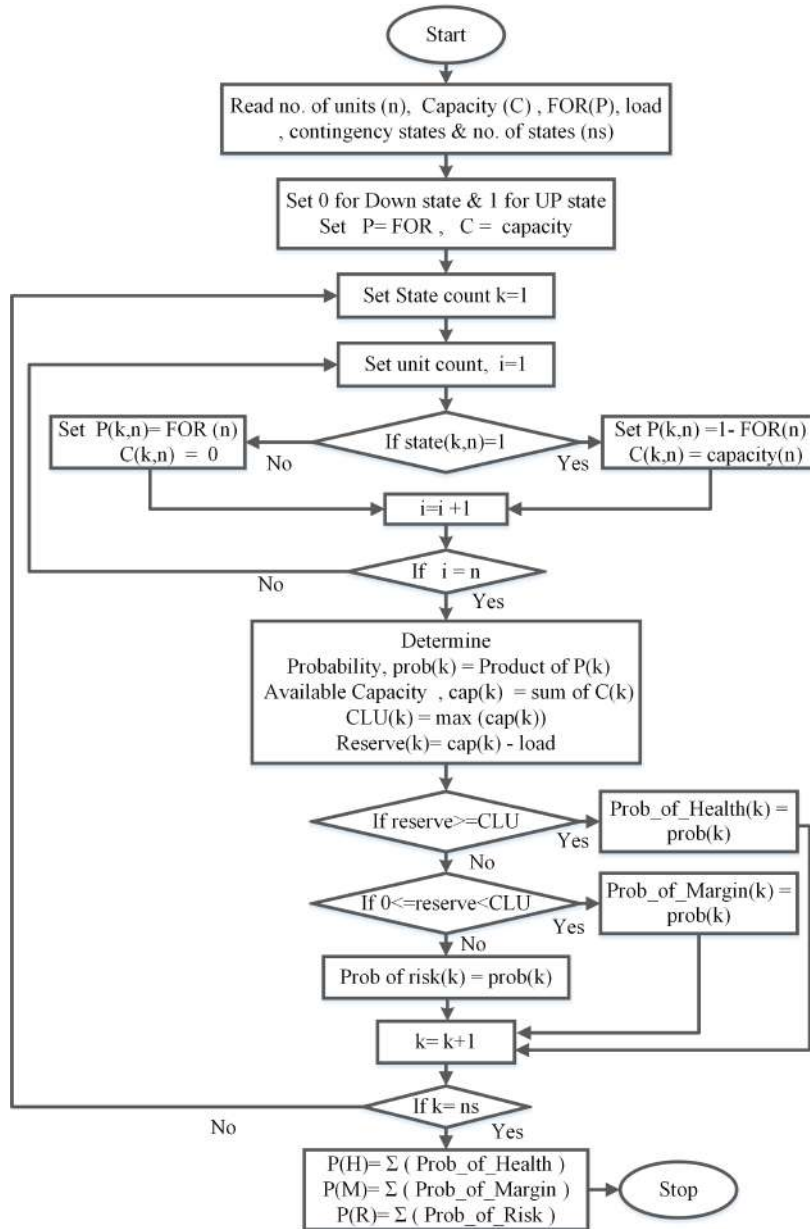


Fig. 3.6 Flowchart to determine the basic well-being indices

3.6 Distribution System Reliability Assessment (DSRA)

A distribution system (DS) is relatively inexpensive compared to generation and transmission systems, and outages have a localized effect. Therefore, less effort has been devoted to quantitatively assessing the adequacy of various alternative designs and reinforcements. Analysis of the customer failure statistics of most utilities reveals that DS makes the highest individual contribution to the unavailability of supply to a customer [20]. Most of the distribution systems are radial in structure. A radial distribution system (RDS) consists of a set of series components, including lines, cables, isolators, busbars, etc. These components are connected reliability-wise in series. It is because, all of these components must be in working state in order to get continuous power supply by the customers. Consequently, the principle of series system illustrated in Section 3.3.1 is applicable directly to these systems.

To measure the reliability of a RDS, a set of reliability indices are developed based on the duration and frequency of interruptions in the system. The primary reliability parameters for DSRA are: average failure rate (λ_s), average outage rate (r_s), and average annual outage time or average annual unavailability (U_s). These indices are evaluated using classical concepts as follows:

$$\lambda_s = \sum_i \lambda_i \quad (3.58)$$

$$U_s = \sum_i \lambda_i r_i \quad (3.59)$$

$$r_s = \frac{\sum_i \lambda_i r_i}{\sum_i \lambda_i} \quad (3.60)$$

where, λ_i , r_i and U_i represent the average failure rate, average outage duration and average annual unavailability in the i^{th} load point. These three indices are fundamentally important tools for examining the system behaviour and response. However, they do not always give a complete representation of the system's performance. In order to reflect the severity or significance of a system outage, several indices were proposed by the IEEE Standards Board

on 8 December 1998. These indices can be categorized primarily into three groups: customer-oriented indices, energy and load oriented indices, and reliability worth indices. The most commonly used indices under these three categories are discussed in the following section.

3.6.1 Distribution System Reliability Indices

1. Customer-oriented Indices

- (a) **System Average Interruption Frequency Index (SAIFI):** It is the average number of sustained outages, per year, per customer over a defined area [20]. It is a measure of how many sustained interruptions an average customer will experience over the course of a year. For a fixed number of customers, the only way to improve the SAIFI is to reduce the number of sustained interruptions experienced by customers. In words,

$$SAIFI = \frac{\text{Total number of customer interruptions}}{\text{Total number of customer served}} \quad (3.61)$$

Mathematically,

$$SAIFI = \frac{\sum \lambda_i N_i}{\sum N_i} \quad (3.62)$$

where λ_i and N_i are the failure rate and number of customers of load point 'i', respectively.

- (b) **System Average Interruption Duration Index (SAIDI):** It is the average length of sustained customer outage experienced by a customer. SAIDI is a measure of how many interruption hours an average customer will experience over the course of a year. For a fixed number of customers, SAIDI can be improved by reducing the number of interruptions or by reducing the duration of these interruptions

[20]. In words,

$$SAIDI = \frac{\sum \text{Customer interruption durations}}{\text{Total number of customer served}} \quad (3.63)$$

Mathematically,

$$SAIDI = \frac{\sum U_i N_i}{\sum N_i} \quad (3.64)$$

- (c) **Customer Average Interruption Duration Index (CAIDI):** It represents the average time required to restore service to the average customer per sustained interruption. CAIDI is a measure of how long an average interruption lasts, and is used as a measure of utility response time to contingencies [20].

$$CAIDI = \frac{\sum \text{Customer interruption durations}}{\text{Total number of customer interruptions}} \quad (3.65)$$

Mathematically,

$$CAIDI = \frac{\sum U_i N_i}{\sum \lambda_i N_i} \quad (3.66)$$

where, U_i is the annual outage time at load point 'i'.

- (d) **Customer Average Interruption Frequency Index(CAIFI):** This index gives the average frequency of sustained interruptions for those customers experiencing sustained interruptions. The customer is counted once regardless of the number of times interrupted for this calculation [20]. In words, the definition is:

$$CAIFI = \frac{\text{Total number of customer interruptions}}{\text{Total number of customers affected}} \quad (3.67)$$

Mathematically,

$$CAIFI = \frac{N_i}{CN} \quad (3.68)$$

where, CN refers to the number of customers who have experienced a sustained interruption during the reporting period.

- (e) **Average service availability index (ASAI):** This index denotes the fraction of time (often in percentage) that a customer has power provided during one year or the specified reporting period [20]. In words, the definition is:

$$ASAI = \frac{\text{Customer hours service availability}}{\text{Customer hours service demand}} \quad (3.69)$$

Mathematically,

$$ASAI = \frac{\sum N_i \times 8760 - \sum U_i N_i}{\sum N_i \times 8760} \quad (3.70)$$

where, N_i and U_i are the number of customers and annual outage time at the i^{th} load point respectively.

2. Energy and Load-oriented indices

One of the important parameters required to measure the energy and load-oriented indices is the average load at each load - point. The average load is expressed by:

$$L_a = L_p f \quad (3.71)$$

where L_p is the peak demand and f is the load factor.

The most commonly used energy and load oriented indices for DSRA are defined below.

- (a) **Average Energy Not Supplied (AENS):** It is the average energy not supplied per customer served per year by the system [20]. Mathematically,

$$AENS = \frac{\text{Total energy not supplied}}{\text{Total number of customers served}} = \frac{\sum L_{a(i)} U_i}{\sum N_i} \quad (3.72)$$

- (b) **Expected Energy Not Supplied (EENS):** It is the expected amount of energy that is not supplied per year at the load points due to an unexpected power outage in the system. The EENS can be utilized by the power utilities to perform an economic and reliability study of a power system [20]. Mathematically,

$$EENS = \sum L_{a(i)} U_i \quad (3.73)$$

where, $L_{a(i)}$ is the average load connected to load point 'i'.

3. Reliability Worth/Cost Indices

Reliability worth is usually quantified in the form of customer interruption costs (CIC). CIC provides an indirect measure of the monetary losses associated with a power outage and serves as input data for cost implications and worth assessments of system planning and operational decisions [153]. The estimation of CIC needs distribution reliability indices of the load points and customer interruption cost data. CIC data are compiled from customer surveys to develop a sector customer damage function (SCDF). The SCDF is a function of customer class and outage duration, which is used to estimate monetary loss incurred by customers due to power failure. The most commonly used reliability worth indices for DSRA are namely ECOST and IEAR. These are defined below.

- (a) **Expected Customer Interruption Cost (ECOST):** It is a measure of reliability worth of a power system. The ECOST is calculated by using the customer interruption cost (CIC) and load point reliability indices [153]. Mathematically,

$$ECOST = \sum L_{a(i)} \lambda_i N_f C_i(d_i) \quad (3.74)$$

where, N_f is the number of failed components responsible for system interruption, C_i is the cost of interruption and d_i is the duration of interruption at load point 'i'.

- (b) **Interrupted Energy Assessment Rate (IEAR):** It links system reliability with CIC. It is expressed in \$/kWh of unsupplied energy. The IEAR for the service area is evaluated as the ratio of ECOST to the total Loss of Expected Energy (LOEE) [153]. Mathematically,

$$IEAR = \frac{\sum L_{a(i)} \lambda_i N_f C_i (d_i)}{\sum L_{a(i)} \lambda_i N_f d_i} \quad (3.75)$$

The relation between ECOST and IEAR is:

$$ECOST = IEAR \times EENS \quad (3.76)$$

where EENS is the expected energy not supplied. This is sometimes referred as Loss of Expected Energy (LOEE).

3.6.2 Distribution System Reliability Indices Calculation

For a practical or large-size distribution system, reliability indices are to be calculated using computer algorithms. The work reported in chapter 5 uses MATLAB platform to evaluate the necessary reliability indices. In this section, a simple RDS is considered (Fig 3.7) to explain the calculation process of the indices.

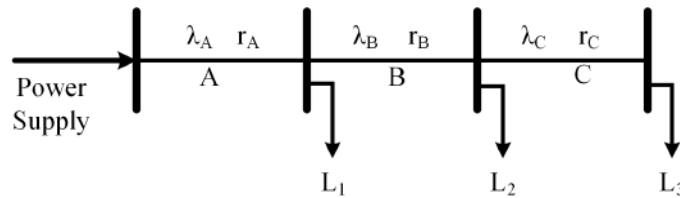


Fig. 3.7 Simple 3-load point RDS

The failure rates and repair times of each line A, B and C are given in Table 3.1 and the load-point reliability indices are presented in Table 3.2

Table 3.1 Component data for the system of Fig. 3.7

| Line | λ (f/yr) | r (hours) |
|------|------------------|-----------|
| A | 0.15 | 8.0 |
| B | 0.20 | 6.0 |
| C | 0.25 | 5.0 |

Table 3.2 Load-point reliability indices for the system of Fig. 3.7

| Load Point | λ_L (f/yr) | r_L (hours) | U_L (hours/yr) |
|------------|--------------------|---------------|------------------|
| L_1 | 0.15 | 8.0 | 1.20 |
| L_2 | 0.35 | 6.8 | 2.40 |
| L_3 | 0.60 | 6.1 | 3.65 |

The results for this example are evaluated using the basic concepts of series network illustrated in Section 3.3.1 and Equations (3.58)- (3.60). The failure of line elements A, B, C are simple open circuits with no compound effects, i.e., the failure of line element C does not effect L_1 or L_2 . This is the same as assuming perfect isolation of faults on line elements A, B and C.

Now, the evaluation of system performance indices can be explained by considering a portion of a distribution system having six load-point busbars. The number of customers and average load connected to these busbars are shown in Table 3.3.

Table 3.3 Details of the distribution system

| Load point | Number of Customers, N | Average load connected, L_a |
|------------|------------------------|-------------------------------|
| 1 | 1000 | 5000 |
| 2 | 800 | 3600 |
| 3 | 600 | 2800 |
| 4 | 800 | 3400 |
| 5 | 500 | 2400 |
| 6 | 300 | 1800 |
| Total | 4000 | 19000 |

Let us assume that four system failures occur in a given calendar year of interest, having the interruption effects shown in Table 3.4.

Table 3.4 Interruption effects in a given calendar year

| Interrupt-ion case | Load point affected | number of customers disconnected (N_C) | Load curtailed, (L_C) | Duration of interruption, d (hours) | Customer hours curtailed, $N_C d$ | Energy not supplied, $L_C d (kWh)$ |
|--------------------|---------------------|--|---------------------------|-------------------------------------|-----------------------------------|------------------------------------|
| 1 | 2 | 800 | 3600 | 3 | 2400 | 10800 |
| | 3 | 600 | 1800 | 3 | 1800 | 8400 |
| 2 | 6 | 300 | 1800 | 2 | 600 | 3600 |
| 3 | 3 | 600 | 2800 | 1 | 600 | 2800 |
| 4 | 5 | 500 | 2400 | 1.5 | 750 | 3600 |
| | 6 | 300 | 1800 | 1.5 | 450 | 2700 |
| Total | | 3100 | 15200 | | 6600 | 31900 |

$$\text{No. of customers affected} = 800 + 300 + 600 + 500 = 2200 = N_a$$

The information given in Tables 3.3 and 3.4 permits all the customer and load -oriented indices to be evaluated as shown below:

$$SAIFI = \frac{\sum N_C}{\sum N} = \frac{3100}{4000} = 0.775 \text{ interruptions/customer}$$

$$CAIFI = \frac{\sum N_C}{N_a} = \frac{3100}{2200} = 1.409 \text{ interruptions/customer affected}$$

$$SAIDI = \frac{\sum N_C d}{\sum N} = \frac{6600}{4000} = 1.65 \text{ hours/customer}$$

$$CAIDI = \frac{\sum N_C d}{\sum N_C} = \frac{6600}{3100} = 2.13 \text{ hours/customer interruption}$$

$$ASAI = \frac{\sum N \times 8760 - \sum N_C d}{\sum N \times 8760} = \frac{4000 \times 8760 - 6600}{4000 \times 8760} = 0.999812$$

$$ENS = \sum L_{Cd} = 31900 \text{ kWh}$$

$$AENS = \frac{\sum L_{Cd}}{\sum N} = \frac{31900}{4000} = 7.98 \text{ kWh/customer}$$

Based on the procedures illustrated above, computer algorithms are developed to solve complex networks. The above mentioned concepts are used in Chapter 5 of this thesis.

3.7 Reliability Test Systems

For power system reliability assessment, different researchers have put forward different methods. To provide a basis for comparing results obtained from various methods, it is desirable to have a reference or ‘test’ system that incorporates the basic data needed in reliability evaluation. For this purpose, the “IEEE Reliability Test System Task Force of the Application of Probability Methods Subcommittee” had prepared several standard test systems for power system reliability studies [154]. Out of those test systems, the Roy Billinton Test System (RBTS) and the distribution system connected to the Bus-2 of it, are used in this research work. A brief description of these two test systems is presented in the following sections.

3.7.1 Roy Billinton Test System (RBTS)

The RBTS is a six-bus composite reliability test system . It was developed for educational purposes at the University of Saskatchewan, Saskatoon, Canada, in 1989. It permits to conduct a large number of reliability studies with reasonable solution time. The details of RBTS are given in Billinton *et al.* [155]

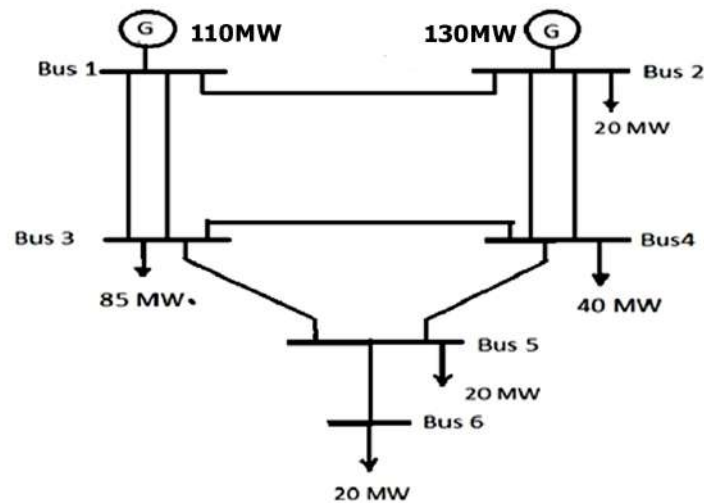


Fig. 3.8 Single-line diagram of RBTS

The single-line diagram of RBTS is given in Fig. 3.8. It has two generator buses and four load buses, nine transmission lines, and eleven generating units. The system voltage level is 230kV and the voltage limits for system buses are assumed to be between 1.05 p.u. and 0.97 p.u. The total installed generation in the system is 240 MW, and the peak load is 185 MW. The distribution network located at bus 3 has industrial, large user, office buildings, residential and commercial customers. Bus 5 has a distribution network with urban-type comprising of residential, government and institutional, office and buildings, and commercial customers. At bus 6, the distribution network is a rural network having agricultural, small industrial, commercial, and residential customers. Bus 2 has a generation system. The distribution network connected to this bus has residential customers, small users, governmental and industrial, and commercial customers. There are four radial feeders connected to this bus. Bus 4 also has the same type of customers as bus 2. The generating unit ratings and reliability data for the RBTS are given in Table A.1 in Appendix A.

3.7.2 RBTS Bus-2 Distribution System

The line diagram of the distribution network located at Bus 2 of the RBTS is shown in Fig. 3.9.

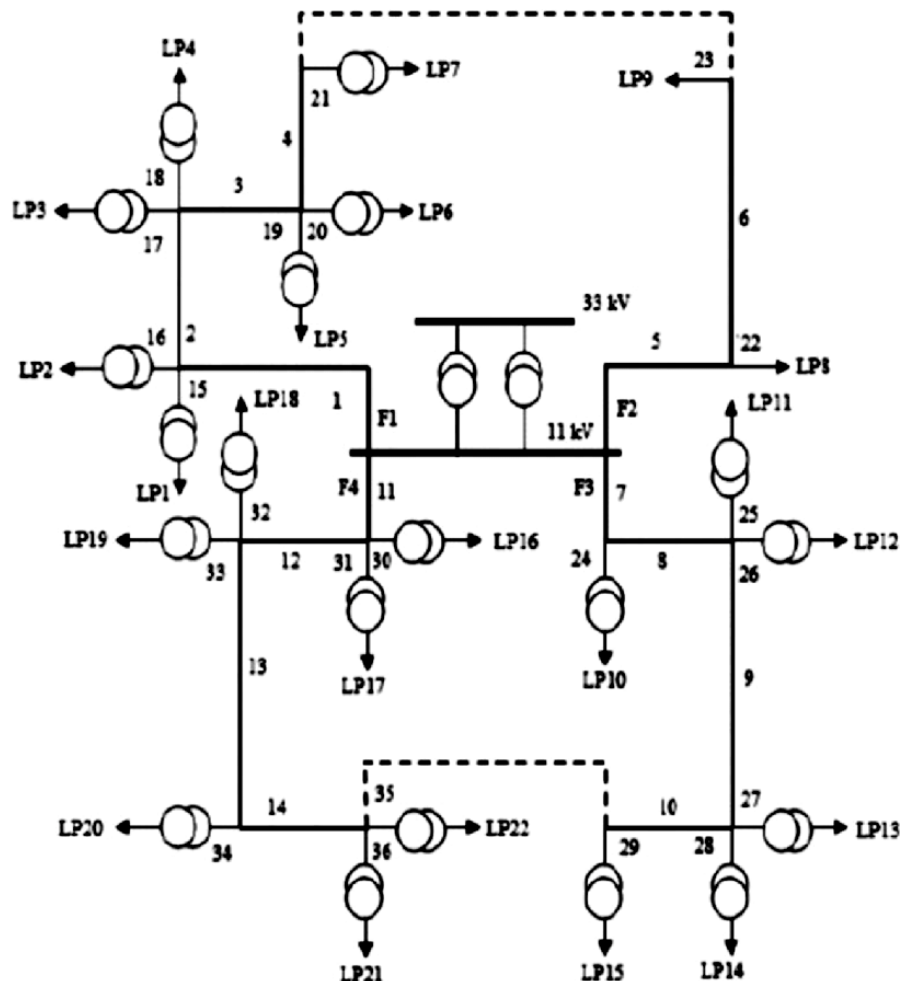


Fig. 3.9 Distribution System at Bus-2 of RBTS

The RBTS Bus-2 Distribution System consists of four radial feeders which supply power to residential customers, small users, governmental, industrial, and commercial customers. The peak load in this distribution system is 20MW, whereas the average load is 12.29MW. The 11 kV feeders are operated as radial feeders, although they are designed as a mesh through normally opened sectionalizing switches. The detailed description of the RBTS

Bus-2 distribution system is available in Refs. [6, 5]. The basic reliability data and other related information on this system are given in the Appendix A.

3.8 Conclusion

This chapter presents a brief description of the different methods and materials that are used in the remaining chapters of this thesis. Two basic reliability evaluation methods are used for system reliability evaluation: Well-being approach and Markov approach. In Chapter 4, the well-being approach is extensively used. Chapter-5 proposes a new technique of reliability evaluation embedding the well-being approach with Markov framework. Chapter 6 uses the well-being approach. On the other hand, Chapters 7 and 8 use the Markov approach. The Roy Billinton Test System and its reliability data are used in Chapter 4, whereas chapters 5 and 6 utilize the Bus-2 Distribution System of the RBTS. The basic reliability concepts presented in Sections 1.2-1.3 are used in Chapters 7 and 8 ■

4

Reliability-Centered Reserve Management in Deregulated Power System

4.1 Introduction

The thrust toward deregulation and delicensing of the electric utility industry has brought significant transformation in modern power systems [156]. Due to deregulation of power distribution, entry barriers for private players for creating competition in the power market are reduced, which enables consumers to purchase the capacity reserve directly from the preferred energy providers based on their reliability levels [1]. This chapter presents an approach to analyze how capacity reserve management in a deregulated environment is done based on consumers' reliability satisfaction. The impact of operating reserve on customer load point reliability is examined. The well-being framework has been applied to develop a reliability-based market model. The proposed concepts have been exemplified in RBTS.

4.1.1 Principle of Operating Reserve

The reliability standard of power supply is traditionally established as a series of technical requirements. In general, reliability requirements are met by providing a group of services, known as ancillary services, which are necessary to protect the system's integrity and guarantee the generation and delivery of electric power throughout the electric grid [16]. These ancillary services include coordinated system operation, frequency regulation, energy balance, and voltage support and generation reserves [157]. In power system operation, scheduling of reserve generation is crucial in order to account for load forecast uncertainties and possible unplanned outages of generation units. Once this capacity is scheduled and spinning, the operator is committed for the period of time it takes to achieve output from other generating units. This time may be of several hours in the case of thermal units but only a few minutes in gas turbines and hydro plants [20].

The reserve capacity that is spinning, synchronized and ready to take up load is generally known as spinning reserve [36]. Some utilities include only this spinning reserve in their system adequacy assessment. Some utilities also include one or more of the following factors: rapid start units such as gas turbines and hydro plants, interruptible loads, assistance from interconnected systems, voltage and /or frequency reductions. These additional factors add to the effective spinning reserve, and the total entity is known as operating reserve [20].

Initially, the concept of the operating reserve was primarily to meet the uncertain load fluctuations in a power system. During off-peak hours, the reserve margin in a system tends to be maximum, whereas, during the peak-load hours, the reserve drops significantly, and sometimes it even becomes negative. Under a negative reserve scenario, some load points must be curtailed, resulting in a severe impact on system reliability. To sustain the power supply reliability at a satisfactory level, the reserve must sufficiently be large during the entire operating period. The purpose of a reliability-centered operating reserve is not only to

satisfy system load under normal operating conditions but also to meet that load even if any fault or unplanned outage occurs in the generating units during the peak or off peak period.

Historically, the size of the operating reserve has been determined by ad hoc or rule-of-thumb methods [20]. The most frequently applied method is that the reserve capacity should be at least equal to the largest generating unit in the system so that even if the largest generator fails the deliver power, the power supply in the system remains uninterrupted [1]. However, this method cannot account for all system parameters. In the operational phase, It may lead to over-scheduling which, although more reliable, is uneconomical, or to under-scheduling which, although less costly to operate, can be very unreliable [20].

A more consistent and realistic method for reserve allocation would be one based on probabilistic methods [21]. A risk index based on such methods enables a consistent comparison to be made between various operating strategies and the economics of such strategies. The acceptable risk level is determined using a deterministic criterion set by operators based on economic and social requirements [20]. A reasonable level can be estimated by evaluating the probabilistic risk index associated with existing operational reserve management techniques. Once a risk level has been defined, sufficient reserve capacity can be scheduled to satisfy that risk level.

4.1.2 Operating Reserve in Conventional Power System

In a conventional, vertically integrated power system (VIPS), the utilities have complete control over all activities in generation, transmission and distribution of power [23]. The allocation and size of operating reserves are centrally managed in such systems to meet the requirements of certain system performance standards [156]. The required reliability level is determined by the system operator under the premise that the customers connected to different load points share the same service reliability levels. The reliability criteria used in this structure are mostly either deterministic or probabilistic. The decision on the size

and scheduling of operating reserve is taken based on a suitable deterministic criterion, while the system risk indices are evaluated using probabilistic criteria [156]. The common deterministic criteria include "Percentage of Peak Load" or "Loss of Largest Unit". Risk indices are mainly "Loss of Load Expectation (LOLE)" and "Loss of Load Probability (LOLP)" [20].

Uniform reserve margin for all types of customers is one of the main drawbacks of a VIPS. An industrial or commercial customer usually requires the highest possible reliability of power supply and is always ready to pay a higher price for a higher reliability margin. However, such a higher reliability margin may not be the requirement of some residential or agricultural customers. It is because they may not afford or may be reluctant to pay for a higher reserve margin. System operators cannot provide the highest reliability margin to all customers due to economic constraints. They also cannot keep the reliability level too low to take care of the residential or agricultural consumers' cost concerns, as it will affect other consumers like industrial or commercial consumers. Therefore, the system operators always face problems in making a trade-off between reliability and cost. This issue is alleviated in a deregulated power system (DPS).

4.1.3 Operating Reserve in Deregulated Power System

The advent of deregulation in the power system has initiated the transition of centralized, monopolistic systems towards a competitive market structure of unbundled generation, transmission, and distribution services [21, 18]. Due to delicensing, the entry barriers for private players for creating competition in the power market are now reduced [17]. Customers can select the energy providers with their own choice. They can purchase power at their preferred reliability levels. Thus, the reliability levels are different at different bulk load points (BLP) in the system. The different reliability levels set by customers can be accomplished by purchasing different capacities of operating reserves. Similarly, the size of the operating

reserve in the agreements can be determined depending on the reliability level demanded by customers. Furthermore, the cost of the reserve capacity can be defined depending on the reliability margin specified by customers.

As reported in Chapter 2 (Section 2.5.1), the reliability-centric operating reserve assessment was not discussed much in the existing literature, particularly for DPS. This chapter presents a probabilistic approach to preparing an operating reserve schedule considering reliability as a constraint. It aims to analyze the impact of operating reserve on customer load point reliability. Some load point reliability indices are introduced for customers to realize their reliability levels. The well-being framework used in VIPS is extended to assess the BLP reliability under deregulated environment. The presented concepts have been demonstrated by conducting two case studies, namely (a) considering the RBTS as a VIPS and (b) considering the RBTS as a DPS.

4.2 Methodology

How much capacity is to be kept as the operating reserve is a deterministic criterion. This criterion is centrally set by the system operator in a VIPS. However, in DPS, the deterministic criteria are selected based on the customer reliability specifications. Depending on the reserve size, system reliability is defined in terms of some probabilistic performance metrics. The well-being analysis technique recognizes that the system operating states created by incorporating the deterministic criteria can be categorized as healthy, alert, and at risk. The probabilities of being in the healthy, alert, and at risk states, i.e., $p(H)$, $p(A)$, and $p(R)$ are designated as the well-being indices. The principle of well-being framework has been discussed in detail in Section 3.5 of the previous chapter.

Figure 4.1 presents the proposed well-being model of a power system for capacity reserve management studies. The system has sufficient reserve capacity in the healthy state to maintain the reliability of the power supply at the pre-specified level. In the alert state, the

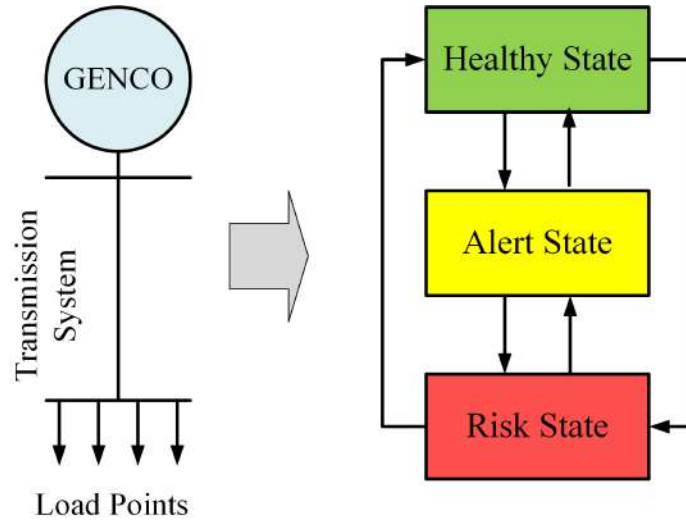


Fig. 4.1 System Well-being Model

reserve capacity is positive; however, the system reliability is less than the desired value. On the other hand, in the risk state, the reserve capacity is negative, i.e., generation is less than the demand, and therefore, the load must be curtailed at some of the load points in the system. The steps to evaluate the system state probabilities are given below:

- **Step 1:** Read the system information i.e. number of generating units, capacity and forced outage rate (F.O.R) of each unit. Also read the contingencies (Units' UP or DOWN states) as well as system load.
- **Step 2:** Find the probability and available capacity for each contingency state. Set the specified operating reserve (SOR).
- **Step 3:** Determine the reserve margin (RM) for each contingency state as,

$$\text{Reserve Margin} = \text{Available capacity} - \text{System load}$$
- **Step 4:** For each state,
 If $RM \geq SOR$, assign the state as healthy state.
 If $0 \leq RM < SOR$, assign the state as alert state.
 If $RM < 0$, assign the state as risk state.
- **Step 5:** Determine the probability of occurrence of each state and Calculate the well-being indices as follows:

$$p(H) = \sum(\text{Healthy state probability})$$

$$p(A) = \sum(\text{Alert state probability})$$

$$p(R) = \sum(\text{Risk state probability})$$

• **Step 6:** Stop

Once the probabilities $p(H)$, $p(A)$, and $p(R)$ are evaluated, the required reserve capacity can be determined to satisfy the single criterion or multiple criteria given below.

1. **Single Criteria:** When the single criterion is used it means that the capacity reserve must be maintained in such a way that the probability of system being in the risk state cannot be greater than the specified risk level.

$$p(R) \leq Sp(R) \quad (4.1)$$

where $Sp(R)$ is the specified risk probability for the system.

2. **Multiple Criteria:** It stresses at satisfying more than one deterministic conditions set by the consumers and operators. Both healthy and risk state probabilities are maintained at acceptable levels by DISCOs purchasing more capacity reserve from different GENCOs.

$$p(H) \geq Sp(H), \text{ and } p(R) \leq Sp(R) \quad (4.2)$$

where $Sp(H)$ is the specified healthy state probability for the system.

The most common deterministic criterion for determining the system well-being indices states that the reserve capacity in the system should be greater than or equal to the capacity of the largest generating unit. However, in a deregulated power market, this thumb rule is not useful. In this study, a new performance index is introduced, which is treated as a deterministic criterion to predict the system's well-being under deregulated environment. The proposed index is termed as 'Capacity Reserve Availability Index (CRAI)' and it is defined as the ratio of the system reserve margin to the total available capacity in the system. Mathematically,

$$\%CRAI = \frac{\text{Available Capacity} - \text{Load}}{\text{Available Capacity}} \times 100\% \quad (4.3)$$

Based on the consumers' reliability requirements, the distribution companies (DISCOs) set the value of CRAI for the generation companies (GENCOs). Accordingly, the GENCOs generate the required power and maintain the desired reserve margin. The flowchart for determining the operating reserve for maintaining the reliability within a margin defined by single or multiple criteria is shown in Fig. 4.2.

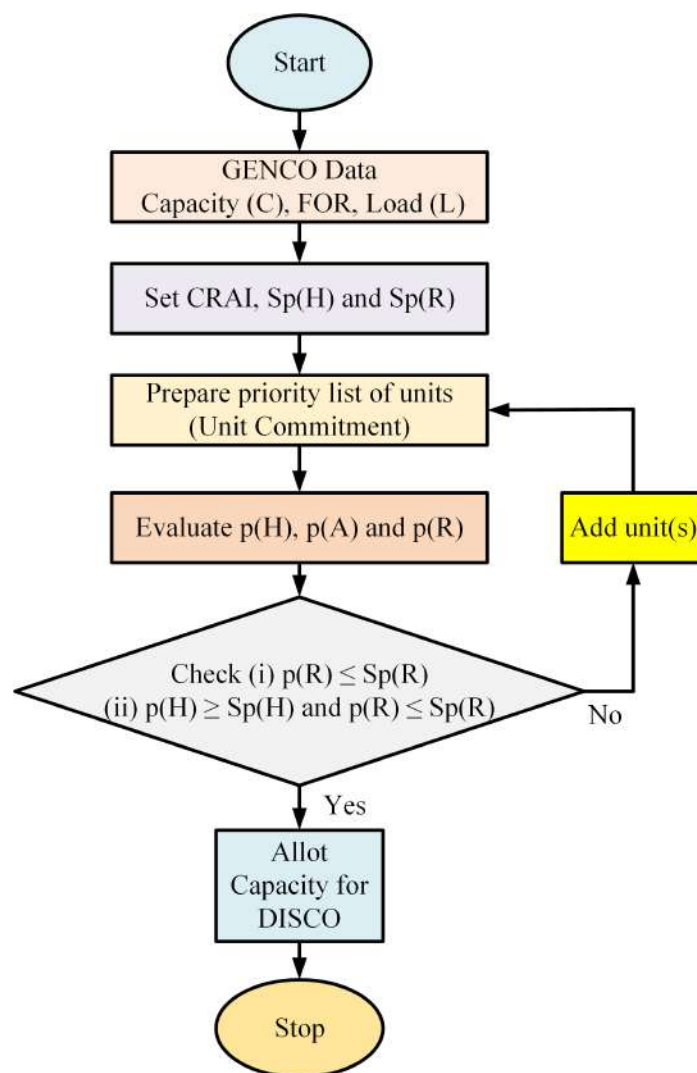


Fig. 4.2 Flowchart for determination of operating reserve

Customers select the potential energy providers based on their requirements. They present their required reliability levels of $p(H)$ and $p(R)$ to the service provider. DISCOs determine the capacity reserve required to fulfill the reliability level presented by consumers. The

DISCOs arrange the operating reserve through agreements with different GENCOs. This renders customers to have full right to select the energy and reserve providers. After making transactions, the GENCOs have an obligation to satisfy customers' reliability requirements. If the transactions are not entirely fulfilled, any associated penalty may also be written into the transactions.

4.3 Description of the Test System

The concepts illustrated in the previous section have been exemplified in the Roy Billinton Test System (RBTS). The single-line diagram of RBTS is shown in Fig. 4.3.

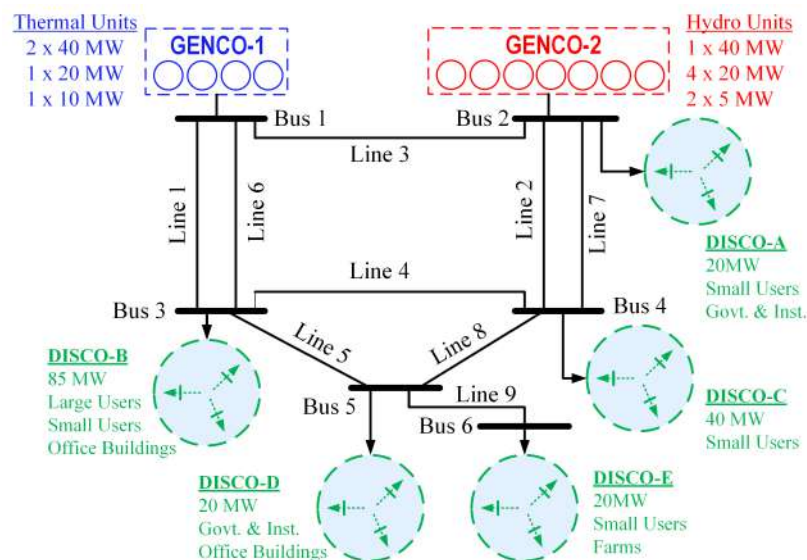


Fig. 4.3 Single-line diagram of RBTS

GENCO 1 consists of two 40MW, one 20MW, and one 10 MW thermal units. These units feed power at Bus 1 of RBTS. GENCO 2 is located at Bus 2. It comprises one 40MW, four 20MW, and two 5 MW hydro units. The bulk load points (BLP) at Bus 2-6 have five different distribution companies (DISCO). DISCO-A supplies 20MW powers to small users and Govt. and institutions at Bus 2. DISCO-B supplies 85MW power to small, large, and office buildings. DISCO-C supplies 40MW power to small users of Bus-4. DISCO-D draws

power from Bus 5 and supplies 20MW power to Govt. and institutions, and office buildings. DISCO-E is located at Bus 6, which delivers 20 MW of power to farms and small users.

The failure and repair information of the generating units of GENCO-1 and GENCO-2 of the RBTS are listed in Table A.2 (Appendix A). Generating units are considered to remain either in operating state (UP) or failed (DOWN) state at a particular time. The unit commitment is done according to the priority loading order given in Table A.2 (Appendix A).

4.4 Case Studies

In this section, the concept of reliability-centered reserve management is quantitatively analyzed by considering the RBTS as a vertically integrated system first, and then as a deregulated power system. It is assumed that the customers connected at the same load point are of the same load type. The transmission system is assumed to be 100% reliable and only the conditions of the generating units are considered. The generating units are assumed to be either in operating (up) state or failed state at a particular time.

4.4.1 Considering RBTS as a Vertically Integrated System

The well-being model of a vertically integrated RBTS is presented in Figure 4.4. As mentioned earlier, in a VIPS, the system reliability level is decided by the system operator, and it remains common for all customers. The combined capacity of all generating units of GENCO-1 and GENCO-2 are utilized centrally to serve the entire system load of 185MW. The transmission utilities do not have any role in ORM. Transmission lines are taken as 100% reliable. Since, the distribution companies (DISCOS) do not have any control over the ORM in VIPS, therefore, the DISCOs can be treated as the bulk load points (BLP). There are five BLPs in the RBTS, as shown in Fig 4.3. To carry out the analysis, the deterministic criteria,

namely, specified risk probability, $Sp(R)$ and the specified healthy state probability, $Sp(H)$ are assumed to be 0.01 and 0.9, respectively.

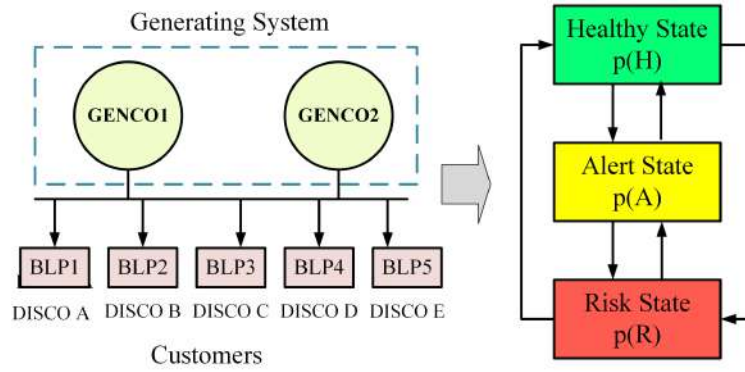


Fig. 4.4 Well-being model for Vertically integrated RBTS

Table 4.1 shows the required number of committed units for different load levels and the corresponding probabilities of different operating states when a specified risk of 0.01 is selected as a unit commitment single criterion. The unit is selected according to the priority loading order defined in Table A.2 in Appendix A.

Table 4.1 System well-being indices for unit commitment using single criterion

| Load Level (MW) | No. of units committed | Generating Capacity (MW) | Operating Reserve (MW) | p(H) | p(A) | p(R) |
|-----------------|------------------------|--------------------------|------------------------|----------|----------|----------|
| 185.0 (100%) | 9 | 230 | 45.0 | 0.838425 | 0.152567 | 0.009007 |
| 166.5 (90%) | 8 | 210 | 43.5 | 0.851020 | 0.141039 | 0.007940 |
| 148.0 (80%) | 7 | 190 | 42.0 | 0.863805 | 0.129325 | 0.006869 |
| 129.5 (70%) | 6 | 180 | 50.5 | 0.885953 | 0.109008 | 0.005038 |
| 111.0 (60%) | 5 | 160 | 49.0 | 0.895083 | 0.100630 | 0.004286 |
| 92.5 (50%) | 5 | 160 | 67.5 | 0.921976 | 0.075947 | 0.002076 |

In Table 4.1, it is observed that the system risk probabilities for all the different load levels satisfy the specified risk criterion. Therefore, the operator can fix the operating reserve schedule as per Table 4.1. However, this schedule does not satisfy the specified multiple criteria as the $p(H)$ values are less than 0.9 for 60% of system load and above. Therefore, the system operators must run additional generator(s) to satisfy the multiple criteria.

Table 4.2 presents the unit commitment schedule to satisfy the multiple criteria, i.e., $p(H) \geq 0.9$ and $p(R) \leq 0.01$, at different loading conditions. When the system load is 90% of the peak load (185MW), the operating reserve must be at least 63.5MW to fulfill both healthy state and risk criteria. For this, nine generating units must be committed to meet the load and maintain the operating reserve following the priority loading order. Table 4.2 shows that the well-being indices of the entire system are highly improved for each load level due to the increase in operating reserve. The healthy state probabilities, $p(H)$ for all the different load levels, except the system peak load (185MW), satisfy both the risk as well as healthy state criteria. It is found that the system does not meet the healthy state criterion at the peak load, even with its maximum capacity of 240MW. Therefore, the operator must purchase additional reserves from other GENCOs to meet the healthy state criteria at the system peak load.

Table 4.2 System well-being indices for unit commitment using multiple criterion

| Load Level (MW) | No. of units committed | Generating Capacity (MW) | Operating Reserve (MW) | $p(H)$ | $p(A)$ | $p(R)$ |
|-----------------|------------------------|--------------------------|------------------------|----------|----------|----------|
| 185.0 (100%) | 11 | 240 | 55.0 | 0.859921 | 0.132880 | 0.007198 |
| 166.5 (90%) | 9 | 230 | 63.5 | 0.918944 | 0.078729 | 0.002326 |
| 148.0 (80%) | 8 | 210 | 62.0 | 0.919964 | 0.077793 | 0.002242 |
| 129.5 (70%) | 7 | 190 | 60.5 | 0.920808 | 0.077019 | 0.002172 |
| 111.0 (60%) | 6 | 180 | 69.0 | 0.921701 | 0.076199 | 0.002099 |
| 92.5 (50%) | 5 | 160 | 67.5 | 0.921976 | 0.075947 | 0.002076 |

To maintain a high-reliability level, the reserve margin should be increased, which results in an increase in the price of electricity. Customers who may not need such a high reliability level and/or not willing to pay such costs will have no other choice because the system reliability is determined and maintained by system operators. This is one of the main issues in VIPS. With deregulation, this problem can be solved.

4.4.2 Considering RBTS as a Deregulated System

In deregulated power market, electricity is treated as a commodity. The deregulation provides customers more choices in selecting the power suppliers (DISCOs). The DISCOs purchase power from GENCOs, fulfilling the economic and reliability constraints. The system operator provides a range of reliability options for customers instead of a predefined fixed reliability criterion for operation. The power transactions in deregulated market is shown in Fig.4.5.

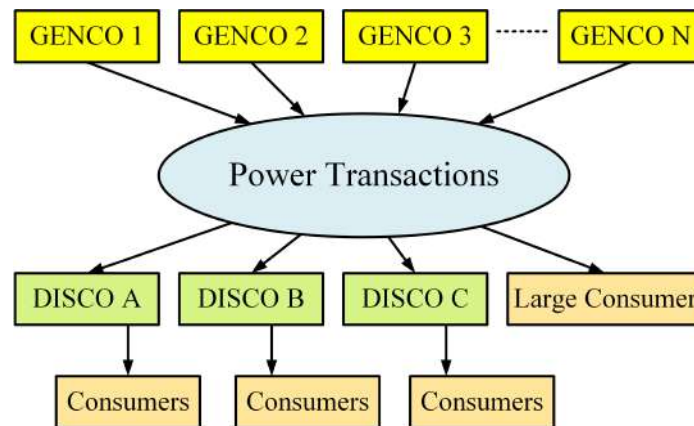


Fig. 4.5 Power transactions in deregulated market

Based on the consumers' reliability requirements, the DISCOs set the value of CRAI for GENCOs, and accordingly, the GENCOs generate the required power and maintains the desired reserve margin.

To demonstrate the concept, the RBTS is considered as a deregulated system. The total generated power is now produced by two different generation companies: GENCO 1 and GENCO 2. Their operations are independent of each other. Both of them prepare their own reserve schedules for their customers. GENCO 1 primarily supplies power to DISCO B only. On the other hand, all other DISCOs prefer GENCO 2 as their electricity provider. Assuming the system load to be fixed at 85 MW for DISCO B, the system well-being indices $p(H)$, $p(A)$, and $p(R)$ are calculated under different reserve capacity and generation schedules.

The variation of CRAI under different generating capacities is shown in Fig. 4.6. The system well-being indices for a set of three different reserves are given in Table 4.3

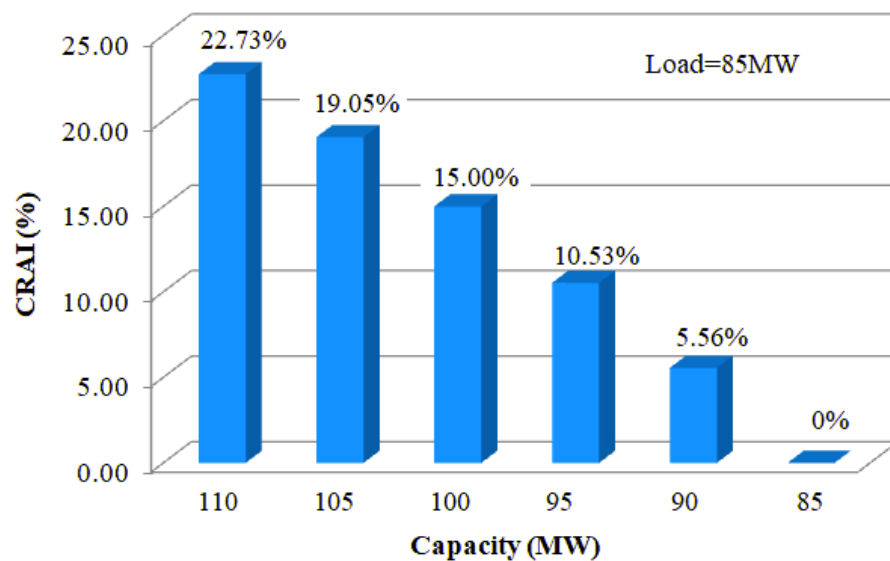


Fig. 4.6 CRAI at different capacities of GENCO 1

Table 4.3 Well-being indices for DISCO B with different reserves allocation

| Load (MW) | GENCO Capacity (MW) | Reserve (MW) | p(H) | p(A) | p(R) |
|-----------|---------------------|--------------|------|----------|----------|
| 85 | 110 | 25 | 0 | 0.940854 | 0.059146 |
| 85 | 100 | 15 | 0 | 0.931495 | 0.068505 |
| 85 | 90 | 5 | 0 | 0.917567 | 0.082433 |

As GENCO 2 has a maximum capacity of 130 MW, and total demand from DISCO A, C, D, and E is 100 MW, so the maximum value of reserve is 30MW. Thus, the GENCO-2 can offer CRAI in the range of 0 to 23.08% to its DISCOs. The value of CRAI at different CRAI is given in Fig. 4.7.

Table 4.4 shows the values of $p(H)$, $p(A)$ and $p(R)$ for the consumers of DISCOs A, C, D and E under different reserves. The load is assumed to be constant at 100MW. The maximum generation capacity of GENCO 2 is 130MW which is shared among the DISCOs.

From Tables 4.3 and 4.4, it is observed that the probabilities of being at risk state increases with the decrease in reserves. The healthy state probability is zero in both cases. If the customers demand a specified risk level of $p(R) \leq 0.01$, (single criteria) the DISCOs must purchase additional reserve from other neighboring GENCOs.

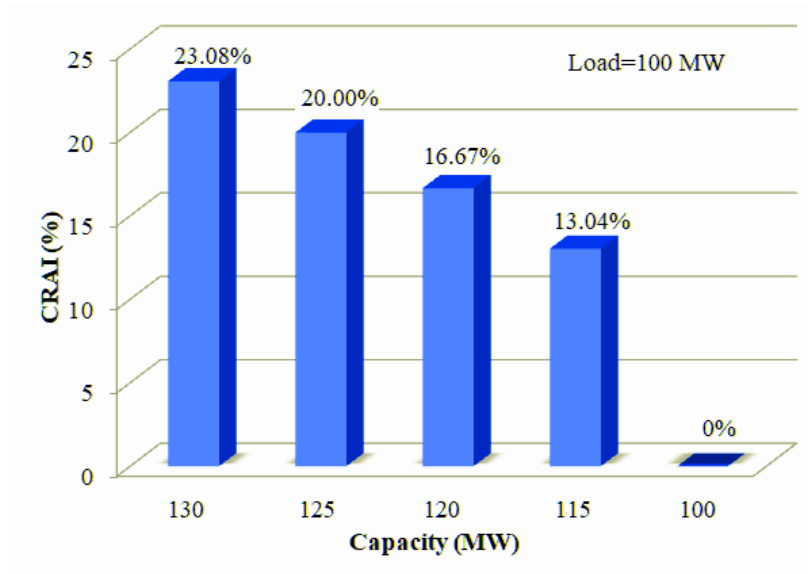


Fig. 4.7 CRAI at different Capacity of GENCO 2

Table 4.4 Well-being indices with different capacity reserves allocation at GENCO 2

| Load (MW) | GENCO Capacity (MW) | Reserve (MW) | p(H) | p(A) | p(R) |
|-----------|---------------------|--------------|------|----------|-----------|
| 100 | 130 | 30 | 0 | 0.978637 | 0.021363 |
| 100 | 125 | 25 | 0 | 0.978636 | 0.021364 |
| 100 | 120 | 20 | 0 | 0.937033 | 0.062967 |
| 100 | 110 | 10 | 0 | 0.937032 | 0.062968 |
| 100 | 100 | 0 | 0 | 0.937030 | 0.0629670 |

If the customers are ready to purchase power at a risk level of 0.1 , i.e., $Sp(R) \leq 0.1$, then the reserve schedules of Tables 4.3 and 4.4 can be fixed for operation. However, if some customers, e.g., farms, govt. institutions or office buildings require higher reliability levels and bid to purchase power with $Sp(H) = 0.9$, the GENCO 1 and GENCO 2 will not be able to fulfill the customers, demand demand [as $p(H)=0$ in Tables 4.3 and 4.4]. In this case, the DISCOs must contract with other GENCOs and arrange the required reserve for their customers.

Suppose, DISCO-B makes an agreement to purchase 30MW power from GENCO2. Due to this transaction, the DISCO B will now be able to offer a $p(H)$ of 0.9177063403 and $p(R)$ of 0.0023356995 to its consumers, satisfying the multiple criteria of $Sp(H)=0.9$ and

$Sp(R)=0.01$. The probabilities of falling to alert and risk states significantly get reduced due to the additional reserve procurement. The improvement in the well-being indices due to the 30MW transaction is shown in Table 4.5.

Table 4.5 Well-being indices after the reserve agreement between DISCO B and GENCO 2

| Purchased reserve (MW) | p(H) | p(A) | p(R) |
|------------------------|--------------|--------------|--------------|
| 0 | 0.0000000000 | 0.9408540310 | 0.0591459690 |
| 30 | 0.9177063403 | 0.0799579601 | 0.0023356995 |

Similarly, suppose, DISCO A, C, D, and E make an agreement with GENCO 1 to purchase 20MW power for its consumers. Under this scenario, the p(H) value increases to 0.9137488004, which is well ahead of the specified value of 0.9. Due to the addition of 20 MW CR, p(A) and p(R) values also reduce to 0.0848689712 and 0.0013822284, respectively. The improvement in the well-being indices due to the 20MW transaction is shown in Table 4.6.

Table 4.6 Well-being indices after the CR agreement between DISCO A,C-E and GENCO 1

| Purchased reserve (MW) | p(H) | p(A) | p(R) |
|------------------------|--------------|---------------|--------------|
| 0 | 0.0000000000 | 0.9786374482 | 0.0213625518 |
| 20 | 0.9137488004 | 0.08486889712 | 0.0013822284 |

Tables 4.5 and 4.6 show that operating reserve agreements among the DISCOs and GENCOs help in fulfilling both single as well as multiple deterministic criteria set by operators and customers. The overall system can be operated at different reliability levels. The load patterns are different for different customer classes, which helps operators to schedule different reserves for different types of customers. The GENCO, which requires supplying power to customers who want low-cost power and do not require high reliability, can sell additional reserves to other DISCOs needing high-reliability power. Setting a high-reliability target or lower risk level will increase the cost of operating reserve. It is, therefore, necessary to maintain an equilibrium between reliability and price in a deregulated system.

4.5 Conclusion

This chapter has made an effort to carry out a reliability assessment for operating reserve management. A probabilistic approach has been presented to prepare operating reserve scheduling in a deregulated environment. In a deregulated system, capacity reserve management is much more complicated than a vertically integrated system. The energy providers are required to supply electricity at a customer-specified reliability range. The features of the reserve agreements provide customers with more options to select the energy provider. If customers want to pay less for operating reserve, they will get less reliable electricity service. In contrast, the high reliability of electricity service will require customers to pay more. Customers can decide their own reliability levels. The concepts presented in this chapter are expected to complement the current researchers and help operators make proper reserve management decisions.

The emergence of renewable distributed generation has made reserve capacity management much simpler. Distributed energy providers can supply the required reserve margin to the DISCOs at the demand side itself. The next chapter is directed at this topic. It will analyze how renewable energy integration impacts system reliability and customer interruption costs in a distribution network.

5

Reliability Modeling and Worth Analysis of a Renewable Energy Incorporated Distribution Network

5.1 Introduction

In the previous chapter, the reported research is directed at determining the operating reserve requirement to satisfy the customer-specific reliability demand in a deregulated power system. This chapter discusses how a coordinated operation of multiple renewable energy sources (RESs) increases the adequacy of the system at considerably lower costs and enables utilities to provide higher service reliability to consumers through smart utilization of the operating reserve.

As explained in chapter 2, a distribution system (DS) is a critical zone in an electrical power system (EPS). It links the bulk system with consumers. In most cases, the structure of the links is radial which makes them susceptible to power outage due to even a single fault event [6]. Statistics show that failures in a DS contribute as much as 85% toward the unavailability of power supply as compared with other parts of EPS [99]. With the integration of distributed generators at some strategic locations of a DS, customer interruptions can be reduced. In addition to this, there are some other methods to minimize the frequency and duration of the interruption, such as network reconfiguration [158, 159], component reliability improvement, rigorous and fast maintenance, etc. However, these methods can contribute to enhancing the system reliability up to a certain extent only. Increasing the size of reserve margin utilizing renewable energy sources is regarded as one of the most convenient and efficient way to improve the power supply reliability in an active distribution network (ADN) [88, 92].

This chapter aims to cover this aspect. To investigate the impact of renewable distributed generation on the reliability of an ADN, three RESs, namely, solar, wind, and tidal energy sources, are connected at three different locations of a radial distribution network (RDN). Following are some of the major contributions of the study covered in this chapter.

- Investigation of reliability and worth of an ADN integrated with solar-wind-tidal energy sources.
- Development of a new approach for quantitative reliability assessment of a system consisting of multiple renewable energy sources.
- Development of two new metrics, namely, "Incremental Energy Benefit (IEB)" and "Incremental Cost Benefit (ICB)", to estimate reliability worth/cost due to the addition of solar, wind, and tidal generations.
- Parameter "Degree of Cleanliness" has been developed to incorporate dust factor in solar power generation.

5.2 Reliability of Active Distribution Network

As stated in Section 2.5.3, modern distribution networks are mostly active networks which not only transmit power but also generate power at strategic locations using small, scattered and preferably renewable power generating units [79]. As shown in Fig. 5.1, the reliability of an ADN is dictated by two factors: (a) adequacy of power supply and (b) reliability of the power carrying network. The adequacy of the power supply depends on the amount of the system's operating reserve, i.e., how much generation is kept as reserve to meet the system load during contingencies. In contrast, the reliability of the power distribution network refers to its ability to provide the generated power to the load points (LPs) with the least possible interruptions. It mostly depends on the network topology, component's time-to-failure (TTF), and time-to restore (TTR). In this study, the ADN under consideration is of radial configuration, which is primarily powered by solar, wind, and tidal energy sources. The reliability of this hybrid generation scheme or system (HGS) is evaluated by introducing a new approach that integrates the Markov Framework with Well-being Framework. For the distribution network (DN), the existing reliability indices, namely, SAIFI, SAIDI, CAIDI, AENS, EENS, ECOST, and IEAR are evaluated and analyzed. Two new metrics are designed in Section 5.4 to measure the energy and cost benefits from the RESs. The mathematical modelings for reliability assessment of the ADN are presented in Sections 5.3 and 5.4.

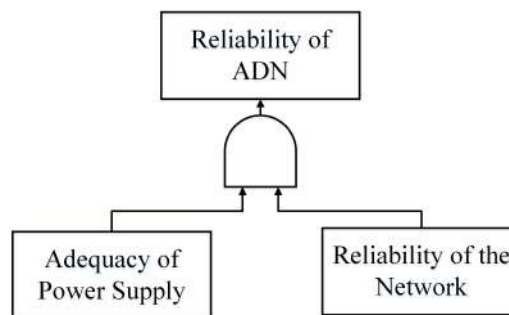


Fig. 5.1 Subdivision of ADN reliability

5.3 Power Generation Model under consideration

The proposed generation scheme consists of a solar power plant (SPP), a wind power plant (WPP), and a tidal power plant (TPP), as shown in Fig. 5.2. The load points' power demand is met primarily by these three renewable plants. However, during abnormal operating conditions or faults in these plants, the network can draw the necessary power from the adjacent grid. The power generation models of SPP, WPP, and TPP are developed in Sections 5.3.1-5.3.3. The renewable HGS's reliability model is developed in Section 5.3.4.

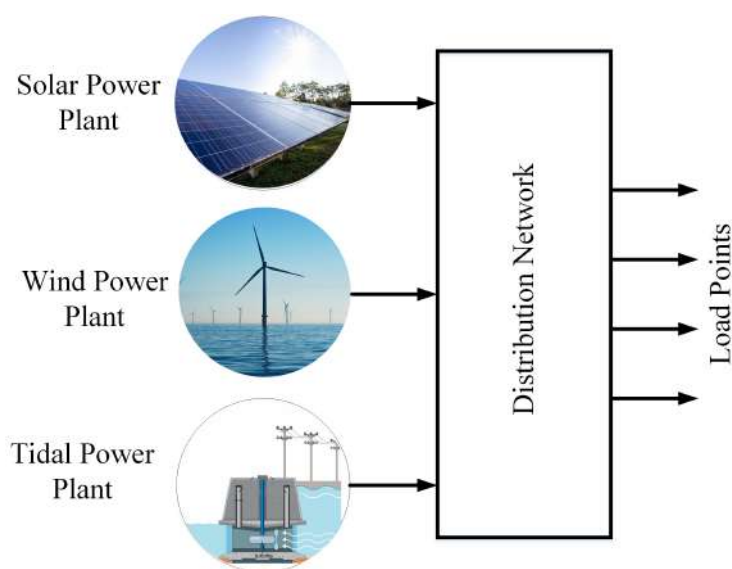


Fig. 5.2 Abstract model of the system under consideration

5.3.1 Modeling of Solar Power Generation

The power generated by a SPP depends on solar irradiation, temperature, weather condition, and degree of cleanliness of the solar panel surface as follows:

- **Solar irradiation:**

The solar irradiation intensity tends to attenuate as it propagates away from the sun's surface, though the wavelengths remain constant. The extraterrestrial irradiation differs

from the solar constant (G_{std}) because of two reasons. The first is the variation in the irradiation emitted by the sun itself. The variation due to this reason is less than 1.5% with different periodicities. The second is the variation (approximately 3%) of the earth-sun distance arising from the earth's slightly elliptic path [160]. The extraterrestrial irradiation in kW/m^2 can be determined using Equation (5.1).

$$G_{ext} = G_{std} \left[1 + 0.033 \cos \left(\frac{360n_d}{365} \right) \right] \quad (5.1)$$

where, n_d is the number of the day in one year. The terrestrial radiation is affected by the changes in atmospheric conditions. The real solar irradiation G_0 that would fall on the surface of the PV panel at a specific geographic location is given by

$$G_0 = G_{ext} \cos \theta_i \quad (5.2)$$

Here, θ_i is the solar incident angle which is calculated using Equation (5.3),

$$\begin{aligned} \cos \theta_i = & (\cos \phi \cos \beta + \sin \phi \sin \beta \sin \omega) \cos \delta \cos \omega + \cos \delta \sin \omega \sin \beta \sin \gamma \\ & + \sin \delta (\sin \phi \cos \beta - \cos \phi \sin \beta \cos \gamma) \end{aligned} \quad (5.3)$$

where, ϕ is the latitude of PV location, δ is the solar declination i.e., the angular displacement of the sun from the earth's equator, β is the slope or tilt angle of the PV panel, ω is the solar hour angle, and γ is the surface azimuth angle.

For a surface facing due south, $\gamma = 0$,

$$\cos \theta_i = \cos(\phi - \beta) \cos \delta \cos \omega + \sin \delta \sin(\phi - \beta) \quad (5.4)$$

For a horizontal surface, $\beta = 0$, $\theta_i = \theta_z$ (zenith angle)

$$\cos \theta_i = \cos \theta_z = \cos \phi \cos \delta \cos \omega + \sin \delta \sin \phi \quad (5.5)$$

For a vertical surface facing due south $\gamma = 0$; $\beta = 90^\circ$

$$\cos \theta_i = -\sin \delta \cos \phi + \cos \delta \cos \omega \sin \phi \quad (5.6)$$

- **Temperature:**

Temperature is an important factor which impacts the PV output. The variation in temperature in a specific day can be expressed as sine function [4] as follows:

$$T = A \sin \omega + B \quad (5.7)$$

where ω is the solar hour angle and

$$A = \frac{T_{max} - T_{min}}{2} \quad (5.8)$$

$$B = \frac{T_{max} + T_{min}}{2} \quad (5.9)$$

where T_{max} and T_{min} are the maximum and minimum temperatures on a particular day, respectively.

- **Weather effect:**

The weather condition can be classified into four main categories, namely, shiny, cloudy, overcast and rainy. Comparing the attenuation tendency data of PV output power under cloudy, overcast and rainy with the standard condition in summer, the weather effect coefficient can be determined [4]. Although the weather variations are different in four seasons, the pattern is quite similar at the same geographical location.

Therefore, the weather change regularity can be estimated using historical weather data of the specific region where the PV system is located. The real solar irradiation (G_0) will get modified by the weather effect coefficient ($\tau_{i,j}$) as follows:

$$G = G_0 \tau_{i,j} \quad (5.10)$$

where, i and j denotes the season and weather condition at a particular region respectively. The value of $\tau_{i,j}$ lies in between 0 and 1. For different seasons and weather conditions, the value of τ is listed in Appendix A.

- **Consideration of dust factor:** Solar power generation is influenced by the “degree of cleanliness” of the PV panel’s surface. If the PV panel is filled with dust layers or any other non-transparent object, then its effective surface area will get reduced, and consequently, the power output will be decreased [137]. The term ‘degree of cleanliness (κ)’ is a new parameter proposed in this chapter. It is defined as the ratio of effective surface area to the total surface area of a PV panel. The value of κ lies in between 0 and 1. For a clean surface, $\kappa = 1$ whereas, for a completely dusty surface, $\kappa = 0$. It can be expressed in another form as follows:

$$\kappa = \frac{\text{Power generated by an unclean PV surface}}{\text{Power generated by a clean PV surface}} \quad (5.11)$$

Considering all the above-mentioned factors, the expression for electrical power generated by a PV panel can be defined as:

$$P_{pv}(G, T) = \begin{cases} \kappa P_{max} \left(\frac{G^2}{G_{std} G_{ref}} \right) (1 + \alpha \Delta T); & \forall G \in [0, G_{ref}) \\ \kappa P_{max} \left(\frac{G}{G_{std}} \right) (1 + \alpha \Delta T); & \forall G \in [G_{ref}, G_{std}) \\ \kappa P_{max} (1 + \alpha \Delta T); & \forall G \geq G_{std} \end{cases} \quad (5.12)$$

where P_{max} is the maximum generation capacity of the PVS, G_{std} is the solar irradiation under standard condition, G_{ref} is the reference irradiance according to the specific geographical location, α is the coefficient of the temperature of the PV cell, and ΔT is the deviation in temperature w.r.t. the nominal value of 25°C .

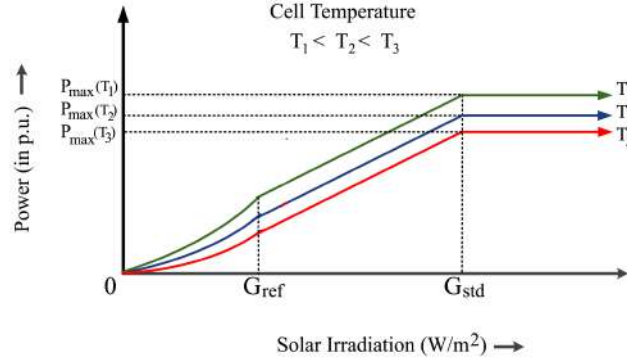


Fig. 5.3 PV power output vs. Solar irradiation characteristics

Thus, the output of a PVS will follow the pattern shown in Fig. 5.3. In order to meet the desired plant capacity, ‘ N ’ number of PV panels are to be installed in the site. In that case, the net power produced by a SPP will be:

$$P_{SPP} = \sum_{i=1}^N P_{pv}^{(i)} \quad (5.13)$$

where, $P_{pv}^{(i)}$ is the power produced by the i^{th} PV panel.

5.3.2 Modeling of Wind Power Generation

The wind speed at a particular site decides how much energy can be extracted from the wind. Historical wind speed data are needed to forecast future hourly data [161]. The hourly wind-speed can be modeled using Weibull pdf as:

$$f(v) = \frac{k}{c} \left(\frac{v}{c}\right)^{k-1} \times e^{-\left(\frac{v}{c}\right)^k} \quad (5.14)$$

where, $f(v)$ is the probability distribution function (pdf) of wind speed (v), k , and c are the shape parameter and scale parameter, respectively. The value of k and c are determined using the mean speed v_m and the standard deviation σ as follows:

$$k = \left(\frac{\sigma}{v_m} \right)^{-1.086} \quad (5.15)$$

$$c = \frac{v_m}{\Gamma(1 + 1/k)} \quad (5.16)$$

To simulate the wind speed chronologically, Weibull cumulative distribution function (CDF) with its inverse given in Equations (5.17) and (5.18)) can be utilized.

$$F(v) = 1 - e \left[- \left(\frac{v}{c} \right)^k \right] \quad (5.17)$$

$$V = -c \ln(1 - u)^{1/k} = -c \ln(u)^{1/k} \quad (5.18)$$

where, $u \in [0, 1]$ is a uniformly distributed random number. Once the Weibull pdf is established for a definite time interval, the power generated by a WTG can be determined using Equation (5.19) [93].

$$P_{WTG}(v) = \begin{cases} 0 & 0 \leq v \leq v_{ci} \\ P_{rated} \left(\frac{v - v_{ci}}{v_r - v_{ci}} \right) & v_{ci} \leq v \leq v_{cr} \\ P_{rated} & v_{cr} \leq v \leq v_{co} \\ 0 & v_{co} \leq v \end{cases} \quad (5.19)$$

where, v_{ci} , v_r and v_{co} denotes the cut-in, rated, and cut-off speeds of wind turbine, respectively. The output power of a single WTG follows the pattern shown in Fig. 5.4. The total plant capacity is obtained by aggregating the outputs of each individual generator.

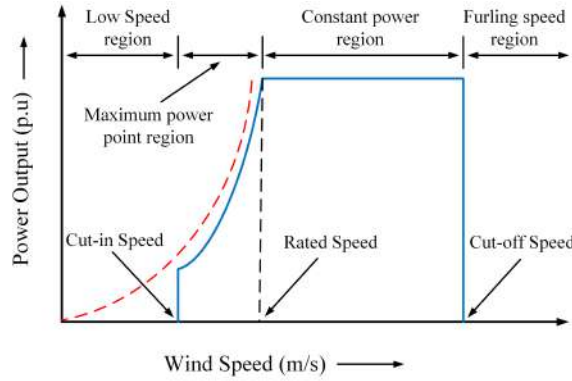


Fig. 5.4 Wind power output vs. wind speed characteristics curve

5.3.3 Modeling of Tidal Power Generation

The rising and falling of ocean water level decide the power production potentiality of a TPP. Along the shore, neap and spring tides with a range of 4–12 m can produce 1 to 10 MW of power per kilometer [98]. Total potential energy of water for a tide height of R meter is:

$$W = \rho g \int_0^R A h dh \quad (5.20)$$

where ρ is the average sea-water density in kg/m^3 , g is the gravitational constant, A is the basin area, dh is the incremental head above the head h .

As the interval of successive high and low tides is 6 hours 12.5 minutes (= 22350 s), this power is to be utilized within this period. Considering $\rho = 1025 kg/m^3$, the average theoretical power generated in one filling or emptying of the basin is:

$$P = \frac{0.5 \times 1025 \times 9.80 \times A \times R^2}{22350} = 0.225AR^2 \text{ Watts} \quad (5.21)$$

However, the actual power generated by a practical system would be less than the average theoretical power given in Equation (5.21) due to frictional losses of the fluid, conversion efficiency (η) of the turbine and generator, and due to the fact that the turbine cannot be run

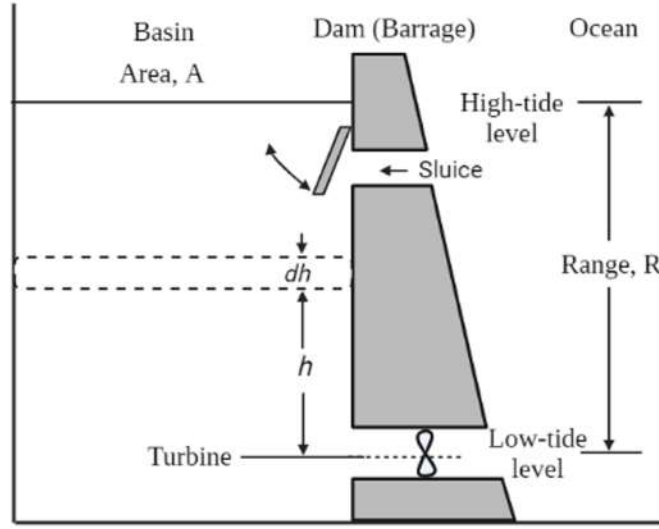


Fig. 5.5 Layout of Tidal Power Plant

down to zero head, and thus full power generation potential cannot be reached. The turbine has to be stopped when the head reaches a minimum value 'r' below which the operation becomes uneconomical. Thus, the actual energy available in single emptying process of the basin will be:

$$W = \eta \rho g \int_r^R A h dh \quad (5.22)$$

or,

$$W = 0.5 \eta \rho g A (R^2 - r^2) \text{ joules} \quad (5.23)$$

The average power generated by a tidal turbine in single emptying is:

$$P_{Tidal} = 0.225 \eta A (R^2 - r^2) \text{ Watts} \quad (5.24)$$

The net power developed by a TPP having 'n' no. of generating units is given by,

$$P_{TPP} = \sum_{i=1}^n P_{Tidal}^{(i)} \quad (5.25)$$

where, $P_{Tidal}^{(i)}$ is the power generated by the i^{th} unit.

5.3.4 Reliability Modeling of the Hybrid Generation System (HGS)

A system transits to a non-operable (DOWN) state during the intended operational period, mainly because of its component failures, unavailability of inputs, scheduled periodic maintenance, or other external faults. However, after repairing the failed components, restoring inputs, and/or clearance of faults, the system returns to the operable (UP) state. This type of system is often modeled as a two-state system in Markov framework. The state-space diagram (SSD) of a two-state system is shown in Fig. 5.6.

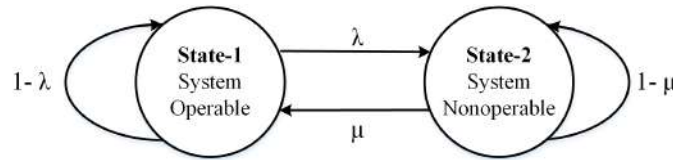


Fig. 5.6 State -space diagram of a two-state system

The probability of the system being at the UP or DOWN state depends on the parameters, failure rate (λ) and restoration rate (μ) of the system. The mean operational time (MOT) of a system is the reciprocal of its failure rate, while the reciprocal of restoration rate gives the mean downtime (MDT) of the system [14].

The conventional generating systems (CGS) generally give either rated or zero output, and so these systems are usually modeled as two-state systems. However, some systems deliver partial outputs during the time of operation. These partial outputs form derated states. The derated state is a common phenomenon of RESs.

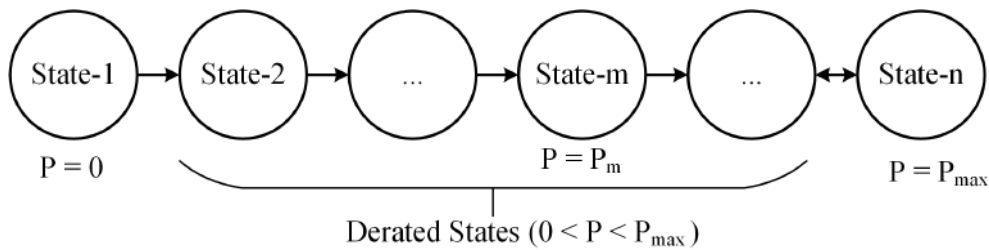


Fig. 5.7 State -space diagram of a n-state system

Depending on the availability of inputs and the values of other variables in Equations (5.12), (5.19) and (5.24), the SPP, WPP and TPP give variable outputs (P) and therefore, will stay at any of the states shown in Fig. 5.7. The capacity of the HGS will vary depending on the UP or DOWN status of the three plants. Because of having derated states, the definitions of 'UP' and 'DOWN' will be different. The system will be considered to be in the UP state even if the system does not deliver the rated output (P_{max}), but gives output in the range, $P_m \leq P \leq P_{max}$. Similarly, the system is considered to be in the DOWN state if $P < P_m$. The value of P_m is decided based on some deterministic criteria, such as system load, prescribed reserve margin, etc.

Using the Markov framework, the state-space model of the HGS can be developed. Since the HGS is comprised of three generating plants, depending on their UP or DOWN status, there will be a total 2^3 number of states where the HGS can reside at a particular moment. The state-space diagram of the HGS is drawn in Fig. 5.8.

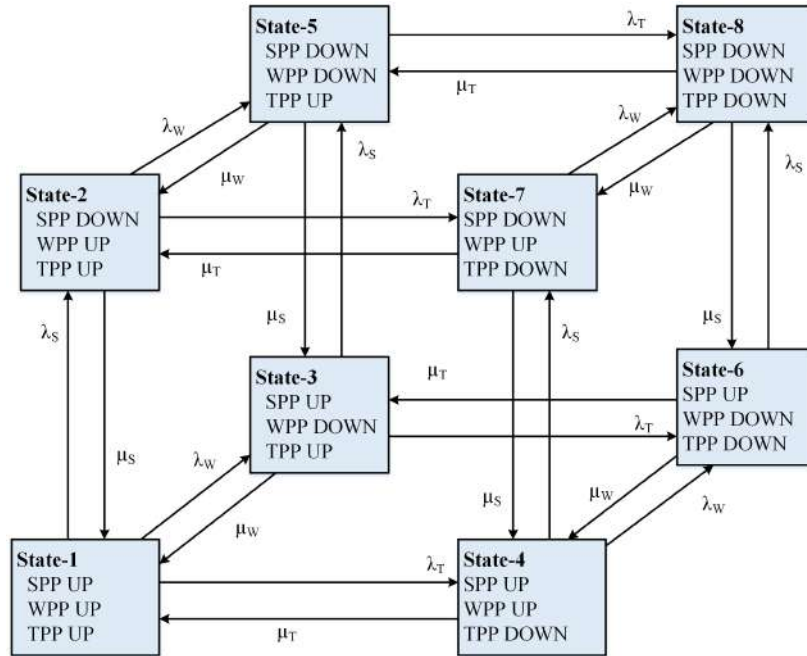


Fig. 5.8 State-space diagram of the HGS

As given in Fig. 5.8, all three renewable energy (RE) plants are operating (UP) in state 1. Two plants are operating in states 2-3, whereas, in states 4-7, only one out of the three plants is operating. Again in state-8, all plants are in non-operable (DOWN) condition. λ_S refers to the failure rate of the SPP, i.e., the number of times that the SPP transits from UP state to DOWN state over the total operational period; while μ_S denotes the restoration rate of SPP, i.e., number of times that the SPP comes back to the UP state from DOWN after going through a repair process. Similarly, λ_W , λ_T are the failure rates, whereas μ_W and μ_T represent the restoration rates of WPP and TPP respectively.

The probability of being the HGS at a particular state is determined using the “matrix multiplication method” [35]. For this, the “Stochastic Transitional Probability Matrix (STPM)” [35] is to be formed. The elements of STPM are the transition rates between two adjacent states of the state-space diagram. The STPM for the HGS model developed in Fig. 5.8 is denoted by $STPM_{HGS}$ and calculated using Equation (5.26).

$$\begin{bmatrix} 1-\lambda_S-\lambda_W-\lambda_T & \lambda_S & \lambda_W & \lambda_T & 0 & 0 & 0 & 0 \\ \mu_S & 1-\mu_S-\lambda_W-\lambda_T & 0 & 0 & \lambda_W & 0 & \lambda_T & 0 \\ \mu_W & 0 & 1-\lambda_S-\mu_W-\lambda_T & 0 & \lambda_S & \lambda_T & 0 & 0 \\ \mu_T & 0 & 0 & 1-\lambda_S-\lambda_W-\mu_T & 0 & \lambda_W & \lambda_S & 0 \\ 0 & \mu_W & \mu_S & 0 & 1-\mu_S-\mu_W-\lambda_T & 0 & 0 & \lambda_T \\ 0 & 0 & \mu_T & \mu_W & 0 & 1-\lambda_S-\mu_W-\mu_T & 0 & \lambda_S \\ 0 & \mu_T & 0 & \mu_S & 0 & 0 & 1-\mu_S-\lambda_W-\mu_T & \lambda_W \\ 0 & 0 & 0 & 0 & \mu_T & \mu_S & \mu_W & 1-\mu_S-\mu_W-\mu_T \end{bmatrix} \quad (5.26)$$

STPM follows the following multiplication principle.

$$\gamma \times STPM_{HGS} = \gamma \quad (5.27)$$

where, γ represents the limiting-state probability vector of the HGS. The elements of this vector are: $p_{HGS}^{(i)}$, where $i \in \{1, 2, 3, \dots, 8\}$.

Again, according to the total probability theorem,

$$\sum_{i=1}^8 p_{HGS}^{(i)} = 1 \quad (5.28)$$

Solving Equations (5.27) and (5.28), the probability, $p_{HGS}^{(i)}$ that the HGS is in state i , where $i \in \{1, 2, 3, \dots, 8\}$ are determined and given in Equations (5.29)-(5.36).

$$P_{HGS}^{(1)} = \frac{\mu_S \mu_W \mu_T}{(\lambda_S + \mu_S)(\lambda_W + \mu_W)(\lambda_T + \mu_T)} \quad (5.29)$$

$$P_{HGS}^{(2)} = \frac{\lambda_S \mu_W \mu_T}{(\lambda_S + \mu_S)(\lambda_W + \mu_W)(\lambda_T + \mu_T)} \quad (5.30)$$

$$P_{HGS}^{(3)} = \frac{\mu_S \lambda_W \mu_T}{(\lambda_S + \mu_S)(\lambda_W + \mu_W)(\lambda_T + \mu_T)} \quad (5.31)$$

$$P_{HGS}^{(4)} = \frac{\mu_S \mu_W \lambda_T}{(\lambda_S + \mu_S)(\lambda_W + \mu_W)(\lambda_T + \mu_T)} \quad (5.32)$$

$$P_{HGS}^{(5)} = \frac{\lambda_S \lambda_W \mu_T}{(\lambda_S + \mu_S)(\lambda_W + \mu_W)(\lambda_T + \mu_T)} \quad (5.33)$$

$$P_{HGS}^{(6)} = \frac{\mu_S \lambda_W \lambda_T}{(\lambda_S + \mu_S)(\lambda_W + \mu_W)(\lambda_T + \mu_T)} \quad (5.34)$$

$$P_{HGS}^{(7)} = \frac{\lambda_S \mu_W \lambda_T}{(\lambda_S + \mu_S)(\lambda_W + \mu_W)(\lambda_T + \mu_T)} \quad (5.35)$$

$$P_{HGS}^{(8)} = \frac{\lambda_S \lambda_W \lambda_T}{(\lambda_S + \mu_S)(\lambda_W + \mu_W)(\lambda_T + \mu_T)} \quad (5.36)$$

Equations (5.29)-(5.36) measure the probability of the HGS being at a particular operating state. For example, $P_{HGS}^{(1)}$ refers to the probability that all three RE plants are operating. Similarly, $P_{HGS}^{(2)}$ refers to the probability that the WPP and TPP are operating but SPP is not operating. Again, $P_{HGS}^{(8)}$ refers to the probability that all RE plants are non-operating.

After determination of the state probabilities of the HGS in Markov framework, the next step is to define the reliability of the system, i.e., how much healthy the system is or how

much risk is involved in the system. For this purpose, the “well-being framework” [103] can be implemented. The well-being approach incorporates some deterministic criteria in a probabilistic framework to define the system’s reliability in a set of risk levels. The deterministic criteria are set by the operator based on the system’s load and operating reserve requirement to meet that load during contingencies. Based on the deterministic criteria and specified risk levels, a set of indices called ‘well-being indices’ are defined.

In the present study, the HGS is considered to have four reliability states: healthy, marginal, emergency, and failed; and accordingly, the well-being indices are defined. The four well-being indices for the HGS are, namely, probability of healthy state, $p(H)$; probability of marginal state, $p(M)$; probability of emergency state, $p(E)$ and probability of failed state, $p(F)$. The deterministic criteria are chosen based on the availability of the three RE plants shown in Fig. 5.8. Using the HGS’s state probabilities that are derived in Markov framework (Equations (5.29)-(5.36)), the well-being indices for the HGS are defined as shown in Fig. 5.9.

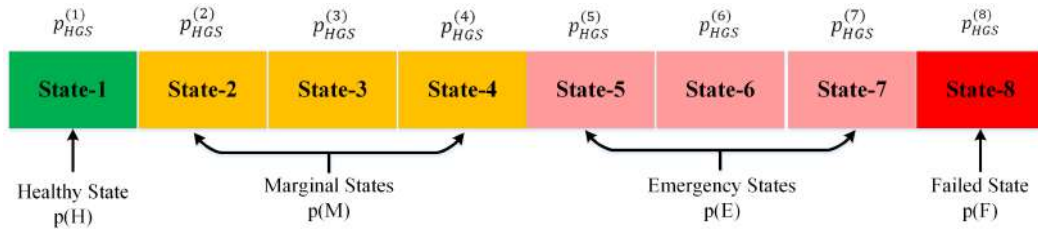


Fig. 5.9 Well-being indices of the HGS

The four well-being indices follow the total probability theorem,

$$p(H) + p(M) + p(E) + p(F) = 1 \quad (5.37)$$

These four indices can be evaluated as shown in Table 5.1:

In the healthy state, all three plants are in operating modes. Solar irradiation level is sufficient to generate the desired power, wind speed is within the range of cut-in and cut-out speeds, and tide height is between r and R . It is the most desirable state since the maximum benefit of RE integration can be achieved here.

Table 5.1 Well-being indices of the HGS

| Index | Contingency level | No. of units operating | Probability |
|-------|-------------------|------------------------|---|
| p(H) | 0 | 3 | $P_{HGS}^{(1)}$ |
| p(M) | 1 | 2 | $P_{HGS}^{(2)} + P_{HGS}^{(3)} + P_{HGS}^{(4)}$ |
| p(E) | 2 | 1 | $P_{HGS}^{(5)} + P_{HGS}^{(6)} + P_{HGS}^{(7)}$ |
| p(F) | 3 | 0 | $P_{HGS}^{(8)}$ |

In the marginal state, at least one among the SPP, WPP, and TPP is in DOWN state. In state-2, the SPP is not in operable condition. Similarly, the WPP is non-operable in state-3, and the TPP is non-operable in state-4. However, in the marginal state, the HGS is supposed to meet the power demand of most of the load points during off-peak hours. Some less prioritized LPs must be curtailed during peak hours if the grid is operated in islanded mode.

In the emergency state, two plants in the HGS are not in operable condition. Only a few high-prioritized load points will get power from the RE sources. The neighboring power utilities may come to the rescue if the system is switched over to grid-connected mode. Some strategic measures like “proper load curtailment policy” or “smart operating reserve management” must be adopted if the system falls to the emergency state.

In the failed state, none of the plants are in operable condition, and the HGS will give zero output power. The system will entirely be dependent on the reliability of the TGS or the neighboring grid’s power supply.

5.4 Reliability Modeling of the Radial Network

Distribution system is a major contributor of system unreliability. A radial distribution network (RDN) is the most common distribution network (DN) in power system due to its simple and economical configuration. It comprises of a set of series components, such as bus bars, distributors, service mains, cables, disconnects (or isolators), circuit breakers, protecting devices, transformers, etc. A customer attached to any LP of such a system needs

all components up to the bulk supply point to be operating so that the continuity of power remains unaffected. The average failure rates (λ) and outage times (r) of these components dictate the reliability of the overall DN. In addition to these, many customer and LP-oriented indices are available to assess the severity or significance of system failures and conduct future reliability prediction analysis [20]. The reliability indices that are used in the present study are SAIFI, SAIDI, CAIDI, AENS, EENS, ECOST and IEAR. The definitions of these indices have been discussed in Section 3.6.1. In addition to these, to quantify and analyze the benefits of adding renewable power sources in an ADN from energy and reliability worth point of view, following metrics have been proposed in this chapter.

1. **Incremental Energy Benefit (IEB):** The reliability worth in terms of energy due to the integration of RESs is expressed by a parameter designated as “Incremental Energy Benefit (IEB)”. It refers to the change in loss of expected energy (LOEE) per customer served per year by the system due to an incremental change in capacity in the system. In other words,

$$IEB = \frac{\Delta LOEE}{\Delta P} = \frac{LOEE_{before \text{ capacity addition}} - LOEE_{after \text{ capacity addition}}}{\text{Incremental change in capacity}} \quad (5.38)$$

2. **Incremental Cost Benefit (ICB):** The reliability worth in terms of cost due to the integration of RESs is expressed by a parameter designated as “Incremental Cost Benefit (ICB)”. It refers to the change in expected customer interruption cost due to an incremental change in capacity in the system. In other words,

$$ICB = \frac{\Delta ECOST}{\Delta P} = \frac{ECOST_{before \text{ capacity addition}} - ECOST_{after \text{ capacity addition}}}{\text{Incremental change in capacity}} \quad (5.39)$$

5.5 Flowchart of the Study

Figure 5.10 shows the flowchart of the present study. The study begins with assessing of the input data for the three RE plants. Using these input data, the generation capacity of the HGS is estimated. The availability of the HGS depends on the UP or DOWN status, failure rates, and recovery rates of the SPP, WPP, and TPP. The hourly load pattern in the system is incorporated with the HGS. In the meantime, the failure modes of the DN are identified, and the basic reliability parameters of the components under consideration are collected. After that, the HGS and DN are integrated to determine the reliability indices.

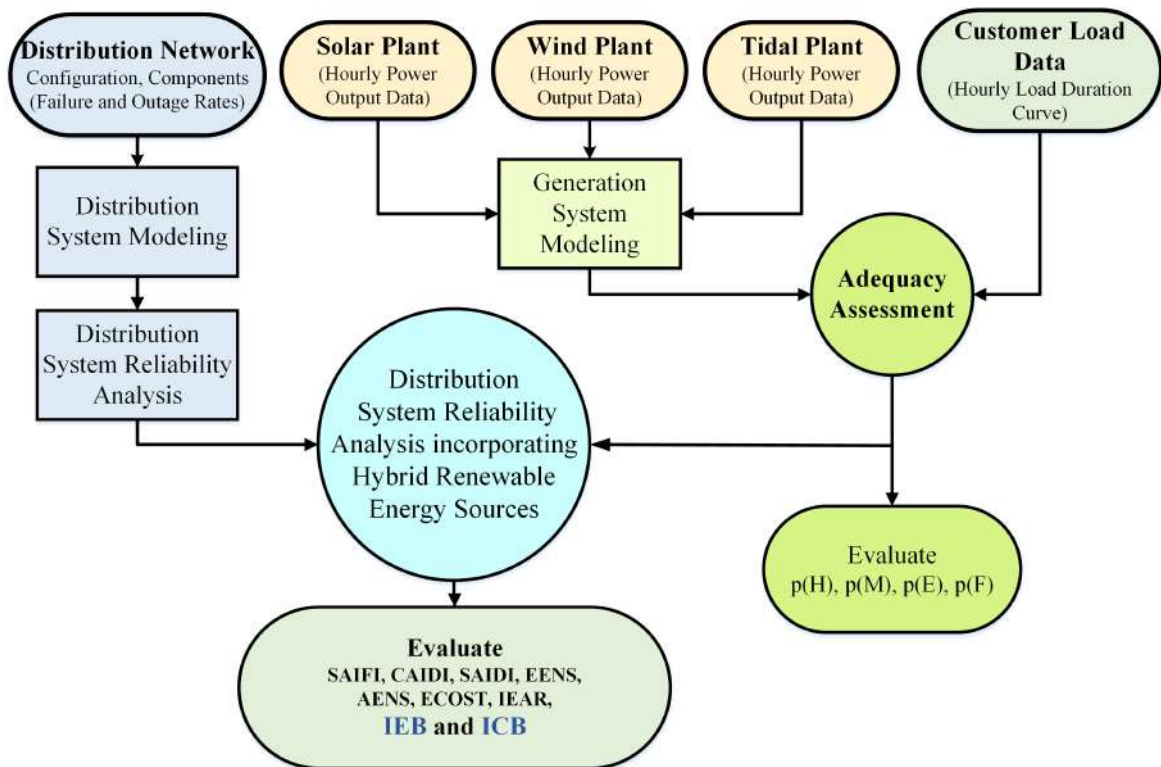


Fig. 5.10 Flowchart of the proposed study

5.6 Description of the Test System

The DS of Bus-2 of the RBTS is considered as test system [5]. The original DN is modified to accommodate the three renewable power plants as shown in Fig. 5.11. The network has 22 LPs, 15 Bus-bars (B/B), 23 transformers (T), and 39 circuit breakers (CB). The solar, wind, and tidal power plants are installed at bus-bar nos. 5, 11, and 12, respectively. The customer types, LPs, and feeder-reliability data of RBTS are used in the study [5, 6]. 33kV bus is exempted from the study, and only the feeders originated from the 11kV bus; their laterals and LPs are considered for analysis. The switching and interrupting devices are considered to have their respective failure rates and outage time as indicated in Appendix A. The transformers attached to each power plant, cable, and other auxiliary devices are assumed to be 100% reliable. The line diagram of the test system is presented in Fig. 5.11.

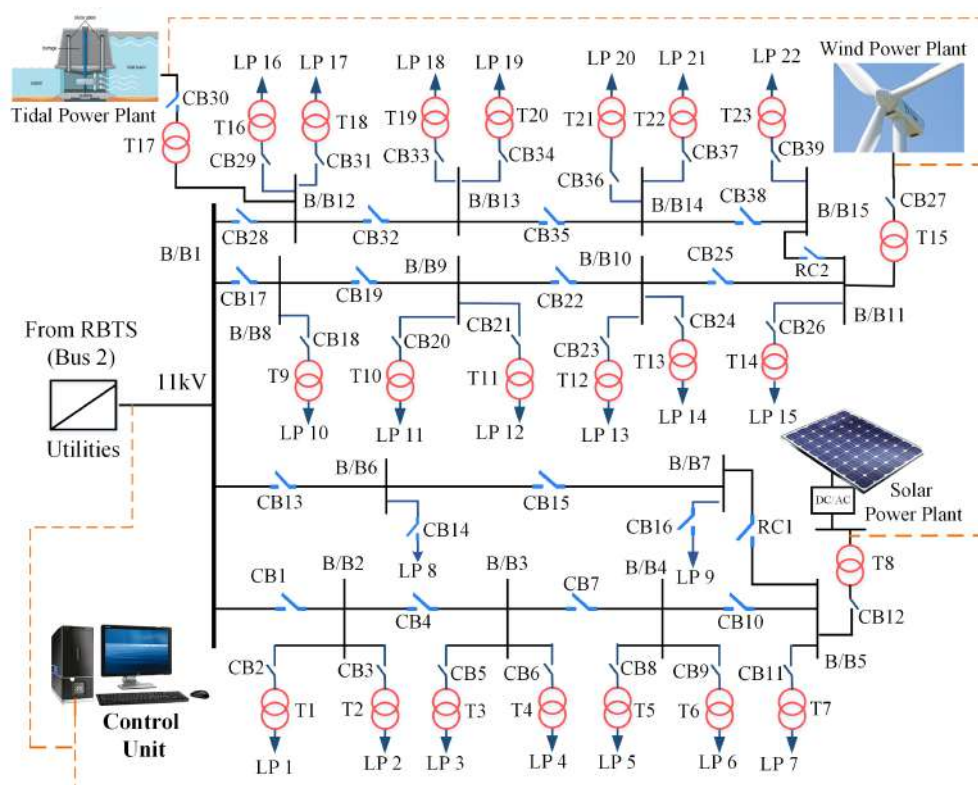


Fig. 5.11 Modified DS of BUS-2 (RBTS) with SPP, WPP and TPP integration

5.7 Results and Discussion

Using the data given in Tables A.3, A.4, A.6, A.7 and A.13 in Appendix A, the developed models in Section 5.2 are exemplified in the test system considered. The input data are taken from the state of the art literature. The proposed methodologies are tested using these data and verified the results for the base test system with the existing works [2, 5, 6]. The case studies are categorized into three parts as follows:

5.7.1 Reliability investigation with a perfect distribution network

If the DN is perfect (i.e., 100% reliable), the entire system's reliability will depend on the adequacy of the power supply only. Under this condition, the reliability of the HGS dictates the the whole integrated system's reliability. Based on generation capacities of SPP, WPP and TPP, the HGS's availability will vary, and that can be examined by evaluating $p(H)$, $p(M)$, $p(E)$ and $p(F)$.

The deterministic criterion considered during the evaluation of well-being indices is that the HGS will be healthy if all three RESs are operated with their respective capacities. As per the data given in Table A.3 (Appendix A), the SPP can generate a maximum of 2 MW power under standard conditions, and it has a failure rate of 0.04 per year, and its average repair time is taken to be 5 hours. Again, the WPP and TPP have the maximum generating capacity of 3MW and 5MW, respectively. Failure rates of these two plants are 0.05 per year and 0.08 per year, respectively. Again average repair time taken by the WPP is 8 hours, and that of the TPP is 10 hours. With these data, the values of $p(H)$, $p(M)$, $p(E)$, and $p(F)$ for the HGS are obtained to be 0.331, 0.463, 0.185, and 0.021, respectively. Their percentage contributions toward the system's reliability are as shown in Fig. 5.12.

Figure 5.12 shows that the probability of the HGS being at the healthy state, i.e., all three RE plants are operating simultaneously at their rated capacities, is 33.1% only. The highest probability (i.e., 44.3%) is associated with the marginal state, where any two RE

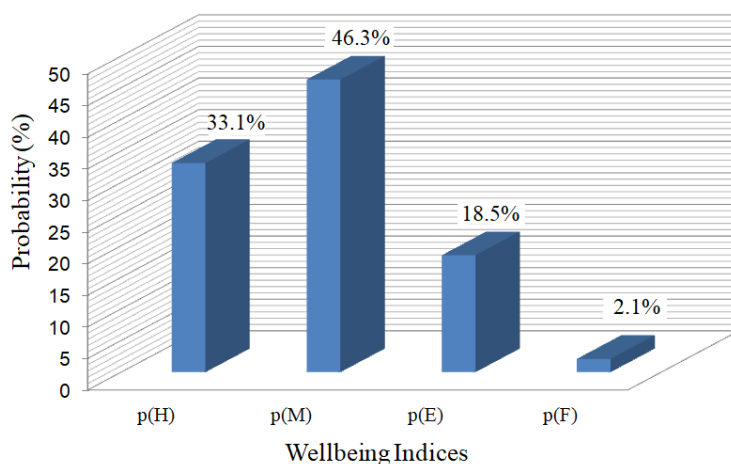


Fig. 5.12 Reliability of the hybrid generation system

plants are operating at a time. The probability of the emergency state, where only one RE plant is operating, is 18.5%. The probability that all three plants are non-operable is found to be 2.1%. The values of the well-being indices are dependent on MOT and MDT of the RE plants, as explained in Section 5.3.4. Due to the low MOT (or high MDT) of RESs, their reliability is quite low as compared to TGS.

5.7.2 Reliability investigation with an imperfect distribution network

If the DN is imperfect (i.e., not 100% reliable), then the reliability of the integrated system will be affected by the reliability of both HGS and the DN. Depending on the UP or DOWN status of the three renewable plants, the DS reliability indices, namely, SAIFI, SAIDI, CAIDI, AENS, EENS, ECOST, and IEAR will vary. The reliability of the entire system can now be analyzed in eight case studies as follows:

- **Case-1:** *All renewable plants are in DOWN states:*

Under this scenario, the HGS is in the failed state (State-8). The power demands from LPs are met by the traditional generating system (TGS) of the RBTS. The consumers at the LPs experience frequent power outages with a longer period of interruption

owing to the absence of DGs in the network. Due to the high frequency and duration of power interruptions, the cost incurred by the customers (ECOST) becomes high. In this state, the values of SAIFI, SAIDI, CAIDI, AENS, EENS, ECOST, and IEAR are found to be 0.13550 f/customer yr, 0.77660 h/customer yr, 5.73137 h/customer interruption, 0.00482 MWh/customer yr, 9.20610 MWh/yr, 40230.2 \$/yr and 4.37112 \$/kWh , respectively.

- **Case-2:** *Only the solar plant is operating:*

The HGS is running in emergency mode. However, the stress on the TGS of RBTS is reduced up to 2 MW due to the availability of SPP. The HGS can satisfy up to 16.27% of the average load and 10% of the peak load of the test system. System's reliability indices, SAIFI, SAIDI, CAIDI, AENS, EENS, and IEAR are improved by 3.82%, 4.03%, 0.21%, 2.49%, 3.99%, and 0.46% respectively. The interruption cost is also reduced by 3.53%, and the net savings in ECOST is 1421.17 \$/yr. The integration of SPP has a better impact on lowering the frequency and duration of power outages as compared to case-1.

- **Case-3:** *Only the wind plant is operating :*

The HGS is operating in the emergency state. However, the stress on the TGS in the test system gets reduced up to 3 MW due to the availability of WPP. The HGS can deliver up to 24.41% of the system's average load and 15% of the peak load. As a result, the ADN sees improvements in SAIFI, SAIDI, CAIDI, AENS, EENS, and IEAR by 4.26%, 5.02%, 0.80%, 6.64%, 7.79%, and 1.19%, respectively. The outage cost is reduced up to 6.67%, while the savings in ECOST is 2685.19 \$/yr.

- **Case-4:** *Only the tidal plant is operating:*

The HGS is in the emergency state. It can deliver up to 5MW power to the LPs in the system. The HGS satisfies up to 40.68% of the system's average load and 25%

of the peak load. The remaining demands are to be met by the TGS available in the RBTS. Due to the availability of the TPP, power interruptions and outage duration are decreased. SAIFI, SAIDI, CAIDI, AENS, EENS, and IEAR are improved by 12.23%, 13.46%, 1.40%, 18.26%, 16.08% and 1.49% respectively. Interruption cost associated with customers is lowered by 14.81% resulting in 5957.64 \$/yr savings in ECOST in the system.

- **Case-5:** *Only the solar and wind plants are operating:*

The HGS is in the marginal state. The dependency on the TGS is reduced up to 5 MW due to the availability of SPP and WPP. The HGS can meet up to 40.68% of the system's average load and 25% of the peak load. SAIFI, SAIDI, CAIDI, AENS, EENS, and IEAR are improved by 18.84%, 19.93%, 1.34%, 18.27%, 24.11% and 2.40% respectively. The expected interruption cost is reduced by 22.27%, and consequently, the system can save up to 8957.64\$/yr from ECOST.

- **Case-6:** *Only the solar and tidal plants are operating:*

The HGS is in the marginal state. However, the burden on the TGS in RBTS is reduced up to 7 MW. The HGS can satisfy up to 56.95% of the average load and 35% of the peak load in the system. The system becomes more reliable with the decrease in the frequency and duration of interruption of power supply. SAIFI, SAIDI, CAIDI, AENS, EENS, and IEAR are improved by 22.89%, 25.30%, 3.13%, 31.76%, 30.99% and 3.64% respectively. Interruption cost is reduced by 28.46%, which results in net savings of 11449.66 \$/yr.

- **Case-7:** *Only the wind and tidal plants are operating:*

The HGS is in the marginal state. The burden on the TGS is reduced up to 8 MW due to the availability of WPP and TPP. The HGS is now capable of satisfying up to 65.09% of the system's average load and 40% of the peak load. SAIFI, SAIDI,

CAIDI, AENS, EENS, and IEAR are improved by 29.25%, 32.15%, 4.10%, 38.38%, 34.34%, and 4.83% respectively. Interruption cost is reduced by 31.15%, resulting in net savings of 11449.66 \$/yr.

- **Case-8:** *All three renewable plants are operating:*

The HGS is in the healthy state and capable of reducing the burden on the TGS up to 10 MW which is equivalent to 81.36% of the system's average demand and 40% of the peak demand. The system's reliability is significantly increased due to the integration of the three RESs. The cost of power outages is reduced by 39.00%. SAIFI, SAIDI, CAIDI, AENS, EENS, IEAR are improved by 51.54%, 54.51%, 6.13%, 54.85%, 43.19%, and 7.34% respectively. Net savings of ECOST is 15691.43 \$/yr.

The simulation results obtained for the eight cases are listed in Table 5.2. The results justify that the reliability and interruption costs are mostly influenced by the operational states of the HGS. With increased capacity through RES integration, the overall system is found to be healthier and more cost-effective.

Table 5.2 Results of the case studies

| Case No. | SAIFI | SAIDI | CAIDI | AENS | EENS | ECOST | IEAR |
|----------|---------|---------|---------|---------|---------|---------|---------|
| 1 | 0.13550 | 0.77550 | 5.73137 | 0.00482 | 9.20610 | 40230.2 | 4.37112 |
| 2 | 0.13032 | 0.74531 | 5.71908 | 0.00470 | 8.83827 | 38809.0 | 4.39102 |
| 3 | 0.12973 | 0.73761 | 5.68573 | 0.00450 | 8.48837 | 37544.9 | 4.42311 |
| 4 | 0.11893 | 0.67210 | 5.65122 | 0.00394 | 7.72565 | 34272.5 | 4.43620 |
| 5 | 0.10997 | 0.62182 | 5.65438 | 0.00394 | 6.98653 | 31272.5 | 4.47612 |
| 6 | 0.10449 | 0.58012 | 5.55206 | 0.00329 | 6.35313 | 28780.5 | 4.53013 |
| 7 | 0.09587 | 0.52693 | 5.49630 | 0.00297 | 6.04487 | 27698.5 | 4.58214 |
| 8 | 0.06567 | 0.35328 | 5.37980 | 0.00218 | 5.22979 | 24538.7 | 4.69211 |

In Table 5.2, the units of SAIFI, SAIDI, CAIDI, AENS, EENS, ECOST and IEAR are f/customer yr, h/customer yr, h/customer interruption, MWh/customer yr, MWh/yr, \$/yr and \$/kWh, respectively. The improvements in the reliability indices under different operating modes of the HGS are graphically demonstrated in Figs. 5.13(a)-(f) and 5.14(a)-(b).

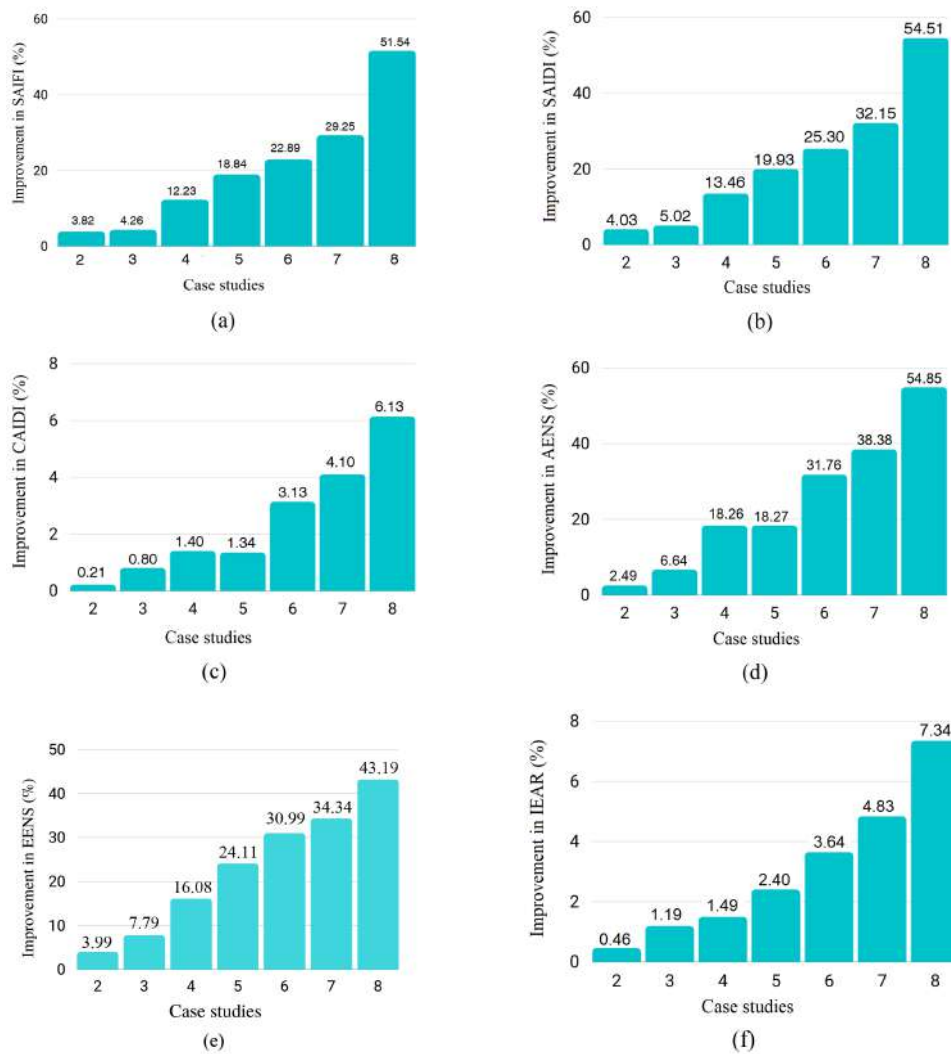


Fig. 5.13 Improvements in (a) SAIFI, (b)SAIDI, (c) CAIDI, (d) AENS , (e) EENS and (f) IEAR under different modes of HGS operation

It is observed that, if the HGS remains in the healthy state, the values of SAIFI, SAIDI, CAIDI, AENS, EENS, ECOST, and IEAR of the system are improved by 51.54%, 54.51%, 6.13%, 54.85%, 43.19%, 39.00%, and 7.34% respectively. Again, if the HGS transits to the marginal state, the average improvements in SAIFI, SAIDI, CAIDI, AENS, EENS, ECOST, and IEAR are obtained as 23.66%, 25.79%, 2.26%, 29.47%, 29.81%, 27.29%, and 3.62% respectively. Even if the HGS falls to the emergency state, these reliability indices are improved by around 6.77%, 7.50%, 0.80%, 9.13%, 9.29%, 8.34%, and 1.04%,

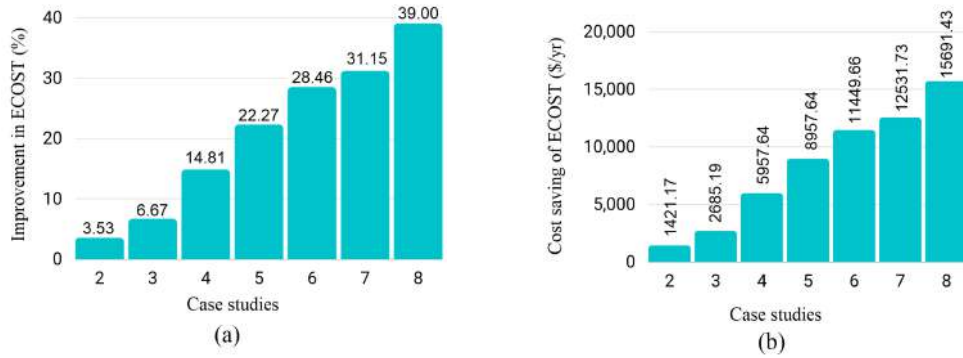


Fig. 5.14 Improvements in (a) ECOST and (b) Savings in ECOST under different modes of HGS operation

respectively. The comparison of results of the eight case studies establishes that an increase in the availability of the HGS comprising of solar, wind, and tidal plants significantly improves the reliability of the ADN by reducing the frequency and period of load curtailment; and thus increases the revenue by lowering the interruption cost associated with customers. Moreover, with RE integration, the reserve margin in the ADN gets significantly increased, and therefore, the generation companies can supply power at the desired reliability level to the consumers.

5.7.3 Reliability worth/cost assessment using the proposed metrics

The annual incremental energy and cost benefits of adding solar, wind, and tidal energy sources in the network are determined using the parameter IEB and ICB given in Equations (5.38) and (5.39). The incremental capacity added to the base test system using solar, wind, and tidal plants are 2MW, 3MW, and 5MW, respectively. Before the RES addition, the system's EENS and ECOST values were 9.20610 MWh/yr and 40230.18 \$/yr, respectively. The IEB for a 2MW of solar energy addition is 0.18392 MWh/yr/MW. Again, the ICB for the same capacity of solar energy addition is 710.58\$/yr/MW. Similarly, the IEB and ICB for adding 3MW of wind energy are 0.23924 MWh/yr/MW and 895.06 \$/yr/MW, respectively. Again, 5 MW of tidal energy addition gives incremental energy and cost benefits of 0.29609 MWh/yr/MW and 1191.53 \$/yr/MW, respectively. Using the results listed in Table 5.2, and

Equations (5.38) and (5.39), the reliability worth in terms of energy and cost benefits are determined for all the operational modes of the HGS given in Fig. 5.8. The results are given in Table 5.3.

Table 5.3 Incremental energy and cost benefits from the HGS under different modes of operation

| Renewable Energy Source(s) Added | Incremental Energy Benefit (IEB) in MWh/yr/MW | Incremental Cost Benefit (ICB) in \$/yr/MW |
|----------------------------------|---|--|
| Solar | 0.18392 | 710.58 |
| Wind | 0.23924 | 895.06 |
| Tidal | 0.29609 | 1191.53 |
| Solar + Wind | 0.44391 | 1791.53 |
| Solar + Tidal | 0.40757 | 1635.67 |
| Wind + Tidal | 0.39515 | 1566.47 |
| Solar + Wind + Tidal | 0.39763 | 1569.14 |

The parameter IEB indicates how much renewable capacity can be added to the ADN to neutralize the loss of expected energy in the system. On the other hand, parameter ICB can be used by a system planner to estimate possible renewable capacity additions based on investment/MW per year.

5.8 Conclusion

This chapter has presented a comprehensive reliability analysis of an active distribution network energized by a hybrid generation system consisting of solar, wind, and tidal energy sources. A new method has been developed combining the Markov and well-being approaches to estimate the reliability of the renewable generating system under different operational modes. The reliability of the distribution network is analyzed by evaluating some standard reliability indices, namely SAIFI, SAIDI, CAIDI, AENS, EENS, ECOST, and IEAR. Two new metrics, namely, IEB and ICB, have been proposed in this chapter to measure the reliability worth of the system in terms of energy and cost benefits from adding renewable DGs. The simulation results justify that renewable DGs have significant impacts on the

reliability of an active distribution network. The system operator can deliver power to the load points at different reliability levels by regulating the operating reserve based on the availability of the RESs. The cost associated with power outages is significantly reduced with increased penetration from the RESs. The result shows that IEB and ICB both increase with the combined operation of multiple RESs. For countries with long coastlines, the combination of solar-wind-tidal energies can effectively meet the power demand satisfying the reliability, economic and environmental constraints. The suggested methodology and outcomes of the study are expected to be useful for the researcher, system planner, policymaker, and operator to conduct further analysis on power system reliability in the presence of new RESs. The present study can further be extended to examine the feasibility, optimal sizing, and location of RESs to maximize the benefits.

The importance of renewable distributed generation significantly increases with the increased size of electric vehicle load. The next chapter is directed at examining how electric vehicle charging can impact the reliability of a distribution network.

6

Reliability Analysis of Distribution Network Integrated with Electric Vehicle

6.1 Introduction

The growing concern of carbon dioxide emissions, greenhouse effects, and a rapid diminution of petroleum resources raise the necessity to develop and utilize new environment-friendly sustainable alternatives to the conventional ICE-driven vehicles. For this reason, electric vehicles (EVs) have received considerable attention worldwide in recent times. However, a critical problem associated with EVs is that their higher penetration causes many issues on the power distribution networks [32, 162]. The increased volume of PEVs in grid-to-vehicle (G2V) mode reduces the grid's reserve capacity, and thus reduces the adequacy of power supply to the load-points(LPs). Again, uncontrolled scheduling of PEV charging distorts the

load curve, causing peaks on the peaks; and pushes the system operator for load curtailment, and thus reduces the system reliability [163].

The distribution system operators (DSOs) are responsible for maintaining the service reliability at the desired level. As DSOs do not have any control over the PEV charging time, duration, and location, the operation becomes more critical. Coordination of plug-in EVs (PEVs) with optimal charging schedules and the provision of the required reserve margin for a daily trip can handle the challenge during peak demand periods. An efficient way to add higher PEV loading is by developing coordinated charging infrastructures and creating provisions for distributed generations in the power network. If the system does not have sufficient reserve margin to satisfy the peak load requirements, load curtailment strategies must be taken by DSOs. As PEV loads are the highly prioritized loads, load curtailments usually affect the system's regular, low-prioritized LPs, and the reliability of these LPs mostly gets disturbed.

In the present chapter, the reliability of a distribution network (DN) is investigated in the presence of coordinated and uncoordinated PEV charging. A wide range of reliability indices has been evaluated to study the impact of PEV loading on the reliability of the DN. Roy Billinton Test System (RBTS) [5] is considered as the test system. Different PEV charging and loading models have been developed. The chapter demonstrates how different volumes of PEV loading impact system reliability and how coordinated charging helps in reducing the impacts.

6.2 Methodology

6.2.1 Battery Charging Model

The equivalent circuit of the battery charging circuit is given in Fig. 6.1. The capacitance of the battery is C . The resistor R is responsible for the ohmic losses in the circuit. V_0 is the

steady-state output voltage of the charger which is represented by a DC voltage source. V_{in} and V_{out} are the input and output voltage of the circuit respectively. The switch is closed at time t to charge the battery.

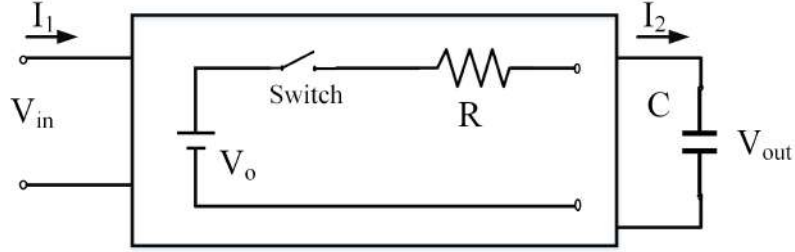


Fig. 6.1 Equivalent circuit of charger

Applying Kirchhoff's voltage law,

$$V_0 = V_R(t) + V_{out}(t) \quad (6.1)$$

If $I(t)$ is the current flowing in the circuit and η is the charging efficiency, then Equation (6.1) becomes:

$$V_0 = I(t)R + \eta V_c \quad (6.2)$$

The voltage across the capacitor, V_c

$$V_c = \frac{1}{C} \int_0^t i(\tau) d\tau \quad (6.3)$$

From Equations (6.2) and (6.3),

$$V_0 = I(t)R + \frac{\eta}{C} \int_0^t i(\tau) d\tau \quad (6.4)$$

Multiplying Equation (6.4) by $\frac{C}{\eta}$, and then differentiating w.r.t. t ,

$$0 = \frac{RC}{\eta} \frac{di(t)}{dt} + i(t) \quad (6.5)$$

Thus, the current in the circuit at time t is,

$$i(t) = \frac{V_0}{R} e^{-\eta \frac{t}{\tau_0}} \quad (6.6)$$

where, $\tau_0 = RC$ is the time constant.

Substituting the value of $i(t)$ in Equation (6.1),

$$V_{out}(t) = V_0 \left(1 - e^{-\eta \frac{t}{\tau_0}} \right) + \bar{V}_0 \quad (6.7)$$

where, \bar{V}_0 is the voltage under pre-charged condition.

The instantaneous power of the battery $P_{out}(t) = V_{out}(t) \times i(t)$ is determined as:

$$P_{out}(t) = P_{max} \left(1 - e^{-\eta \frac{t}{\tau_0}} \right) + P_0 \quad (6.8)$$

where, $P_{out}(t)$, P_{max} and P_0 are the instantaneous, maximum and initial powers in the battery respectively. The value of t varies from 0 to t_{req} , where t_{req} is the time required to make the battery full charged.

6.2.2 Vehicle Charging Demand Model

The power status in the battery at time t is given by:

$$P_{PEV}(t) = P_{PEV,max} \left(1 - e^{-\alpha t / t_{max}} \right) + P_{PEV,0} \quad (6.9)$$

where, α is the battery charging constant and $t \in [0, t_{req}]$. t_{max} is the maximum time required to get full charged from the zero initial power. $P_{PEV,max}$ is the maximum capacity of the PEV battery, and $P_{PEV,0}$ is the initial power status of the PEV battery.

The value of t_{req} varies with the battery initial power status as follows:

1. if $P_{PEV,0} = 0$, then $t_{req} = t_{max}$
2. if $P_{PEV,0} = P_{PEV,max}$ then $t_{req} = 0$
3. if $0 < P_{PEV,0} < P_{PEV,max}$ then t_{req} is to be calculated as follows:

As $P_{PEV}(t) = P_{PEV,max}$ at time $t = t_{req}$, Equation (6.9) becomes:

$$P_{PEV,max} = P_{PEV,max} \left(1 - e^{-\alpha t_{req}/t_{max}} \right) + P_{PEV,0} \quad (6.10)$$

Thus, the required charging time is,

$$t_{req} = -\frac{t_{max}}{\alpha} \ln \left(\frac{P_{PEV,0}}{P_{PEV,max}} \right) \quad (6.11)$$

Now the instantaneous power status in charging mode is determined as:

$$P_{PEV}(t) = \begin{cases} P_{PEV,max} \left(1 - e^{-\frac{\alpha t_{req}}{t_{max}}} \right) + P_{PEV,0}; \forall t < t_{req} \\ P_{PEV,max}; \forall t \geq t_{req} \end{cases} \quad (6.12)$$

The total power demand for full charge of a PEV at time t is:

$$P_{PEV,dem}(t) = P_{PEV,max} - P_{PEV}(t) \quad (6.13)$$

Suppose, the vehicle starts charging at t_1 hour and takes t_{req} to get full charged. Thus, the time spent by the PEV at the charging station is $t_2 = t_1 + t_{req}$ hours. However, if the charging is stopped at t_3 due to power outage or any failures in the system, then the PEV battery status at that time is determined as:

$$P_{PEV,t_3} = P_{PEV,max} \left(1 - e^{-\alpha(t_3-t_1)/t_{max}} \right) + P_{PEV,0} \quad (6.14)$$

where $(t_3 - t_1)$ is the charging duration of the vehicle at the charging station. If the system is restored at t_4 and $t_4 \geq t_2$ then the battery power status remains the same. However, if $t_4 < t_2$, the power status of the battery will be:

$$P_{PEV,t_2} = \begin{cases} P_{PEV,max} \left(1 - e^{-\frac{\alpha(t_2 - t_4)}{t_{max}}} \right) + P_{PEV,t_3}; & \forall (t_2 - t_4) < t_{req} \\ P_{PEV,max}; & \forall (t_2 - t_4) \geq t_{req} \end{cases} \quad (6.15)$$

The power that is not charged due to the system failure i.e., the power required to achieve $P_{PEV,max}$ after the interruption is given by Equation (6.16).

$$P_{PEV,req} = \begin{cases} P_{PEV,max} - P_{PEV,t_3}; & \forall t_4 \geq t_2 \\ P_{PEV,max} - P_{PEV,t_2}; & \forall t_4 < t_2 \end{cases} \quad (6.16)$$

6.2.3 Time Distribution Modeling of schedulable PEV

To develop the time distribution model, two types of probability events are used in a 24-hour period. Using maximum likelihood estimation on normalized statistical data, the probability distribution function (pdf) of the first trip start time $f_{t-start}(x)$ and the last trip end time $f_{t-end}(x)$ are determined. Event A denotes that the PEV's first trip start time is in $t_e - t_f$. Here, the vehicle does not take part in the centralized charge dispatch. The probability of event A is determined using Equation (6.17)

$$\rho(A) = \int_{t_e}^{t_f} f_{t-start}(x) dx \quad (6.17)$$

Event B denotes that the end time $T - end$ for the last trip is the neighborhood of moment t , referred as $U(t, \frac{1}{2}\Delta T)$, where ΔT is the time step. The probability of event B is determined

using Equation (6.18)

$$\rho(B) = \rho(T_{end}|T_{end} \in U(t, \frac{1}{2}\Delta T)) = \int_{(t-\frac{1}{2}\Delta T)}^{(t+\frac{1}{2}\Delta T)} f_{t-end}(x)dx \quad (6.18)$$

In a centralized charging mode, the probability of scheduable dispatch $\rho_{dispatch}(t)$ of PEV at t is estimated by Equation (6.19).

$$\rho_{dispatch}(t) = \begin{cases} 0; \forall t \in [t_e, t_f] \\ (1 - \rho(A)) \times \rho(B); \forall t \notin [t_e, t_f] \end{cases} \quad (6.19)$$

6.2.4 PEV Load Modeling

The factors affecting the PEV load include the type of the EV, charging mode, user habits and other EV parameters like driving characteristics, state of charge (SOC) etc. The driving distance and end time are uncertain. The type of EVs can be classified as buses, private cars, electric taxis based on their driving patterns. In practice, PEVs are mostly charged at constant power mode. Applying the maximum likelihood estimation technique, the pdf of logarithmic normal distribution for daily driving distance is determined as:

$$f_d(x) = \frac{1}{x\sigma_d\sqrt{2\pi}} e^{-\left[\frac{(\ln x - \mu_d)^2}{2\sigma_d^2}\right]} \quad (6.20)$$

The logarithmic normal distribution parameter i.e., standard deviation σ_d and mean value μ_d for buses, taxis and private cars are listed in Table 6.1

Table 6.1 Logarithmic normal distribution parameters

| Parameter | Taxis | Bus | Private Car |
|------------|-------|------|-------------|
| σ_d | 5.09 | 4.38 | 3.20 |
| μ_d | 0.30 | 0.32 | 0.88 |

The driving end time of private car is estimated using Equation (6.21).

$$f_s(x) = \frac{1}{x\sigma_s\sqrt{2\pi}} e^{-\left[\frac{(\ln x - \mu_s)^2}{2\sigma_s^2}\right]} \quad (6.21)$$

where, standard deviation $\sigma_s = 3.5$ and mean value $\mu_s = 17.5$. As the EV load pattern is uncertain, the Monte Carlo simulation technique is applied to estimate the daily load curve of electric private cars. The simulation steps are as follows:

- **Step1:** Set the initial values of the required parameters. Maximum travel distance is d_{max} . Maximum battery capacity is $P_{PEV,max}$, Charging power is P , Number of EVs is M , simulation time is N .
- **Step2:** Estimate the charging load of each car. Based on the pdf of the daily driving distance and driving end time, random numbers d and T are generated.

The charging load at different time periods i from 0 to 24 hours is,

$$P_m = \begin{cases} P, & i = T, T+1, T+2, \dots, T+[t]-1 \\ 0, & \text{others} \end{cases} \quad (6.22)$$

where, $[t]$ is the smallest integer that does not exceed t . The net PEV charging loads for time period, $i = 0$ to 24 hours is given by Equation (6.23).

$$P_i = \sum_{m=1}^M P_m \quad (6.23)$$

- **Step3:** The variance coefficient ε_i used to estimate the load data of N group of electric cars is:

$$\varepsilon_i = \frac{\sqrt{V_i(\bar{L})}}{\bar{L}_i} = \frac{\sigma_i(\bar{L})}{\sqrt{N}\bar{L}_i} \quad (6.24)$$

where, $V_i(\bar{L}_i)$ is variance, \bar{L}_i is expected value, $\sigma_i(\bar{L}_i)$ is standard deviation.

If the simulation attains the defined number of N and result converges, the process should be stopped. The same procedure is applicable to electric buses and taxis. The parameters are to be set according to the type of PEVs.

6.2.5 Reliability of the Network

As explained in Chapter 2, the reliability of a distribution system (DS) reflects its ability to supply power without interruption [108]. A DN comprises a set of series components, such as bus bars, distributors, service mains, cables, disconnects (or isolators), circuit breakers, protecting devices, transformers, etc. A customer attached to any LP of such a system needs all components up to the bulk supply points to be operating so that the continuity of power remains unaffected. The average failure rates (λ) and outage times (r) of these components dictate the reliability of the overall DN. In addition to these, many customer and LP-oriented indices are available to assess the severity or significance of system failures and conduct future reliability prediction analysis. The reliability indices that are used in the present study are ASAI, SAIFI, SAIDI, CAIDI, and ENS. The evaluation procedure and detailed description of these indices have been discussed in Chapter 3.

6.3 Description of the Test System

The DS of Bus-2 of the IEEE-RBTS is considered as the test system [5]. The network has four feeders, 22 Load points (LPs), 15 Bus-bars (B/B) and 22 transformers (T). The customer types, LPs, and feeder-reliability data of RBTS are used in the study which are available in Appendix A as well as in Ref. [5]. The 33kV bus is exempted from the study, and only the feeders originated from the 11kV bus; their laterals and LPs are considered for analysis. The switching and interrupting devices are assumed to have their respective failure rates and outage time as indicated in Table 6.2 which are taken from [5]. The transformers

attached to each power plant, cable, and other auxiliary devices are assumed to be 100% reliable. The single line diagram of the test system is presented in Fig. 6.2.

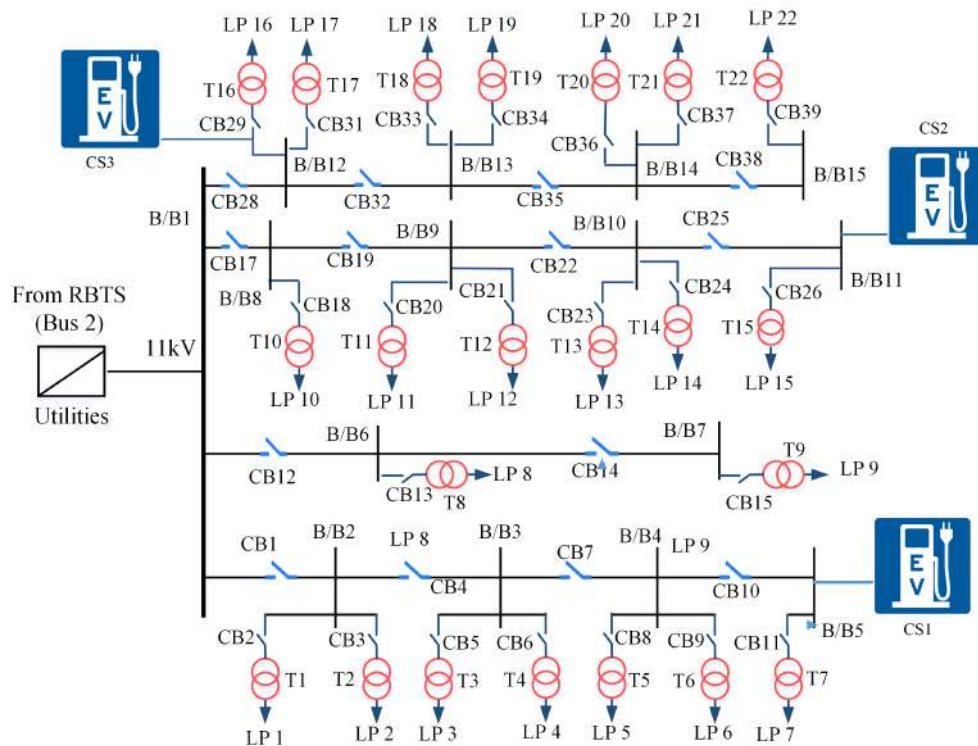


Fig. 6.2 Distribution Network at BUS-2 of IEEE-RBTS

The reliability parameters of the line and transformers are given in Table 6.2.

Table 6.2 Reliability parameters of elements of the DN

| Component | Failure rate | Repair time (/h) |
|-------------|------------------------|------------------|
| Network | 0.065 times/(km. yr) | 5 |
| Transformer | 0.015 times/ (set. yr) | 200 |
| Switch | 0.06/(set. yr) | 4.5 |

6.4 Results and Discussion

To analyze the impact of EV charging on the reliability of a DS, three charging stations are installed at busbar nos. 5, 11, and 12, respectively, as shown in Fig. 6.2. PEV loads are

considered as the most prioritized load. The following three cases are considered to examine how the increase in PEV loads affects the reliability of the DS.

Case-1: No PEV is connected to the charging points

Case-2: 100 PEVs connected to each of the three charging stations

Case-3: 200 PEVs connected to each of the three charging stations

The selected PEVs are considered to have identical ratings with following assumptions:

- Battery capacity is 57 kWh
- Endurance capacity 316 km
- The vehicle is connected for charging immediately after arriving
- The battery is charged to the maximum capacity each time it is connected for charging

The daily load curve of a particular day is taken as an example. According to the above model, the impact of different EV quantities on the daily load curve after assessing the DN is analyzed. The simulation results are shown in Fig. 6.3. The figure shows that when EVs are disorderly charged, the peak load period overlaps with the initial load, causing a peak on the peak. The load increase during this period will affect the reliability of the DN.

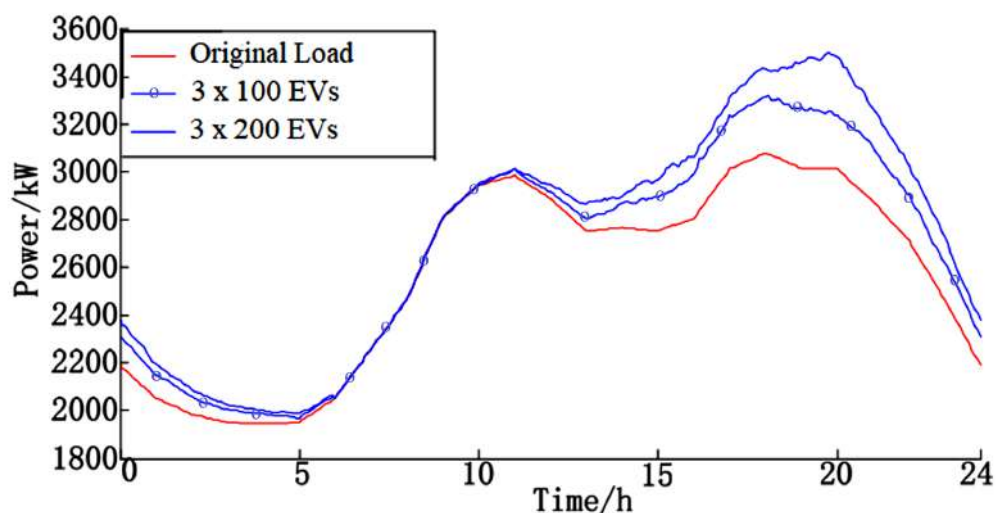


Fig. 6.3 Impact of different sizes of EV loads on system load curve

Table 6.3 shows that simulation results for the three case studies. It has been found that with increase in PEV volume, the expected ENS has reduced significantly. However, there is no impact on SAIFI, SAIDI, CAIDI and ASAI due to addition of the PEV loads.

Table 6.3 Impact of PEV charging on DS reliability

| Reliability Index | Case 1 | Case 2 | Case 3 |
|--------------------|--------|--------|--------|
| SAIFI (f/customer) | 0.215 | 0.215 | 0.215 |
| SAIDI (h/customer) | 3.812 | 3.812 | 3.812 |
| CAIDI (h/customer) | 5.331 | 5.331 | 5.331 |
| ASAI (%) | 99.981 | 99.981 | 98.981 |
| ENS (MWh/yr) | 44.374 | 45.76 | 50.43 |

Now, the reliability of the system is assessed in two different operation modes-(a) uncontrolled and (b) controlled charging. 100 private cars, 50 buses and 75 taxis are connected to each charging stations on continuous basis. The characteristics of different PEVs are given in Table 6.4

Table 6.4 Parameters of the different PEVs

| Parameters | Private Cars | Buses | Taxis |
|-------------------------|--------------|-------|-------|
| Battery Capacity (kWh) | 57 | 125 | 75 |
| Endurance Capacity (km) | 316 | 150 | 415 |
| Charging rate (C) | 0.5 | 1 | 2 |

The results obtained in the simulation are presented in Table 6.5.

Table 6.5 DS Reliability under different PEV charging modes

| Reliability Index | Uncontrolled mode | Controlled mode |
|--------------------|-------------------|-----------------|
| SAIFI (f/customer) | 1.536 | 1.336 |
| SAIDI (h/customer) | 5.612 | 4.312 |
| CAIDI (h/customer) | 3.653 | 3.297 |
| ASAI (%) | 97.9359 | 99.9633 |
| ENS (MWh/yr) | 51.91 | 48.26 |

It is observed in Table 6.5 that the system reliability indices get improved significantly in the controlled charging mode as compared to the uncontrolled scenario. It is because, in the

uncontrolled charging mode as the charging process is stochastic and distributive. As a result, load distribution is nonuniform in the uncontrolled mode. In contrast, the controlled charging mode provides the system operator to manage the load distributions among the load points.

6.5 Conclusion

This chapter has made an effort to investigate the reliability of a distribution system (DS) in the presence of plug-in EV loads. The battery charging model, PEV charging demand model, time distribution model, and PEV load models have been developed to examine how the PEV loading impacts the reliability of a DS. The concepts are exemplified in the IEEE-RBTS Bus-2 distribution system. It is found that PEV loading does not change the SAIFI, SAIDI, CAIDI, and ASAI values but significantly affects the ENS. Again, with a controlled charging schedule, the values of these indices can be improved up to a certain extent. The concepts presented in the chapter may complement the ongoing researches on PEV loading. Furthermore, the study can be extended to analyze how renewable distributed generations and optimum location of charging infrastructures help to maintain the reliability of the DS at the satisfactory level.

7

Reliability, Availability and Maintainability Analysis of Plug-in Electric Vehicle

7.1 Introduction

In the previous chapter, the reported research explains how the integration of a plug-in EV (PEV) impacts the reliability of a distribution network. The present chapter aims to investigate how the reliability of power supply from a grid influences the operational effectiveness of a PEV. In addition to that, it will address the “system reliability”, “availability,” and “maintainability” issues associated with a PEV. For this, a composite reliability model of a PEV system has been developed in this chapter.

As stated earlier, electric vehicle has been a centre of discussion in recent times. It has found growing global importance mainly due to its environment-friendly and low-cost operation [164]. However, reliability, availability, and maintainability are some of the major

issues involved in EVs [8]. While purchasing a vehicle, people are mainly concerned about the vehicle's reliability, safety, cost, and maintainability [165]. PEVs are designed with a large number of electrical components and systems (e.g., battery, motor-drive, controllers, energy management systems, etc.). These systems are highly failure-prone. Therefore, such vehicles offer less reliability than mechanically driven ICE-based vehicle systems. To achieve higher reliability, the vehicle system must be designed with reliable components. Among all the parts, the battery's reliability is the most sensitive to the reliability of a PEV [119]. The vehicle's protective schemes must also fulfill the minimum reliability criteria to ensure safety to the personnel. Although a highly reliable vehicle system demands a higher price, it reduces the frequency of maintenance and lowers the servicing cost [14].

The operation of a PEV is often affected by the reliability of a charging station. For a reliable charging station, the reliability of the power supply is a dominant factor. In many countries, load shedding is a major issue [166]. Because of frequent load shedding, charging stations offer less charging hours to a discharged PEV. As a result, the operational effectiveness or availability of a PEV decreases considerably.

A thorough RAM investigation of a vehicle system helps manufacturers to identify the failure-prone zones in the design and to estimate their contributions to the overall system failure. It encourages searching for more reliable alternatives. RAM analysis ascertains the critical performance metrics, such as Survivability, Mean Time to Failure, Mean Down Time, and Frequency of Failure [167]. Apart from these, RAM analysis is also essential from the customer's point of view. A large investment is associated while purchasing a PEV, and such investments deserve dedicated research in order to ensure that the most critical reliability criteria are satisfied. The components' reliability information can help to follow proper maintenance strategies and improve the vehicle's health [168].

As mentioned in Section 2.5.5 of Chapter 2, existing literature have reported very few reliability-oriented researches for a PEV system. Some research works have focused only at

some vital components of a PEV system. The existing literature also has not yet discussed how the availability of a PEV depends on the grid power supply and the charging system's reliability. This study aspires to fill these knowledge gaps by examining the RAM issues of a PEV system from all probable aspects. Following are some of the novel contributions of the study presented in this chapter.

- Development of a mathematical model for RAM assessment of a PEV system. The model incorporates the reliability characteristics of all the critical components of the vehicle system.
- Investigation on how the fault events are logically related to each other, how the reliability of the PEV depends on these fault events, and how the vehicle's availability gets improved with proper maintenance strategies.
- Development of a new probabilistic index for evaluating the reliability of a charging station. With the help of this index, the study analyzes how the reliability of power supply influences the operational effectiveness of a PEV.

The Markov framework has been implemented for developing the RAM model of a PEV. As mentioned in Chapter 3 most of the analytical techniques only consider the failure characteristics in reliability studies and assume that the repair process is instantaneous or negligible. It is an inherent limitation and thus requires additional methods if this assumption is not valid. Markov framework alleviates this limitation. It can incorporate the stochastic behaviors of both the failure and repair process. The basic concepts of Markov modeling is discussed in Section 3.4 with the help of a single component repairable system (Fig. 3.4).

7.2 PEV Configuration

Figure 7.1 presents the schematic diagram of a typical PEV system. The entire vehicle system can be divided into four major functional blocks or subsystems: (a) Energy Source

Subsystem (ESS), (b) Electric Propulsion Subsystem (EPS), (c) Auxiliary System (AS), and (d) Mechanical Transmission System (MTS) [165].

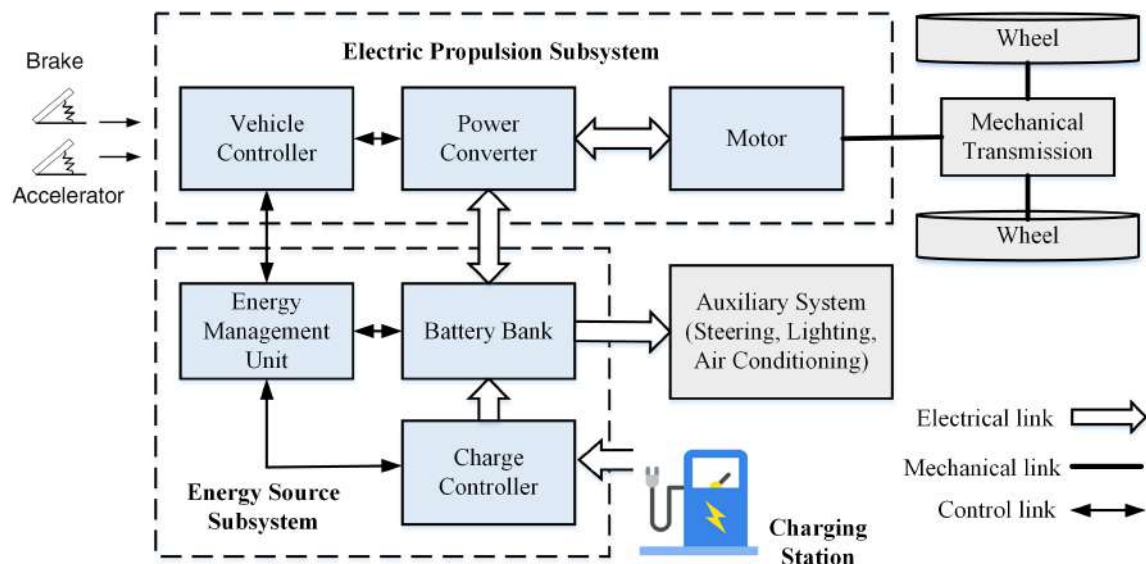


Fig. 7.1 Schematic diagram of a typical plug-in electric vehicle (PEV) system.

The ESS is comprised of a Charge Controller (CC), Battery Bank (BB), and Energy Management Unit (EMU), whereas the EPS consists of a Vehicle Controller (VC), a Power Converter (PC), and a Motor. The motor's shaft torque is transferred to the wheels through a mechanical transmission mechanism. The AS controls the auxiliary power supply that is required for power steering, lighting, air conditioning, etc. [165]

The heart of an EV is the EPS. The motor receives the electrical power from the battery bank through the PC at proper voltage and current level and transforms it into mechanical power to propel the vehicle.

The VC sends the control signals to the PC, depending on the command from the accelerator and brake pedals. The PC regulates the power flow between the ESS and motor. During braking, the PC receives the regenerative power from the motor and restores it in the battery, provided that the ESS is receptive. Most of the EV batteries have the ability to store regenerated energy. The EMU cooperates with the VC to initiate the process of energy

recovery from regenerative braking. It also monitors the state of charge (SOC) and state of health (SOH) of the battery bank in real-time and asks the CC to act accordingly [169].

7.3 Reliability Modeling of PEV System

Figure 7.2 shows the fault-tree of the PEV system. It represents all of the possible fault events associated with the vehicle system, their logical combinations, and their correlations to the system failure. The mathematical models developed for RAM assessment are based on the principle that is defined by this fault-tree.

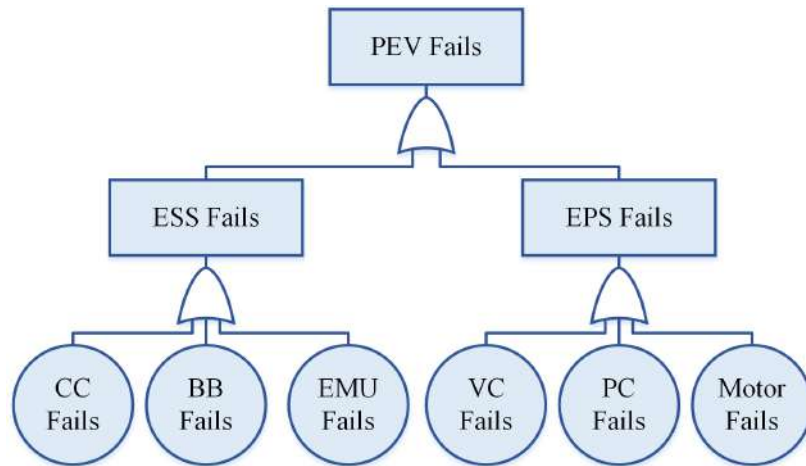


Fig. 7.2 Fault-tree diagram of the PEV system.

In this study, the battery, charge controller, vehicle controller, drives, motor, and energy management unit failures constitute the basic events. It is assumed that the failure and repair characteristics of these components are already known and exponentially distributed. Repair commences immediately if the component is repairable and the repair facility is available. Otherwise, it waits in the queue to avail the first opportunity of service. If the component is not repairable or the repair cost is close to the component's price, then the component is replaced. The restoration rate will get modified accordingly. The proposed reliability model focuses on the vehicle's main link, i.e., ESS and EPS. The AS and MTS are considered to

be 100% reliable. The reliability modelings of various subsystems of the PEV system are discussed in Sections 7.3.1, 7.3.2 and 7.3.3.

7.3.1 Modeling of Energy Source Subsystem

The ESS consists of three main components: CC, BB, and EMU, as mentioned in Section 7.2. Among these, battery is the most crucial component from the vehicle's reliability perspective. At any instant, the battery may stay either in the operational (UP) state or in the nonoperational (DOWN) state. In the operational state, the battery has enough electrostatic energy to supply the power that is required by the EPS and AS. The battery goes to the DOWN state because of two reasons: (a) it has not sufficient electrostatic energy (discharged state) and (b) it loses the ability to store charge (damaged state).

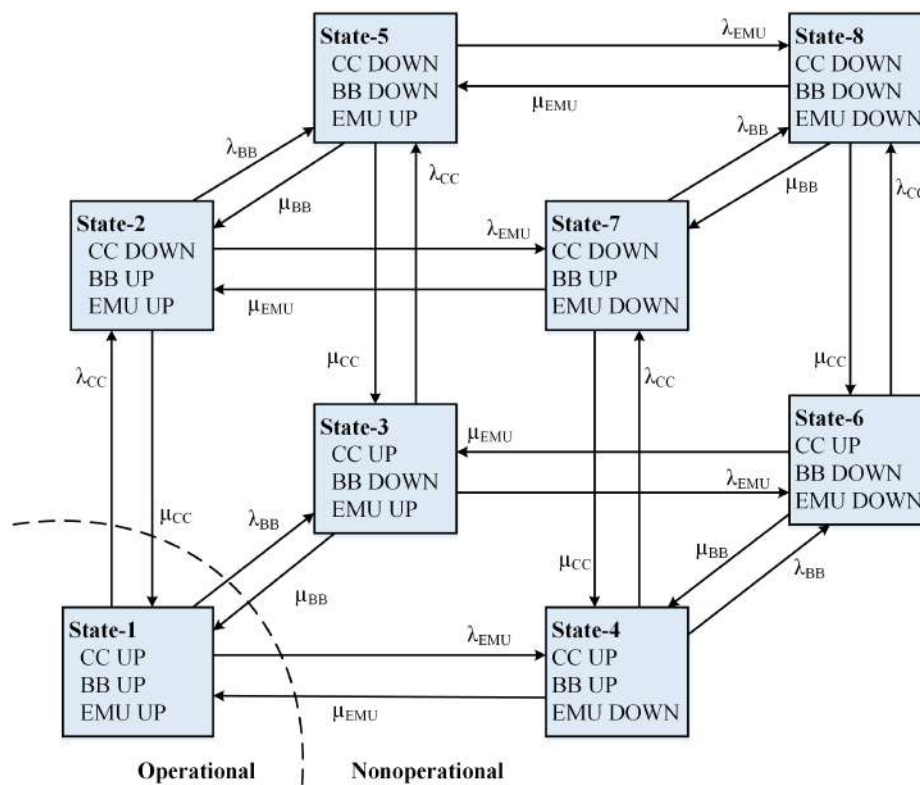


Fig. 7.3 State-space diagram of the Energy Source Subsystem.

Similarly, the CC and EMU also have two possible states (UP and DOWN) at any time 't'. Therefore, the entire ESS will have a total 2^3 no. of transitional states. Figure 7.3 shows the state-space model of the ESS illustrating the transitions among all of the possible states. $\lambda_{CC}, \lambda_{BB}, \lambda_{EMU}$ represent the failure rates and $\mu_{CC}, \mu_{BB}, \mu_{EMU}$ represent the restoration rates of the CC, BB, and EMU, respectively. Equation (7.1) shows the STPM of a three-components system.

$$STPM = \begin{bmatrix} 1-\lambda_1-\lambda_2-\lambda_3 & \lambda_1 & \lambda_2 & \lambda_3 & 0 & 0 & 0 & 0 \\ \mu_1 & 1-\mu_1-\lambda_2-\lambda_3 & 0 & 0 & \lambda_2 & 0 & \lambda_3 & 0 \\ \mu_2 & 0 & 1-\lambda_1-\mu_2-\lambda_3 & 0 & \lambda_1 & \lambda_3 & 0 & 0 \\ \mu_3 & 0 & 0 & 1-\lambda_1-\lambda_2-\mu_3 & 0 & \lambda_2 & \lambda_1 & 0 \\ 0 & \mu_2 & \mu_1 & 0 & 1-\mu_1-\mu_2-\lambda_3 & 0 & 0 & \lambda_3 \\ 0 & 0 & \mu_3 & \mu_2 & 0 & 1-\lambda_1-\mu_2-\mu_3 & 0 & \lambda_1 \\ 0 & \mu_3 & 0 & \mu_1 & 0 & 0 & 1-\mu_1-\lambda_2-\mu_3 & \lambda_2 \\ 0 & 0 & 0 & 0 & \mu_3 & \mu_1 & \mu_2 & 1-\mu_1-\mu_2-\mu_3 \end{bmatrix} \quad (7.1)$$

If the suffix 1, 2, and 3 used in λ and μ are replaced by CC, BB, and EMU, respectively, then Equation (??) will represent the STPM of the ESS model.

The probability of occurrence of each state of the ESS model that is shown in Fig. 7.3 can be determined using Equations (7.2)–(7.9).

$$P_{ESS}^{(1)} = \frac{\mu_{CC}\mu_{BB}\mu_{EMU}}{(\lambda_{CC} + \mu_{CC})(\lambda_{BB} + \mu_{BB})(\lambda_{EMU} + \mu_{EMU})} \quad (7.2)$$

$$P_{ESS}^{(2)} = \frac{\lambda_{CC}\mu_{BB}\mu_{EMU}}{(\lambda_{CC} + \mu_{CC})(\lambda_{BB} + \mu_{BB})(\lambda_{EMU} + \mu_{EMU})} \quad (7.3)$$

$$P_{ESS}^{(3)} = \frac{\mu_{CC}\lambda_{BB}\mu_{EMU}}{(\lambda_{CC} + \mu_{CC})(\lambda_{BB} + \mu_{BB})(\lambda_{EMU} + \mu_{EMU})} \quad (7.4)$$

$$P_{ESS}^{(4)} = \frac{\mu_{CC}\mu_{BB}\lambda_{EMU}}{(\lambda_{CC} + \mu_{CC})(\lambda_{BB} + \mu_{BB})(\lambda_{EMU} + \mu_{EMU})} \quad (7.5)$$

$$P_{ESS}^{(5)} = \frac{\lambda_{CC}\lambda_{BB}\mu_{EMU}}{(\lambda_{CC} + \mu_{CC})(\lambda_{BB} + \mu_{BB})(\lambda_{EMU} + \mu_{EMU})} \quad (7.6)$$

$$P_{ESS}^{(6)} = \frac{\mu_{CC}\lambda_{BB}\lambda_{EMU}}{(\lambda_{CC} + \mu_{CC})(\lambda_{BB} + \mu_{BB})(\lambda_{EMU} + \mu_{EMU})} \quad (7.7)$$

$$P_{ESS}^{(7)} = \frac{\lambda_{CC}\mu_{BB}\lambda_{EMU}}{(\lambda_{CC} + \mu_{CC})(\lambda_{BB} + \mu_{BB})(\lambda_{EMU} + \mu_{EMU})} \quad (7.8)$$

$$P_{ESS}^{(8)} = \frac{\lambda_{CC}\lambda_{BB}\lambda_{EMU}}{(\lambda_{CC} + \mu_{CC})(\lambda_{BB} + \mu_{BB})(\lambda_{EMU} + \mu_{EMU})} \quad (7.9)$$

The ESS will be operational if, and only if, all of its components are in UP states, i.e., the ESS will be working in state-1 only. Thus, the availability of the ESS (A_{ESS}) will be equal to $P_{ESS}^{(1)}$ and it can be determined from Equation (7.2). In the remaining seven states, at least one component is in the failed state, which makes the whole ESS non-operable. Thus, the unavailability of the ESS (U_{ESS}) will be the net probability of these seven states, and it can be calculated using Equation (7.10).

$$U_{ESS} = \sum_{i=2}^8 P_i \quad (7.10)$$

Eliminating the DOWN states from Equation (7.1), the STPM reduces to a truncated matrix (Q) that is given by Equation (7.11).

$$Q = \begin{bmatrix} 1 - \lambda_{CC} - \lambda_{BB} - \lambda_{EMU} \end{bmatrix} \quad (7.11)$$

The mean time that the ESS spent in state-1 is determined using Equation (7.12).

$$M = [I - Q]^{-1} \quad (7.12)$$

∴ The mean operating time (MOT) of the ESS is:

$$MOT_{ESS} = \frac{1}{\lambda_{CC} + \lambda_{BB} + \lambda_{EMU}} \quad (7.13)$$

The effective failure rate of the ESS will be:

$$\lambda_{ESS} = \frac{1}{MOT_{ESS}} = \lambda_{CC} + \lambda_{BB} + \lambda_{EMU} \quad (7.14)$$

Again, the Mean Down Time (MDT) or Mean-time-to-repair (MTTR) of the ESS can be calculated using Equation (7.15).

$$MDT_{ESS} = \frac{1 - A_{ESS}}{A_{ESS} \times \lambda_{ESS}} \quad (7.15)$$

∴ The effective restoration rate of the ESS will be:

$$\mu_{ESS} = \frac{1}{MDT_{ESS}} = \frac{A_{ESS} \times \lambda_{ESS}}{1 - A_{ESS}} \quad (7.16)$$

7.3.2 Modeling of the Electric Propulsion Subsystem

The stochastic model for the EPS (Fig.7.4) is comprised of a vehicle controller (VC), a power converter (PC), and a motor, each of having two operational states (i.e., UP and DOWN).

The model architecture is similar to that of the ESS. For the successful operation of the EPS, it is necessary to remain all of its components in the working (UP) state. This

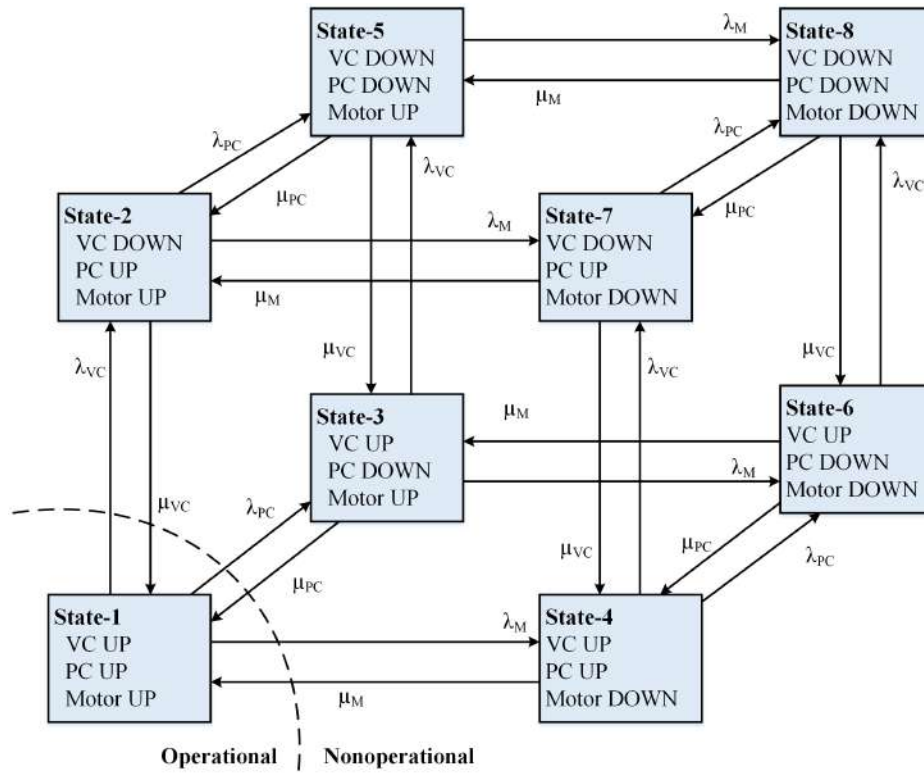


Fig. 7.4 State-space diagram of the Electric Propulsion Subsystem.

means that the EPS will be operational in state-1 only. Therefore, the availability of the EPS will be equal to the limiting state probability of state-1, which can be calculated using Equation (7.17).

$$A_{EPS} = P_{EPS}^{(1)} = \frac{\mu_{VC}\mu_{PC}\mu_M}{(\lambda_{VC} + \mu_{VC})(\lambda_{PC} + \mu_{PC})(\lambda_M + \mu_M)} \quad (7.17)$$

The effective failure and restoration rates of the EPS can be determined using Equations (7.18) and (7.19), respectively.

$$\lambda_{EPS} = \lambda_{VC} + \lambda_{PC} + \lambda_M \quad (7.18)$$

$$\mu_{EPS} = \frac{A_{EPS} \times \lambda_{EPS}}{1 - A_{EPS}} \quad (7.19)$$

7.3.3 Modeling of the PEV System

After evaluating the reliability parameters (i.e., failure rates and restoration rates) of the ESS and EPS blocks, the reliability model for the PEV system can be constructed, as shown in Fig. 7.5.

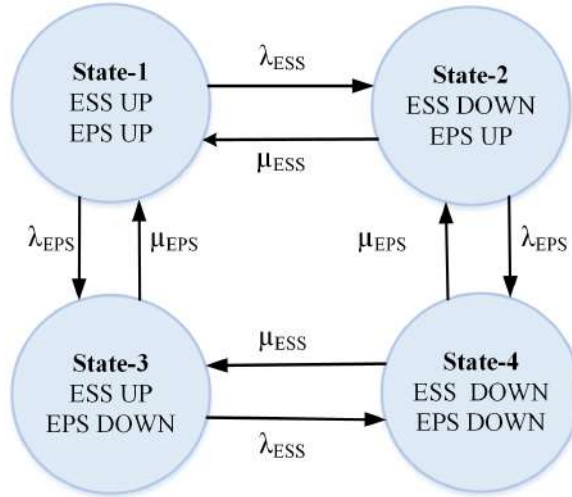


Fig. 7.5 State-space diagram of the PEV system.

Depending on the operating status of the ESS and EPS, the PEV system may remain in any one of the four probable states that are mentioned in Fig. 7.5. The transition rates between two adjacent states will define the STPM, as follows:

$$STPM_{PEV} = \begin{bmatrix} 1 - \lambda_{ESS} - \lambda_{EPS} & \lambda_{ESS} & \lambda_{EPS} & 0 \\ \mu_{ESS} & 1 - \mu_{ESS} - \lambda_{EPS} & 0 & \lambda_{EPS} \\ \mu_{EPS} & 0 & 1 - \lambda_{ESS} - \mu_{EPS} & \lambda_{ESS} \\ 0 & \mu_{EPS} & \mu_{ESS} & 1 - \mu_{ESS} - \mu_{EPS} \end{bmatrix} \quad (7.20)$$

In order to make the vehicle operational, ESS and EPS must both be in working state. Thus, the availability of the PEV is equal to the probability of occurrence of state-1, which can be determined using Equation (7.21).

$$A_{PEV} = P_{PEV}^{(1)} = \frac{\mu_{ESS}\mu_{EPS}}{(\lambda_{ESS} + \mu_{ESS})(\lambda_{EPS} + \mu_{EPS})} \quad (7.21)$$

If the transitions that are associated with the nonoperational states are eliminated, the STPM of the PEV reduces to Equation (7.22).

$$Q_{PEV} = \begin{bmatrix} 1 - \lambda_{ESS} - \lambda_{EPS} \end{bmatrix} \quad (7.22)$$

The mean-time-to-first-failure (MTTFF) which decides the *warranty period* of the vehicle, can be determined using Equation (7.23).

$$MTTFF_{PEV} = [I - Q_{PEV}]^{-1} = [\lambda_{ESS} + \lambda_{EPS}]^{-1} \quad (7.23)$$

Again, the mean down time of the vehicle can be determined using Equation (7.24).

$$MDT_{PEV} = \frac{1 - A_{PEV}}{A_{PEV} \times \lambda_{PEV}} \quad (7.24)$$

∴ The effective failure rate and repair rate of the vehicle can be estimated using Equations (7.25) and (7.26), respectively.

$$\lambda_{PEV} = \frac{1}{MTTFF_{PEV}} = \lambda_{ESS} + \lambda_{EPS} \quad (7.25)$$

$$\mu_{PEV} = \frac{1}{MDT_{PEV}} = \frac{A_{PEV} \times \lambda_{PEV}}{1 - A_{PEV}} \quad (7.26)$$

The reliability of the PEV system at time, t can be determined using Equation (7.27).

$$R_{PEV}(t) = e^{-\lambda_{PEV}t} \quad (7.27)$$

Additionally, the maintainability of the PEV at time, t can be calculated using Equation (7.28).

$$M_{PEV}(t) = 1 - e^{-\mu_{PEV}t} \quad (7.28)$$

7.4 Charging Station's Role on PEV's Availability

The reliability of a charging station (CS) plays a vital role in the availability of a PEV. A charging station's reliability depends on two factors: (a) Reliability of power supply, and (b) Reliability of the charging system.

If the charging station is subjected to a power outage, the vehicle will have to wait for a longer time to get recharged and, hence, the Mean Down Time of the PEV increases. The vehicle will be remaining nonoperational (forced outage) until the power supply is restored. The higher the downtime, the lesser will be the availability. It can be justified from Equation (7.29).

$$Availability = \frac{Mean\ Operable\ Time}{Mean\ Operable\ Time + Mean\ Down\ Time} \quad (7.29)$$

In addition to a reliable power supply, a reliable charging system is also important for reducing the downtime of a vehicle. Charging systems experience forced outages due to internal faults and they remain out of service for a certain period. An unreliable charging system provides fewer charging hours to a PEV.

In order to investigate how a charging station's reliability impacts the availability of a PEV, a two-state battery model is integrated with a two-state CS model. The state-space diagram of this composite model is shown in Fig. 7.6.

Figure 7.6 shows that the battery is in the UP state (charged) in states 1 and 2 only. The vehicle has the maximum availability in state-1 (provided all other PEV components are operating well). In state-2, the vehicle is operable, but the availability is restricted by

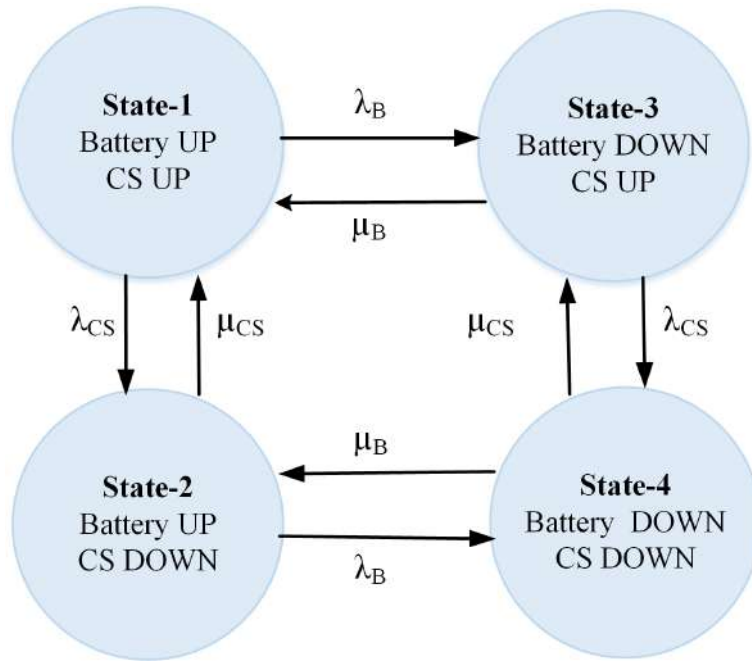


Fig. 7.6 State-space diagram of the CS-Battery Model.

the discharging rate of the battery (λ_B) and restoration rate of the CS (μ_{CS}). In state-3, the vehicle is in discharged mode and, hence, unavailable to operate. Here, the unavailability is controlled by the charging rate of the battery (μ_B) and failure rate of CS (λ_{CS}). The vehicle is also not operable in state-4, and its availability will depend on μ_{CS} and μ_B .

The probability that the PEV may enter into the aforesaid four states can be determined using Equations (7.30)–(7.33).

$$P_1 = \frac{\mu_B \mu_{CS}}{(\lambda_B + \mu_B)(\lambda_{CS} + \mu_{CS})} \quad (7.30)$$

$$P_2 = \frac{\mu_B \lambda_{CS}}{(\lambda_B + \mu_B)(\lambda_{CS} + \mu_{CS})} \quad (7.31)$$

$$P_3 = \frac{\lambda_B \mu_{CS}}{(\lambda_B + \mu_B)(\lambda_{CS} + \mu_{CS})} \quad (7.32)$$

$$P_4 = \frac{\lambda_B \lambda_{CS}}{(\lambda_B + \mu_B)(\lambda_{CS} + \mu_{CS})} \quad (7.33)$$

The power supply's reliability at a particular charging station can be determined with the help of a probabilistic index, called Average Service Availability Index (ASAI) [7]. Although it is a distribution system's reliability index, it can also be applied in the charging station with few modifications. The modified ASAI is defined, as follows:

$$\begin{aligned} ASAI &= \frac{\text{Charging hours available for service}}{\text{Charging hours demanded}} \\ &= \frac{\sum N_i \times 8760 - \sum U_i N_i}{\sum N_i \times 8760} \end{aligned} \quad (7.34)$$

where, N_i is the no. of vehicles to be recharged and U_i is the annual outage time at the i^{th} charging point.

Now, considering the charging system as a single component having an effective failure rate of λ_C and restoration rate of μ_C , the reliability of the CS at time 't' can be determined using Equation (7.35).

$$R_{CS}(t) = (ASAI).e^{-\lambda_C t} \quad (7.35)$$

The availability of the CS can be determined using Equation (7.36).

$$A_{CS}(t) = (ASAI). \left[\frac{\mu_C}{\lambda_C + \mu_C} \right] \quad (7.36)$$

The mean operable time of the CS can be calculated using Equation (7.37).

$$MOT_{CS} = \int_0^{\infty} R_{CS}(t) dt = \frac{ASAI}{\lambda_C} \quad (7.37)$$

The effective failure rate of the CS can be determined using Equation (7.38).

$$\lambda_{CS} = \frac{1}{MOT_{CS}} = \frac{\lambda_C}{ASAI} \quad (7.38)$$

The effective restoration rate of the CS can be obtained using Equation (7.39).

$$\mu_{CS} = \frac{A_{CS} \times \lambda_{CS}}{1 - A_{CS}} \quad (7.39)$$

Now, the availability of the PEV at different stochastic operational situations of a charging station can be investigated using Equations (7.30)–(7.33).

7.5 Results and Discussion

The developed mathematical models have been implemented to a typical PEV system in order to carry out the RAM assessment. Tables A.8 and A.9 in Appendix provides the reliability data and other relevant information required for the analysis. The component reliability data are realized from Military Handbook MIL-HDBK-217E and MIL-HDBK-217F. The case study is categorized in two parts, as follows:

7.5.1 RAM Assessment of the PEV System

Figure 7.7 shows the reliability, availability, and maintainability characteristic curves for the PEV system. It indicates that the vehicle's reliability is exponentially decreasing and it becomes 67.99%, 46.23%, and 31.43% after a period of 5, 10, and 15 years, respectively. However, due to maintenance (i.e., inclusion of repair rates), its operational effectiveness increases significantly and it becomes 85.52%, 84.12%, and 83.96%, respectively, after the said periods. The improvement can be noticed by comparing the reliability and availability curves that are shown in Fig. 7.7. Again, as time passes, the vehicle's maintenance rate has to be increased, so that its availability increases and attains the maximum (steady-state) value. As the maintainability curve approaches 1 (i.e., 100%), the availability curve becomes saturated and cannot be further improved with standard restoration rates.

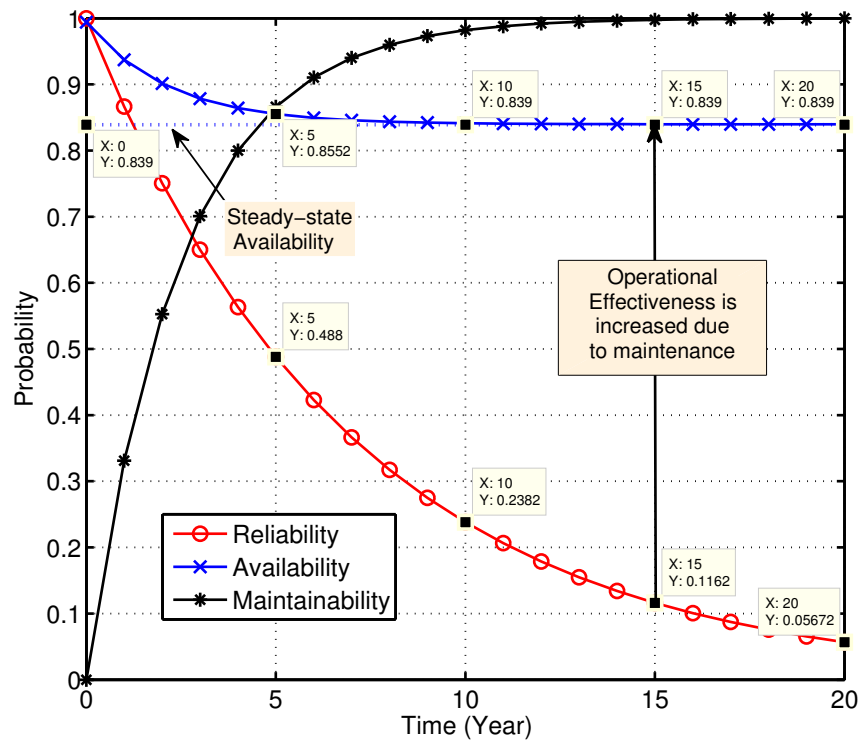


Fig. 7.7 Reliability, Availability, and Maintainability curves for the PEV.

For further improvement in steady-state availability, three possible options are available: (a) using components having lower failure rate, (b) using spare components as standby redundancy, and (c) increasing the repair or restoration rates. The first two options are only possible at the manufacturing stage and restricted by the design and cost constraints. The failure properties are usually stochastic, and the operator cannot do much on it. However, the repair time and restoration rates of faulty components can be controlled by the operator up to a certain level. If the vehicle's defective part is replaced or repaired at a higher rate, then the vehicle's availability increases significantly.

Figure 7.8 graphically illustrates how the vehicle's operational effectiveness improves with higher restoration rates (RR). It is observed that, if the RR is increased by 25%, the steady-state availability of the PEV improves by 3.50%. Similarly, 50%, 75%, and 100% increment in restoration rates of the failed components will give 5.92%, 7.69%, and 9.04% improvement of steady-state availability, respectively.

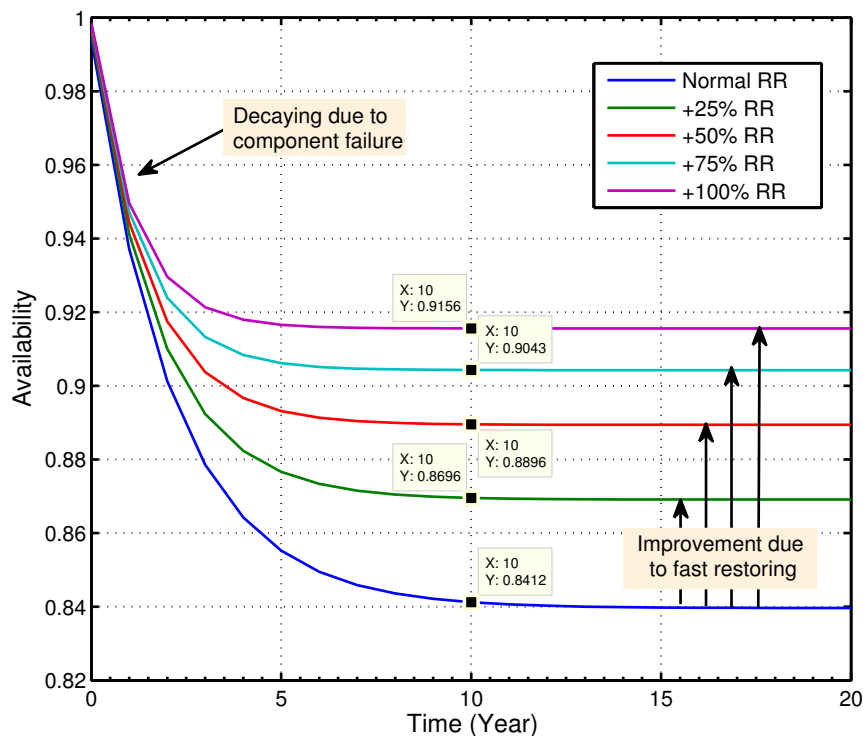


Fig. 7.8 Vehicle's availability at different restoration rates (RR).

7.5.2 Impact of *ASAI* on the PEV

In Section 7.5.1, RAM analysis of the PEV is performed while assuming that the charging station is 100% reliable. However, in practice, this assumption does not hold good, as no system is 100% reliable.

The reliability and availability of a charging station are mainly dependent on three parameters namely, *ASAI*, λ_c , and μ_c , as mentioned in Section 7.4. Using the charging station's data given in Table A.9 in Appendix A, the value of *ASAI* is found to be 90.47%. Corresponding to this value, the charging station offers 71.78% reliability and 83.91% availability to the PEV after five years of operation.

Figure 7.9 shows the availability of a five years old PEV system at different values of *ASAI*. The results show that the vehicle's availability or operational effectiveness is highly dependent on the value of *ASAI*. At zero *ASAI*, a vehicle coming for recharge will be lying ineffective at the charging station. As *ASAI* increases, the PEV's availability increases.

For example, at 50% *ASAI*, the availability of the PEV becomes 73.97%. At 100% *ASAI*, the availability of the vehicle (after five years of operation) becomes 79.33%. It cannot reach the 100% mark due to the unreliability contributed by the charging unit and other components of the PEV. If all the other components are 100% available, then only the PEV can achieve 100% availability at 100% *ASAI* value.

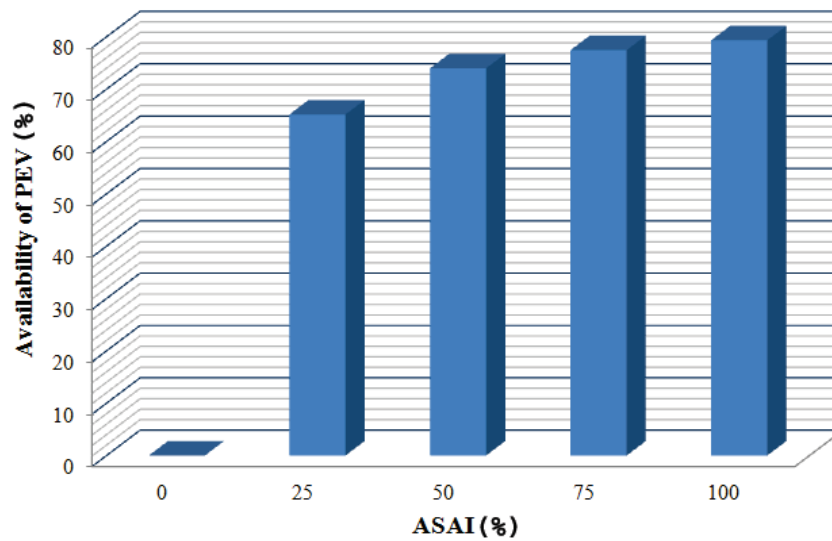


Fig. 7.9 Availability of PEV at different *ASAI*.

In many developing countries, where frequent power outages occur, *ASAI* can be a useful indicator for the vehicle owners. The knowledge of *ASAI* will help the PEV owner in the effective and reliable operation of their vehicles. However, modern charging stations are equipped with captive power plants (most preferably by renewable energy) to reach the *ASAI* close to 100%. A battery with a high charging rate can save the charging hours of a charging station. It reduces the MDT of a discharged PEV. Again, a slow discharging rate increases the MOT of the vehicle. It helps to improve the availability of a PEV.

7.6 Conclusion

In this chapter, RAM assessment of a PEV system is done using Markov Framework. The study justifies that the reliability and availability of a PEV deteriorate with time, due to its components' failures. However, with timely repair or replacement of the faulty components, the vehicle's operational effectiveness can be improved significantly. Although a vehicle owner does not have the option to control the system's stochastic failures, the restoration process of faulty components can be accelerated up to a certain level. It will increase the availability of the vehicle. Again, it is observed that the availability of a PEV highly depends on the charging station's reliability. A charging station's reliability mostly relies on the reliability of the power supply. The present study demonstrates this aspect with the help of a modified reliability index, *ASAI*. Because of frequent load shedding in the rural areas of many developing countries, *ASAI* can be a useful indicator for vehicle owners. There is a noticeable literature gap on this topic. The concepts that have been introduced in this chapter can inspire further research on the RAM issues of a vehicle system. There is a scope for further continuation of the study concentrating on reliability worth assessment. It will assist manufacturers in designing more reliability-centric, but cost-effective PEV models.

The dependency on the grid power supply can be reduced/eliminated by facilitating the charging station with RESs. Solar and/or wind energy are the most widely used RESs to feed a charging station. Furthermore, the grid-dependency of a PEV can be alleviated by mounting a photo-voltaic system on the roof of the vehicle system itself. Reliability investigation on this type of EV is presented in the next chapter.

8

Reliability Modeling and Availability Analysis of Solar Electric Vehicle

8.1 Introduction

In the previous chapter, it has been discussed that the reliability and availability of an electric vehicle (EV) are much more dependent on the reliability and availability of a charging station. It also illustrates how the reliability of power supply from the grid impacts the operational effectiveness of a plug-in (PEV). The present chapter aims to address how an EV embedded with an onboard photovoltaic system (PVS) can solve these issues, and can be a better EV option from reliability perspective.

As stated in Section 2.5.6, EV can be a potential solution to the emission problem of the transport sector. However, the electricity required for an EV still needs to be produced, in part by fossil fuels in many countries. Thus, attaining a truly carbon-free solution on

the horizon is not fulfilled. There are some other issues also in EVs. The lack of charging infrastructure at the desired location limits the adaptability of these vehicles. Unlike a conventional vehicle, a plug-in EV needs a much longer refueling time [32], and people may not have enough time to recharge the vehicle at a public charging station (CS). Moreover, load shedding is a common problem in many developing countries. It reduces the reliability of the CS and adversely affects the operation of a plug-in EV. A solar electric vehicle (SEV), which is powered entirely or considerably by direct solar energy utilizing photovoltaic (PV) technology, seems to be one of the best last-mile solutions to these problems providing a grid-free and continuous charging facility [129]. The ability to recharge during the running as well as parking period is one of the most outstanding advantages of a SEV.

The operation of a SEV mainly depends on the reliability of its onboard photovoltaic system (PVS). The power generated by PVS is intermittent in nature and affected by various factors like solar irradiation, vehicle's geographic location, ambient temperature, weather condition, dust deposition, wind speed etc.[135–138]. Designing a PVS on the roof of the vehicle to produce reliable electrical power for charging the battery at a standard rate is a major challenge for the SEV manufacturers. Most manufacturers try to mitigate this challenge by providing a standby power source such as plug-in option, fuel cell, swappable spare battery, etc. The standby power supply option significantly improves the reliability of the SEV. Apart from the power source, the reliability of other electrical components of the SEV such as battery, energy management system, propulsion system, controllers, etc. have also considerable impacts on the overall operational effectiveness of the vehicle. For a better survivability, the vehicle system must be manufactured with a reliable design using reliable components [139]. Moreover, the vehicle's protective schemes must fulfill the minimum reliability criteria to ensure safety to the personnel. Although a system with high reliability incurs higher manufacturing costs, it reduces the frequency of maintenance and therefore, lowers the service costs [63].

As reported in Section 2.5.6, the reliability assessment of a solar-energized EV is still an unexplored research area. Most of the studies carried out so far were confined to the design and performance analysis of a few selected components of a SEV system. This chapter concentrates on those research gaps, and carries out a comprehensive reliability and availability assessment of a SEV facilitated with a standby plug-in option. It aims to investigate how the availability of a SEV is dictated by the reliability of its onboard PV system and how a standby plug-in facility improves the reliability and availability of a SEV. The study also examines how the SEV's fault events are logically correlated and responsible for its failure and how proper maintenance strategies can improve its availability. The standby redundancy concepts of reliability engineering have been applied in the power supply system. Markov framework [140] has been used to construct the state-space models and determine the critical performance metrics of the SEV system. This framework can incorporate both failure and repair characteristics of a system. In contrast, all other reliability frameworks count only the failure characteristics of components stating that the repair process is instantaneous and negligible. Since repair process or maintenance has a significant role in a vehicle's reliable operation, therefore, Markov concepts can provide a better estimation of 'system reliability' of a vehicle. The upshot of this study is expected to complement the ongoing researches on SEV design and maintenance. Some of the significant contributions of the study covered in this chapter are stated below:

- A composite reliability model for a SEV system is proposed, which includes all critical factors and components that can influence the reliability and availability of the vehicle.
- A new probabilistic index, termed as *mPAI*, is proposed to determine the availability of power generated by the onboard PV System. This index helps to investigate the effectiveness of a SEV at a particular geographic location.

- A distribution system reliability index, called *ASAI*, is modified and proposed for evaluating the reliability of a CS. This index helps to examine the improvement of SEV's reliability due to the addition of the standby plug-in facility.
- Reliability-centric sensitivity analyses have been carried out to investigate the impacts of key parameters on the performance of a SEV.

In this chapter, Section 8.2 presents the schematic diagram and description of the SEV system. Section 8.3 presents the detailed reliability modeling of the vehicle system. Section 8.4 presents the results and discussion of several case studies to exemplify the proposed reliability models. The conclusion is drawn in Section 8.5.

8.2 Description of the SEV System

The schematic diagram of the SEV system under study is shown in Fig. 8.1. The entire vehicle system is divided into three major functional blocks: Power Supply System (PSS), electrical propulsion system (EPS), and mechanical transmission system (MTS) [170]. The PV system (PVS) mounted on the exterior body (usually on the roof) of the SEV and the standby plug-in system together constitute the PSS. Under normal operating conditions (NOC), the PVS generates electrical power, which is stored in the battery bank after passing through a controlled and protective mechanism. The standby plug-in option provides the flexibility to recharge the vehicle at a charging station (CS). The EPS includes an energy storage system (ESS), a motor-drive system (MDS), a vehicle controller (VC), and an energy management system (EMS). The MTS mainly consists of a gear mechanism, steering, and wheels, etc. [170, 171].

The input command to the vehicle comes from a driver in the form of an accelerator command or braking command. This command proceeds to the VC, which then acts and gives information to the electric drive to initiate the action. When the accelerator command

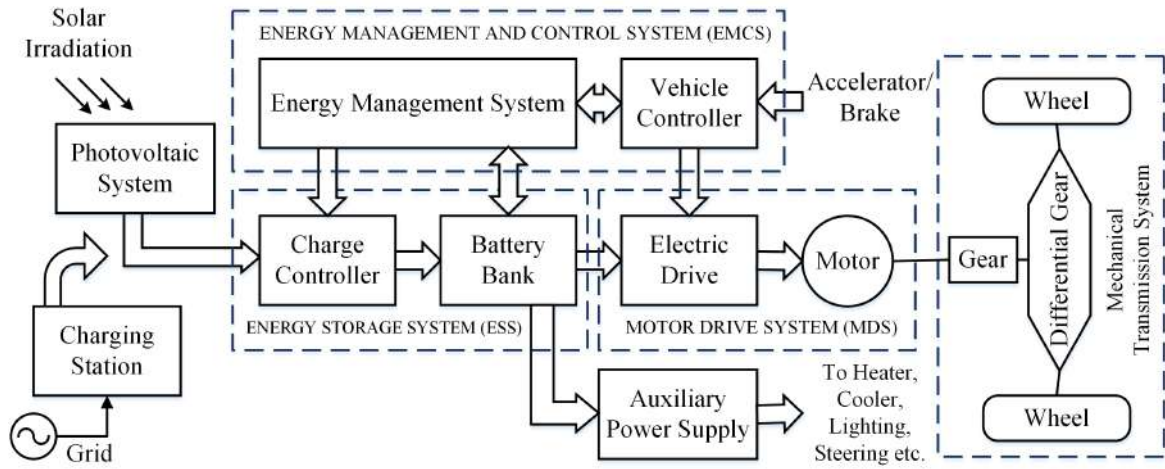


Fig. 8.1 Schematic diagram of the SEV under study

is given, the power is transferred from the battery to the wheels via MDS. When the braking action is commanded, the drive initiates the regenerative braking mechanism provided the ESS is receptive [170]. Most EV batteries can accept regenerated energy. The EMS monitors the parameters in real-time and sends information to VC to regulate the regenerative braking and reduce waste of energy. It takes care of the state of charge (SOC) and state of health (SOH) of the battery bank [172–175]. The EMS also controls the heating and cooling process and manages the auxiliary power supply.

8.3 Reliability Modeling of SEV

As defined earlier, the term ‘reliability’ denotes the probability that a system is operable for a certain period without a single failure [139, 140]. Reliability mainly depends on the design and topological layout of the system in addition to the failure characteristics of its constituting components [139]. The proposed reliability model concentrates on the electrical link of the SEV and considers that the MTS and connecting cables are 100% reliable. The vehicle’s electrical link starts with the power supply scheme, and the charge controller (CC), battery bank, motor, drive, EMS and the vehicle controller (VC) are the core components

in the link. These components are assumed to be single entities, i.e., further decomposition is not required. All these components are reliability-wise in series. The vehicle will be operational (i.e., in UP state) if each of these components is in operable condition. Failure of a single component will lead the SEV to a state of ineffectiveness (DOWN). It is assumed that the reliability characteristics of these components are known, and they follow the properties of the exponential probability density function [140]. Whenever a component fails, repair commences immediately if the repair facility is available; if not, then the failed unit waits in the line for getting the first opportunity to repair or replace. The detailed mathematical modelings of various subsystems of the SEV are illustrated categorically in the following subsections.

8.3.1 Fault-Tree model of the SEV under study

The reliability model proposed in this study is based on the principle defined by the fault-tree [140] shown in Fig. 8.2.

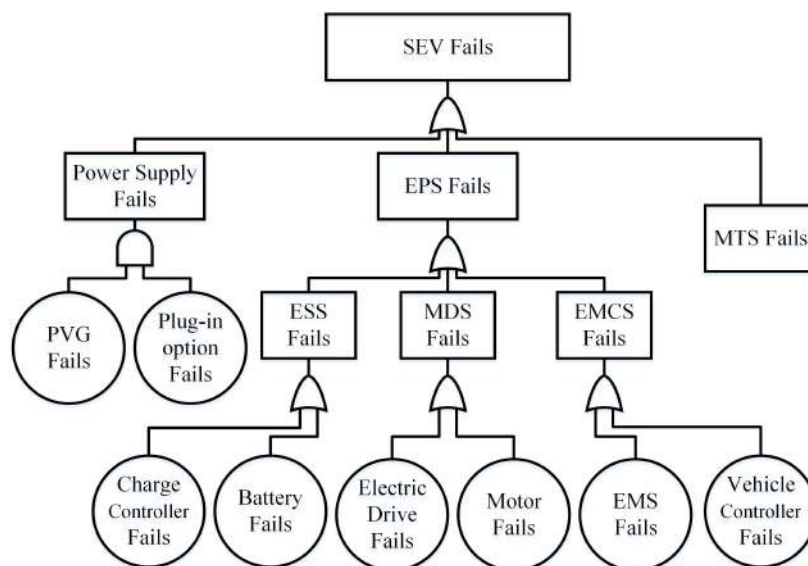


Fig. 8.2 Fault-tree of the SEV under study

The fault-tree diagrammatically represents all probable fault events, their logical correlations, and their contributions to the SEV's failure. This schematic approach of fault-tree analysis helps to find out the root causes of failure. The "basic events" in the fault-tree are the failure events of the components of the electrical link, namely charge controller, battery, electric drive, motor, VC, EMS and power supply. The "top event" is the "SEV failure". The failure probabilities of basic events are combined with logical AND and OR gates to obtain the failure probabilities of intermediate events and finally the top event, i.e., SEV failure.

The power supply scheme fails if both PV generation and plug-in systems fail. The EPS will fail if at least one component constituting the basic events fails. The vehicle will fail to operate if at least one subsystem among the PSS, EPS, and MTS fails. Based on this principle, the critical performance metrics of the SEV system, such as failure rate (FR), repair or replacement rate (RR), mean operating time (MOT), mean restoration time (MRT), availability, forced outage rate (FOR), mean-time-to-first-failure, (MTTFF), etc.[139, 140] are determined.

8.3.2 Modeling of Power Supply System (PSS)

The power supply scheme of the SEV is presented in Fig. 8.3. It consists of an onboard PVS and a plug-in system. The PVS acts as a primary source of power supply. Under NOC, the PVS provides continuous power to its battery. The battery stores this energy during the vehicle's parking time, which can be utilized during the inadequate solar irradiation period. However, in the event of a forced outage of the PVS, or any other emergency situation, the vehicle uses the plug-in option to recharge the battery at a charging station (CS). Thus, the CS acts as a standby redundancy [140] source. The change-over switch connects the PVS or CS to the charge-controller.

The reliability modelings of these two sources are described in Sections 8.3.2.1 and 8.3.2.2, and the reliability of the PSS is evaluated in Section 8.3.2.3.

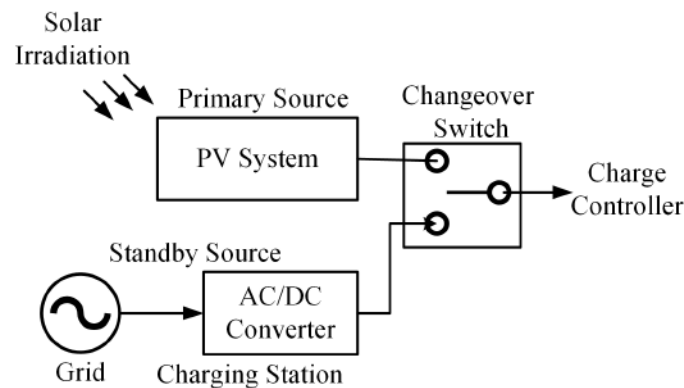


Fig. 8.3 Power supply scheme for the SEV under study

8.3.2.1 Modeling of PV Generation (PVG)

The power generated by a PV system (P) is a function of solar irradiance (G) and surface temperature (T) of the PV panel [136, 151] which can be defined by Equation (8.1).

$$P(G, T) = \begin{cases} P_{max} \left(\frac{G^2}{G_{std} G_{ref}} \right) (1 + \alpha \Delta T); & \forall G \in [0, G_{ref}) \\ P_{max} \left(\frac{G}{G_{std}} \right) (1 + \alpha \Delta T); & \forall G \in [G_{ref}, G_{std}) \\ P_{max} (1 + \alpha \Delta T); & \forall G \geq G_{std} \end{cases} \quad (8.1)$$

where P_{max} is the maximum generation capacity of the PV system, G_{std} is the solar irradiation under standard condition, G_{ref} is the reference irradiance according to the specific geographical location, α is the coefficient of the temperature of the PV panel, and ΔT is the deviation in temperature from the nominal value of $25^\circ C$.

The temperature variation in a particular day can be expressed by Equation (8.2).[136]

$$T = A \sin \omega + B \quad (8.2)$$

where ω is the solar hour angle and

$$A = \frac{T_{max} - T_{min}}{2} \quad (8.3)$$

$$B = \frac{T_{max} + T_{min}}{2} \quad (8.4)$$

where T_{max} and T_{min} are the maximum and minimum temperatures on a particular day, respectively. Depending on the values of G and T , the PVS will produce variable power output in the range of $[0, P_{max}]$. An n -state generation model has been developed to represent the PVG, and is shown in Fig. 8.4. In state-1, the output power is zero, whereas in state- n , the PVG delivers the maximum power. Between these two states, there are $(n - 2)$ no. of derated states with generation capacity of $(0 < P_i < P_{max})$ where, P_i is the generated power in the i^{th} state.

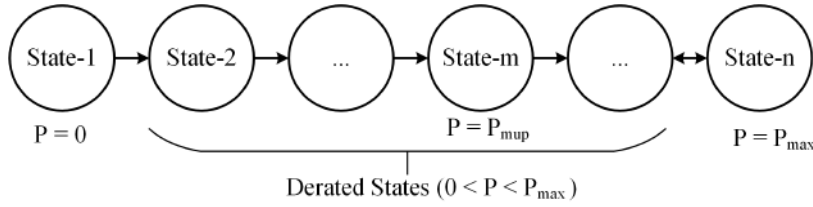


Fig. 8.4 n -state model of PVG.

A certain amount of the generated power is used to meet the net ohmic losses in the system's resistive components. Moreover, if the generated useful power is not adequate to charge the battery at the standard rate, the vehicle's downtime will increase, and consequently, its availability will get reduced. The vehicle will be operable if and only if the battery fulfils the MDS's power requirement. Therefore, the PV modules must produce at least the *minimum useful power* (P_{mup}) for the successful operation of the SEV. It is an important deterministic criterion for a SEV's PVG design. The PVG model will be considered operating only in the states where, $P_i \in [P_{mup}, P_{max}]$. The remaining states will be treated as failed states. To estimate the reliability of PVG, a new index, termed as, Minimum Power Availability Index ($mPAI$) is proposed in this chapter, which is defined as follows:

The probability of producing at least the minimum useful power from the available solar irradiation with a 100% reliable PV system is defined as the minimum power availability index ($mPAI$).

The value of $mPAI$ lies in the range of $[0, 1]$. The necessary steps to determine the $mPAI$ are as follows:

Step 1: Generate/measure solar irradiance (G) with step size δG within the minimum and maximum irradiation values at the vehicle's location, and also temperature (T), in the range $T \in [T_{min}, T_{max}]$ with step size δT for the intended period.

Step 2: Determine ' P ' using Equation (8.1) for all G and T .

Step 3: Construct an n -state model for P such that, $P \in [0, P_{max}]$

Step 4: Determine the probability of occurring P_i at state ' i ' using Equation (8.5).

$$Prob(P_i) = \frac{\text{No. of occurrence of } P_i}{\text{Total no. of states or samples considered}} \quad (8.5)$$

Step 5: Determine $mPAI$ as:

$$mPAI = \sum_{i=m}^n Prob(P_i); \forall P_i \in [P_{mup}, P_{max}] \quad (8.6)$$

The solar panels are designed in a series-parallel combination of a large number of solar cells which usually have low failure rates. The warranty period offered by most manufacturers on PV modules is around 20 to 25 years [176]. The common faults noticed in the PVS generally occur in the DC/DC converter [177], reverse blocking diodes, and other electronic components, which result in an interruption in the solar generation for a particular period [178]. If the entire PV system has an effective failure rate (EFR)[140] of λ_{PVS} and effective restoration rate (ERR)[140] of μ_{PVS} , then the reliability of PVG (R_{PVG}) at time ' t ' will be:

$$R_{PVG}(t) = mPAI \times e^{-\lambda_{PVS}t} \quad (8.7)$$

and the steady-state availability [140] of PVG (A_{PVG}) will be:

$$A_{PVG} = mPAI \times \frac{\mu_{PVS}}{\lambda_{PVS} + \mu_{PVS}} \quad (8.8)$$

The MOT of PVG is determined using Equation (8.9).

$$MOT_{PVG} = \int_0^{\infty} R_{PVG}(t) dt = \frac{mPAI}{\lambda_{PVS}} \quad (8.9)$$

The EFR of PVG (λ_{PVG}) is determined using Equation (8.10).

$$\lambda_{PVG} = \frac{1}{MOT_{PVG}} = \frac{\lambda_{PVS}}{mPAI} \quad (8.10)$$

8.3.2.2 Modeling of plug-in system

The plug-in system's reliability is dictated by the reliability of the charging station (CS) connected to it. A charging station's reliability mainly depends on two factors: (a) reliability of the power supply and (b) reliability of the charging system. Frequent power outages or prolonged interruptions reduce the service hour (MOT) of a charging station, and consequently decrease the effectiveness or availability. Therefore, in areas where load shedding is a common issue, the operation of a plug-in EV is severely impacted.

As stated in the previous chapter, the power supply's reliability at a grid-connected charging station can be estimated using the Average Service Availability Index (ASAI). This index is proposed as follows:

The ratio of total charging hours available for service to the total charging hours demanded is defined as the average service availability index (ASAI) of a charging station.

Mathematically,

$$ASAI = \frac{\sum N_i \times 8760 - \sum U_i N_i}{\sum N_i \times 8760} \quad (8.11)$$

where, N_i is the number of EVs and U_i is the interruption time per year at the i^{th} charging point.

Besides the power supply's reliability, the reliability of the charging system also influences the reliability of a charging station. A system with frequent component failures offers less

service time [139]. Charging system is an AC/DC converter system. If the converter system has an EFR of λ_c and ERR of μ_c , then the CS will have reliability of R_{CS} at time t , which is given by

$$R_{CS}(t) = ASAI \times e^{-\lambda_c t} \quad (8.12)$$

and the availability of the CS (A_{AS}) will be

$$A_{CS} = ASAI \times \left[\frac{\mu_c}{\lambda_c + \mu_c} \right] \quad (8.13)$$

The MOT of the CS can be determined using Equation (8.14):

$$MOT_{CS} = \int_0^{\infty} R_{CS}(t) dt = \frac{ASAI}{\lambda_c} \quad (8.14)$$

and the EFR (λ_{CS}) using Equation (8.15):

$$\lambda_{CS} = \frac{1}{MOT_{CS}} = \frac{\lambda_c}{ASAI} \quad (8.15)$$

8.3.2.3 Reliability evaluation of the power supply system (PSS)

As shown in Fig. 8.3, the PSS is comprised of a primary system (PVG) and a standby system (CS). By principle, a standby system takes over the operation only when the primary system fails [139]. Switching over to the standby system from the primary system or vice versa is done using either an automatic or manually controlled switch, whose reliability also affects the overall system's reliability. Incorporating the properties of a standby system [140], the Equation (8.16) has been developed for estimating the reliability of the PSS at time t .

$$R_{PSS}(t) = e^{-\lambda_{PVG}t} + \frac{r_{sw}\lambda_{PVG}}{\lambda_{CS} - \lambda_{PVG}}(e^{-\lambda_{PVG}t} - e^{-\lambda_{CS}t}) \quad (8.16)$$

where, λ_{PVG} and λ_{CS} are the EFR of PVG and the CS respectively, which are determined using Equations (8.10) and (8.15) respectively. r_{sw} is the reliability of the change-over switch.

8.3.3 Modeling of Energy Storage System (ESS)

The ESS consists of a battery bank and a charge controller (CC). The battery has a pivotal role in the reliable operation of a SEV. The availability of a battery is analyzed by developing a 3-state Markov model. The state-space diagram of the proposed battery model is given in Fig. 8.5.

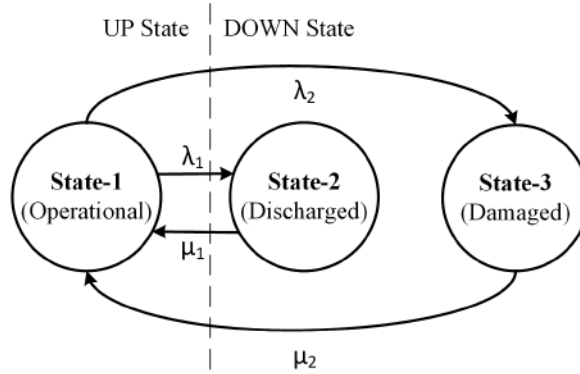


Fig. 8.5 Three-state model of a battery.

In state-1 (operational), the battery's physical condition is good, and sufficient electro-static energy is available to meet the power required by the MDS. In state-2 (discharged), the battery's physical condition is good but does not have sufficient energy. In state-3 (damaged), the battery loses its capability to store energy, and therefore it must be either replaced or repaired. The transition from state-1 to state-2, i.e., λ_1 depends on the discharge rate whereas, the restoration of state-1 from state-2 depends on the charging rate (μ_1) of the battery. The transition rate λ_2 corresponds to the failure rate, and μ_2 denotes the repair rate (if repairable) or replacement rate (if non-repairable) of the battery.

The probability of transition from one state to its adjacent states is determined by constructing the stochastic transitional probability matrix (STPM) [140]. The STPM of the battery is given by Equation (8.17).

$$STPM_B = \begin{bmatrix} 1 - \lambda_1 - \lambda_2 & \lambda_1 & \lambda_2 \\ \mu_1 & 1 - \mu_1 & 0 \\ \mu_2 & 0 & 1 - \mu_2 \end{bmatrix} \quad (8.17)$$

The battery is operational in state-1 only. Eliminating the matrix elements associated with the DOWN states, the STPM reduces to a truncated matrix (Q) as given in Equation (8.18).

$$Q = [1 - \lambda_1 - \lambda_2] \quad (8.18)$$

The average time spent at state-1 before approaching to DOWN states can be determined using Equation (8.19).

$$M = [I - Q]^{-1} \quad (8.19)$$

where 'I' is the unit matrix. M represents the MOT or Mean Time Between Failures (MTBF)[140]. Thus, for the battery,

$$MOT_B = \frac{1}{\lambda_1 + \lambda_2} \quad (8.20)$$

∴ The EFR of the battery is,

$$\lambda_B = \frac{1}{MOT_B} = \lambda_1 + \lambda_2 \quad (8.21)$$

Similarly, considering only the DOWN state transitions in the STPM, a new truncated matrix (Q_t) is formed as follows:

$$Q_t = \begin{bmatrix} 1 - \mu_1 & 0 \\ 0 & 1 - \mu_2 \end{bmatrix} \quad (8.22)$$

The average time intervals taken in the DOWN states is estimated using Equation (??).

$$M_t = [1 - Q_t]^{-1} \quad (8.23)$$

M_t is known as mean-time-to-repair (MTTR) or mean restoration time(MRT)[140]. Using Equations (??) and (??), MRT of the battery is determined as,

$$MRT_B = [I - Q_t]^{-1} = \frac{1}{\mu_1} + \frac{1}{\mu_2} \quad (8.24)$$

∴ The ERR of the battery is,

$$\mu_B = \frac{1}{MRT_B} = \frac{\mu_1 \mu_2}{\mu_1 + \mu_2} \quad (8.25)$$

The availability[139], i.e., the probability that the battery will remain in the UP state at time ‘t’ is given by Equation (8.26).

$$A_B(t) = \frac{\mu_B}{\lambda_B + \mu_B} + \frac{\lambda_B}{\lambda_B + \mu_B} e^{-(\lambda_B + \mu_B)t} \quad (8.26)$$

The steady-state value of the battery’s availability is,

$$A_B = \frac{\mu_B}{\lambda_B + \mu_B} \quad (8.27)$$

The charge controller(CC) facilitates controlled charging based on the SOC of the battery. The failure of the CC occurs mainly due to overheating or electrical faults in its components [178, 179]. If λ_{cc} and μ_{cc} represent the EFR and ERR of the CC respectively, then its steady-state availability will be:

$$A_{CC} = \frac{\mu_{CC}}{\lambda_{CC} + \mu_{CC}} \quad (8.28)$$

Based on the UP and DOWN status of the CC and the battery, a 4-state Markov model is developed for the ESS as shown in Fig. 8.6.

In state-1, both battery and charge controller are operating. In state-2, the battery is in DOWN state. In state-3, the battery is operating; however, the controller is in DOWN state.

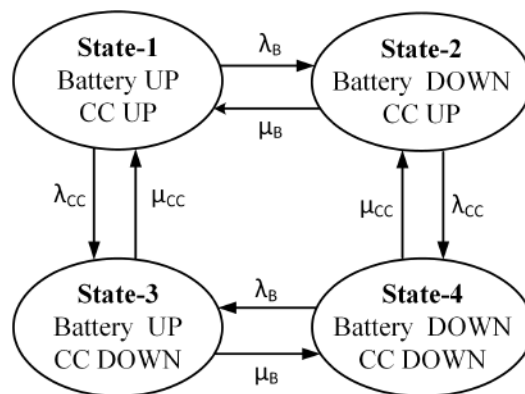


Fig. 8.6 State-space diagram of the ESS model

In state-4, both components are in DOWN state. The STPM of the ESS will be as follows:

$$STPM_{ESS} = \begin{bmatrix} 1 - \lambda_B - \lambda_{CC} & \lambda_B & \lambda_{CC} & 0 \\ \mu_B & 1 - \mu_B - \lambda_{CC} & 0 & \lambda_{CC} \\ \mu_{CC} & 0 & 1 - \lambda_B - \mu_{CC} & \lambda_B \\ 0 & \mu_{CC} & \mu_B & 1 - \mu_B - \mu_{CC} \end{bmatrix} \quad (8.29)$$

The ESS is operable in state-1 only. Therefore, the ESS's steady-state availability (A_{ESS}) is equal to the probability of occurrence of state-1, which is determined using Equation (8.30).

$$A_{ESS} = \frac{\mu_B \mu_{CC}}{(\lambda_B + \mu_B)(\lambda_{CC} + \mu_{CC})} \quad (8.30)$$

After elimination of the nonoperational states, the STPM reduces to the truncated matrix (Q_{ESS}) shown in Equation (8.31).

$$Q_{ESS} = [1 - \lambda_B - \lambda_{CC}] \quad (8.31)$$

∴ The MOT of the ESS is:

$$MOT_{ESS} = [I - Q_{ESS}]^{-1} = \frac{1}{\lambda_B + \lambda_{CC}} \quad (8.32)$$

and the MRT of the ESS is:

$$MRT_{ESS} = \frac{1 - A_{ESS}}{A_{ESS}(\lambda_B + \lambda_{CC})} \quad (8.33)$$

The EFR (λ_{ESS}) and the ERR (μ_{ESS}) of the ESS are determined using Equations (8.34) and (8.35) respectively.

$$\lambda_{ESS} = \frac{1}{MOT_{ESS}} = \lambda_B + \lambda_{CC} \quad (8.34)$$

$$\mu_{ESS} = \frac{1}{MRT_{ESS}} = \frac{A_{ESS}(\lambda_B + \lambda_{CC})}{1 - A_{ESS}} \quad (8.35)$$

8.3.4 Modeling of Motor-Drive System (MDS)

The MDS is the core system of an EV. It consists of a motor and an electric drive system. The choice of MDS is mainly defined by two factors: driver expectation and vehicle constraints [128, 172]. The drive receives electrical energy from the battery and feeds into the motor in varying amounts, thereby regulates the speed, torque, and direction of rotation of the motor. The drive consists of a power converter, control module, driver module, communication module, and electronic components such as bus-bar capacitors, IGBT, etc.[146, 170]. The MDS will go out of service if any one of these components fails to operate.

The state space diagram of the MDS is given in Fig. 8.7. The MDS has four transition states. λ_M , λ_D are the failure rates, and μ_M , μ_D are the repair rates of the motor and drive system, respectively. The MDS is operational in state-1 only, where both the motor and the

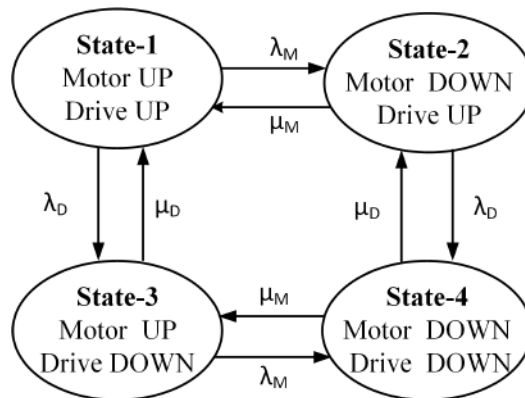


Fig. 8.7 State-space diagram of the Motor-Drive system

drive are operating. The STPM of the MDS is determined using Equation (8.36).

$$STPM_{MDS} = \begin{bmatrix} 1 - \lambda_M - \lambda_D & \lambda_M & \lambda_D & 0 \\ \mu_M & 1 - \mu_M - \lambda_D & 0 & \lambda_D \\ \mu_D & 0 & 1 - \lambda_M - \mu_D & \lambda_M \\ 0 & \mu_D & \mu_M & 1 - \mu_M - \mu_D \end{bmatrix} \quad (8.36)$$

The availability of the MDS (A_{MDS}) is determined using Equation (8.37).

$$A_{MDS} = \frac{\mu_M \mu_D}{(\lambda_M + \mu_M)(\lambda_D + \mu_D)} \quad (8.37)$$

The MOT and MRT of the MDS are determined using Equations (8.38) and (8.39) respectively.

$$MOT_{MDS} = \frac{1}{\lambda_M + \lambda_D} \quad (8.38)$$

$$MRT_{MDS} = \frac{1 - A_{MDS}}{A_{MDS}(\lambda_M + \lambda_D)} \quad (8.39)$$

The EFR (λ_{MDS}) and ERR (μ_{MDS}) of the MDS are calculated using Equations (8.40) and (8.41) respectively.

$$\lambda_{MDS} = \frac{1}{MOT_{MDS}} = \lambda_M + \lambda_D \quad (8.40)$$

$$\mu_{MDS} = \frac{1}{MRT_{MDS}} = \frac{A_{MDS}(\lambda_M + \lambda_D)}{1 - A_{MDS}} \quad (8.41)$$

8.3.5 Modeling of Energy Management and Control System(EMCS)

The VC and the EMS together constitute the EMCS of the vehicle. At a particular instant, VC and EMS may stay either in the UP state or DOWN state. Their failures may be in the form of hardware or software problems or both. Based on their individual operational status, a 4-state Markov model for the EMCS is constructed. The state-space diagram of the model is shown in Fig. 8.8. The layout of the EMCS model is similar to that of ESS or MDS. The

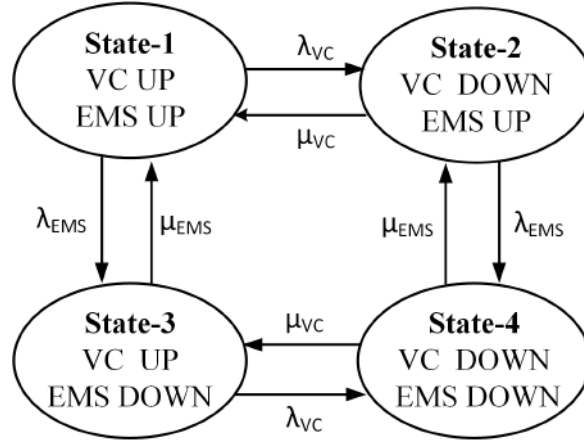


Fig. 8.8 State-space diagram of the EMCS

STPM of the EMCS is given by Equation (8.42).

$$STPM_{EMCS} = \begin{bmatrix} 1 - \lambda_{VC} - \lambda_{EMS} & \lambda_{VC} & \lambda_{EMS} & 0 \\ \mu_{VC} & 1 - \mu_{VC} - \lambda_{EMS} & 0 & \lambda_{EMS} \\ \mu_{EMS} & 0 & 1 - \lambda_{VC} - \mu_{EMS} & \lambda_{VC} \\ 0 & \mu_{EMS} & \mu_{VC} & 1 - \mu_{VC} - \mu_{EMS} \end{bmatrix} \quad (8.42)$$

where, $\lambda_{VC}, \lambda_{EMS}$ are the failure rates and μ_{VC}, μ_{EMS} are the repair rates of the vehicle controller and the EMS respectively.

The availability of the EMCS (A_{EMCS}) is determined using Equation (8.43).

$$A_{EMCS} = \frac{\mu_{VC}\mu_{EMS}}{(\lambda_{VC} + \mu_{VC})(\lambda_{EMS} + \mu_{EMS})} \quad (8.43)$$

The EFR (λ_{EMCS}) and ERR (μ_{EMCS}) of the EMCS are determined using Equations (8.44) and (8.45) respectively.

$$\lambda_{EMCS} = \lambda_{VC} + \lambda_{EMS} \quad (8.44)$$

$$\mu_{EMCS} = \frac{A_{EMCS}(\lambda_{VC} + \lambda_{EMS})}{1 - A_{EMCS}} \quad (8.45)$$

8.3.6 Modeling of Electrical Propulsion System (EPS)

Once the performance metrics of the ESS, MDS, and EMCS are determined, the entire EPS can be modeled as shown in Fig. 8.9. Since each of these three subsystems has two operational states (i.e., UP and DOWN), therefore, there will be a total of 2^3 states in the EPS model. In state-1, all three subsystems are operative. In state-2, the ESS is in a DOWN state, but the MDS and EMCS are operational. Again, none of the ESS, MDS, and EMCS is functional in state-8. The probabilities of occurrence of these states are given by Equations (8.46)-(8.53).

$$P_{EPS}^{(1)} = \frac{\mu_{ESS}\mu_{MDS}\mu_{EMCS}}{(\lambda_{ESS} + \mu_{ESS})(\lambda_{MDS} + \mu_{MDS})(\lambda_{EMCS} + \mu_{EMCS})} \quad (8.46)$$

$$P_{EPS}^{(2)} = \frac{\lambda_{ESS}\mu_{MDS}\mu_{EMCS}}{(\lambda_{ESS} + \mu_{ESS})(\lambda_{MDS} + \mu_{MDS})(\lambda_{EMCS} + \mu_{EMCS})} \quad (8.47)$$

$$P_{EPS}^{(3)} = \frac{\mu_{ESS}\lambda_{MDS}\mu_{EMCS}}{(\lambda_{ESS} + \mu_{ESS})(\lambda_{MDS} + \mu_{MDS})(\lambda_{EMCS} + \mu_{EMCS})} \quad (8.48)$$

$$P_{EPS}^{(4)} = \frac{\mu_{ESS}\mu_{MDS}\lambda_{EMCS}}{(\lambda_{ESS} + \mu_{ESS})(\lambda_{MDS} + \mu_{MDS})(\lambda_{EMCS} + \mu_{EMCS})} \quad (8.49)$$

$$P_{EPS}^{(5)} = \frac{\lambda_{ESS}\lambda_{MDS}\mu_{EMCS}}{(\lambda_{ESS} + \mu_{ESS})(\lambda_{MDS} + \mu_{MDS})(\lambda_{EMCS} + \mu_{EMCS})} \quad (8.50)$$

$$P_{EPS}^{(6)} = \frac{\mu_{ESS}\lambda_{MDS}\lambda_{EMCS}}{(\lambda_{ESS} + \mu_{ESS})(\lambda_{MDS} + \mu_{MDS})(\lambda_{EMCS} + \mu_{EMCS})} \quad (8.51)$$

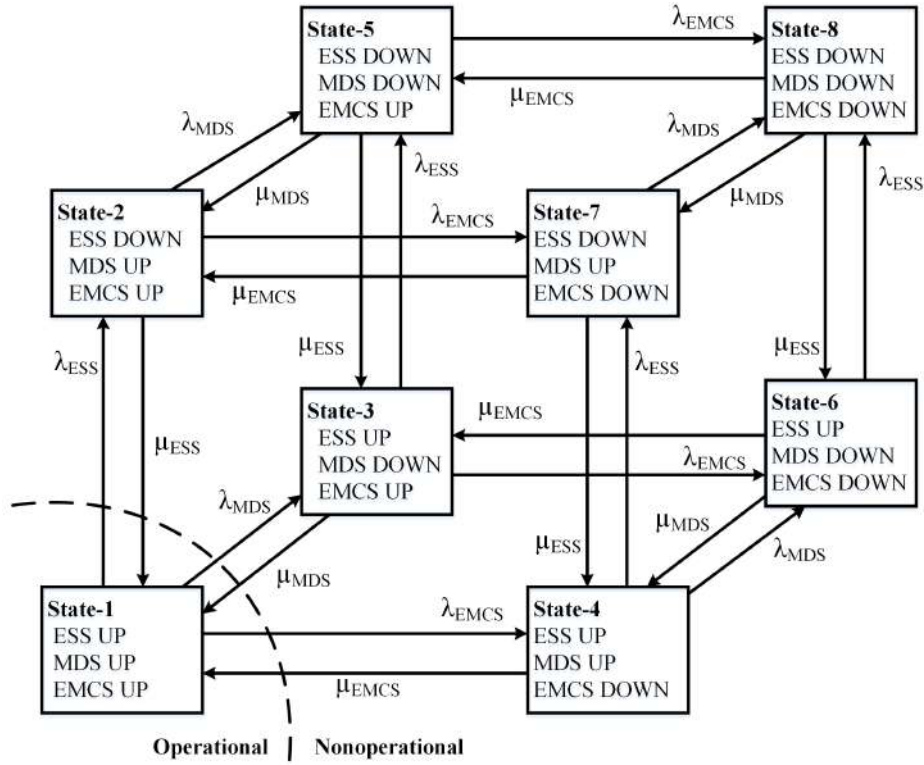


Fig. 8.9 State-space diagram of the EPS

$$P_{EPS}^{(7)} = \frac{\lambda_{ESS}\mu_{MDS}\lambda_{EMCS}}{(\lambda_{ESS} + \mu_{ESS})(\lambda_{MDS} + \mu_{MDS})(\lambda_{EMCS} + \mu_{EMCS})} \quad (8.52)$$

$$P_{EPS}^{(8)} = \frac{\lambda_{ESS}\lambda_{MDS}\lambda_{EMCS}}{(\lambda_{ESS} + \mu_{ESS})(\lambda_{MDS} + \mu_{MDS})(\lambda_{EMCS} + \mu_{EMCS})} \quad (8.53)$$

where, $P_{EPS}^{(i)}$ is the probability of occurrence of state i . The values of λ_{ESS} , μ_{ESS} , λ_{MDS} , μ_{MDS} , λ_{EMCS} , and μ_{EMCS} are determined using Equations (8.34), (8.35), (8.40), (8.41), (8.44) and (8.45), respectively.

Fig. 8.9 shows that the EPS will be operable if, and only if, it is in state-1. In this case, the steady-state availability of the EPS (A_{EPS}) will be equal to $P_{EPS}^{(1)}$ and it can be determined using Equation (8.46). The forced outage rate (FOR) or unavailability [140] of the EPS will be the algebraic sum of probabilities of all non-operable states, which is evaluated using Equation (8.54).

$$FOR_{EPS} = \sum_{i=2}^8 P_{EPS}^{(i)} \quad (8.54)$$

The EFR (λ_{EPS}) and ERR (μ_{EPS}) of the EPS can be determined using Equations (8.55) and (8.56)) respectively using similar approach as illustrated in Section 8.3.3.

$$\lambda_{EPS} = \lambda_{ESS} + \lambda_{MDS} + \lambda_{EMCS} \quad (8.55)$$

$$\mu_{EPS} = \frac{A_{EPS}\lambda_{EPS}}{1 - A_{EPS}} \quad (8.56)$$

\therefore The reliability of the EPS at time 't' is given by Equation (8.57).

$$R_{EPS}(t) = e^{-\lambda_{EPS}t} \quad (8.57)$$

8.3.7 Composite Reliability Modeling of the SEV System

The reliability block diagram (RBD)[139] of the SEV system consisting of the PSS, EPS, and MTS is shown in Fig. 8.10. R_{PVG} , R_{CS} , R_{EPS} , R_{MTS} and R_{PSS} denotes the reliability of PVG, CS, EPS, MTS and PSS respectively.

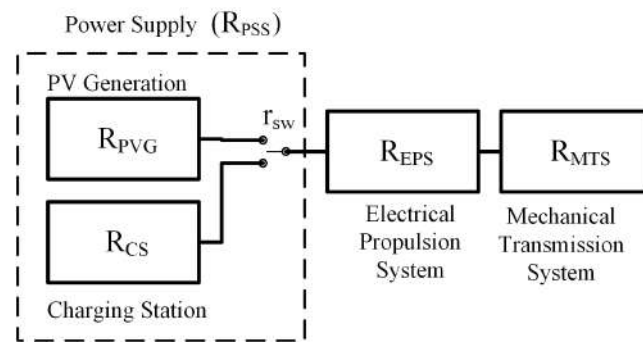


Fig. 8.10 Reliability block diagram of the SEV.

Since the RBD is a series combination of the PSS, EPS, and MTS, the overall reliability of the SEV (R_{SEV}) will be equal to the product of the individual reliability of these subsystems and it has been evaluated using Equation (8.58).

$$R_{SEV}(t) = R_{PSS}(t) \times R_{EPS}(t) \times R_{MTS}(t) \quad (8.58)$$

Assuming R_{MTS} as 100% reliable, and using Equations (8.16), (8.57), and (8.58), the reliability of the SEV with standby plug-in facility is given by Equation (8.59).

$$R_{SEV}(t) = \left[e^{-\lambda_{PVG}t} + \frac{r_{sw}\lambda_{PVG}}{\lambda_{CS} - \lambda_{PVG}} (e^{-\lambda_{PVG}t} - e^{-\lambda_{CS}t}) \right] \times e^{-\lambda_{EPS}t} \quad (8.59)$$

where, r_{sw} is a manufacturer specification and the values of λ_{PVG} , λ_{CS} , λ_{EPS} are determined using Equations (8.10), (8.15) and (8.55), respectively.

The mean-time-to-first-failure (MTTFF)[139], which is a useful parameter to decide the warranty period of the SEV as it predicts the average failure-free operation period of a system, is determined using Equation (8.60).

$$MTTFF_{SEV} = \frac{1}{\lambda_{PVS} + \lambda_{ESS} + \lambda_{MDS} + \lambda_{EMCS}} \quad (8.60)$$

8.4 Results and Discussion

The reliability models proposed in Section 8.3 have been exemplified using a typical SEV system. The input data used to carry out the studies are listed in Tables A.10, A.11 and A.12 in Appendix A. Sections 8.4.1, 8.4.2 and 8.4.3 present the results and analyses of the following studies:

- Determination of reliability of the SEV system.
- Comparison of reliability of SEV with and without plug-in facility.
- Determination of availability of the SEV.
- Impact of maintenance on availability of a SEV system.
- Impact of failure characteristics of components on reliability of a SEV system.
- Impact of the proposed index, $mPAI$ on availability of a SEV system.

8.4.1 Reliability Assessment of SEV

The reliability assessment of a SEV needs to be categorized into two parts: (a) Reliability assessment of the physical SEV system, which includes the onboard PVS and the EPS, and (b) Reliability assessment of output power of the PSS, which includes PVG and the CS.

With an EFR of 0.04 f/yr, the PVS provides 92.40% reliability after five years of operation, which is reasonably good, as explained in Section 8.3.2. On the other hand, the constituent components of the EPS, namely ESS, MDS, and EMCS, provide 89.05%, 85.73%, and 85.43% reliability respectively, after the same operating period. Since these components are reliability-wise in series, the effective reliability of the EPS will become 65.22% after five years.

As time progresses, the reliability of each subsystem further decreases. Table 8.1 shows the results of the assessment carried out for five years, ten years, fifteen years, and twenty years respectively. It shows that the reliability of the PVS reduces to 73.17% in ten years. It is further decreased by 34.46% and 46.52% in the next five and ten years, respectively. On the other hand, the EPS's reliability reduces to 42.53% in the next five years. It will be only 27.74% and 18.09% reliable after 15 years and 20 years of operation, respectively. Based on the component reliability information, manufacturers can estimate the vehicle system's warranty period and offer customers the best possible service policy accordingly.

Table 8.1 Reliability of key subsystems of the SEV

| | Reliability (%) | | | |
|------|-----------------|----------|----------|----------|
| | t=5 yrs | t=10 yrs | t=15 yrs | t=20 yrs |
| PVS | 92.40 | 73.17 | 57.94 | 45.88 |
| ESS | 89.05 | 79.29 | 70.61 | 62.88 |
| MDS | 85.73 | 73.49 | 63.00 | 54.01 |
| EMCS | 85.43 | 72.99 | 62.35 | 53.27 |
| EPS | 65.22 | 42.53 | 27.74 | 18.09 |

The reliability of PSS depends on the reliability of PVG and the availability of the standby source, i.e., CS. Using the PVG data given in Table A.11 (Appendix A). and Ref.[180], $mPAI$ is estimated with the help of Equation (8.6). The value of $mPAI$ is found to be 85.71% under NOC. This yields the reliability of PVG equal to 0.8571 multiplied by the PVS's reliability at time t given in Table 8.1. Similarly, $ASAI$ is determined using Equation (8.11) and the CS data given in Table A.12 (Appendix A). The value of $ASAI$ is obtained as 90.47%. With this $ASAI$, the charging system having an EFR of 0.06 f/yr provides availability of 83.91%. The reliability of the PSS is determined using Equation (8.16). For a five years old SEV, the PSS's reliability is found to be 96.61%. However, with time, this value reduces and becomes 89.01% and 79.46% after ten and fifteen years of operating time, respectively.

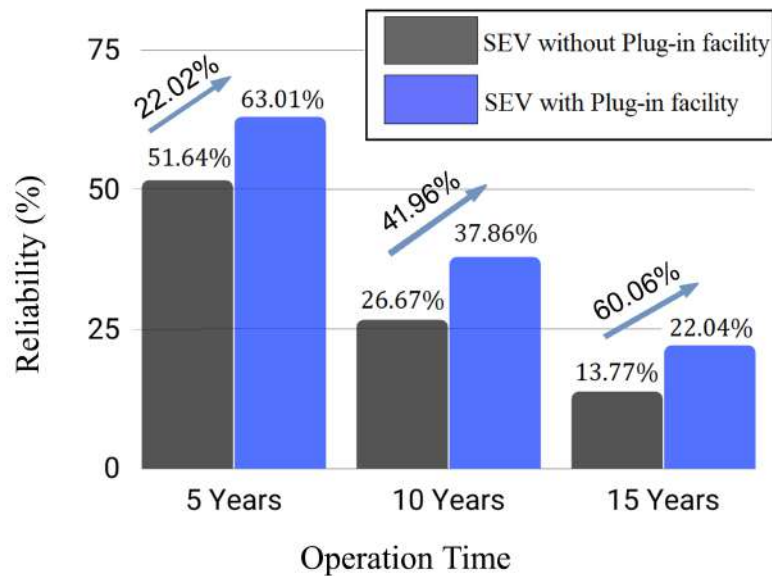


Fig. 8.11 Comparison of reliability of SEV with and without plug-in facility

Figure 8.11 shows a comparative reliability assessment of a SEV with and without the plug-in facility. It is obtained that the overall reliability of a five-year-old SEV with no plug-in option is only 51.64%. However, if a standby plug-in facility is added, the reliability of the SEV becomes 63.01%, providing an improvement of 22.02%. If the same assessment is done for a ten-year-old SEV, an improvement of 41.96% is observed due to the addition

of a plug-in option. Similarly, after 15 years of operation, the percentage improvement in reliability due to the addition of a plug-in facility is found to be 60.06%. Thus, from a long-term reliability perspective also, a SEV with a standby plug-in facility will be more beneficial.

Figure 8.12 shows the vehicle's reliability curves given by Equation (8.59), with an operating period of 20 years, utilizing all available power source options.

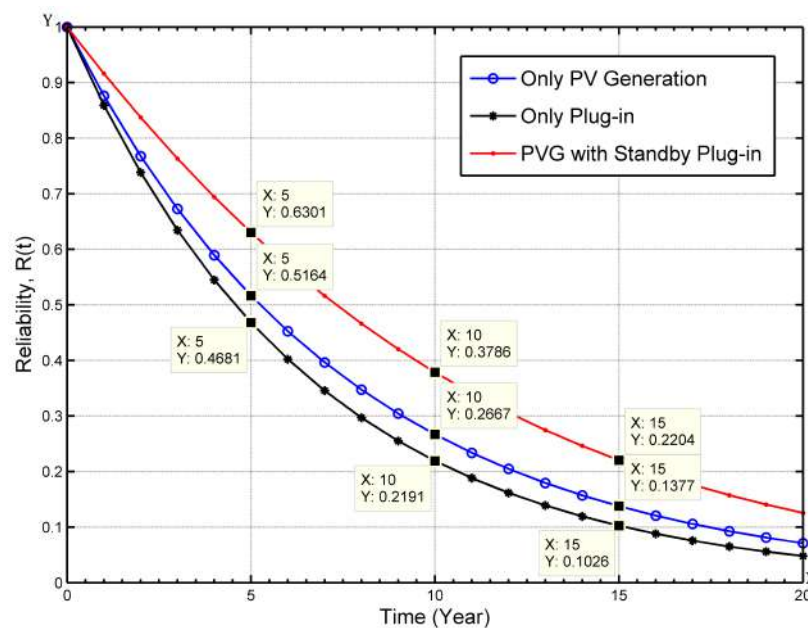


Fig. 8.12 Reliability of a SEV with different energy source options

The plots drawn in Fig. 8.12 indicate that a solar energized EV predicts higher reliability under NOC as compared to a plug-in EV of identical rating. The reason behind it is, PVG has the ability to provide continuous charging current to the battery under NOC, whereas charging through plug-in is a discrete process. A plug-in EV always runs in discharging mode unlike a SEV, which limits the driving range and hence reduces its effectiveness. However, under abnormal operating conditions (i.e., night hours, bad weather conditions, forest road, covered bridge, tunnel road, etc.), a SEV also runs in discharging mode and acts just like a plug-in EV. PVG with a standby plug-in option alleviates the drawbacks of charging through a single energy source, and improves the vehicle's reliability.

8.4.2 Availability Assessment of SEV

Availability refers the probability that a system is operating at time, t . It is often linked with maintainability, i.e., the probability that the system is restored to operating mode within a specified time. Availability, therefore, is affected by both FR and RR.

Figure 8.13 shows the vehicle's availability curves, simulated for 20 years of operating period. It is observed that the vehicle's reliability [Plot-(i)] is exponentially decaying and found to be 22% after 15 years of operation. However, at the same time, the availability [Plot-(ii)] of the SEV becomes 67.86%. The improvement noticed in the operational effectiveness is due to the consideration of the maintenance process. If the DOWN components are restored at their normal speeds of restoration (as given Table A.10 in Appendix A), then the vehicle's availability raises to 67.85% from 15.76% (which is for an unmaintained SEV) after 18 years of operation.

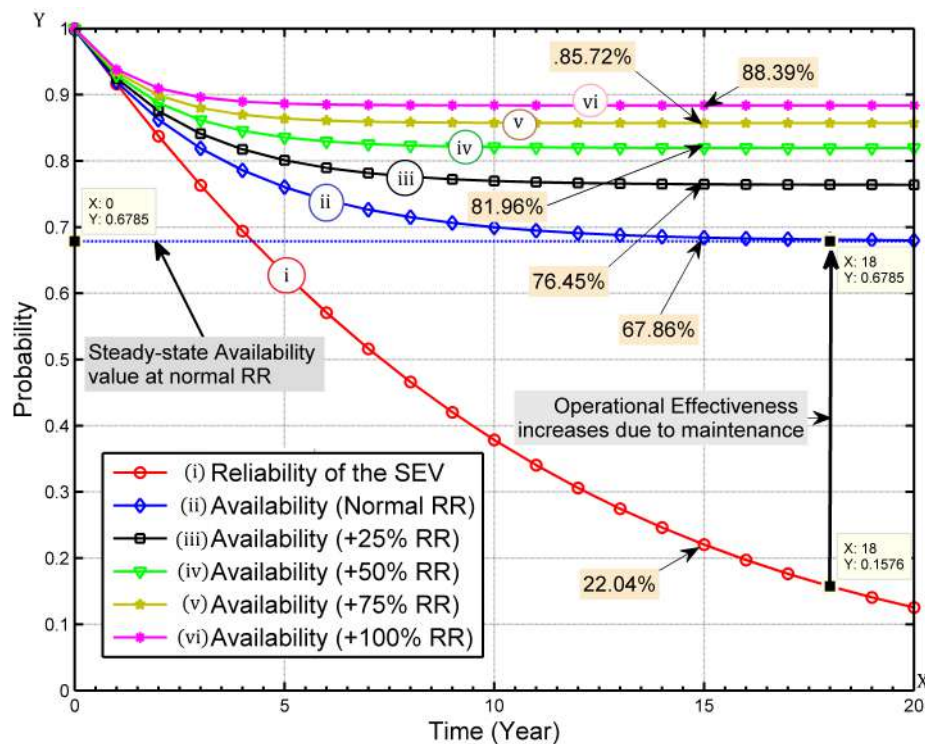


Fig. 8.13 Effectiveness of the SEV with different maintenance strategies.

After attaining the steady-state value (i.e., 67.85%), further improvement in availability cannot be achieved at normal RR. In that case, there are three feasible options to improve the availability: (a) using components of higher reliability (i.e., low failure rates), (b) increasing redundant components (i.e., standby or parallel mode), and (c) improving the RR of the failed components. The options (a) and (b) can be executed in the manufacturing stage only and are restricted mainly due to economic as well as design constraints. The third option is associated with the customer and service provider and, therefore, easily implementable from the user end.

The plots (ii)-(vi) drawn in Fig. 8.13 attempt to demonstrate how quick response in repair or replacement can lessen the ill-effect of failure and improves availability. Graph (iii) shows that if the normal RR is increased by 25%, the vehicle gains 12.62% improvement in its steady-state availability. Similarly, 50%, 75%, and 100% increment in normal RR of the faulty elements will improve the SEV's availability by 20.78%, 26.34%, and 30.27%, respectively. Thus, with proper knowledge on failure rates of all critical components and adopting quick restoration strategies for the faulty parts, users can improve the vehicle's availability and maintain its reliability at a satisfactory level.

Figure 8.14 shows how a reduction in FR enhances the availability of a SEV. It is observed that with a 25% decrement in FR [Plot (b)], the steady-state availability of the SEV gets improved by 8.83% from its base value of 68.1% [Plot (a)]. Similarly, plots (c) and (d) show that 50% and 75% reductions in FR boost the availability of the SEV by 19.19% and 31.64%, respectively. However, it is not so easy to have control over FR since it is stochastic in nature. With a strong design, correct manufacturing techniques, less complexity, experienced handling, and rigorous maintenance policies, the FR of a component or a system can be reduced up to some extent.

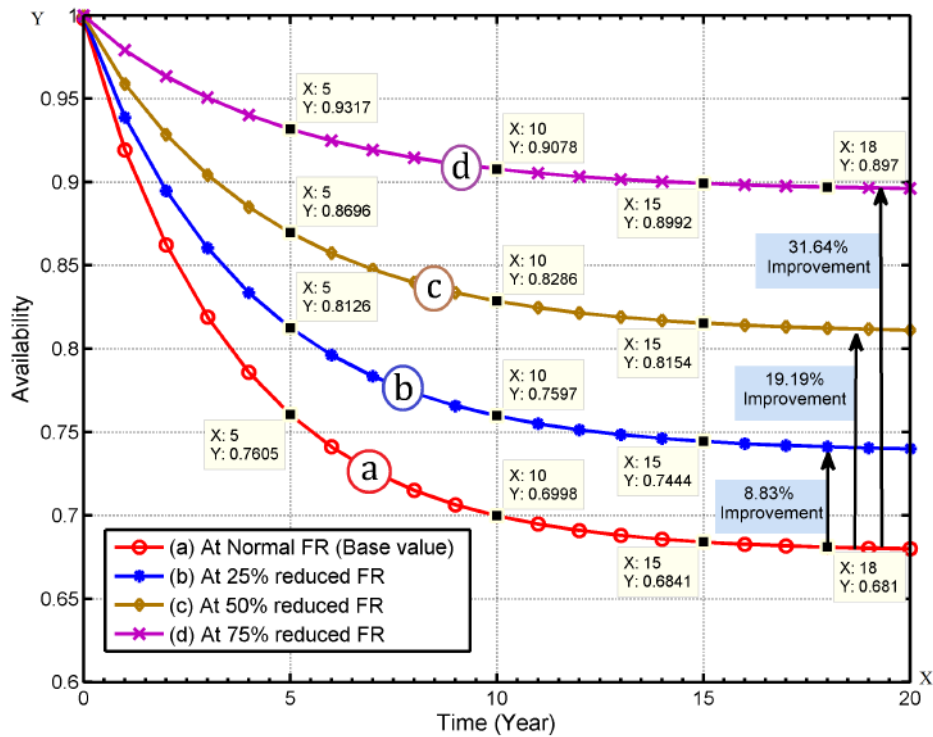


Fig. 8.14 Comparison of availability of the SEV with different component failure rates(FR)

8.4.3 Impact of $mPAI$ on SEV's Availability

Being the primary source of power supply of a SEV, the PVG's reliability plays the most significant role in the vehicle's availability. The model developed in section 8.3.2 reveals how the reliability of PVG is influenced by the solar irradiation values, and consequently by the $mPAI$. Greater the value of $mPAI$, higher will be the availability of power supply to the battery, and hence higher will be the availability of the SEV. This is justified by the results graphically presented in Fig. 8.15.

Figure 8.15 presents the availability of the SEV at different levels of $mPAI$. It shows that at zero $mPAI$, the SEV becomes completely ineffective (zero availability), provided no plug-in option in the vehicle. The availability of the vehicle gets improved with increased $mPAI$. At 100% $mPAI$, availability attains the maximum value of 63.80%. The remaining 36.20% is the unavailability of the SEV system due to the forced outages of other critical subsystems.

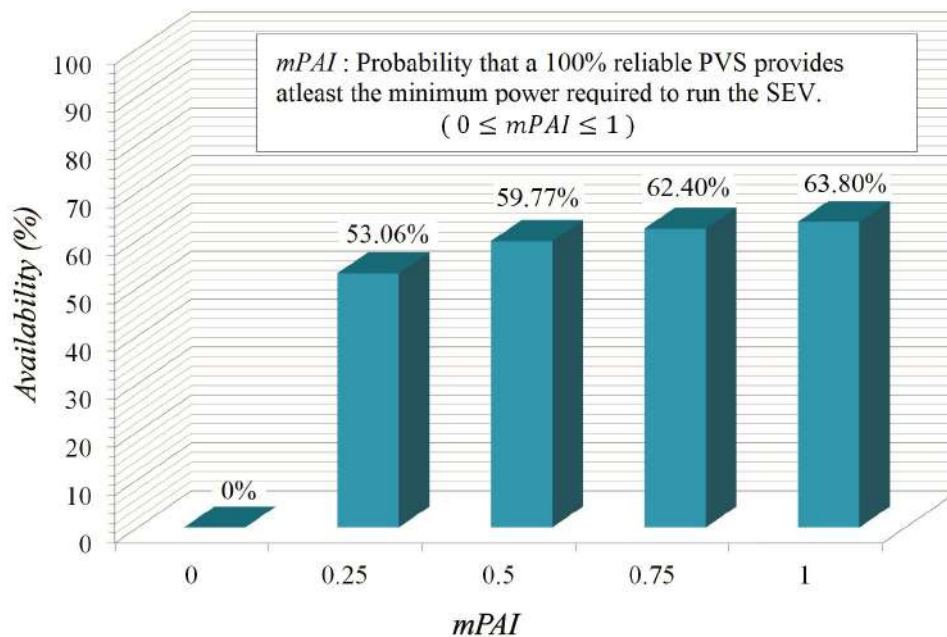


Fig. 8.15 Availability of the SEV at different *mPAI*

Although reliability cannot be 100% in practice, availability can approach to 100% mark for a well-maintained system. Therefore, at 100% *mPAI*, a well-maintained SEV can be 100% available. Since *mPAI* can predict how much solar irradiation must be available for the successful and reliable operation of a SEV, therefore, this index can be treated as a useful parameter for designing area-specific SEVs.

8.5 Conclusion

In this chapter, an effort has been made to develop a composite reliability model of a SEV system for investigating the reliability and availability of the vehicle. The proposed model mainly concentrates on the power supply scheme (PSS) and the electrical propulsion system (EPS) of the SEV. The PSS is comprised of an onboard PV system supported by a standby plug-in system. A multi-state reliability model of the EPS has been developed in Markov framework considering the contributions of all major failure-prone electrical components.

To determine the reliability of photovoltaic generation (PVG), a new probabilistic index, named *mPAI*, has been proposed. This index helps to estimate the operational readiness or availability of a SEV at a particular geographical location. The study quantitatively justifies that the SEVs are more reliable than plug-in EVs under NOC. Another reliability index, *ASAI* is proposed to examine the contribution of the plug-in option for improving the reliability of the SEV. The result shows that SEV with a standby plug-in facility is the best EV option from the reliability perspective. The chapter also demonstrates how quick response in maintenance helps to enhance the availability of the vehicle. Reliability analysis of a SEV is still an unexplored area of research. The concepts presented in this chapter can complement the ongoing researches on SEV design and maintenance. To examine how vehicle speed impacts *mPAI* is one of the future scopes of this research. The study can further be extended for dynamic reliability assessment, maintenance-based reliability modeling, maintainability prediction, spare parts provisioning, and reliability vs. cost trade-off analysis for a SEV.

9

Conclusions and Future Scope

9.1 Conclusions

This chapter outlines the conclusions based on the literature review and on the results of the various analyses performed in the present work. The conclusions are presented in the two categories, viz.

- General conclusions based on literature review.
- Specific conclusions pertaining to the reliability evaluation of some emerging areas of modern power and energy systems.

9.1.1 General Conclusions

The conclusions based on literature review are as follows:

1. Modern power systems are very complex. Due to the integration of renewable distributed generation and large volumes of electric vehicle loading, the complexities have further been increased. This makes “power system reliability” a critical parameter for assessing system performance.
2. Measurement of actual reliability provides feedback to planners on the performance of the executed plans and to operations personnel on the reliability effects of operating and maintenance practices.
3. Reliability and economics must be treated together in order to perform cost-benefit studies, but methods are not yet sufficiently developed, and the data are not yet available.
4. In the past, most of the reliability studies were based on some deterministic criteria. Later, probabilistic approaches got more preferences over the deterministic approaches in order to incorporate the system’s stochastic behavior. Modern techniques often consider both deterministic as well as probabilistic criteria for system reliability assessment.
5. System well-being analysis is a very useful method for power system reliability (PSR) assessment. It can incorporate both deterministic and probabilistic approaches and, therefore, provide a more realistic system reliability assessment.
6. Markov modeling is another useful framework that has widely been used in literature. Markov model incorporates both failure and repair processes of a system. Furthermore, it can easily model systems having derated or intermittent states.
7. Most of the existing PSR studies have been directed at conventional power systems where reliability is an operator’s decision. The deregulation in the power system

- makes reliability a customer-centric criterion in system operation. Customers have the authority to choose energy providers based on their ability to supply electricity at the customer-defined reliability levels.
8. The existing literature is rich in renewable energy studies. Integration of renewable energy sources with power distribution networks helps to improve the reliability of the power supply. However, it also increases the operational challenges in the system.
 9. Maximum benefits in terms of interruption cost and energy can be achieved only if multiple renewable energy sources are integrated with a grid. It is because most of the RESs follow an intermittent pattern in power generation.
 10. Electric vehicle (EV) is one of the fascinating subjects of research at present. Many researchers have studied the impact of EV load on the grid. However, there are very limited literature available emphasizing reliability issues.
 11. Plug-in EVs are being widely accepted all over the world mainly because of their environment-friendly and oil-independent operation. However, reliability, availability, and maintainability (RAM) are some of the critical issues associated with a plug-in EV. Most of the literature has addressed the reliability concerns of some selected key components of an EV system. However, RAM issues of the entire EV system have not been explored yet.
 12. The arrival of EVs makes transportation an electrical engineering subject. The increased volume of EV load brings many challenges in grid operation. Again, the grid-dependency of plug-in EV limits its operational effectiveness. A solar EV has no such limitation as it can generate the required power itself utilizing solar energy. Therefore, SEV is going to be the future of e-mobility. Furthermore, it can be the ideal solution for clean and sustainable transportation. There are ample scopes of research on this subject.

9.1.2 Specific Conclusions

The following conclusions are drawn from the present studies:

1. In a deregulated power system, operating reserve management is much more complicated than a vertically integrated system. The energy providers are required to supply electricity at a customer-specified reliability range. The features of the reserve agreements provide customers with more options to select the energy provider. If customers want to pay less for operating reserve, they will get less reliable electricity service. In contrast, the high reliability of electricity service will require customers to pay more. Customers can decide their own reliability levels. To prepare an operating reserve schedule as per customers' reliability-specifications, this thesis presents a method in well-being framework. The concepts are exemplified in RBTS. It has been observed that GENCO-1 and GENCO-2 in RBTS are capable of maintaining the single risk criterion. However, they alone cannot satisfy the multiple reliability criteria set by customers. For that, both the GENCOs must purchase additional reserves from the wholesale power market through a bilateral agreement.
2. To improve the reliability of power supply, sufficient reserve margin must be available in the system. With a large volume of renewable energy integration, the operating reserve and hence the reliability of power supply can be enhanced. This thesis has proposed an approach for a comprehensive reliability assessment of a power distribution network energized by solar, wind, and tidal energy sources. Two new metrics, IEB and ICB, have been proposed to measure the reliability worth of the system in terms of energy and cost benefits from adding renewable energy sources (RESs). The simulation results justify that renewable distributed generations have significant impacts on the PSR. The system operator can deliver power to the load points at different reliability levels by regulating the operating reserve based on the availability of the RESs. The cost associated with power outages is significantly reduced with increased penetration

- from the RESs. The result shows that IEB and ICB both increase with the combined operation of multiple RESs. Thus, for countries with long coastlines, the combination of solar, wind and tidal energies can effectively meet the power demand satisfying the reliability, economic and environmental constraints.
3. The importance of renewable distributed generation further increases with the increased volume of electric vehicle (EV) load. A critical problem associated with plug-in EVs (PEVs) is that their higher penetration causes many issues on the power distribution network. The increased volume of PEVs in grid-to-vehicle (G2V) mode reduces the grid's reserve capacity and thus reduces the adequacy of power supply to the load points. Again, uncontrolled scheduling of PEV charging distorts the load curve, causing peaks on the peaks; and pushes the system operator for load curtailment, and thus reduces the system reliability. To investigate the PEV load's impact on the reliability of a distribution network, an approach has been presented in this thesis. It is observed that PEV loading does not change the SAIFI, SAIDI, CAIDI, and ASAI values but significantly affects the ENS. With a controlled charging schedule, these indices' values can be improved to a certain extent. With proper regulations and incentives, consumers can be encouraged to go for controlled schedule charging of PEVs, so that the overall reliability of the power supply remains at a satisfactory level throughout the period.
 4. Electric vehicles have received considerable importance in recent times due to the growing environmental and energy security concerns. However, there are many issues in EV operation, and most of these are related to its reliability availability and maintainability (RAM). The study presented in this thesis reports that the availability of a PEV highly depends on the charging station's reliability, which mainly relies on the reliability of the grid's power supply. Because of frequent load shedding in many developing countries, the operation of a PEV is severely impacted. This thesis

introduces an index called *ASAI*, which can measure the reliability of a charging station. Furthermore, the study presented in this thesis justifies that the reliability and availability of a PEV deteriorate with time due to its components' failures. However, with timely repair or replacement of the faulty components, the vehicle's operational effectiveness can be improved significantly. Although a vehicle owner does not have the option to control the system's stochastic failures, the restoration process of faulty components can be accelerated up to a certain level. It will increase the availability of the vehicle.

5. The dependency on the grid power supply can be reduced/eliminated by facilitating the charging station with RESs. Solar and/or wind energy are the most widely used RESs to feed a charging station. Furthermore, the grid-dependency of a PEV can be alleviated by mounting a photovoltaic system (PVS) on the roof of the vehicle system itself. To investigate the reliability and operational effectiveness of a solar powered EV, this thesis has developed a composite reliability model considering all the electrical components of the vehicle. A solar electric vehicle's (SEV) reliability is mostly impacted by the reliability of power generated by its onboard PVS. To determine the reliability of photovoltaic generation (PVG), a new probabilistic index, named *mPAI*, has been proposed in this thesis. This index helps to estimate the operational readiness or availability of a SEV at a particular geographical location. The study quantitatively justifies that the SEVs are more reliable than plug-in EVs under normal operating conditions. Another reliability index, *ASAI* is proposed to examine the contribution of the plug-in option for improving the reliability of the SEV. The result shows that SEV with a standby plug-in facility is the best EV option from the reliability perspective. The thesis also demonstrates how quick response in maintenance helps to enhance the availability of the vehicle. Reliability analysis of a SEV is still an unexplored area of

research. The concepts presented in this thesis can complement the ongoing researches on SEV design and maintenance.

9.2 Future Scope

Reliability is an important design parameter, which must be analyzed during the planning, designing, and operating phases of a system. Assessment of power system reliability has great significance and importance since its failure has cascaded impacts on society and the economy. As power systems are being complexed day-by-day due to the addition of many new concepts and facilities, the need for sophisticated methodologies to assess reliability is highly increased. Most of the existing techniques have their own limitations and are not suitable to address the new challenges. Thus, the development of new methodologies and also the inclusion of multiple new probable factors in the existing techniques can be the scopes of future research. Based on the studies reported in this thesis, some probable future scopes of research have been outlined as follows:

1. **Reliability-cost pricing assessment in deregulated power market:** In this thesis, an approach has been presented to prepare a customer-reliability-specific operating reserve schedule. The cost of reserve margin is not considered in the assessment. In a deregulated environment, customer can choose their reliability level by paying the required cost of reserve. For higher reliability, the cost of reserves will be more. Thus, there must be a trade-off in reliability vs. cost. This aspect can be added to future research.
2. **Application of IEB and ICB:** The reliability worth of integrating renewable energy sources (RESs) with distribution systems is one of the less focused areas in power system reliability studies. In this thesis, two new parameters, namely Incremental Energy Benefit (IEB) and Incremental cost Benefit (ICB), are introduced to measure

the benefits of RESs integration. Application of these two metrics can be extended to other renewable-energy incorporated systems.

3. **Reliability assessment in Vehicle-to-Grid mode:** The present study illustrates how the reliability of a distribution network gets impacted due to the increased EV charging. Thus, this study considers the negative impact of EV integration. However, EVs can be treated as portable DGs and can be used to boost the reliability of a grid. During the off-peak hours, EV takes charge from the grid (grid-to-vehicle), and during the peak hours, the vehicle supplies the energy to the grid (Vehicle-to-Grid). This concept has been addressed in many recent literature; however, reliability-centric researches are still very limited. The impact of EV integration in vehicle-to-grid mode on the reliability of a distribution network can be a future scope of the present study.
4. **Maintainability prediction, reliability-cost trade off, and dynamic reliability assessment of EV:** The research reported in Chapter 7 of this thesis shows how a proper maintenance strategy is essential for the higher availability of an EV. A comprehensive maintainability prediction analysis can help to investigate all the factors associated with the maintainability of an EV and prepare a proper corrective and preventive maintenance schedule accordingly. In addition to that, a reliability-cost trade-off assessment is very important to find an optimum reliability point at a reasonable cost of EV components. These two aspects can be incorporated in future studies. Again, the present research has dealt with the steady-state reliability assessment of EVs. Dynamic reliability assessment can be a good scope of future research.
5. **Further study on mPAI:** The present study has not considered the impact of wind speed on mPAI. The reliability of the SEV has been determined at stationary conditions. How a vehicle's speed impacts the value of mPAI can be a potential future scope of the study reported in this thesis.

References

- [1] L. Goel, Z. Song, and P. Wang, "Well-being analysis of spinning reserve in a bilateral power market," *Electric Power Systems Research*, vol. 69, no. 1, pp. 37–42, 2004.
- [2] T. Adefarati and R. C. Bansal, "Reliability assessment of distribution system with the integration of renewable distributed generation," *Applied Energy*, vol. 185, pp. 158–171, jan 2017.
- [3] B. K. Talukdar, B. C. Deka, and A. K. Goswami, "Reliability analysis of an active distribution network integrated with solar, wind and tidal energy sources," *International Transactions on Electrical Energy Systems*, p. e13201, 2021.
- [4] H. Wang, N. Zhu, and X. Bai, "Reliability model assessment of grid-connected solar photovoltaic system based on Monte-Carlo," *Applied Solar Energy (English translation of Geliotekhnika)*, vol. 51, pp. 262–266, oct 2015.
- [5] R. N. Allan, R. Billinton, I. Sjarief, L. Goel, and K. S. So, "A Reliability Test System For Educational Purposes - Basic Distribution System Data and Results," *IEEE Transactions on Power Systems*, vol. 6, no. 2, pp. 813–820, 1991.
- [6] L. Goel, R. Billinton, and R. Gupta, "Basic data and evaluation of distribution system reliability worth," pp. 271–277, 1992.
- [7] R. Billinton and R. N. Allan, *Reliability Evaluation of Power Systems*, pp. 220–248. Boston: Springer US, 1996.
- [8] B. K. Talukdar and B. C. Deka, "An approach to reliability, availability and maintainability analysis of a plug-in electric vehicle," *World Electric Vehicle Journal*, vol. 12, no. 1, 2021.
- [9] B. K. Talukdar, B. C. Deka, and A. K. Goswami, "An approach to reliability modeling and availability analysis of a solar electric vehicle with standby plug-in facility," *International Transactions on Electrical Energy Systems*, p. e13147, 2021.
- [10] R. Allan and R. Billinton, "Probabilistic assessment of power systems," *Proceedings of the IEEE*, vol. 88, no. 2, pp. 140–162, 2000.
- [11] W. L. Roy Billinton, *Reliability Assessment of Electric Power Systems Using Monte Carlo Methods*. New York: Springer Science, 1st ed., 1994.
- [12] L. Goel and C. Feng, "Well-being framework for composite generation and transmission system reliability evaluation," *IEE Proceedings - Generation, Transmission and Distribution*, vol. 146, p. 528, sep 1999.

- [13] A. Verma, D. Srividya, and R. Karanki, *Power System Reliability*, pp. 305–321. London: Springer London, 2010.
- [14] E. Balagurusamy, *Reliability Engineering*. New Delhi: Tata McGraw Hill Education Private Limited, 14th ed., 2013.
- [15] M. Pereira and N. Balu, “Composite generation/transmission reliability evaluation,” *Proceedings of the IEEE*, vol. 80, no. 4, pp. 470–491, 1992.
- [16] M. H. Hashemi, S. Zolfaghari, and A. Zolfaghari, “Reserve management in restructured power system considering loads reliability,” *European Journal of Engineering Research and Science*, vol. 2, pp. 34–38, 12 2017.
- [17] C. T. Pawan and D. Singh, “Restructuring and Deregulation of Power system- A Review,” *International Journal of Current Research*, vol. 10, pp. 70474–70478, June 2018.
- [18] V. V. Venu and A. K. Verma, “Reliability of electric power systems: Challenges in the deregulated environment - a research perspective,” *International Journal of Systems Assurance Engineering and Management*, vol. 1, no. 1, pp. 24–31, 2010.
- [19] A. Rahimi and A. Sheffrin, “Effective market monitoring in deregulated electricity markets,” *IEEE Transactions on Power Systems*, vol. 18, no. 2, pp. 486–493, 2003.
- [20] R. Billinton and R. N. Allan, “Distribution systems—basic techniques and radial networks,” in *Reliability Evaluation of Power Systems*, pp. 220–248, Springer US, 1996.
- [21] A. Ehsani, A. M. Ranjbar, A. Jafari, and M. Fotuhi-Firuzabad, “Reliability evaluation of deregulated electric power systems for planning applications,” *Reliability Engineering and System Safety*, vol. 93, no. 10, pp. 1473–1484, 2008.
- [22] A. Ehsani, A. M. Ranjbar, A. Jafari, and M. Fotuhi-Firuzabad, “Reliability evaluation of deregulated power system considering competitive electricity market,” *Iranian Journal of Science and Technology, Transaction B: Engineering*, vol. 31, no. 6, pp. 603–616, 2007.
- [23] Y. Mobarak and K. Nithiyananthan, “Vertically integrated utility power system structures for egyptian scenario and electricity act,” *Journal of Advanced Research in Dynamical and Control Systems*, vol. 11, p. 766, 07 2019.
- [24] C. Li, X. Liu, W. Zhang, Y. Cao, X. Dong, F. Wang, and L. Li, “Assessment method and indexes of operating states classification for distribution system with distributed generations,” *IEEE Transactions on Smart Grid*, vol. 7, no. 1, pp. 481–490, 2016.
- [25] C. Borges and V. Martins, “Active distribution network integrated planning incorporating distributed generation and load response uncertainties,” in *2012 IEEE Power and Energy Society General Meeting*, vol. 26, pp. 2164–2172, 2012.
- [26] Z. Hu and F. Li, “Cost-benefit analyses of active distribution network management, part i: Annual benefit analysis,” *IEEE Transactions on Smart Grid*, vol. 3, no. 3, pp. 1067–1074, 2012.

- [27] C. L. T. Borges, "An overview of reliability models and methods for distribution systems with renewable energy distributed generation," *Renewable and Sustainable Energy Reviews*, vol. 16, no. 6, pp. 4008–4015, 2012.
- [28] M. Al-Muhaini and G. T. Heydt, "Evaluating future power distribution system reliability including distributed generation," *IEEE Transactions on Power Delivery*, vol. 28, no. 4, pp. 2264–2272, 2013.
- [29] H. Wu, S. Li, and Y. Ren, "Reliability modeling of electric vehicles and its impact on distribution network," in *2018 IEEE PES Asia-Pacific Power and Energy Engineering Conference (APPEEC)*, pp. 229–234, 2018.
- [30] J. Gemassmer, C. Daam, and R. Reibsch, "Challenges in grid integration of electric vehicles in urban and rural areas," *World Electric Vehicle Journal*, vol. 12, no. 4, 2021.
- [31] Y. Lim, H. M. Kim, S. Kang, and T. H. Kim, "Vehicle-to-grid communication system for electric vehicle charging," in *Integrated Computer-Aided Engineering*, vol. 19, pp. 57–65, 2012.
- [32] M. Elsis, M. Soliman, M. A. Aboelela, and W. Mansour, "Model predictive control of plug-in hybrid electric vehicles for frequency regulation in a smart grid," *IET Generation, Transmission and Distribution*, vol. 11, no. 16, pp. 3974–3983, 2017.
- [33] Q. Su, G. Zhang, J. Lai, S. Feng, and W. Shi, "Green solar electric vehicle changing the future lifestyle of human," *World Electr. Veh. J.*, vol. 4, p. 128–132, 2010.
- [34] M. N. Hassanzadeh, M. Fotuhi-Firuzabad, and A. Safdarian, "Wind energy penetration with load shifting from the system well-being viewpoint," *International Journal of Renewable Energy Research*, vol. 7, no. 2, pp. 977–987, 2017.
- [35] R. Billinton and R. N. Allan, *Reliability Evaluation of Engineering Systems*. Springer US, 1992.
- [36] Q. Wang, "Advances of wholesale and retail electricity market development in the context of distributed energy resources," in *New Technologies for Power System Operation and Analysis* (H. Jiang, Y. Zhang, and E. Muljadi, eds.), pp. 99–142, Academic Press, 2021.
- [37] R. Allan and R. Billinton, "Probabilistic assessment of power systems," *Proceedings of the IEEE*, vol. 88, no. 2, pp. 140–162, 2000.
- [38] R. Billinton, "Evaluation of reliability worth in an electric power system," *Reliability Engineering & System Safety*, vol. 46, no. 1, pp. 15–23, 1994. Special Issue On Power System Reliability.
- [39] J. Oteng-Adjei and R. Billinton, "Evaluation of interrupted energy assessment rates in composite systems," *IEEE Transactions on Power Systems*, vol. 5, no. 4, pp. 1317–1323, 1990.
- [40] R. Billinton and R. Ghajar, "Evaluation of the marginal outage costs of generating systems for the purposes of spot pricing," *IEEE Transactions on Power Systems*, vol. 9, no. 1, pp. 68–75, 1994.

- [41] A. Sankararishnan and A. Billinton, "Effective techniques for reliability worth assessment in composite power system networks using monte carlo simulation," *IEEE Transactions on Power Systems*, vol. 11, no. 3, pp. 1255–1261, 1996.
- [42] K. Kariuki and R. Allan, "Evaluation of reliability worth and value of lost load," *IEE Proceedings - Generation, Transmission and Distribution*, vol. 143, pp. 171–180(9), March 1996.
- [43] J. C. O. Mello, M. Pereira, A. M. L. da Silva, and A. C. G. Melo, "Application of chronological load modeling in composite reliability worth evaluation," *Electric Power Systems Research*, vol. 40, pp. 167–174, 1997.
- [44] J. van Casteren, M. Bollen, and M. Schmiege, "Reliability assessment in electrical power systems: the weibull-markov stochastic model," *IEEE Transactions on Industry Applications*, vol. 36, no. 3, pp. 911–915, 2000.
- [45] A. Heidari, V. G. Agelidis, and H. Zayandehroodi, "Reliability worth analysis of distributed generation enhanced distribution system considering the customer cost model based on optimal radial basis function neural network," in *2013 IEEE 7th International Power Engineering and Optimization Conference (PEOCO)*, pp. 641–646, 2013.
- [46] S. Küfeoğlu and M. Lehtonen, "A review on the theory of electric power reliability worth and customer interruption costs assessment techniques," in *2016 13th International Conference on the European Energy Market (EEM)*, pp. 1–6, 2016.
- [47] A. U. Rehman, A. U. Rehman, and S. Mehmood, "Reliability assessment and cost analysis of over loaded distribution system with distributed generation," in *2016 International Conference on Computing, Electronic and Electrical Engineering (ICE Cube)*, pp. 244–250, 2016.
- [48] W. Zhu, M. Han, J. V. Milanović, and P. Crossley, "Methodology for reliability assessment of smart grid considering risk of failure of communication architecture," *IEEE Transactions on Smart Grid*, vol. 11, no. 5, pp. 4358–4365, 2020.
- [49] M. Bhavaraju, "Composite system reliability evaluation," *International Journal of Electrical Power & Energy Systems*, vol. 10, no. 3, pp. 174–179, 1988.
- [50] R. Billinton and M. P. Bhavaraju, "Transmission planning using a reliability criterion, part i: A reliability criterion," *IEEE Transactions on Power Apparatus and Systems*, vol. PAS-89, no. 1, pp. 28–34, 1970.
- [51] R. Billinton, "Overall approach to the reliability evaluation of composite generation and transmission systems," *IEE Proceedings C (Generation, Transmission and Distribution)*, vol. 127, pp. 72–81(9), March 2010.
- [52] R. Billinton, T. K. P. Medicherla, and M. S. Sachdev, "Application of common-cause outage models in composite system reliability evaluation," *IEEE Transactions on Power Apparatus and Systems*, vol. PAS-100, no. 7, pp. 3648–3657, 2004.

- [53] R. Billinton, P. K. Vohra, and S. Kumar, "Effect of station originated outages in a composite system adequacy evaluation of the IEEE reliability test system," *IEEE Transactions on Power Apparatus and Systems*, vol. PAS-104, no. 10, pp. 2649–2656, 2009.
- [54] R. Allan and J. Ochoa, "Modeling and assessment of station originated outages for composite systems reliability evaluation," *IEEE Transactions on Power Systems*, vol. 3, no. 1, pp. 158–165, 2006.
- [55] S. Kumar and R. Billinton, "Adequacy evaluation of a small area in a large composite power network," *IEEE Transactions on Power Systems*, vol. 4, no. 2, pp. 551–558, 2003.
- [56] R. Billinton and W. Zhang, "An adequacy equivalent approach for composite power system reliability evaluation," in *IEEE WESCANEX 95. Communications, Power, and Computing. Conference Proceedings*, vol. 1, pp. 163–168 vol.1, 2003.
- [57] R. Billinton and W. Zhang, "State extension for adequacy evaluation of composite power systems-applications," *IEEE Transactions on Power Systems*, vol. 15, no. 1, pp. 427–432, 2005.
- [58] G. C. Oliveira, M. V. F. Pereira, and S. H. F. Cunha, "A technique for reducing computational effort in monte-carlo based composite reliability evaluation," *IEEE Power Engineering Review*, vol. 9, no. 11, pp. 29–29, 1989.
- [59] R. Billinton, "Hybrid approach for reliability evaluation of composite generation and transmission systems using monte-carlo simulation and enumeration technique," *IEE Proceedings C (Generation, Transmission and Distribution)*, vol. 138, pp. 233–241(8), May 1991.
- [60] J. Ubeda and R. Allan *IEE Proceedings C (Generation, Transmission and Distribution)*, vol. 139, pp. 81–86(5), March 1992.
- [61] R. Billinton and J. J.R., "Application of sequential monte carlo simulation to evaluation of distributions of composite system indices," *IEE Proceedings - Generation, Transmission and Distribution*, vol. 144, pp. 87–90(3), March 1997.
- [62] A. Abdulwhab and R. Billinton, "Generating system wellbeing index evaluation," *International Journal of Electrical Power and Energy Systems*, vol. 26, no. 3, pp. 221–229, 2004.
- [63] K. Aggarwal, *Maintainability and Availability, Topics in Safety Reliability and Quality*, p. 24. Netherlands: Springer, 1993.
- [64] P. Subudhi and S. Krithiga, "Pv and grid interfaced plug-in ev battery charger operating in p-vg, p-v and v-g modes," *IJRTE*, vol. 8, pp. 3431 – 3443, 2019.
- [65] S. Gobhinath, S. Boobalan, R. Ashwin, J. Meshach, and K. Rajkumar, *A Practical Approach in Design and Fabrication of Solar-Powered Four-Wheeled Electric Vehicle*, p. 601–607. Singapore: Springer, 2020.

- [66] S. Khan, A. Ahmad, F. Ahmad, M. Shafaati Shemami, M. Saad Alam, and S. Khateeb, "A comprehensive review on solar powered electric vehicle charging system," *Smart Sci.*, vol. 6, p. 54–79, 2018.
- [67] R. Billinton, "Reliability considerations in the new electric power utility industry," *Proceedings of the 1997 Canadian Electricity Conference Expo*, pp. 1–10, 1997.
- [68] R. Billinton and M. Fotuhi-Firuzabad, "A reliability framework for generating unit commitment," *Electric Power Systems Research*, vol. 56, pp. 81–88, 2000.
- [69] C. Singh, "Role of reliability , risk and probabilistic analysis in the competitive environment," *IEEE Conference Proceedings*, 1999.
- [70] M. Shahidehpour and M. Alomoush, "Restructured electric power systems: Operation, trading, and volatility [book review]," *Computer Applications in Power, IEEE*, vol. 15, pp. 60 – 62, 05 2002.
- [71] J. Zhu, G. Jordan, and S. Ihara, "The market for spinning reserve and its impacts on energy prices," *2000 IEEE Power Engineering Society, Conference Proceedings*, vol. 2, no. c, pp. 1202–1207, 2000.
- [72] A. E.H and I. M.D, "Reserve markets for power system reliability," *IEEE Trans.Power Syst*, vol. 15, pp. 228–233, 01 2000.
- [73] M. R. Tur, "Deployment of reserve requirements into the power systems considering the cost, lost, and reliability parameters based on sustainable energy," *The International Journal of Electrical Engineering & Education*, vol. 58, no. 2, pp. 621–639, 2021.
- [74] M. R. Tur, S. Ay, A. Erduman, A. Shobole, and M. Wadi, "Impact of demand side management on spinning reserve requirements designation," *International Journal of Renewable Energy Research*, vol. 7, pp. 946–953, 01 2017.
- [75] A. Helseth, M. Haugen, H. Farahmand, B. Mo, S. Jaehnert, and I. Stenkløv, "Assessing the benefits of exchanging spinning reserve capacity within the hydro-dominated nordic market," *Electric Power Systems Research*, vol. 199, p. 107393, 2021.
- [76] S. S. Reddy, P. R. Bijwe, and A. R. Abhyankar, "Optimal dynamic emergency reserve activation using spinning, hydro and demand-side reserves," *Frontiers in Energy*, vol. 10, no. 4, pp. 409–423, 2016.
- [77] A. da Silva, L. de Resende, L. da Fonseca Manso, and R. Billinton, "Well-being analysis for composite generation and transmission systems," *IEEE Transactions on Power Systems*, vol. 19, no. 4, pp. 1763–1770, 2004.
- [78] R. Billinton and J. E. Billinton, "Distribution System Reliability Indices," *IEEE Transactions on Power Delivery*, vol. 4, no. 1, pp. 561–568, 1989.
- [79] Z. Esau and D. Jayaweera, "Reliability assessment in active distribution networks with detailed effects of PV systems," *Journal of Modern Power Systems and Clean Energy*, vol. 2, no. 1, pp. 59–68, 2014.

- [80] L. S. Vladimír Krepl, Husam I. Shaheen, Ghaeth Fandi, T. H. Zdenek Muller, Josef Tlustý, 7, and S. G. 8, "The Role of Renewable Energies in the Microgrids," *Energies*, vol. 24, no. 1, 2019.
- [81] D. Bogdanov, M. Ram, A. Aghahosseini, A. Gulagi, A. S. Oyewo, M. Child, U. Caldera, K. Sadvoskaia, J. Farfan, L. De Souza Noel Simas Barbosa, M. Fasihi, S. Khalili, T. Traber, and C. Breyer, "Low-cost renewable electricity as the key driver of the global energy transition towards sustainability," *Energy*, vol. 227, p. 120467, 2021.
- [82] BP, "Statistical Review of World Energy globally consistent data on world energy markets .." <https://www.bp.com/content/dam/bp/business-sites/en/global/corporate/pdfs/energy-economics/statistical-review/bp-stats-review-2020-full-report.pdf>, 2020.
- [83] S. Jai, "One Sun, One World, One Grid: All you need to know about mega solar plan | Business Standard News." https://www.business-standard.com/article/current-affairs/one-sun-one-world-one-grid-all-you-need-to-know-about-solar-strategy-120081500417_1.html, 2020.
- [84] V. Kalkhambkar, B. Rawat, R. Kumar, and R. Bhakar, "Optimal allocation of renewable energy sources for energy loss minimization," *Journal of Electrical Systems*, vol. 13, no. 1, pp. 115–130, 2017.
- [85] B. Kroposki, B. Johnson, Y. Zhang, V. Gevorgian, P. Denholm, B. M. Hodge, and B. Hannegan, "Achieving a 100% Renewable Grid: Operating Electric Power Systems with Extremely High Levels of Variable Renewable Energy," *IEEE Power and Energy Magazine*, vol. 15, no. 2, pp. 61–73, 2017.
- [86] J. L. López-Prado, J. I. Vélez, and G. A. Garcia-Llinás, "Reliability evaluation in distribution networks with microgrids: Review and classification of the literature," *Energies*, vol. 13, p. 6189, dec 2020.
- [87] Z. A. Haidar and A. M. Al-Shaalan, "Reliability Evaluation of Renewable Energy Share in Power Systems," *Journal of Power and Energy Engineering*, vol. 6, pp. 40–47, 2018.
- [88] V. S. Bhadoria, N. S. Pal, V. Shrivastava, and S. P. Jaiswal, "Reliability Improvement of Distribution System by Optimal Siting and Sizing of Disperse Generation," *International Journal of Reliability, Quality and Safety Engineering*, vol. 24, no. 6, pp. 1–11, 2017.
- [89] S. Ullah, A. M. Haidar, P. Hoole, H. Zen, and T. Ahfock, "The current state of Distributed Renewable Generation, challenges of interconnection and opportunities for energy conversion based DC microgrids," nov 2020.
- [90] H. Eluri and M. G. Naik, "Challenges of RES with Integration of Power Grids, Control Strategies, Optimization Techniques of Microgrids: A Review," *International Journal of Renewable Energy Research*, vol. 11, no. 1, pp. 1–19, 2021.
- [91] A. Escalera, B. Hayes, and M. Prodanović, "A survey of reliability assessment techniques for modern distribution networks," *Renewable and Sustainable Energy Reviews*, vol. 91, no. February, pp. 344–357, 2018.

- [92] A. Man-Im, W. Ongsakul, and N. Madhu, "Reliability Enhanced Multi-objective Economic Dispatch Strategy for Hybrid Renewable Energy System with Storage," *Journal of the Operations Research Society of China*, 2020.
- [93] V. Kalkhambkar, R. Kumar, and R. Bhakar, "Joint optimal allocation methodology for renewable distributed generation and energy storage for economic benefits," *IET Renewable Power Generation*, vol. 10, no. 9, pp. 1422–1429, 2016.
- [94] T. T. Chuong, N. Van Hung, and N. H. Nam, "Assessment of Wind Turbine Generators on Reliability of Distribution Network," *Journal of Electrical Engineering and Technology*, vol. 14, no. 6, pp. 2217–2224, 2019.
- [95] J. Lin, L. Cheng, Y. Chang, K. Zhang, B. Shu, and G. Liu, "Reliability based power systems planning and operation with wind power integration: A review to models, algorithms and applications," *Renewable and Sustainable Energy Reviews*, vol. 31, pp. 921–934, 2014.
- [96] K. Murali and V. Sundar, "Reassessment of tidal energy potential in India and a decision-making tool for tidal energy technology selection," *The International Journal of Ocean and Climate Systems*, vol. 8, no. 2, pp. 85–97, 2017.
- [97] C. P. Nazir, "Coastal power plant: A hybrid solar-hydro renewable energy technology," *Clean Energy*, vol. 2, no. 2, pp. 102–111, 2018.
- [98] M. S. Chowdhury, K. S. Rahman, V. Selvanathan, N. Nuthammachot, M. Suklueng, A. Mostafaiepour, A. Habib, M. Akhtaruzzaman, N. Amin, and K. Techato, "Current trends and prospects of tidal energy technology," *Environment, Development and Sustainability*, vol. 23, no. 6, pp. 8179–8194, 2021.
- [99] F. Xavier and B. Llavall, "Reliability Worth Assessment of Radial System With Distributed Generation," no. July, p. 55, 2011.
- [100] B. Khan, H. H. Alhelou, and F. Mebrahtu, "A holistic analysis of distribution system reliability assessment methods with conventional and renewable energy sources," *AIMS Energy*, vol. 7, no. 4, pp. 413–429, 2019.
- [101] A. Alferidi and R. Karki, "Development of probabilistic reliability models of photovoltaic system topologies for system adequacy evaluation," *Applied Sciences*, vol. 7, no. 2, 2017.
- [102] R. Karki and R. Billinton, "Reliability/cost implications of utilizing wind energy in small isolated power systems," *Wind Engineering*, vol. 24, no. 5, pp. 379–388, 2000.
- [103] R. Billinton, S. Aboreshaid, and M. Fotuhi-Firuzabad, "Well-being analysis for hvdc transmission systems," *IEEE Transactions on Power Systems*, vol. 12, no. 2, pp. 913–918, 1997.
- [104] B. Liang, W. Liu, F. Wen, and M. A. Salam, "Well-being analysis of power systems considering increasing deployment of gas turbines," *Energies*, vol. 10, no. 7, 2017.

- [105] W. Wangdee, "Deterministic-based power grid planning enhancement using system well-being analysis," *Journal of Modern Power Systems and Clean Energy*, vol. 6, no. 3, pp. 438–448, 2018.
- [106] S. Kalaiarasi, A. Merceline Anita, and R. Geethanjali, "Analysis Of System Reliability Using Markov Technique," *Global Journal of Pure and Applied Mathematics*, vol. 13, no. 9, pp. 5265–5273, 2017.
- [107] A. Mohammad, R. Zamora, and T. T. Lie, "Integration of electric vehicles in the distribution network: A review of PV based electric vehicle modelling," *Energies*, vol. 13, no. 17, 2020.
- [108] Y. Wang, H. Su, W. Wang, and Y. Zhu, "The impact of electric vehicle charging on grid reliability," *IOP Conference Series: Earth and Environmental Science*, vol. 199, no. 5, 2018.
- [109] D. Božič and M. Pantoš, "Impact of electric-drive vehicles on power system reliability," *Energy*, vol. 83, pp. 511–520, 2015.
- [110] N. H. Tehrani and P. Wang, "Probabilistic estimation of plug-in electric vehicles charging load profile," *Electric Power Systems Research*, vol. 124, pp. 133–143, 2015.
- [111] S. Deb, A. K. Goswami, P. Harsh, J. P. Sahoo, R. L. Chetri, R. Roy, and A. S. Shekhawat, "Charging coordination of plug-in electric vehicle for congestion management in distribution system integrated with renewable energy sources," *IEEE Transactions on Industry Applications*, vol. 56, no. 5, pp. 5452–5462, 2020.
- [112] E. Sortomme, M. M. Hindi, S. D. J. MacPherson, and S. S. Venkata, "Coordinated charging of plug-in hybrid electric vehicles to minimize distribution system losses," *IEEE Transactions on Smart Grid*, vol. 2, no. 1, pp. 198–205, 2011.
- [113] S. Deilami, A. S. Masoum, P. S. Moses, and M. A. S. Masoum, "Real-time coordination of plug-in electric vehicle charging in smart grids to minimize power losses and improve voltage profile," *IEEE Transactions on Smart Grid*, vol. 2, no. 3, pp. 456–467, 2011.
- [114] S. Han, S. Han, and K. Sezaki, "Estimation of achievable power capacity from plug-in electric vehicles for v2g frequency regulation: Case studies for market participation," *IEEE Transactions on Smart Grid*, vol. 2, no. 4, pp. 632–641, 2011.
- [115] S. Han, S. Han, and K. Sezaki, "Development of an optimal vehicle-to-grid aggregator for frequency regulation," *IEEE Transactions on Smart Grid*, vol. 1, no. 1, pp. 65–72, 2010.
- [116] W. Kempton and J. Tomić, "Vehicle-to-grid power fundamentals: Calculating capacity and net revenue," *Journal of Power Sources*, vol. 144, no. 1, pp. 268–279, 2005.
- [117] K. Clement-Nyns, E. Haesen, and J. Driesen, "The impact of vehicle-to-grid on the distribution grid," *Electric Power Systems Research*, vol. 81, pp. 185–192, jan 2011.

- [118] X. Shu, Y. Guo, W. Yang, K. Wei, Y. Zhu, and H. Zou, "A Detailed Reliability Study of the Motor System in Pure Electric Vans by the Approach of Fault Tree Analysis," *IEEE Access*, vol. 8, pp. 5295–5307, 2020.
- [119] Q. Xia, Z. Wang, Y. Ren, B. Sun, D. Yang, and Q. Feng, "A reliability design method for a lithium-ion battery pack considering the thermal disequilibrium in electric vehicles," *Journal of Power Sources*, vol. 386, pp. 10–20, May 2018.
- [120] Q. Xia, Z. Wang, Y. Ren, L. Tao, C. Lu, J. Tian, D. Hu, Y. Wang, Y. Su, J. Chong, H. Jin, and Y. Lin, "A modified reliability model for lithium-ion battery packs based on the stochastic capacity degradation and dynamic response impedance," *Journal of Power Sources*, vol. 423, pp. 40–51, May 2019.
- [121] B. Sakhdari and N. Azad, "An Optimal Energy Management System for Battery Electric Vehicles," *IFAC-PapersOnLine*, vol. 48, no. 15, pp. 86–92, 2015.
- [122] I. Bolvashenkov and H.-G. Herzog, "Approach to predictive evaluation of the reliability of electric drive train based on a stochastic model," in *2015 International Conference on Clean Electrical Power (ICCEP)*, (Taormina, Italy), pp. 486–492, IEEE, June 2015.
- [123] B. S. Ammaiyappan and S. Ramalingam, "Reliability investigation of electric vehicle," *Life Cycle Reliability and Safety Engineering*, vol. 8, no. 2, pp. 141–149, 2019.
- [124] M. Khalilzadeh and A. Fereidunian, "A Markovian approach applied to reliability modeling of bidirectional DC-DC converters used in PHEVs and smart grids," *Iranian Journal of Electrical & Electronic Engineering*, vol. 12, dec 2016.
- [125] A. Sierra Rodriguez, T. de Santana, I. MacGill, N. Ekins-Daukes, and A. Reinders, "A feasibility study of solar pv-powered electric cars using an interdisciplinary modeling approach for the electricity balance, co2 emissions, and economic aspects: The cases of the netherlands, norway, brazil, and australia," *Progress in Photovoltaics: Research and Applications*, vol. 28, no. 6, pp. 517–532, 2020.
- [126] R. N. Colvile, E. J. Hutchinson, J. S. Mindell, and R. F. Warren, "The transport sector as a source of air pollution," *Atmos. Environ.*, vol. 35, no. 9, p. 1537–1565, 2001.
- [127] C. L. Canals, E. Martinez-Laserna, B. Amante García, and N. Nieto, "Sustainability analysis of the electric vehicle use in europe for co2 emissions reduction," *J. Clean. Prod.*, vol. 127, p. 425–437, 2016.
- [128] N. Wassan, A. Furneaux, and S. Salhi, *Role of Green Technology Vehicles in Road Transportation Emissions – Case of the UK*, pp. 27–62. Wiley-ISTE, 2019.
- [129] Q. Su, G. Zhang, J. Lai, S. Feng, and W. Shi, "Green solar electric vehicle changing the future lifestyle of human," *World Electr. Veh. J.*, vol. 4, p. 128–132, 2010.
- [130] "H. com editors, "william cobb demonstrates first solar-powered car," history. <https://www.history.com/this-day-in-history/william-cobb-demonstrates-first-solar-powered-car> (accessed may 25, 2021),"
- [131] "'stella," solar team eindhoven. <https://solarteameindhoven.nl/stella-vie/stella/> (accessed may 23, 2021),"

- [132] ““long range solar electric vehicle | lightyear one.” <https://lightyear.one/lightyear-one> (accessed may 20, 2021),”
- [133] ““sion electric car,” sono motors. <https://sonomotors.com/en/sion/> (accessed may 20, 2021),”
- [134] ““solar electric vehicles.” <https://www.humblemotors.com/> (accessed may 20, 2021),”
- [135] T. Adefarati and R. C. Bansal, “Reliability assessment of distribution system with the integration of renewable distributed generation,” *Appl. Energy*, vol. 185, p. 158–171, 2017.
- [136] H. Wang, N. Zhu, and X. Bai, “Reliability model assessment of grid-connected solar photovoltaic system based on monte-carlo,” *Appl. Sol. Energy*, vol. 51, p. 262–266, 2015.
- [137] W. Zhao, Y. Lv, Z. Wei, W. Yan, and Q. Zhou, “Review on dust deposition and cleaning methods for solar PV modules Review on dust deposition and cleaning methods for solar PV modules,” vol. 032701, no. April, 2021.
- [138] M. Q. Tran, M. Elsis, K. Mahmoud, M. Lehtonen, and M. M. Darwish, “Robust design of ANFIS-based blade pitch controller for wind energy conversion systems against wind speed fluctuations,” *IEEE Access*, vol. 9, pp. 37894–37904, 2021.
- [139] E. Balagurusamy, *Reliability Engineering*, p. 24. Green Park Extension, New Delhi 110016: McGraw Hill Education (India) Private Limited, 2017.
- [140] R. Billinton and R. N. Allan, *Reliability Evaluation of Engineering Systems*, pp. 280–308. Boston: Springer US, 1992.
- [141] R. Taleb and H. Saidi, “IRAMY inverter control for solar electric vehicle,” *International Journal of Power Electronics and Drive Systems*, vol. 7, no. 3, pp. 1012–1022, 2016.
- [142] A. Sankar and R. Seyezhai, “Simulation and implementation of solar powered electric vehicle,” *Circuits and Systems*, vol. 7, pp. 643–661, 2016.
- [143] M. M. Ismail, A. F. Bendary, and M. Elsis, “Optimal design of battery charge management controller for hybrid system PV/wind cell with storage battery,” *International Journal of Power and Energy Conversion*, vol. 11, no. 4, pp. 412–429, 2020.
- [144] Q. Xia, Z. Wang, Y. Ren, B. Sun, D. Yang, and Q. Feng, “A reliability design method for a lithium-ion battery pack considering the thermal disequilibrium in electric vehicles,” *J. Power Sources*, vol. 386, pp. 10–20, 2018.
- [145] Q. Xia, “A modified reliability model for lithium-ion battery packs based on the stochastic capacity degradation and dynamic response impedance,” *J. Power Sources*, vol. 423, pp. 40–51, 2019.
- [146] X. Shu, Y. Guo, W. Yang, K. Wei, Y. Zhu, and Z. H., “A detailed reliability study of the motor system in pure electric vans by the approach of fault tree analysis,” *IEEE Access*, vol. 8, p. 5295–5307, 2020.

- [147] B. Sakhdari and N. L. Azad, "An optimal energy management system for battery electric vehicles," *IFAC-Pap*, vol. 48, p. 86–92, 2015.
- [148] B. S. Ammaiyappan and S. Ramalingam, "Reliability investigation of electric vehicle," *Life Cycle Reliab. Saf. Eng.*, vol. 8, p. 141–149, 2019.
- [149] I. Bolvashenkov and H.-G. Herzog, "Approach to predictive evaluation of the reliability of electric drive train based on a stochastic model," *International Conference on Clean Electrical Power (ICCEP)Taormina, Italy*, p. 486–492, 2015.
- [150] A. Alferidi and R. Karki, "Development of probabilistic reliability models of photovoltaic system topologies for system adequacy evaluation," *Appl. Sci.*, vol. 7, p. 176, 2017.
- [151] C. L. T. Borges, "An overview of reliability models and methods for distribution systems with renewable energy distributed generation," *Renew. Sustain. Energy Rev.*, vol. 16, p. 4008–4015, 2012.
- [152] C. Ebeling, *An Introduction to Reliability and Maintainability Engineering*. New Delhi: Tata McGraw Hill Education Private Limited, 7th ed., 2000.
- [153] R. Billinton, "Evaluation of reliability worth in an electric power system," *Reliability Engineering and System Safety*, vol. 46, no. 1, pp. 15–23, 1994.
- [154] Subcommittee, Probability Methods, "IEEE Reliability Test System," *IEEE Transactions on Power Apparatus and Systems*, vol. PAS-98, no. 6, pp. 2047–2054, 1979.
- [155] R. Billinton, S. Kumar, N. Chowdhury, K. Chu, K. Debnath, L. Goel, E. Khan, P. Kos, G. Nourbakhsh, and J. Oteng-Adjei, "A reliability test system for educational purposes-basic data," *IEEE Power Engineering Review*, vol. 9, no. 8, pp. 67–68, 1989.
- [156] A. Ehsani, A. M. Ranjbar, A. Jafari, M. Fotuhi-Firuzabad, D. . D. k. S. Pawan C . Tapre, I. D. Analysis, R. Concrete, T. Sokolova, A. Ehsani, A. M. Ranjbar, A. Jafari, M. Fotuhi-Firuzabad, S. B. Raikar, and K. M. Jagtap, "Reliability evaluation of deregulated power system considering competitive electricity market," *Iranian Journal of Science and Technology, Transaction B: Engineering*, vol. 31, no. 6, pp. 603–616, 2018.
- [157] J. F. Prada, "The Value of Reliability in Power Systems : Pricing Operating Reserves. energy laboratory, massachusetts institute of technology, 1999.." Massachusetts Institute of Technology. Energy Laboratory.
- [158] B. K. Talukdar, B. C. Deka, A. K. Goswami, and D. Saha, "Reconfiguration of Radial Distribution Network Implementing TLBO Algorithm for Loss Minimization and Reliability Improvement," pp. 157–164, 2020.
- [159] D. L. Duan, X. D. Ling, X. Y. Wu, and B. Zhong, "Reconfiguration of distribution network for loss reduction and reliability improvement based on an enhanced genetic algorithm," *International Journal of Electrical Power and Energy Systems*, vol. 64, pp. 88–95, 2015.

- [160] B. H. Khan, *Non-Conventional Energy Resources - B H Khan - Google Books*. New Delhi: Tata McGraw Hill Education Private Limited, 2nd ed., 2010.
- [161] Y. M. Atwa, E. F. El-Saadany, M. M. Salama, R. Seethapathy, M. Assam, and S. Conti, "Adequacy evaluation of distribution system including wind/solar DG during different modes of operation," *IEEE Transactions on Power Systems*, vol. 26, pp. 1945–1952, nov 2011.
- [162] M. Brenna, F. Foiadelli, C. Leone, and M. Longo, "Electric Vehicles Charging Technology Review and Optimal Size Estimation," *Journal of Electrical Engineering & Technology*, vol. 15, pp. 2539–2552, Nov 2020.
- [163] S. A. A. Rizvi, A. Xin, A. Masood, S. Iqbal, M. U. Jan, and H. Rehman, "Electric vehicles and their impacts on integration into power grid: A review," in *2018 2nd IEEE Conference on Energy Internet and Energy System Integration (EI2)*, pp. 1–6, 2018.
- [164] R. Colville, E. Hutchinson, J. Mindell, and R. Warren, "The transport sector as a source of air pollution," *Atmospheric Environment*, vol. 35, pp. 1537–1565, Mar. 2001.
- [165] M. Ehsani, *Modern electric, hybrid electric, and fuel cell vehicles: fundamentals, theory, and design*. Power electronics and applications series, Boca Raton: CRC Press, 2005.
- [166] O. I. Oluwasuji, O. Malik, J. Zhang, and S. D. Ramchurn, "Solving the fair electric load shedding problem in developing countries," *Autonomous Agents and Multi-Agent Systems*, vol. 34, p. 12, Dec. 2019.
- [167] F. Corvaro, G. Giacchetta, B. Marchetti, and M. Recanati, "Reliability, availability, maintainability (ram) study, on reciprocating compressors api 618," *Petroleum*, vol. 3, no. 2, pp. 266–272, 2017.
- [168] K. K. Aggarwal, *Reliability Engineering*, vol. 3 of *Topics in Safety, Reliability and Quality*. Dordrecht: Springer Netherlands, 1993.
- [169] M. Ehsani, F.-Y. Wang, and G. L. Brosch, eds., *Transportation Technologies for Sustainability*. New York: Springer-Verlag, 2013.
- [170] M. Ehsani, Y. Gao, and A. Emadi, *Modern Electric, Hybrid Electric, and Fuel Cell Vehicles: Fundamentals, Theory, and Design*, p. 558. Boca Raton: CRC Press., 2017.
- [171] C. C. Chan, A. Bouscayrol, and K. Chen, "Electric, hybrid, and fuel-cell vehicles: Architectures and modeling," *IEEE Trans. Veh. Technol.*, vol. 59, p. 589–598, 2010.
- [172] M. Ehsani, F. Y. Wang, and G. L. Brosch, eds., *Plug-in Hybrid Electric Vehicles*, pp. 870–881. New York, NY: Springer New York, 2013.
- [173] G. Lacey, G. Putrus, and E. Bentley, "Smart ev charging schedules: supporting the grid and protecting battery life," *IET Electr. Syst. Transp.*, vol. 7, p. 84–91, 2017.
- [174] A. Mohamed, V. Salehi, T. Ma, and O. Mohammed, "Real-time energy management algorithm for plug-in hybrid electric vehicle charging parks involving sustainable energy," *IEEE Trans. Sustain. Energy*, vol. 5, p. 577–586, 2014.

- [175] M. Elsis, N. Bazmohammadi, J. M. Guerrero, and M. A. Ebrahim, "Energy management of controllable loads in multi-area power systems with wind power penetration based on new supervisor fuzzy nonlinear sliding mode control," *Energy*, vol. 221, p. 119867, apr 2021.
- [176] S. Anand and B. G. Gundlapalli, S. K. and Fernandes, "Transformer-less grid feeding current source inverter for solar photovoltaic system," *IEEE Trans. Ind. Electron.*, vol. 61, p. 5334–5344, 2014.
- [177] M. Khalilzadeh and A. Fereidunian, "A markovian approach applied to reliability modeling of bidirectional dc-dc converters used in phevs and smart grids," *Iranian Journal of Electrical and Electronic Engineering*, vol. 12, no. 3, 2016.
- [178] P. R. Mishra and J. C. Joshi, "Reliability estimation for components of photovoltaic systems," *Energy Convers. Manag.*, vol. 37, p. 1371–1382, 1996.
- [179] T. T. Pham, T. C. Kuo, D. M. Bui, M. T. Cao, T. P. Nguyen, and T. D. Nguyen, "Reliability evaluation of an aggregate battery energy storage system under dynamic operation," *IEEE International Conference on Power Electronics, Smart Grid and Renewable Energy (PESGRE2020), Cochin, India*, p. 1–8, 2020.
- [180] "POWER Data Access | SSE-Renewable Energy; Temporal average-Daily; Lat: $26^{\circ}8'5.9548''N$; Lon: $91^{\circ}43'52.9572''E$ (Guwahati, India); Duration: Jan 1,2020-Jan 1,2021; Meteorology: Temp range at 2 meters, clear sky; Available at- ." <https://power.larc.nasa.gov/data-access-viewer/>. (accessed April 8, 2021).



Input Data Set

All the input data which are used in case studies throughout the thesis are presented here.

Table A.1 Generating Unit Rating and Reliability Data of RBTS [1]

| Unit Size (MW) | Type | No. of units | Failure rate (1/yr) | Repair rate (1/yr) | Scheduled main- tenance(week/yr) |
|-------------------|---------|-----------------|------------------------|-----------------------|-------------------------------------|
| 5 | Hydro | 2 | 2.0 | 198.0 | 2 |
| 10 | thermal | 1 | 4.0 | 196.0 | 2 |
| 20 | Hydro | 4 | 2.4 | 157.6 | 2 |
| 20 | Thermal | 1 | 5.0 | 195.0 | 2 |
| 40 | Hydro | 1 | 3.0 | 147.0 | 2 |
| 40 | Thermal | 2 | 6.0 | 194.0 | 2 |

Table A.2 Priority order of generating units of RBTS [1]

| Priority loading order | Bus no | Unit capacity (MW) | Failure Rate (f/year) | Repair Rate (hr) | FOR |
|------------------------|--------|--------------------|-----------------------|------------------|--------|
| 1 | 2 | 40 | 3 | 60 | 0.0201 |
| 2 | 2 | 20 | 2.4 | 55 | 0.0148 |
| 3 | 2 | 20 | 2.4 | 55 | 0.0148 |
| 4 | 1 | 40 | 6 | 45 | 0.0299 |
| 5 | 1 | 40 | 6 | 45 | 0.0299 |
| 6 | 1 | 20 | 5 | 45 | 0.0102 |
| 7 | 1 | 10 | 4 | 45 | 0.0250 |
| 8 | 2 | 20 | 2.4 | 55 | 0.0148 |
| 9 | 2 | 20 | 2.4 | 55 | 0.0148 |
| 10 | 2 | 5 | 2 | 45 | 0.0102 |
| 11 | 2 | 5 | 2 | 45 | 0.0102 |

Table A.3 Specifications of SPP, WPP and TPP [2, 3]

| Description | Solar Plant | Wind Plant | Tidal Plant |
|--|--|---|--|
| Installed capacity | 2 MW | 3 MW | 5 MW |
| Nominal Rating | 200W | 3MW | 5 MW |
| Efficiency | 18.70% | 45% | 69% |
| Life time | 20 years | 25 years | 25 years |
| Unit Price | 3000 \$/kW | 2290 \$/kW | 3500\$/kW |
| Maintenance cost (% of the capital cost) | 3% | 1% | 3% |
| Other Technical Specifications | $V_{OC}=22.30V$, $P_{max}=200W$, $T = 30^{\circ}C$, $\kappa=0.9$, $\alpha = -0.005/^{\circ}C$ | $V_{ci}=3m/s$, $v_{co}=25m/s$, Swept area= $6362 m^2$ | $R=6m, r=2m$, $\rho = 1025kg/m^2$, $A=1km^2$ |

Table A.4 Weather effect coefficient (τ) for SPP [4]

| Conditions | spring | Summer | Autumn | Winter |
|------------|--------|--------|--------|--------|
| Sunshine | 0.68 | 0.42 | 0.60 | 0.74 |
| Cloudy | 0.24 | 0.26 | 0.35 | 0.17 |
| Overcast | 0.05 | 0.14 | 0.02 | 0.03 |
| Rainy | 0.03 | 0.18 | 0.03 | 0.06 |

Table A.5 Customer Data at BUS-2 of RBTS [5]

| No. of load points | load points (LP) | Customer Type | Average load per LP (MW) | Peak load per LP (MW) | No. of customers |
|--------------------|----------------------|---------------|--------------------------|-----------------------|------------------|
| 5 | 1-3, 10, 11 | residential | 0.535 | 0.8668 | 210 |
| 4 | 12, 17-19 | residential | 0.450 | 0.7291 | 200 |
| 1 | 8 | small user | 1.00 | 1.6279 | 1 |
| 1 | 9 | small user | 1.15 | 1.8721 | 1 |
| 6 | 4, 5, 13, 14, 20, 21 | govt/inst | 0.566 | 0.9167 | 1 |
| 5 | 6,7, 15, 16, 22 | commercial | 0.454 | 0.7500 | 10 |
| TOTAL | | | 12.291 | 20.00 | 1908 |

Table A.6 Component Reliability Data for BUS-2 of RBTS [6]

| Component Type | Failure rate (f/yr) | Repair time (hr) | Replacement time (hr) | Switching time (hr) |
|----------------|---------------------|------------------|-----------------------|---------------------|
| Transformers | 0.015 | 200.0 | 10.0 | 1.0 |
| Breakers | 0.006 | 4.0 | — | 1.0 |
| Busbars | 0.001 | 2.0 | — | 1.0 |
| Lines | 0.065 | 0.50 | — | 1.0 |
| Cables | 0.040 | 30.0 | — | 3.0 |

Note: Lines and cables failure rates are in f/yr-km

Table A.7 Interruption Cost (\$/kW) of different consumer types [7]

| Interruption duration | Residential user | Commercial user | Small user | Govt/Inst. |
|-----------------------|------------------|-----------------|------------|------------|
| 1 min | 0.001 | 0.381 | 0.060 | 0.044 |
| 20 min | 0.093 | 2.969 | 0.343 | 0.369 |
| 1 hr | 0.482 | 8.552 | 0.649 | 1.492 |
| 4 hr | 4.914 | 31.317 | 2.064 | 6.558 |
| 8 hr | 15.690 | 83.003 | 4.120 | 26.040 |

Table A.8 Component Reliability Data for PEV [MIL-HDBK-217E,F]

| Component | Failure Rate, λ (per yr) | Restoration Rate, μ (per yr) |
|------------------------|----------------------------------|----------------------------------|
| Charge controller | 0.00741 | 0.285 |
| Battery bank | 0.00746 | 0.668 |
| Energy management unit | 0.01624 | 0.556 |
| Power converter | 0.01255 | 0.342 |
| Motor | 0.01825 | 0.586 |
| Vehicle controller | 0.01525 | 0.345 |
| Charging system | 0.06000 | 0.768 |

Table A.9 Charging Station Data for PEV [8]

| Charging Point/Station(i) | No.of Vehicles (N) (per yr) | Annual Outage (U) (hour) |
|---------------------------|-----------------------------|--------------------------|
| 1 | 1200 | 1000 |
| 2 | 1400 | 950 |
| 3 | 1100 | 700 |
| 4 | 700 | 850 |
| 5 | 1300 | 900 |
| 6 | 1500 | 750 |
| 7 | 1000 | 800 |
| 8 | 800 | 650 |

Table A.10 Reliability data of a typical SEV [MIL-HDBK-217E,F]

| Component/Subsystem | Failure Rate (per yr) | Restoration Rate (per yr) |
|-------------------------------------|-----------------------|---------------------------|
| PV system | 0.04000 | 0.552 |
| Charge controller | 0.00741 | 0.285 |
| Battery | 0.00746 | 0.668 |
| Electric drive | 0.01255 | 0.342 |
| Motor | 0.01825 | 0.586 |
| Vehicle controller | 0.01525 | 0.345 |
| Energy management system | 0.01624 | 0.556 |
| Converter station (Charging System) | 0.06000 | 0.768 |

Table A.11 PV Generation Data [9]

| Parameter | Symbol | Value |
|--------------------------------------|-----------|---------------------------|
| Standard solar irradiation | G_{std} | 1000 W/m^2 |
| Reference solar irradiation | G_{ref} | 150 W/m^2 |
| Maximum temperature | T_{max} | 70°C |
| Minimum temperature | T_{min} | 5°C |
| Temp. coefficient of PV arrays | α | $-0.005/^{\circ}\text{C}$ |
| PV generation capacity | P_{max} | 1 pu |
| Minimum useful power | P_{mup} | 0.1 pu |
| Reliability of the changeover switch | r_{sw} | 0.98 |

Table A.12 Charging Station Data for SEV [9]

| Charging Point/Station(i) | No.of Vehicles (N)(Per Year | Annual Outage (Hour) |
|---------------------------|-----------------------------|----------------------|
| 1 | 700 | 850 |
| 2 | 1200 | 1000 |
| 3 | 1000 | 800 |
| 4 | 1100 | 700 |
| 5 | 1300 | 900 |
| 6 | 1500 | 750 |
| 7 | 1400 | 950 |
| 8 | 800 | 650 |

Table A.13 Radial System Reliability Parameter: RBTS (Bus-2) [6]

| Load point | Failure Rate (f/yr) | Repair time (hr) | Annual Outage Time (hr/yr) |
|------------|---------------------|------------------|----------------------------|
| 1 | 0.23925 | 3.03 | 0.7252 |
| 2 | 0.25225 | 3.13 | 0.7902 |
| 3 | 0.25225 | 3.13 | 0.7902 |
| 4 | 0.23925 | 3.03 | 0.7252 |
| 5 | 0.25225 | 3.13 | 0.7903 |
| 6 | 0.24900 | 3.11 | 0.7740 |
| 7 | 0.25225 | 2.98 | 0.7513 |
| 8 | 0.13975 | 3.88 | 0.5427 |
| 9 | 0.13975 | 3.60 | 0.5038 |
| 10 | 0.24250 | 3.00 | 0.7285 |
| 11 | 0.25225 | 3.13 | 0.7902 |
| 12 | 0.25550 | 3.16 | 0.8065 |
| 13 | 0.25225 | 2.93 | 0.7383 |
| 14 | 0.25550 | 2.95 | 0.7545 |
| 15 | 0.24250 | 3.00 | 0.7285 |
| 16 | 0.25225 | 3.13 | 0.7902 |
| 17 | 0.24250 | 3.06 | 0.7415 |
| 18 | 0.24250 | 3.00 | 0.7285 |
| 19 | 0.25545 | 3.11 | 0.7935 |
| 20 | 0.25550 | 3.11 | 0.7935 |
| 21 | 0.25225 | 2.93 | 0.7383 |
| 22 | 0.25550 | 2.95 | 0.7545 |



List of Publications

[A] Publications in Journal

1. Talukdar, B.K.; Deka, B.C., Goswami, A.K., “Reliability analysis of an active distribution network integrated with solar, wind and tidal energy sources”, *International transactions on electrical energy systems*, (2021), DOI: 10.1002/2050-7038.13201, **(SCI expanded and SCOPUS indexed)**.
2. Talukdar, B.K.; Deka, B.C., Goswami, A.K., “An approach to reliability modeling and availability analysis of a solar electric vehicle with stand-by plug-in facility”, *International transactions on electrical energy systems*, (2021), DOI: 10.1002/2050-7038.13147, **(SCI expanded and SCOPUS indexed)**.
3. Talukdar, B.K.; Deka, B.C. “An Approach to Reliability, Availability and Maintainability Analysis of a Plug-In Electric Vehicle”. *World Electric Vehicle Journal*, 2021, 12, 34. <https://doi.org/10.3390/wevj12010034> **(SCOPUS indexed)**.
4. Talukdar, B.K.; Deka, B.C. “An Approach to solve Unit Commitment Problems considering Reliability as a Constraint,” *International Journal of Computer Sciences and Engineering*, Vol.04, Issue.07, pp.30-33, 2016. **(UGC Approved)**.

[B] Publication as Book Chapter

1. Talukdar, B.K.; Deka, B.C., Goswami, A.K., Saha, D, “Reconfiguration of Radial Distribution Network Implementing TLBO Algorithm for Loss Minimization and Reliability Improvement”, in *‘Intelligent Techniques and Applications in Science and Technology’*, Springer International Publishing, (2020), DOI: 10.1007/978-3-030-42363-6-19.

[C] Publications in IEEE Conferences

1. Talukdar, B.K.; Deka, B.C., Goswami, A.K., “Reliability Centered Capacity reserve Management in Deregulated Power Market”, *IEEE International Conference on Power Electronics, Smart Grid, and Renewable Energy (IEEE-PESGRE-22)*, January 2-5, 2022 **(Published in IEEE Explore)**
2. Talukdar, B.K.; Deka, B.C., Bhuyan, M.J., “Reliability Analysis of Electric Vehicle integrated Distribution Network”, *2nd IEEE IAS International Conference on Computational Performance Evaluation (ComPE-2021)*, December 1-3, 2021. **(Published in IEEE Explore)**

[D] Publications in other International/ National Conferences

1. B.K.Talukdar, B.C. Deka, “Modeling of a Photovoltaic System and Reliability Assessment", Proceedings of *International Conference on Renewable and Alternate Energy (ICRAE-2018)* 4th-6th December, 2018.
2. Talukdar, B.K.; Deka, B.C., Goswami, A.K., “Distribution System Reliability Assessment Incorporating Distributed Generation”, Proceedings of *National Conference on ‘Recent Advances in Science and Technology’*, (NCRAS-2019), May 15-17, 2019.
3. Talukdar, B.K.; Deka, B.C “An Approach to Adequacy Assessment of Renewable Microgrid”, Proceedings of *National Conference on Emerging Trends in Energy and Electrical Systems (ETEES-2019)*, March 29-30, 2019
4. Talukdar, B.K.; Deka, B.C., “Effects of Wind Power on Bulk System Reliability Evaluation Using Well-Being Framework”, Proceedings of *National Conference on Non-Conventional Energy: Harvesting Technology and Its Challenges (NCEHTC-2017)*, November 17-18, 2017.
5. Talukdar, B.K.; Deka, B.C., “Adequacy Assessment of a System utilizing Solar and Wind Energy Sources”, Proceedings of *National Exhibition & Conference on New and Renewable Energy (NECONRE-2017)*, October 6-7, 2017. ■

**POWER SYSTEM RELIABILITY ANALYSIS
WITH SPECIAL EMPHASIS ON
RENEWABLE DISTRIBUTED GENERATION
AND ELECTRIC VEHICLE**



BIPUL KUMAR TALUKDAR

DEPARTMENT OF ELECTRICAL ENGINEERING

ASSAM ENGINEERING COLLEGE

**THIS THESIS IS SUBMITTED TO
GAUHATI UNIVERSITY FOR THE AWARD OF DEGREE OF
DOCTOR OF PHILOSOPHY**

**FACULTY OF ENGINEERING
GAUHATI UNIVERSITY
2022**

Recommendation:

Power system reliability (PSR) refers to the probability of a power system performing its intended function, i.e., to provide electrical power to all of its customers at a reasonable cost with an assurance of continuity and quality. However, it is neither technically nor economically feasible to plan, construct and operate a power system with zero likelihood of failure. System failures are stochastic in nature. The probability of customers being interrupted can be reduced up to a certain extent by increased investment and proper planning during the designing phase or the operating phase, or both. For this, it is extremely important to assess the reliability of the entire system considering all aspects like load growth, available operating reserve, capacity expansion, transmission constraints, etc. A thorough analysis of PSR helps system planners, designers, and operators to monitor the system's overall risk level. It also provides information on the weak zone in the system and helps to prepare preventive and corrective maintenance schedules for its components.

Over the years, PSR has been an operational issue for the power system operators (PSOs). However, deregulation of power industry makes PSR more customer-centric and price-specific. In a deregulated power system (DPS), customers have more freedom to select not only the energy utilities but also to purchase power at their preferred reliability levels. Therefore, maintaining PSR as per customers' specifications becomes challenging for the PSOs in DPSs. Centralized operations that aid in easier decision-making at all levels are no more relevant in the deregulated environment. Cost-based mechanisms of vertically integrated utilities have transitioned to price-based mechanisms in horizontally operated power systems. A judicious reliability-centered operating reserve management (ORM) strategy is vital in such environments. This research covers this aspect. Reliability assessment of a power system under deregulated scenario is one of the objectives of this research.

For a highly reliable power supply, the adequacy of operating reserve is an important factor. With the integration of renewable distributed generation (DG), smart management of the operating reserve becomes possible, enabling high efficiency and reliability of power supply at reasonably lower costs. However, integration of large volumes of renewable energy sources (RESs) brings some technical challenges and complexities in power system operation. Therefore, modern power system requires enhanced techniques to evaluate its reliability and minimize the frequency and duration of outages. In this research work, a method has been proposed to develop a reliability model of a system having multiple RESs. The thesis analyzes

the reliability worth in terms of energy and costs due to the integration of solar, wind, and tidal energy sources with the help of two new performance metrics.

In addition to RESs, the emergence of electric vehicles (EVs) brings many new aspects to PSR studies. EVs can be treated as variable loads (in grid-to-vehicle mode) and also as portable DG (in vehicle-to-grid mode). The increased volume of plug-in EVs in grid-to-vehicle mode reduces the grid's reserve capacity and thus reduces the reliability of power supply to its customer load-points. Moreover, uncontrolled scheduling of EV charging distorts the load curve, causing peaks on the peaks; and pushes the system operator for load curtailment, and thus reduces the system reliability. The present research considers this aspect also. It analyzes how the reliability of a distribution network is impacted due to the charging of plug-in EVs.

The operational effectiveness of a plug-in EV is primarily dependent on the availability of a reliable charging station at the desired location. Thus, the grid's reliability directly impacts the operation of an EV. Furthermore, EVs are built with a large number of electrical components, which makes EVs more failure-prone as compared to conventional vehicles. This thesis presents an approach to conducting comprehensive reliability, availability, and maintainability studies of a plug-in EV covering all the above-mentioned aspects. In addition to this, the thesis also investigates the reliability and availability of a solar-powered vehicle. The study quantitatively justifies that a solar EV with a standby plug-in facility can be the most effective EV option from reliability perspective.

The present studies implement the Markov modeling concepts and well-being framework to develop different reliability models. In addition to the conventional reliability indices, some newly designed reliability metrics have been proposed in this thesis. Developed models are exemplified in some standard test systems. Input data sets are collected from the state of the art literature. Calculations are carried out through programming/simulations in MATLAB/Simulink

The cost of reserve margin is not considered in the present research. In a deregulated environment, customer can choose their reliability level by paying the required cost of reserve. For higher reliability, the cost of reserves will be more. Thus, there must be a trade-off in reliability vs. cost. This aspect can be added to future research.

The reliability worth of integrating renewable energy sources (RESs) with distribution systems is one of the less focused areas in power system reliability studies. In this thesis, two new

parameters, namely Incremental Energy Benefit (IEB) and Incremental cost Benefit (ICB), are introduced to measure the benefits of RESs integration. Application of these two metrics can be extended to other renewable-energy incorporated systems.

The present study illustrates how the reliability of a distribution network gets impacted due to the increased EV charging. Thus, this study considers the negative impact of EV integration. However, EVs can be treated as portable DGs and can be used to boost the reliability of a grid. During the off-peak hours, EV takes charge from the grid (grid-to-vehicle), and during the peak hours, the vehicle supplies the energy to the grid (Vehicle-to-Grid). This concept has been addressed in many recent literatures; however, reliability-centric researches are still very limited. The impact of EV integration in vehicle-to-grid mode on the reliability of a distribution network can be a future scope of the present study.

The research reported in Chapter 7 of this thesis shows how a proper maintenance strategy is essential for the higher availability of an EV. A comprehensive maintainability prediction analysis can help to investigate all the factors associated with the maintainability of an EV and prepare a proper corrective and preventive maintenance schedule accordingly. In addition to that, a reliability-cost trade-off assessment is very important to find an optimum reliability point at a reasonable cost of EV components. These two aspects can be incorporated in future studies. Again, the present research has dealt with the steady-state reliability assessment of EVs. Dynamic reliability assessment can be a good scope of future research.

The present study has not considered the impact of wind speed on mPAI. The reliability of the SEV has been determined at stationary conditions. How a vehicle's speed impacts the value of mPAI can be a potential future scope of the study reported in this thesis.